Stony Brook University

Transformation of mammary epithelial cells by regulators of cell polarity

A Dissertation Presented

By

Marissa E. Nolan

To

The Graduate School

in Partial Fulfillment of the

Requirements

for the Degree of

Doctor of Philosophy

in

Genetics

Stony Brook University

May 2008

Stony Brook University

The Graduate School

Marissa Ellen Nolan

We, the dissertation committee for the above candidate for the

Doctor of philosophy, hereby recommend

acceptance of this dissertation

Dr. Senthil Muthuswamy - Dissertation Advisor
Associate Professor, Cold Spring Harbor Laboratory

Dr. Howard Crawford – Chairperson of Defense
Assistant Professor, Department of Pharmacological Sciences, Stony Brook University

Dr. Yuri Lazebnik
Professor, Cold Spring Harbor Laboratory

Dr. Scott W. Lowe
Investigator, HHMI and Deputy Director, Cancer Center, Cold Spring Harbor Laboratory

Dr. Jonathan Chernoff
Senior Member, Fox Chase Cancer Center

This dissertation is accepted by the Graduate School

Lawrence Martin
Dean of the Graduate School

Abstract of the Dissertation

Transformation of mammary epithelial cells by regulators of cell polarity

By

Marissa E. Nolan

Doctor of Philosophy

In

Genetics

Stony Brook University

2008

During the progression to breast cancer, organized growth-arrested epithelial cells become hyperproliferative and lose their polarized glandular organization. Many studies have shown that proliferation is a driving force behind cancer formation, however little is known about the mechanisms that disrupt polarized acinar structures. To determine how breast cancer progresses we need to understand not only the mechanisms of cell proliferation, but also the mechanisms that regulate epithelial cell polarity and how these pathways may become altered during cell transformation.

We found that the polarity regulator, Par6, is overexpressed in precancerous breast lesions and in advanced carcinoma. When Par6 was ectopically expressed in the non-transformed human breast epithelial cell line, MCF-10A, we found that Par6 promoted hyperproliferation. We determined that Par6 promoted proliferation through activation of the MAPK pathway and that this proliferative effect depended on Par6/aPKC/Cdc42 interaction. MCF-10A cells, when plated on basement membrane,

form acinar-like structures that recapitulate the resting acinar structures within human breast tissue. Acinar structures derived from Par6 overexpressing cells are hyperproliferative and resemble the precancerous breast lesions observed *in vivo*. The fact that overexpression of Par6 was found in both early and late stage lesions, suggests that Par6 may impart an advantage that promotes cell transformation.

Activation of the oncogene ErbB2 in acinar structures also resembles early breast lesions, termed ductal carcinoma in situ (DCIS). Both DCIS and ErbB2 transformed acini are characterized by disruption of acinar organization and hyperproliferation. We found that activated ErbB2 recruits Par6/aPKC and that this interaction is required for ErbB2-induced disruption of cell polarity, but not re-initiation of cell proliferation. This finding suggests that ErbB2 uses at least two distinct pathways to promote transformation; one to initiate proliferation and the other to disrupt epithelial cell polarity. We also found that downregulation of the cytoarchitectural regulator RhoA promoted invasion of ErbB2 transformed acinar structures. This suggests that further deregulation of the cell organization by disrupting cellular cytoarchitecture can promote invasion of ErbB2 transformed acini. Collectively, the studies of this dissertation found that inference with the normal expression and function of the regulators of cell polarity can promote proliferation and transformation of mammary epithelial cells.

Table of Contents

List of Figures

Chapter 1.

Chapter 2.

Chapter 3.

Chapter 4.

Chapter 5.

Chapter 6.

Appendix.

List of Abbreviations

10A.ErbB2: MCF-10A cells expressing chimeric ErbB2

2D: two-dimensional

3-D: Three-dimensional

ADH: Atypical ductal hyperplasia

AKT: V-AKT murine thymoma viral oncogene homolog

AREG: amphiregulin

BM: basement membrane

BrdU: 5-Brmo-2'-deoxyuridine

C. elegans: caenorhabditis elegans

Cdc42: cyclin division cycle protein

cDNA: Complementary deoxyribonucleic acid

c-Met: Mesenchyml epithelial transition factor

c-Myc: Cellular oncogene from avian myelocytomatosis

CRIB: Cdc42/Rac interactive binding

DAPI: 4', 6-diamidine-2-phenylinodole-dihydrochlodride

DCIS: Ductal Carcinoma in situ

DNA: Deoxyribonucleic acid

ECM: Extracellular matrix

EDTA: Ethylenediamine tetraacetic acid

EGF: Epidermal growth factor

EGFR: Epidermal growth factor receptor

EHS: Englebreth-Holm-Swarm tumor

EMT: Epithelial to mesenchyml transition

ER: Estrogen receptor

ErbB: v-erb-b2 erythroblastic leukemia viral oncogene homolog

ERK: Extracellular signal-related kinase

ERM: Ezrin-radixin-moesin

FACS: fluorescence-activated cell sorting

FAK: focal adhesion kinase

FKBP: FK506 binding protein

GAPDH: glyceraldehyde-3-phosphate dehydrogenase

GDP: Guanine Di-phosphate

GM130: Golgi marker 130

gp135: Golgi protein 135

GTP: Guanine tri-phosphate

HA: Hemagglutinin

HEK 293T: Human embryonic kidney

HER: Human epidermal growth factor receptor

HGF: Hepatocyte growth factor

HPV: Human papillomavirus

HTLV-1: human T-cell leukemia virus type-1

IBC: Invasive breast cancer

IF: Immunofluorescence

IP: Immunoprecipitation

JNK: Jun N-terminal kinase

Lgl: Lethal giant Larvae

LTR: long terminal repeat

MAPK: Mitogen active protein kinase

MCF-10A: Michigan Cancer Foundation -10 Adherent

MDCK II: Madin-Darby Canine Kidney II

MOI: Multiplicity of infection

ng: Nanogram

NP-40: Nonylphenylpolyethylene glycol detergent

NSCL: Non-small cell lung cancer

P: Phosphorous

PALS: Protein associated with Lin-7

Par1: Partitioning defective -1

Par3: Partitioning defective-3

Par4: Partitioning defective-4

Par6: Partitioning defective-6

PATJ: Pals1-associated tight junction

PCR: Polymerase chain reaction

PDZ: PSD95(post synaptic density)/Discs-large/ZO-1

PI3: Phosphotidyl 3'-inositol kinase

aPKC: Atypical protein kinase C

PLCγ: Phospholipase C gamma

Q-PCR: Quantitative real time PCR

Rac1: Ras-related C3 botulinum toxin substrate

Ras: V-ras neuroblastoma RAS viral oncogene homolog

RhoA: Ras homolog gene family, member A

RhoN19A: Dominant negative RhoA

RIPA: Radioimmuno-precipitation Assay

RNA: Ribonucleic acid

RTK's: Receptor Tyrosine Kinases

SDS-PAGE: Sodium dodecyl sulfate-polyacrylamide gel electrophoresis

shRNA: Short hairpin RNA

siRNA: Small interfering RNA

Src: Sarcoma viral oncogene

STAT3: Signal Transducer and Activator of Transcription 3

TDLU: terminal ductal-lobular unit

TGFβ: transforming growth factor beta

TJ: Tight junction

TNE: Tris-NP-40-EDTA

Tris-HCl: Tris (hydroxymethyl) aminomethane hydrochloride

Triton X-100: Polyehylene glycol tert-octylphenyl ether

Tyr: Tyrosine

ZO-1: Zonula occluden

µg: Microgram

µl: Microliter

Acknowledgements

First I would like to thank Senthil Muthswamy for taking me into his lab and being an excellent mentor. When I first met Senthil, I was truly inspired by the way he thought about science. I had never thought about the problems of carcinoma in terms of organization before I joined the lab. I have enjoyed studying and learning under Senthil and thank him for all his efforts in training me as a scientist.

I would also like to thank the members of my committee, Jonathan Chernoff, Howard Crawford, Scott Lowe and Yuri Lazebnik for their time and guidance throughout my graduate career. I would especially like to thank Jonathan for all travel he endured for my meetings. I would also like to thank Howard for reading my manuscript, traveling from Stony Brook and for all his support and guidance as the chair of my committee.

Thanks to my collaborators for helping me generate the Par6 story. Min Yu for breast tumor RNA, Lakshmi Muthuswamy for analysis of ER positive tumors and ROMA data, Srinjin Basu for being so observant, Sanjun Lee for the microarray analysis of HELUs and Craig Allred. Erin Cline from James Nelson's laboratory at Stanford provided a Par6 antibody. There ErbB2/Par6 story was lead by both Teresa Haire and Victoria Aranda in collaboration with Joseph Calarco**,** Avi Z. Rosenberg, James P. Fawcett, Tony Pawson.

I would like to acknowledge the people within the CSHL community that helped me with reagents, protocols and scientific discussions: David Mu, Khalid Siddiqu, Niraj Tolia, John Kurland, Amy Leung, Darren Burgess, Rotem Karini, Ross Dickens, Lawrence X, Maria Chen, Mona Spector, Lars Zender, Mike Hemann, Jack Zilfou, David Simpson and the Demerec building. Also the neighboring Lazebnik lab, Amy, Himena,

Cathy and Dom for always having a reagent when were ran out, especially Amy for all the chats and lunches.

The members of the Muthuswamy lab past and present, Teresa Haire, Avi Rosenberg, Lixing Zhan, Bin Xu, Bin Xaing, Izabela Sukja-Wok, Ming Chen, Samit Chaterjee, Kenneth Bergami, Min Yu, Kim Gram, Victoria Aranda Alexandra Lucs and the waves and waves of rotation students. They have been a wonderful group of people to work with and have generated a pleasurable working environment, assistance with experiments and reagents Through the years the lab overall has faced many struggles. The most difficult challenge for me was not scientific; it was dealing with the loss of Teresa. Teresa was an amazing technician before she left for graduate school. She had such dedication and drive. It was because of here that the lab ran so smoothly the first few years. She was also a wonderful person and friend and will be missed.

I would also like to thank my Stony Brook classmates for their support, especially in the first year of graduate school. Andrea, Adam, Carmine, Doug, Kristen, Jackie, Nihal, Togay, Paul, Alexandra, Tarah, and Dan. We spent quite a bit of time studying and socializing in the fishbowl. I would especially like to thank my roommate for the first 3 years of Grad school Kristen for her friendship. The Genetics Graduate program administrators and directors have been provided immeasurable support through my first years, Peter Gergen, Pam Sims and Teresa Kunkel helped ease my transition into graduate school. Currently, Jerry Thompson and Kate Bell are providing support and guidance as I navigate the SBU red tape.

Working at CSHL has provided me an opportunity to meet some amazing people from all over the world. The community of Post-docs and graduate students have

generated a wonderful work/play environment. I have enjoyed meeting up at Delbruck happy hour or the bar with the members of the Martinesn lab, Mikel, Dani, Keith, SJ and Milos. In addition to socializing, Volleyball and yoga have provided a wonderful form of stress relief. I would like to thank the 2007 volleyball champions: David, Galen, Charlie, Oliver, Amy, and Cathy. Never underestimate the underdog. My passion for yoga began and grew through Kashia, Vic, Cathy and Anne; it is wonderful to have people to practice with. I would especially like thank Catherine Cormier for being such a wonderful supportive friend, volleyball and yoga partner, shopping buddy and a great person to talk science with.

The decision to join the Muthuswamy lab was made in at the same time as my classmate Alexandra Lucs. I would like to thank Sasha for being my rock and always willing to take the time to talk science, politics and whatever else came up. A special thanks to Sasha's family, David, Tatiana and Gabriella, for generating a wonderful family atmosphere where, Dan and I were always welcome for dinner. Also I would like to thank Kitty and Tatiana for brightening up my mornings when they visited especially during the first few years of grad school.

Victoria, my Mentoria! I would like to thank Vic for all of her help with everything, for all the coffee breaks and pep talks. She has provided me with invaluable assistance scientifically and has helped me improve my communication skills like no other, especially in preparation of this document. Victoria has been a wonderful friend and the best baymate a grad student could ask for! We have laughed, cried and supported each other and my experience in grad school wouldn't have been the same if she hadn't joined the lab.

To my family, my parents have been a wonderful resource for support and love. I wouldn't be where I am today if it were not for them. They inspire me every single day. My three sisters, Melanie, Michelle and Meaghan, who have been so supportive during my years of graduate school even if they make me refrain from talking science over the the holidays. My grandmothers, who were and are women of love and understanding. I would also like to thank my friends Amy, Erin, Jenny and Darby for their love and support. My husband's family, Mama Nolan, Kevin and his family, James, Diane and her family all have been very understanding and supportive over the past years.

Lastly I would like to thank my wonderful husband who began this journey with me. I have seen his development as a scientist, from the intellectual questions he posed while he was half asleep in grad gen to the amazing scientist that he has become and continues to be. I would have never thought that the young first year that I met in the fishbowl would turn out to be the perfect husband. Daniel has been my literal support net from the first biochemistry exam through dissertation writing. I could not have done this without him. It has been an amazing journey and it has only just begun.

Chapter 1: Introduction

Breast cancer

Breast cancer is the most prevalent cancer in women in the United States and Europe with over 600,000 new cases a year (Ferlay et al. 2007; ACS 2008). Despite recent advances in targeted therapy and early diagnosis, breast cancer remains the second most common form of cancer deaths in the United States and the third most deadly cancer in Europe (Ferlay et al. 2007; ACS 2008). Breast cancer cannot be regarded as one single disease. In fact, because of the genetic diversity of tumors, it can be considered multiple diseases with diverse histopathology and clinical outcomes (Simpson et al. 2005). The current understanding of breast cancer is confounded by this heterogeneity which presents a major obstacle to development of new treatments and the improvement of existing therapies.

Common genetic alterations in breast cancer

Breast cancer appears to develop from normal breast tissue. One hallmark of cancer progression is genetic instability, which results in acquired genetic changes such as, gene loss or amplification, point mutation and chromosomal translocation (Aldaz et al. 1995; O'Connell et al. 1998; Waldman et al. 2000; Osborne et al. 2004). Some of these genetic changes will be advantageous to the cell and promote cell proliferation, survival and motility. These genetic changes allow the cells to proliferate, possibly giving rise to populations of cells with the ability to grow into a malignant tumor. Some of these genetic changes and the cellular pathways associated with them have been

identified. These pathways are currently being targeted with therapeutics; however the diversity of breast cancers makes the broad application of a single therapy difficult. These cancerous pathways are not only diverse but highly interactive and necessary for the survival of normal breast cells, further complicating the benefits of current therapeutics. Our understanding of cancer pathways and how to target them has become more comprehensive in the past decade. However, we still face many challenges in understanding the different types of breast lesions to ensure that the disease is diagnosed and treated accordingly.

The identification of oncogenes, tumor suppressors and their associated pathways has contributed to our knowledge of cancer formation. Oncogenes are genes that promote the formation of cancer. One of the most prominent oncogenes in breast cancer is the erythroblastic leukemia viral oncogene homolog ErbB2. ErbB2/HER2, is over-expressed in 25-35% of breast cancers and this overexpression correlates with a poor clinical prognosis (Slamon et al.1987; Slamon et al. 1989). ErbB2 is one member of the ErbB family of receptor tyrosine kinases. These receptor play a role during the normal development of the mammary gland and during tumorigenesis (Yarden and Sliwkowski 2001). There are four members in this family, ErbB1 (EGFR, HER), ErbB2 (HER2), ErbB3 and ErbB4. These receptors can homo and heterodimerize with each other upon interaction with their respective ligands. Once dimerization occurs, the receptors become activated by autophosphorylation of several tyrosine residues in the cytoplasmic domain, initiating downstream signal transduction cascades that result in cell proliferation, differentiation, migration and apoptosis (Yarden and Sliwkowski 2001). Oncogenic ErbB2 can autonomously activate at high expression levels that are observed in tumors.

The downstream signaling cascade that results from ErbB2 activation, such as Ras/MAPK and PI3K/AKT activation leads to an increase in cell proliferation, migration, resistance to apoptosis and altered cell-cell interactions. The importance of ErbB2 in breast cancer is underscored by the success of the current therapies that target ErbB2 and also target the cellular pathways that ErbB2 activates. ErbB2 is targeted by the humanized monoclonal antibody called, Herceptin (Carter et al. 1992) with a response rate of 11-26% (Baselga et al, 1996; Cobleigh et al 1999; Vogel et al 2002; Slamon et al 2002). In addition therapies against PI3K pathway (Rapamycin) and Ras/MAPK pathway (Farnesyl transferase inhibitor, Zarnestra) have been used and yield a 8.5% and 12% response rate respectively (Johnston et al. 2003; Mita et al. 2003).

Other oncogenes that have been associated with breast cancer are, Cyclin D1 and c-myc. Cyclin D1 is genomically amplified in 10-20% and overexpressed in 40-50% of invasive breast cancer with high proliferation rates. Presumably this occurs because an increase in Cyclin D1 levels pushes cells through the G1-S-phase transition of the cell cycle promoting hyperprolifertion. The low molecular weight form of Cyclin E is overexpressed in 20-30% of breast cancer (Keyomarsi et al. 2002) and functions in a similar manner as overexpression of cyclin D1. *The regulators of Cyclins are targeted with cell cycle inhibitors with limited response rates in patients (Osborne et al. 2004).* Another oncogene is c-myc, which encodes a transcriptional regulator that can regulate genes responsible or cell proliferation, differentiation and apoptosis. c-myc is overexpressed in 15-25% of breast tumors and can be associated with more aggressive tumors (Varley et al. 1987; Nass and Dickson 1997). Clinical trials using c-myc

antisense therapy are currently ongoing to determine if this is a viable therapy (Osborne et al. 2004; Devi et al. 2005).

In addition to gain of function and oncogenic stimulation, loss of a tumor suppressor gene, such as p53, can promote breast cancer. p53 is a transcriptional regulator of the cell cycle and mutations in this protein promotes aberrant cell cycle progression. Mutations in p53 occur in 20-30% of breast cancer (Hollstein et al. 1991) and is associated with poor prognosis (Fitzgibbons et al. 2000; Ioakim-Liossi et al. 2001). Gene therapy replacing the function of mutated p53 gene is currently being optimized to reduce the side effect of the gene delivery systems (Osborne et al. 2004; Li et al. 2007).

The identification of the above aberrant pathways in breast cancer furthers our understanding of the disease. The majority of these pathways promote hyperproliferation, however, breast cancer is more complex than just highly proliferative cells. Although targeted therapies have proven successful, their limited response rates emphasize the need for a deeper understanding into the interactive molecular pathways and alternative explanations for cancer progression. For example, very little is known about the pathways that promote disorganization of breast tissue a common feature of all cancerous lesions. Therefore, it is also important to be able to classify and diagnose these lesions at a molecular level to identify therapeutic strategies that will be effective.

Breast cancer subtypes

Standard features of clinical prognosis are patient age, tumor size, lymph node status, tumor grade and endocrine receptor or ErbB2 status (Peppercorn et al. 2008). These types of tumor classification systems are rudimentary and recent studies have

determined 5 different tumor subtypes based on molecular profiling. Microarray analysis was performed on tumors and normal breast tissue. The tumors, in three separate studies, consistently segregated into five distinct subtypes of breast cancer that can be correlated with clinical prognosis. These subtypes are: Basal-like, ErbB2 positive, Normal-like, Luminal A and Luminal B (Perou et al. 2000; Sorlie et al. 2001; Sorlie et al. 2003). These five different subtypes were verified in subsequent studies performed on patients in different ethinic groups (Yu et al. 2004), inflammatory breast cancer (Van Laere et al. 2006) and in a large scale analysis of over 1000 invasive breast tumors (Abd El-Rehim et al. 2005) .

Luminal A tumors are the most common form of breast cancer and are usually low grade with a low risk of reoccurrence. Generally they are positive for estrogen (ER) and progesterone receptors (PR) and are negative for ErbB2. Luminal A tumors are also responsive to endocrine therapy and less responsive to chemotherapy. Luminal B tumors are more variable than luminal A, in that they have a variable grade, variable response to chemotherapy, are sometimes ErbB2 positive and are usually responsive to endocrine therapy. Luminal B tumors are also more proliferative compare to Luminal A. ErbB2 positive tumors are usually high grade, have amplification in ErbB2, are negative for ER and PR, are highly proliferative and respond anti-ErbB2 therapy with a higher risk of recurrence. Basal–like tumors are high grade with a higher risk of recurrence than Luminal tumors and are responsive to chemotherapy but have no known targeted therapy. They lack hormone receptors, lack ErbB2 amplification and are highly proliferative. Normal-breast like subtype presents an enigma to researchers because there are no

significant alterations that are different from the normal breast tissue (Perou et al. 2000; Sorlie et al. 2001; Sorlie et al. 2003; Peppercorn et al. 2008).

This system of subtype classification aids in our understanding of breast cancer as a heterogeneous disease. This system of classification better predicts response to targeted therapies and generates a more accurate prognosis. However, aside from endocrine and ErbB2 targeted therapy, the influence of these molecular subtypes remains limited. Current efforts are focused on understanding the different response and resistance rates to targeted therapy. These types of studies will only aid in the identification of new targets that within these subtypes.

A model for breast cancer progression

The hallmark changes associated with both benign hyperplastic breast disease and breast cancer are increased epithelial cell proliferation rates and disruption of normal breast tissue organization (Ronnov-Jessen et al. 1996; Porter et al. 2003). These characteristics of breast cancer lesions could occur because the mechanisms that control normal cell proliferation and organization have been altered. Many studies have shown that oncogenes disrupt pathways responsible for growth control such as cyclin D1 and ErbB2. However, few studies have determined how the mechanisms that control acinar organization could be deregulated during the progression to carcinoma. Therefore it is important to classify the lesions with disrupted organization and understand what other alterations correlate with these lesions. Understanding organizational disruption will give us new insights into the process breast cancer progression.

A modified Wellings-Jenson model has been proposed by D.C. Allred (Figure 1.1) (Wellings and Jensen 1973; Wellings et al. 1975; Allred et al. 2001). This model arose from histological observation of multiple types of breast lesions. These observations placed lesions with different histological classification on a continuum, from normal breast structures to pre-malignant disease to invasive breast carcinoma. It is important to note that this is a model and breast cancer need not be a linear progression. Indeed this model oversimplifies the heterogeneity of breast disease and does not place lobular carcinoma within this progression model. However, regardless of where the lesion lies on a histological continuum, the histopathological and molecular changes associated with each lesion can be classified together. Therefore this model provides a framework for classifying breast lesions with similar organizational and molecular features that occur throughout the progression to breast cancer (Allred et al. 2001).

According to this model, the earliest breast lesions are the hyperplastic enlarged lobular units (HELU), which are derived from terminal ductal lobular units (TDLU) (Figure 1.1.A). The cells within HELUs are hyperproliferative and have the ability to grow in an organized manner resulting in an enlargement of the acini with a single layer of columnar epithelium (Lee et al. 2006)(Suzuki et al. 2000). These lesions also have a reduction in apoptosis and an increase in expression of both estrogen receptor and epidermal growth factor (EGF) family of growth factors (Cotran et al. 1989; Lee et al. 2006). The hyperproliferation of HELUs is thought to be driven by the increase in the expression estrogen and progesterone receptor (Lee et al. 2006), which are strong inducers of proliferation in the development and differentiation of the human breast (Anderson and Clarke 2004). Consistent with increased proliferation and inhibition of

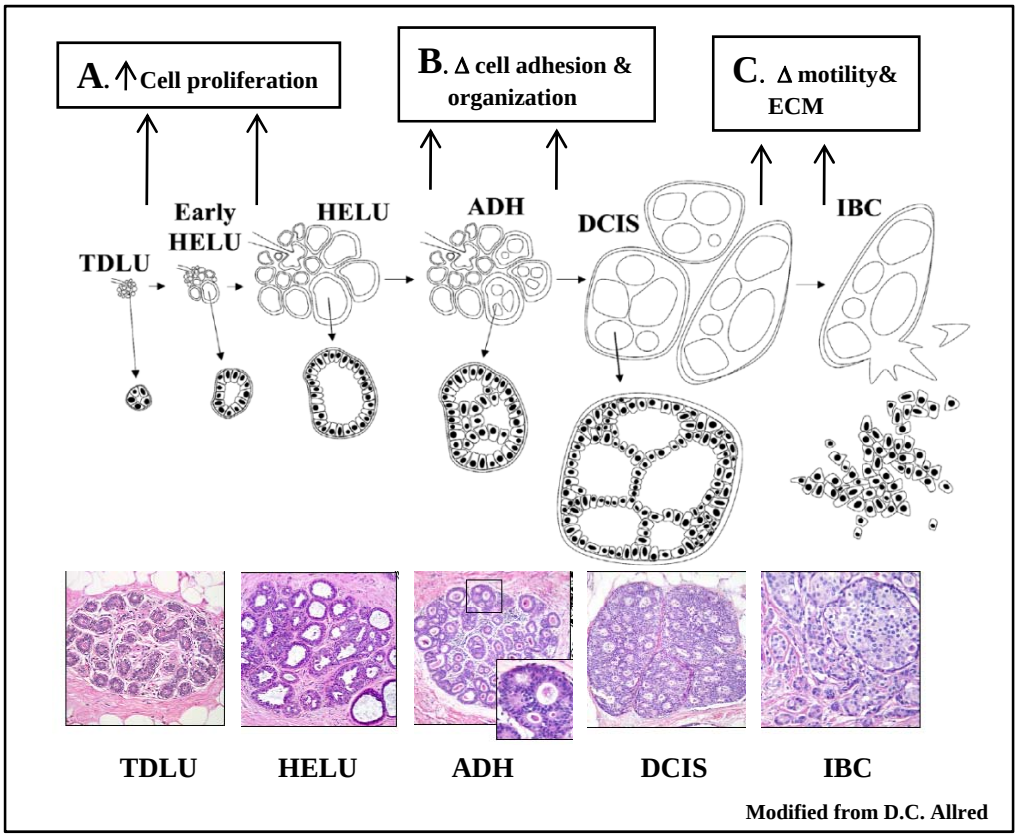

Figure 1.1. Modified Wellings-Jensen model of breast cancer progression

(A) HELU structures have an increase in cell proliferation. **(B)** ADH and DCIS are characterized by changes in cell adhesion and organization. **(C)** IBC is characterized by breakdown of ECM and increased motility of cancer cells (Lee *et al* 2006)**.**

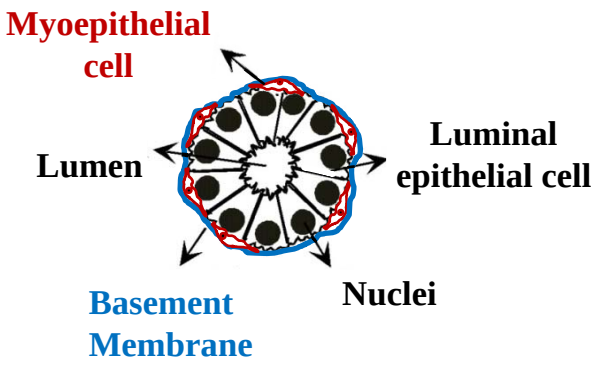

Figure 1.2. Organization of a mammary epithelia acinus

Single layer of luminal epithelial cells surrounding a hollow lumen. These cells are surrounded by a layer of myoepithelial cells and basement membrane.

apoptosis, it has been shown that HELUs have a 2-fold elevated risk of developing into breast cancer over TDLUs (Bodian et al. 1993; Dupont et al. 1993). However, this progression is not obligatory and not all HELUs will progress to atypical ductal hyperplasia (ADH) or beyond.

ADH is associated with changes to acinar organization and cell-cell adhesion and these lesions a have a 5-fold increased risk of progressing to breast cancer (Bodian et al. 1993; Dupont et al. 1993). ADH may or may not progress to ductal carcinoma in situ (DCIS), a commonly diagnosed form of pre-malignant breast disease that has a 10-fold risk of developing to breast cancer (Bodian et al. 1993; Dupont et al. 1993). The epithelial cells within DCIS display an improper architecture and fill the lumen to form abnormal structures with multiple layers of cells that lack proper apical-basal polarity (Figure 1.1.B) (Corn and El-Deiry 2002). While these proliferative changes associated with DCIS have been well studied, the precise mechanisms by which cell and tissue architecture is disrupted in DCIS is not known (Allred et al. 1992; Rudas et al. 1997). During progression to invasive carcinoma (IBC) further disruption of acinar organization and cell-cell adhesion occurs (Figure 1.1.C). The invasive cells within IBC breakdown the extracellular matrix and can invade the surrounding stroma. While the specific genetic changes that occur in IBC are not known, an increase in proteins such as matrix metalloproteases (MMPs), and downregulation of tissue inhibitors of metalloproteases (TIMPs) have been implicated in the enzymatic degradation of the matrix (Nakopoulou et al. 2003; Burstein et al. 2004; Roy et al. 2004). It has been suggested that DCIS are precursors for IBC, because the gene expression profile is similar between these two lesions (O'Connell et al. 1998; Ma et al. 2003; Seth et al. 2003; Simpson et al. 2005).

These similarities are even more apparent in lesions that were isolated from the same breast, lending further support to the idea that DCIS is a precursor of carcinoma (Ma et al. 2003; Seth et al. 2003).

In order to study how oncogenes and alterations in epithelial cell organization can promote breast cancer progression we need to establish a model system that recapitulates acinar organization. Using a three-dimensional human breast epithelial cell culture system (discussed in the following sections) we can disrupt epithelial cell organization, promote hyperplasia or progression to invasive breast carcinoma. We can use this modified Wellings-Jensen model of histological continuity to correlate the phenotypes that we observe in culture with the stages of breast cancer.

Organization of mammary epithelial cells in vivo

In order to understand a breast afflicted with cancer, we must first understand its normal organization. The human breast is organized into a network of ducts and lobules. Lobules are comprised of a multiple units referred to as terminal ductal lobular units (TDLU). Each TDLU contains of a cluster of individual structures referred to as an acinus. An acinus is composed of a single layer of polarized luminal epithelium, surrounded by a layer of myoepithelial cells that are organized around a hollow lumen. Encompassing these structures are layers of basement membrane, extracellular matrix (ECM) proteins and connective tissue (Figure 1.2). The luminal epithelial cells, within an acinus, display apical-basal polarity which is defined by the asymmetric distribution of membrane proteins and junctional complexes (tight junctions, gap junctions, and adherens junctions) (Hilkens et al. 1984; Petersen and van Deurs 1986; Drubin and

Nelson 1996; Ronnov-Jessen et al. 1996). Each cell within the acinus has three main surfaces, the lateral surface that contacts neighboring cells, the basal surface that maintains contacts with myoepithelial cells and basement membrane, and an apical surface that faces a hollow lumen. The ECM that surrounds each acinus provides both physical support and critical signals that regulate epithelial cell shape, proliferation, organization, polarization and differentiation (Fata et al. 2004; Sternlicht 2006). Breast epithelial cells are tightly regulated *in vivo* and during pregnancy. For example, hormonal signals result in dramatic but highly organized changes to prepare for lactation, such as, cell proliferation, glandular growth, expansion of the acini and polarization of the luminal epithelial cells, (Battersby and Anderson 1988; Suzuki et al. 2000). The mechanisms that govern breast development and growth during pregnancy are the same mechanisms that could become disrupted during cancer progression, therefore it is important to study these mechanisms to gain a deeper understanding of both breast development and cancer progression.

Three dimensional MCF-10A cell culture system

In order to understand how loss of epithelial cell organization occurs during breast cancer it is important to use a system that recapitulates epithelial organization *in vivo* . We chose to use an *in vitro* three-dimensional model system that generates organized growth-arrested structures, which share several properties with acini structures *in vivo* (Debnath et al. 2003a). We use the non-transformed, human breast epithelial cell line MCF-10A. The MCF-10A cell line spontaneously arouse, without chemical or mutagenic alteration, from mortal cells isolated from a patient with fibrocystic breast

disease (Soule et al. 1990). MCF-10A cells share properties of normal breast epithelium such as dependency on exogenous growth factors for proliferation, lack of anchorage independent growth and lack of tumorigenicity in nude mice. Importantly, MCF-10A cells form organized acini-like structures with low rates of proliferation when plated on reconstituted basement membrane called Matrigel™.

Matrigel™ is generated from the basement membrane secretions of the Englebreth-Holm-Swarm (EHS) tumor and it is primarily composed of collagen IV, laminin and entactin (Kleinman et al. 1982; Kleinman et al. 1986). When plated on Matrigel, single MCF-10A cells undergo programmed morphogenesis and proliferate to form a ball of cells by day 6-8 (Figure 1.3.A and B). At this time, the cells located in the middle of the ball begin to undergo apoptosis or autophagic cell death (Reginato et al. 2005) and clear the center forming a lumen. By day 12-14, the acini are fully polarized growth-arrested structures. This means that the acinar structures, regardless of the presence of exogenous growth factors, have low rates of proliferation and remain the same size (Figure 1.3.B). The apical-basal axis of polarity of each epithelial cell in the acinar structure can be determined by observing the basal deposition of laminin V (Figure 1.3.C), the apical localization of the golgi apparatus and the basal-lateral localization of the cell-cell adherens junction marker, E-Cadherin.

While MCF-10A cells have normal epithelial cell characteristics, it should be noted that they do have minimal genomic rearrangements, including a loss of *p16/p14ARF* and an amplification in *c-myc* (Debnath et al. 2003a). These rearrangements are commonly seen in mammary epithelial cells that grow in culture and could potentially alter the phenotypes observed when these cells are manipulated with exogenous

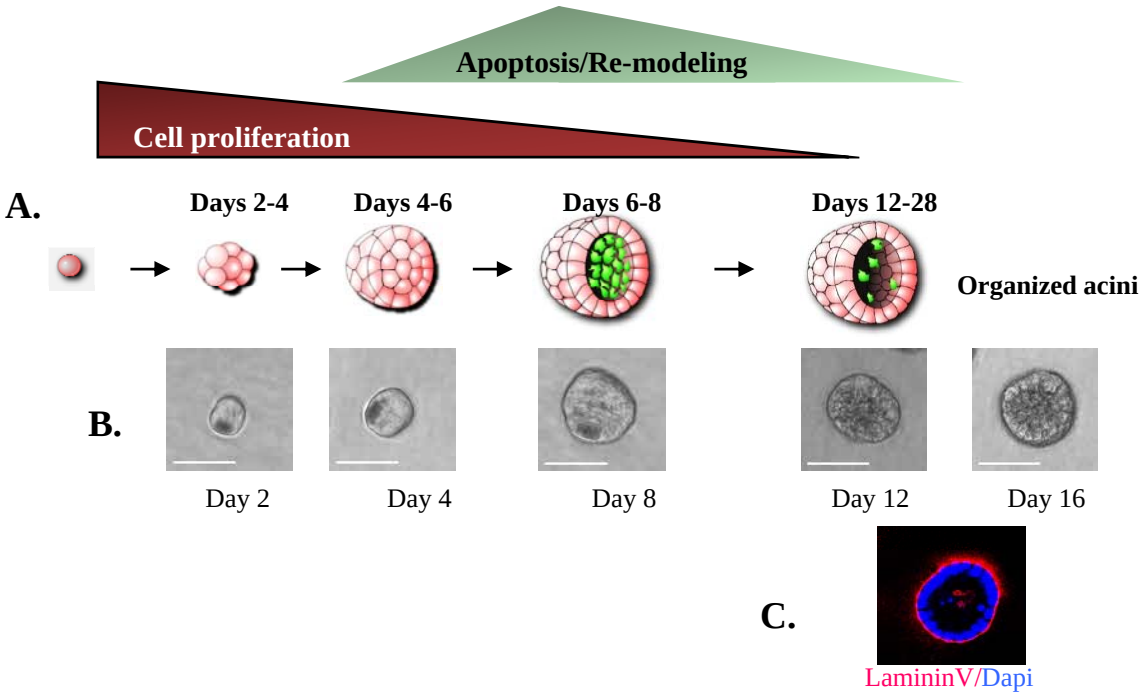

Figure 1.3. Three-dimensional MCF-10A cell model system

(A) Cartoon depicting the programmed morphogenesis of MCF-10A cells when plated on Matrigel. Single MCF-10A cells proliferate and form a sphere of cells (day 1-8). The center of the sphere undergoes apoptosis and remodeling (day 5-12) eventually forming an organized growth arrested acinar structure (day 12- 6). **(B)** Phase images of MCF-10A acinar structures on different days of morphogenesis. **(C)** Immunofluorescence staining of a polarized acinar structure as defined by a single layer of nuclei (DAPI, blue) and basal secretion of Laminin V (Red).

oncogenes (Debnath et al. 2003a). It should also be noted that while MCF-10A cells make polarized cell-cell contacts through the adherens junctions, they do not from close-knit tight junctions (Fogg et al. 2005). Although tight junction proteins such as zona occludens are localized properly to the apical-lateral boarder, the staining pattern is fragmented. Therefore, the cells do not have a continuous barrier between apical-lateral boarder that can prevent proteins and lipids from diffusing between the apical to basal surfaces (Fogg et al. 2005).

Despite these caveats, MCF-10A cells resemble normal breast epithelial cells and are more convenient to manipulate and culture than primary breast epithelial cells. Moreover, MCF-10A cells form acini like structures that have similar properties to structures derived from another normal breast epithelial cell line (Petersen et al. 1992). Therefore, MCF-10A cells grown on Matrigel is an attractive *in vitro* model system to use in the discovery of new mechanisms involved in the transformation of organized breast epithelial cells.

Oncogenes induce disruption of three-dimensional acini organization

Using the MCF-10A three-dimensional models system described above, it was discovered that activation of ligand inducible ErbB transforms polarized growth-arrested acinar structures. Stimulation of ErbB2 reinitiates proliferation, blocks apoptosis, and promotes acinar disorganization and the formation of multi-acinar structures with filled lumens (Muthuswamy et al. 2001). This study was important because it showed that ErbB2 not only stimulates proliferation but also disrupted the organization of the acinar structures that resemble DCIS lesions seen in vivo.

In addition to ErbB2, other oncogenes have been reported to disrupt epithelial cell morphogenesis and cell organization in this MCF-10A three-dimensional system. Inducible activation of the serine/threonine kinase AKT during acinar morphogenesis, not only increased proliferation, but also induced changes in individual cell size and shape, therefore distending and distorting the organization of the acini structures (Debnath et al. 2003b). Co-overexpression of colony stimulating factor receptor (CSF-1R) and the ligand, colony stimulating factor 1 (CSF-1), during acinar morphogenesis severely disrupted the acinar structures. These disrupted acinar structures had an increase in cell proliferation rates and a progressive loss of acinar organization and cell-cell adhesion (Wrobel et al. 2004). The same study also observed that co-overexpression of the receptor tyrosine kinase c-Met and its ligand hepatocyte growth factor (HGF) also disrupted the organization of the acini structures by stimulating tubule formation (Wrobel et al. 2004). Taken together these studies show that different oncogenic stimuli can disrupt epithelial cell organization. Interestingly, each of these stimuli elicited a proliferative response yet they each had a different morphological effect on acinar organization, i.e. promoting tubule formation or by distorting individual cell size and shape. The histopathological features of breast cancer lesions are diverse. For example, changes are seen in the cell shape (columnar cell metaplasia) and some lesions have cells that disorganize and multi-layer (atypical columnar cell metaplasia) (Shaaban et al. 2002). Because of the heterogeneity of breast tumors and the different histopathological features, it is important to study how oncogenes can affect not only proliferation but also how they can affect epithelial cell organization in order to comprehend their entire oncogenic effect.

Establishment of epithelial cell polarity

Cell polarity is the asymmetry of cell shape as defined by the asymmetric distribution of membranes and proteins. There are various types of cell polarity that range from asymmetric cell division in the drosophila neuroblast to the polarization of the axon extension from the cell body of a neuron (Figure 1.4.A and B). Single cell organisms such as budding yeast also have cell polarity and this is necessary to distribute proteins to daughter cells during the cell division (Figure 1.4.C). The major feature of organized epithelial cells is apical-basal polarity. This type of polarity establishes barriers that control the diffusion of ions and solutes between distinct compartments (Figure 1.4.D) (Nelson 2003).

Epithelial cell polarity is established through a series of polarity protein complex interactions that create and maintain the spatial asymmetric distribution of membranes. The exact biochemical interactions that are responsible for the establishment of apical-basal cell polarity are not fully understood. However, the overall hierarchy of these complex interactions has been determined in model systems such as *Drosophila* and in mammalian epithelial cells. The interactions between three protein complexes, the Par complex, the scribble complex and the crumbs complex, have been identified (Macara 2004b).

The Par complex is an apical junctional complex and is localized at the cell membrane where the apical and basolateral membrane meet (Figure 1.5.A). The Par complex contains the scaffolding molecules, partitioning defective protein 3 (Par3) and partitioning defective protein 6 (Par6), whose purposes are to bring different proteins together. Par6 can bind the atypical protein kinase C (aPKC) and the RhoGTPases,

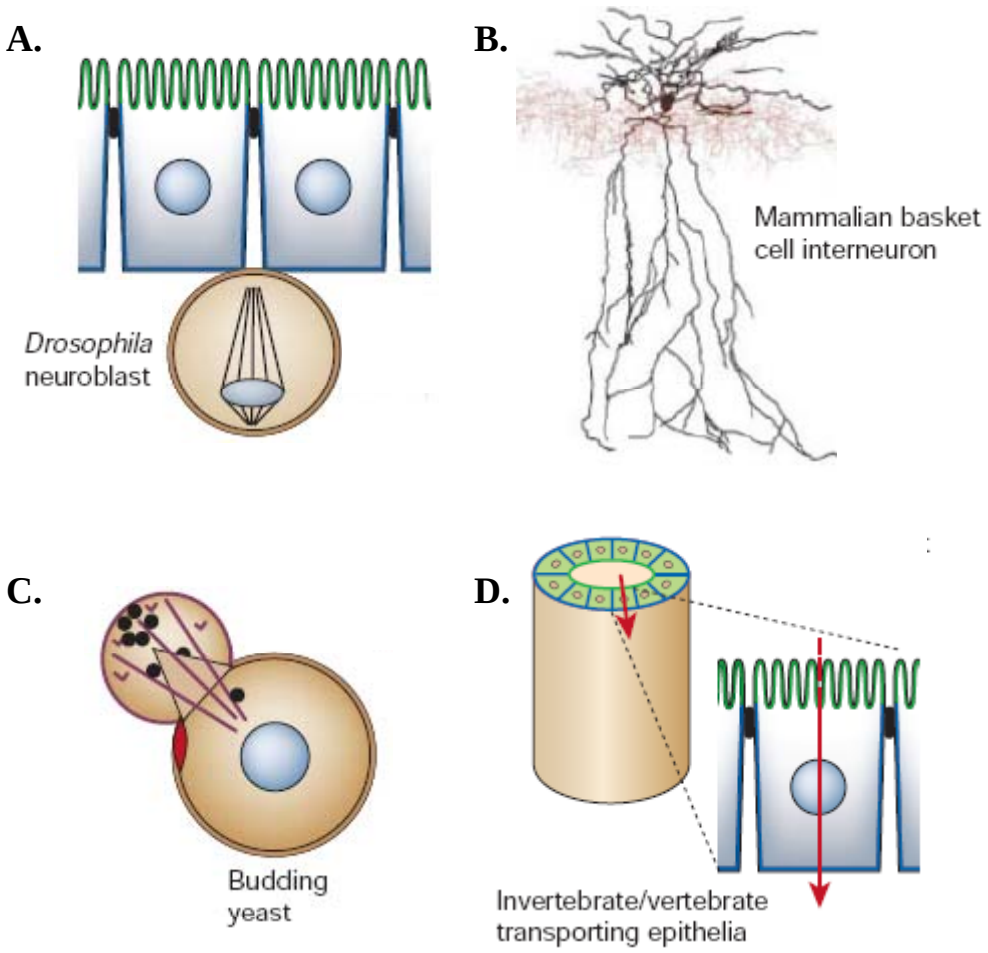

Figure 1.4. Different forms of cell polarity

(A) Asymmetric cell division of a drosophila neuroblast **(B)** Polarized basket cell neuron, showing the asymmetric distribution of the axons in red and the dendrites/soma in black **(C)** Asymmetric distribution of proteins during cell division of budding yeast **(D)** Epithelial cell apical-basal cell polarity. Ionic homeostasis is maintained by the asymmetrically localized tight junctions of polarized epithelial cells (Adapted from Nelson, 2003)

Cdc42/Rac (Joberty et al. 2000; Johansson et al. 2000; Lin et al. 2000; Qiu et al. 2000). Par6 contains a PDZ (PSD95/Dlg/ZO-1) domain, a PB1 (Phox/Bem1) and a semi-CRIB (Cdc42/Rac1 Interactive Binding) domain (Figure 1.6.A). The PB1 domain of Par6 forms a constitutive complex with PB1 domain of aPKC. Par6 binds Par3 through PDZ domain interactions and Par6 binds the activated GTP binding proteins Cdc42/Rac1 through both the semi-CRIB and PDZ domains (Joberty et al. 2000; Johansson et al. 2000; Lin et al. 2000; Qiu et al. 2000). Together these proteins interact to form an active Par complex that is recruited to the apical/lateral boarder in *Drosphila* or to the tight junctions in mammalian systems. This recruitment occurs on cue after the cell forms cell-cell contacts via adhesion molecules called Cadherins (Wang et al. 1990; Knust and Bossinger 2002; O'Brien et al. 2002).

The Par complex interacts with two other polarity complexes namely the baso-lateral Scribble complex that contains Scribble, Lethal giant larvae (Lgl), Discs large (Dlg) (Figure 1.5.B and 1.6.B) and the apical Crumbs complex that contains Crumbs, protein associated with Lin-7 (Pals), Pals1-associated tight junction (PATJ) protein (Figure 1.5.C and 1.6.C) (Ohno 2001; Lemmers et al. 2002; Humbert et al. 2003). The recruitment of the Par complex to the tight junction initiates the formation of the apical membrane. The spread of the apical membrane is inhibited by the activity of the basolaterally localized Scribble complex. Par6/aPKC can phosphorlyate Lgl and this phosphorylation restricts the localization of the Par complex to the apical junctional boarder and restricts the Scribble/Lgl complex to the basolateral membrane (Betschinger et al. 2003; Hurd et al. 2003; Plant et al. 2003; Yamanaka et al. 2003). In addition, the apical Crumbs complex is recruited by PALS1 binding to Par6-Par complex and together

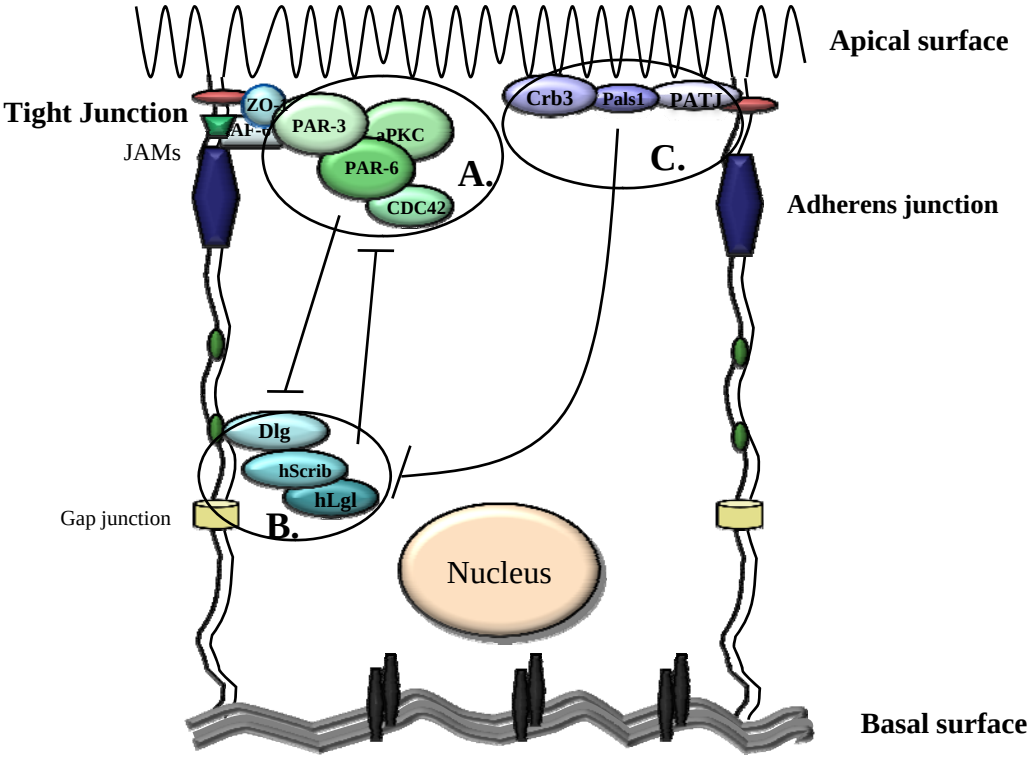

Figure 1.5. Establishment of apical-basal cell polarity

Typical organization of an polarized mammalian epithelial cell with asymmetric distribution of membranes and proteins. Diagram shows the interaction of the different polarity complexes. The Par complex **(A)** is recruited to the tight junctions located at the apical-lateral boarder. The Par complex and the Scribble complex **(B)** restricts each others localization to the apical and basolateral membranes respectively. The Par complex **(A)** also recruits the apical Crumbs complex **(C)** and together they restrict the basal localization of the Scribble **(B)** complex through phosphorylation of Lgl. This cross-talk regulates the establishment of apical-basal polarity.

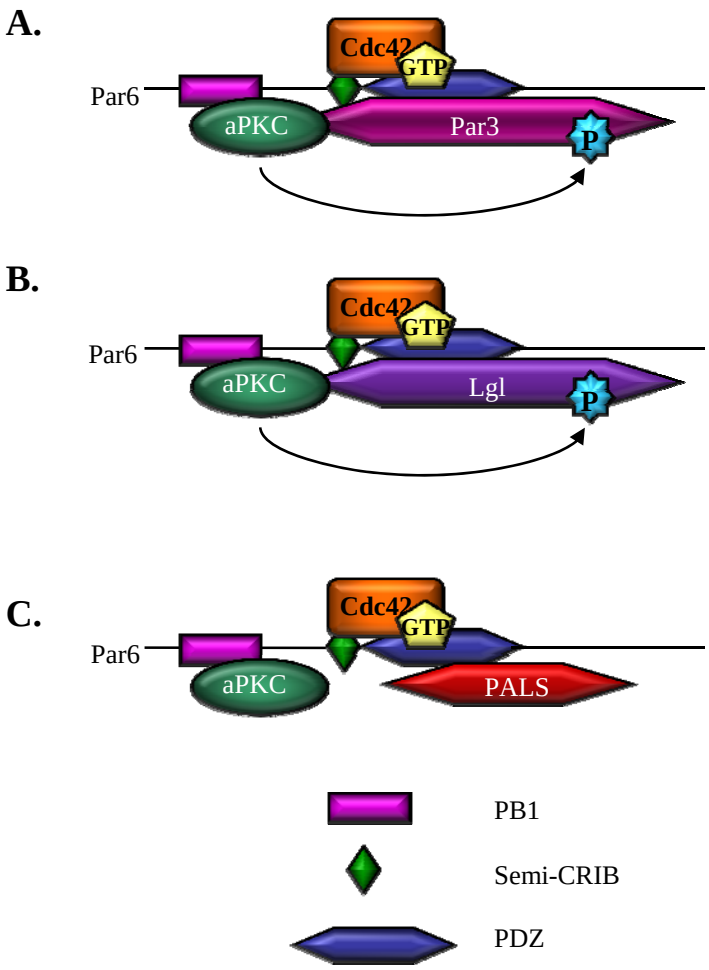

Figure 1.6. The known Par6 interactions

(A-C) Par6 interacts with Cdc42 through both the semi-CRIB and PDZ domains and interacts with Par3, Lgl and PALS1 via PDZ domain. Par6 forms a constitutive complex with aPKC through PB1 domain interactions and **(A)** aPKC can phosphorlate Par3. **(C)** Par6/aPKC can also phosphorylate Lgl. **(C)** Par6 binds PALS1 in a Cdc42-GTP dependent manner. (Adapted from Macara, 2004)

they further antagonize the activity of the Scribble complex by blocking the spread of the basolateral membrane (Betschinger et al. 2003; Hurd et al. 2003; Plant et al. 2003; Wang et al. 2004). This concerted effort maintains the apical membrane identity (Tanentzapf and Tepass 2003) and together this series of protein-protein interactions establish the epithelial apical-basal cell polarity.

Regulators of the cytoskeleton

The organization of the cytoskeleton plays a major role in epithelial cell polarity. During cell polarization, the actin cytoskeleton reorganizes in response to cell-cell contacts from the adherens interactions. The cytoskeleton attaches at the cell cortex of each membrane, for example, filamentous actin (F-actin) binds to catenin-cadherin proteins complexes at the adherens junctions (Fukata and Kaibuchi 2001). A family of proteins called the RhoGTPase (Rho, Rac and Cdc42) regulate this binding of F-actin to the adherens junction (Fukata and Kaibuchi 2001; Nelson 2003). Other studies have connected RhoGTP to other biological functions including cell cycle control, gene expression and cell migration (Sahai and Marshall 2002).

Rho family of GTPase, are known regulators of the cytoskeleton. For example activation of RhoA regulates the formation of actomyosin bundles (stress fibers) and focal adhesion complexes. Rac regulates the formation of lamellipodia which are membrane protrusions composed of actin and Cdc42 promotes the formation of filopodia or membrane ruffling (Hall 2005). These small GTP binding proteins that cycle between active GTP bound and inactive GDP bound states. These proteins are regulated by guanine exchange factors (GEFs) that promote the exchange of GDP for GTP and

activation of the proteins (Figure 1.7.A). Their activation is turned off by GTPase activating proteins (GAPs) which enhance the GTPase activity promoting hydrolysis of GTP to GDP (Figure 1.7.B). In addition to these two regulators of GTPase, Rho proteins are affected by Guanine dissociation inhibitors (GDIs), which interact with RhoGDP and prevent the exchange of GDP to GTP (Figure 1.7.C). These regulators control the specific spatial and temporal regulation of the RhoGTPase proteins ensuring proper activation (Sahai and Marshall 2002); (Fukata and Kaibuchi 2001).

Alterations in the polarity proteins disrupt epithelial cell polarity

In mammalian epithelial cells the border between apical and lateral membrane is defined by the presence of tight junctions. Tight junctions are protein complexes between cells that act as a barrier, regulating ionic homeostasis between differ biological compartments (Tsukita et al. 1999). Studies performed in established models systems show that overexpression or loss of polarity proteins disrupts tight junctions and thus apical-basal polarity. Overexpression of Par6 in mammalian epithelial cells delays the assembly of the Par complex and tight junction formation (Ohno 2001; Gao et al. 2002a). Tight junction assembly is inhibited by activation of Cdc42 and inactivation of aPKC (Joberty et al. 2000). In vertebrate development overexpression of aPKC or loss of function, disrupts cell polarity and tight junction formation (Chalmers et al. 2005). Loss of Pals1 and PATJ delays formation of structural and the barrier function of tight junctions, and prevents lumen formation in a three-dimensional model system of MDCK cells grown as cysts (Straight et al. 2004). Loss of the polarity protein and serine

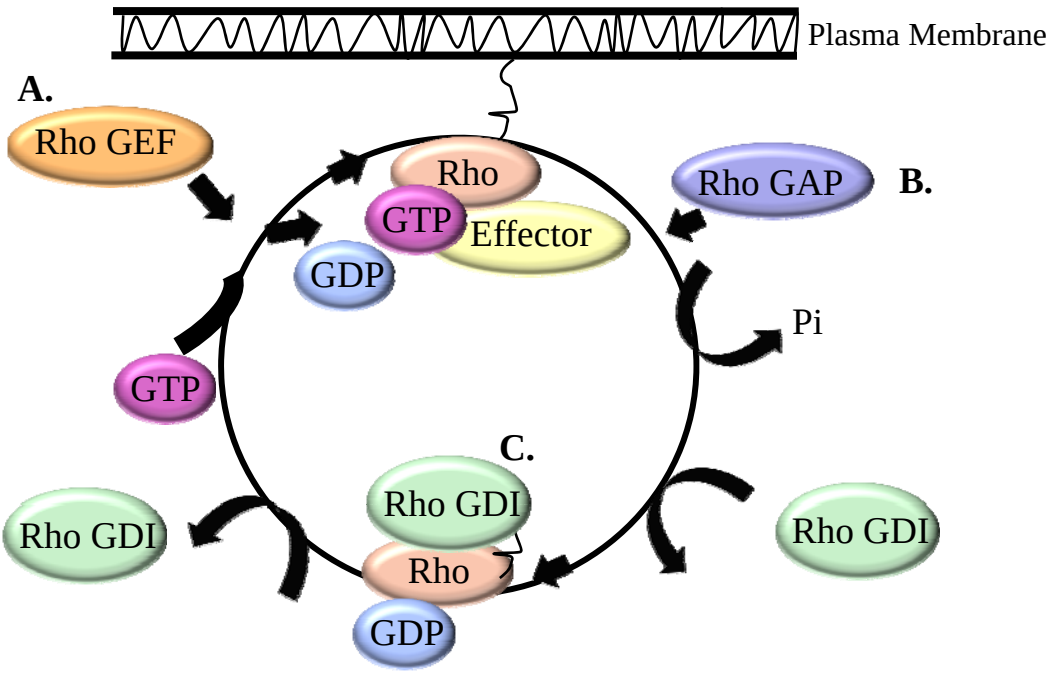

Figure 1.7 Regulation of RhoGTPase

(A) RhoGTPase is activated by guanine exchange factors that replace GDP with GTP. **(B)** GTPase activating proteins **(**GAPs) enhance the intrinsic activity of the GTPase promoting the formation of RhoGDP. **(C)** Rho proteins remain inactive by the binding of guanine dissociation factors (GDIs) (Adapted from Fukata, 2002)

threonine kinase (Par4) LKB1 also disrupts polarity formation in epithelial cells (Forcet et al. 2005). Therefore, interference with many of the polarity proteins can affect the development of epithelial cell polarity and disrupt the barrier function of tight junctions in epithelial cells.

Cell polarity is also affected by the regulation of the actin cytoskeleton and studies of the RhoGTPase have shown that interference with these proteins also disrupted cell polarity. The *C. elegans* homolog of RhoA (RHO-1) is essential for asymmetric distribution of Cdc42 during polarity establishment of embryos (Schonegg and Hyman 2006). In mammalian systems, activation of Raf reduced RhoA activity by promoting expression of the RhoA antagonist, RND3/RhoE. Expression of RND3 promoted loss of cell polarity and induced multilayers in polarized MDCK cells (Hansen et al. 2000). Another study showed that either activation or inhibition of both RhoA or Rac1 activity disrupted tight junctions and barrier function (Jou and Nelson 1998; Jou et al. 1998). These studies show the importance of RhoGTPase in different cellular contexts and link Rho to altered cell organization. Collectively, the studies outlined above exemplify the fact that deregulation of polarity and cytoarchitectural regulators disrupt normal cell organization and polarity. Since we know that cell organization is disrupted in cancer and that cell organization is affected by the expression of oncogenes, then perhaps these organizational regulators are being targeted and altered in cancer.

Polarity proteins and oncogenesis

Pioneering studies in *Drosophila melanogaster* have linked cell polarity proteins with growth control. Loss of polarity regulators have been shown to increase cell

proliferation and also promote the disruption of cell polarity in the epithelial cells (Bilder et al. 2000). Loss of polarity regulators can also cooperate with Ras to promote invasion and metastasis in *Drosophila* (Brumby and Richardson 2003; Pagliarini and Xu 2003). These studies are one of the first to relate activation of an oncogene to loss of a cell polarity regulator (Brumby and Richardson 2003; Pagliarini and Xu 2003) and show that interference with the polarity machinery can promote neoplastic transformation. Whether the same mechanisms occur to promote carcinogenesis in humans has yet to be determined.

Evidence suggests that alterations in the polarity machinery may also directly contribute to oncogenesis in human cancers. The human homologue of the *Drosophila* tumor suppressors lgl, dlg and scribble, have been shown to be targeted by viral oncoproteins. Various oncogenic viral proteins such as human T-cell leukemia virus (HTLV-1) tax and adenoviral Ad9 E4 ORF1 can target Dlg1. This interaction is thought to disrupt the binding of Dlg1 to the tumor suppressor adenomatous polyposis coli (APC) which leads to increased proliferation (Kiyono et al. 1997; Lee et al. 1997; Suzuki et al. 1999). The human papillomavirus (HPV) protein E6 can target Dlg1 and scribble for degradation and infection with HPV. Infection with HPV has been associated with an increased risk of cervical cancer (Kiyono et al. 1997; Lee et al. 1997; Nakagawa and Huibregtse 2000; Pim et al. 2000). More recent reports show the loss of scribble, Dlg, and Lgl expression strongly correlates with progression to malignancy (Cavatorta et al. 2004; Schimanski et al. 2005; Gardiol et al. 2006; Kuphal et al. 2006). Mutations in the polarity protein LKB1 (Par4) have also been correlated with Peutz-Jeghers cancer syndrome which is characterized by benign tumors of the gastrointestinal tract (Jenne et

al. 1998). More recently, it was shown that Par6β is located within a 1.5 megabase amplicon in a subset of estrogen receptor positive human breast tumors and this correlated with overexpression of Par6β mRNA. This suggests that Par6β overexpression could be a tumor promoting factor in breast cancer (Bergamaschi et al. 2006; Chin et al. 2006; Ginestier et al. 2006; Hicks et al. 2006). Another member of the Par complex, aPKC is overexpressed in non-small cell lung carcinoma (NSCL) and ovarian carcinoma. Increased expression of aPKC promotes aberrant proliferation and loss of cell polarity in ovarian epithelia (Eder et al. 2005; Regala et al. 2005a; Regala et al. 2005b). The RhoGTPase family of cytoarchitectural regulators, RhoA, Rac1 and Cdc42 are over-expressed in human breast, colon, lung and pancreatic cancers (Fritz et al. 1999). Taken together the studies above suggest that alterations to polarity regulator proteins can contribute to carcinoma because these proteins are altered in human cancers. While the precise mechanisms by which these alterations promote cancer are not understood, these studies highlight the need to study polarity proteins in carcinoma.

Study aims

The majority of human breast tumors lack defined tissue organization, suggesting that the regulators of tissue organization and cell polarity are no longer able to function properly. Therefore, it is possible that the normal function of these proteins is disrupted upon cancer initiation as well as throughout the progression to malignant disease. Activation of certain oncogenes in three-dimensional cell culture systems not only promotes hyperproliferation but also disrupts acinar organization. Interestingly, viral oncoproteins target polarity regulators, while alterations in the polarity machinery are

correlated with cancer progression. How the polarity proteins can be altered during cancer progression is unclear. The aim of this thesis is to determine if overexpression or loss of function of the polarity and cytoarchitectural regulators can contribute to cell transformation in the MCF-10A three-dimensional models system.

To address this question, I have broken down my thesis into 4 main chapters. In the second and third chapters, I sought to determine the effect of Par6 overexpression in organized human breast epithelial cells and how Par6 overexpression relates to breast cancer. Here I report a novel function for the polarity protein Par6 in promoting proliferation, through activation of the MAPK pathway and I determined that Par6 is overexpressed in human breast cancer. In the fourth chapter, we wanted to determine if oncogenic ErbB2 needed to disrupt epithelial cell polarity in order to transform organized breast epithelial cells. We found that oncogenic ErbB2 uses the Par polarity complex to disrupt cell polarity without affecting cell proliferation. Thus we identified a mechanism by which oncogenes can target the polarity machinery to promote transformation. Finally, in the fifth chapter, I sought to determine if inhibition of the cytoarchitectural regulators RhoA, Rac and Cd42 interfered or cooperated with ErbB2 induced transformation. I found that oncogenic ErbB2 and the downregulation of RhoA using a dominant negative cooperated to promote invasion of ErbB2 transformed structures. Together the data presented in this thesis show that the regulators of epithelial cell organization can be targeted in the progression to breast cancer.

Chapter 2: The Polarity protein Par6 promotes proliferation of mammary epithelial cells

Introduction:

Par6 is a scaffolding molecule that was originally identified as a regulator of asymmetric cell division during embryonic development of *C. elegans* (Kemphues et al. 1988). Par6 is highly conserved throughout evolution and is involved in different biological functions. In mammalian epithelia, Par6 regulates establishment of apical-basal polarity (Chapter 1)(Yamanaka et al. 2001; Gao et al. 2002b) and cell death (Kim et al. 2007). It also regulates directional migration of astrocytes and keratinocytes (Etienne-Manneville and Hall 2001; Kodama et al. 2003), and axon specification in neurons (Shi et al. 2003; Solecki et al. 2004). The precise mechanism by which Par6 regulates these processes remains to be fully understood.

Par6 is known to be involved in multiple protein-protein interactions (Chapter 1, Figure 1.4 and 1.5)(Brajenovic et al. 2004; Macara 2004b). The most prominent is with the members of the Par polarity complex, which consists of Par3, atypical protein kinase (aPKC) and Cdc42/Rac (Joberty et al. 2000; Johansson et al. 2000; Lin et al. 2000; Qiu et al. 2000). Par6 also interacts with members of the other polarity complexes, such as crumbs, Lgl and PALS1. (Betschinger et al. 2003; Hurd et al. 2003; Plant et al. 2003; Wang et al. 2004).

The interactions of Par6 with the Par complex are required for Par6-mediated regulation of biological processes. For instance, Par6 regulates aPKC induced

phosphorylation of Lgl (Plant et al. 2003), Par1 (Suzuki et al. 2004) and Numb proteins (Smith et al. 2007) during establishment of apical-basal polarity in epithelial cells. Likewise, Par6-associated aPKC regulates glycogen synthase kinase 3β (GSK3β) activity to induce polarized migration of astrocytes (Etienne-Manneville and Hall 2003a) and to promote cell death during 3D epithelial morphogenesis (Kim et al. 2007). Thus, the Par6 complex can serve as a signaling node that regulates diverse biological processes by inducing activation of different effector pathways.

Deregulation of Par6 may cause cell transformation. Mammalian Par6 was originally identified as a protein that interacts with Tax, an oncogene of HTLV-1 (human T-cell leukemia virus type-1) (Rousset et al. 1998). Subsequently, Par6 cooperates with activated Rac1/Cdc42 to transform fibroblasts (Qiu et al. 2000). Par6 is required for TGFβ induced epithelial to mesenchymal transition (EMT) by regulating TGFβ-induced degradation of RhoA (Ozdamar et al. 2005). We have demonstrated a role for Par6 during ErbB2 induced transformation of mammary epithelial acini. Activation of ErbB2 recruited Par6/aPKC and this interaction was necessary for ErbB2 induced disruption of cell polarity and three-dimensional epithelial organization (Aranda et al. 2006)(Chapter 4). Together the above studies suggest that Par6 can function as a scaffold for oncogenic signaling. Interestingly, among the three isoforms of Par6, (gene name *Pard6*) (*Pard6a, Pard6b*, and *Pard6c*), the *Pard6b* isoform is located in a region of the genome that is frequently amplified in breast cancer and this correlates with increased *Pard6b* mRNA expression (Bergamaschi et al. 2006; Chin et al. 2006; Ginestier et al. 2006; Hicks et al. 2006). The fact that Par6 is genomically amplified suggests that an increase in Par6 expression is beneficial for breast epithelial cells. Perhaps increased expression of Par6

by itself could play a role transformation, in addition to its known role in oncogenic ErbB2 and activated Rac transformation.

In this chapter, I investigated the effects of Par6 overexpression in cultured cells. I demonstrate that expression of Par6 induces epidermal growth factor (EGF) independent proliferation of normal mammary epithelial cells by inducing activation of mitogen activated protein kinase (MAPK) signaling. This function of Par6 is dependent on Par6's ability to interact with aPKC/Cdc42, demonstrating that the Par complex regulates cell proliferation pathways. Therefore, overexpression of Par6 can promote aberrant proliferation which is one characteristic of transformed cells.

Results:

Overexpression of Par6 promotes EGF independent proliferation:

To determine the effect of overexpressing Par6, we expressed two different isoforms of Par6, *Pard6a* (protein referred to as Par6α) and *Pard6b* (protein referred to as Par6β) in the EGF-dependent, non-transformed human breast epithelial cell line MCF-10A (Figure 2.1.A and B). We noticed no morphological changes in Par6 expressing cells (Figure 2.2.A and C). However, when EGF was removed from the media, overexpression of Par6 maintained MCF-10A cells in cell cycle (Figure 2.2.A and C). Par6 expressing cells had a three-fold increase in the number of cells in S-phase compared to control cells (Figure 2.2.B and D).

To rule out nonspecific effects of viral infections, such as viral integration induced disruption of a cell cycle regulator gene or a tumor suppressor, we generated multiple pooled populations of Par6 overexpressing cells. It was also important to determine if the location of the epitope tag affected the ability of Par6 to bind its effectors and if the location of the epitope tag affected Par6 induced proliferation. Therefore, we generated multiple independent stable cell line populations with variable levels of both Par6α as N-terminal (Flag-Par6α) (Appendix A.2.A.) and C-terminal (Par6-Flagα) epitope fusion in MCF-10A cells (Data not shown and Figure 2.3). The specific construct that was used in each experiment is indicated in each figure legend. In all cell lines tested, expression of Par6, induced proliferation of MCF-10A cells in the absence of exogenous growth factors. Moreover, we found that Par6 induced proliferation was not limited to MCF-10A cells. We overexpressed Par6 in an EGF-dependent pluripotent

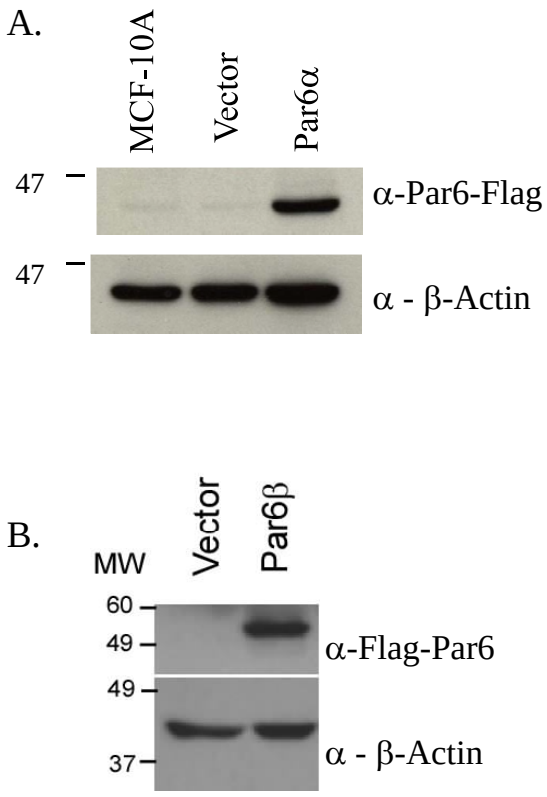

Figure 2.1. Expression of Par6α and β in MCF-10A cells.

Immunoblots of extracts from MCF-10A cells stably expressing **(A)** Par6α-Flag or **(B)** Flag-Par6β. The membranes were probed with an antibody against the epitope flag to detect Par6 expression and an antibody against β-actin as a protein loading control.

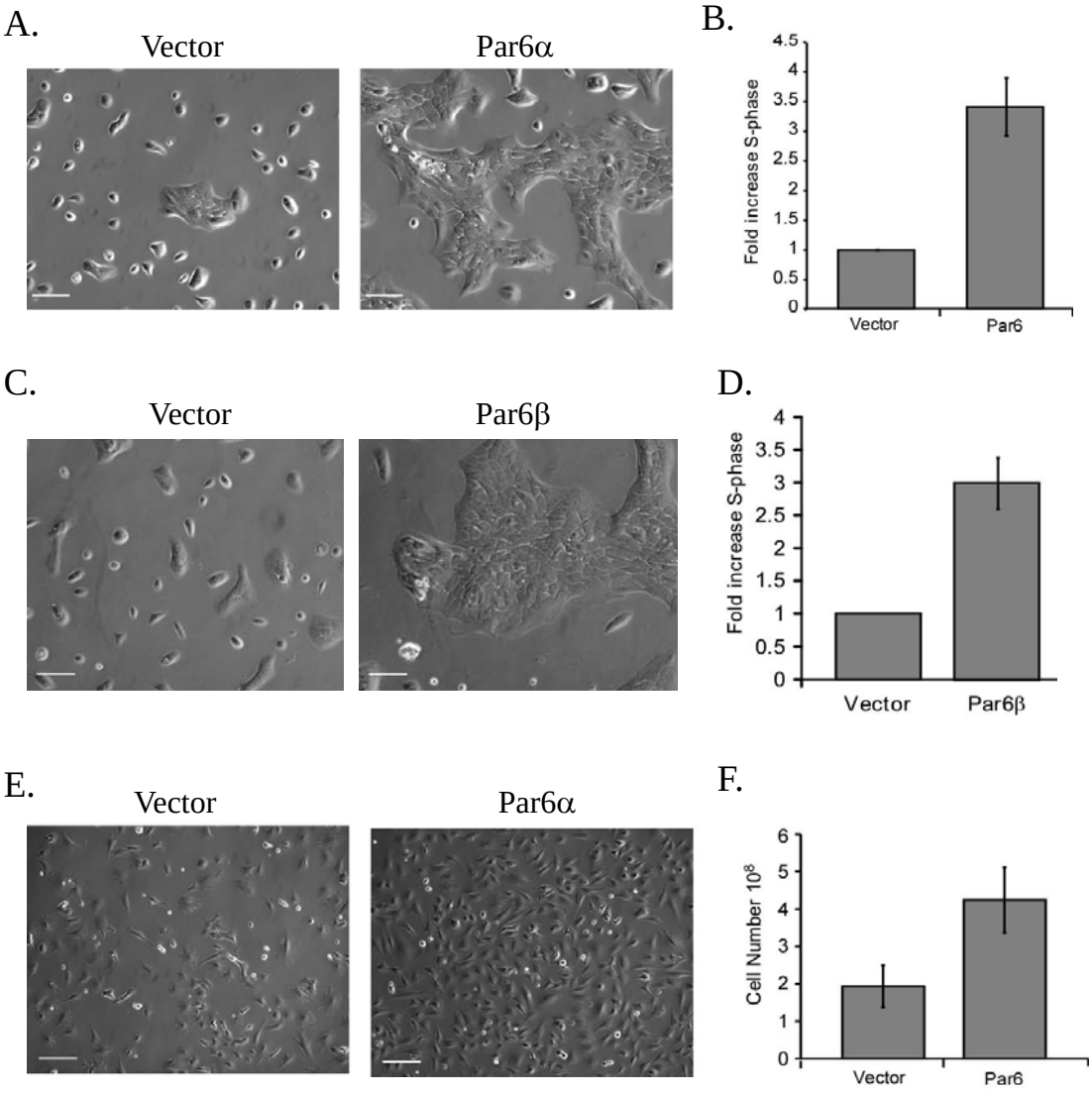

Figure 2.2. Par6 promotes proliferation of mammary epithelial cells.

(A,C) Phase contrast images showing growth inhibited vector control MCF-10A cells compared to growing Flag-Par6α and Flag-Par6β. overexpresssing cells in EGF-free media. The scale bar represents 100 μm. **(B,D)** Cell cycle analysis of cells grown for 3 days in EGF free media. Data are fold increase in S-phase of Par6 cells compared to control cells and are means +/- S.D. of three independent experiments. **(E)** Phase images showing growth inhibited vector control of Comma1D cells compared to growing Par6α-Flag overexpresssing in EGF free media. The scale bar represents 100 μm. **(F)** Proliferation analyses of cells grown for three days in EGF free media by estimating the cell number with a hemocytometer. Data are means +/- S.D. from three independent experiments.

mouse mammary epithelial cells line Comma 1Dβgeo (Danielson et al. 1984) (herein referred to as Comma-1D). Expression of Par6 induced EGF independent proliferation as monitored by changes in cell number (Figure 2.2 E and F).

Taken together the experiments above demonstrate that expression of Par6, regardless of isoform, location of epitope tag or level of protein expression, induced growth factor independent proliferation. This pattern of Par6 induced proliferation in two cell lines demonstrates this phenomenon may be a general aspect of mammary epithelial cells. Thus, my results identify an unexpected role for the polarity gene Par6, to promote cell proliferation.

Par6 induced cell proliferation requires interaction with aPKC and Cdc42

To gain insight into the mechanisms by which Par6 induces cell proliferation, we carried out structure-function analysis of Par6. Previous studies had mapped the Par6 residues involved in the binding to its known adaptor/effector partners, mostly members of the Par complex and other polarity regulator complexes (Lin et al. 2000; Noda et al. 2003; Wilson et al. 2003; Yamanaka et al. 2003; Wang et al. 2004). This information was used to generate Par6 mutants that are defective in binding to members of the Par6 complex such as Par3, Cdc42, Lgl and aPKC. The following genetic alterations were made by site directed mutagenesis: a Lysine to Alanine mutation in the PB1 (Phox/Bem1p) domain ($Par6^{K19A}$) to abolish binding to aPKC, a deletion of Proline 136 in the semi-CRIB binding domain ($Par6^{\Delta Pro136}$) to disrupt binding to Cdc42, and a Methione to Tryptophan substitution in the PDZ domain ($Par6^{M235W}$) to disrupt binding to

Lgl (Figure 2.3.D). Each mutant was expressed in MCF-10A cells and confirmed by co-immunoprecipitation analysis (Figure 2.3.A, B, C). As expected, $Par6^{K19A}$ failed to associate with aPKC and retained its ability to associate with Cdc42 (Figure 2.3.B). In addition, we found that this mutant also lost its ability to interact with Par3 and Lgl (Figure 2.3.A and C). The $Par6^{\Delta Pro136}$ mutant was defective in its ability to bind Cdc42 (Figure 2.3.B), but associated with Par3, aPKC and Lgl (Figure 2.3.A and C). The $Par6^{M235W}$ mutant did not bind Cdc42 or Lgl and was defective in binding Par3 but still associated with aPKC (Figure 2.35.A, B, and C).

The Par6 mutants were analyzed for EGF-independent cell proliferation. None of the mutants induced EGF-independent cell proliferation (Figure 2.3.E). The inability of $Par6^{K19A}$ to promote proliferation demonstrated that aPKC binding was necessary and that Cdc42 binding is not sufficient. Conversely, the $Par6^{\Delta Pro136}$ mutant demonstrated that aPKC, Par3 and Lgl were not sufficient and that Cdc42 was necessary to promote proliferation. The inability of $Par6^{M235W}$to promote proliferation showed that both Cdc42 and Lgl binding was necessary and aPKC and Par3 binding was not sufficient to induce EGF-independent proliferation. To summarize the mutational analysis we determined that Par6 requires both aPKC and Cdc42 in order to promote proliferation. Because the binding of Cdc42 to Par6 induces aPKC kinase activity (Etienne-Manneville and Hall 2001; Yamanaka et al. 2001) it is likely that Par6-aPKC-Cdc42 forms a core complex to promote EGF-independent cell proliferation of mammary epithelial cells. It is also possible that the other binding partners of Par6 such as, PALS1 or Crumbs could be playing a role in Par6 induced proliferation. However, it is unlikely that it is PALS1, because PALS1 binds at the same location in the PDZ domain as Lgl and this binding

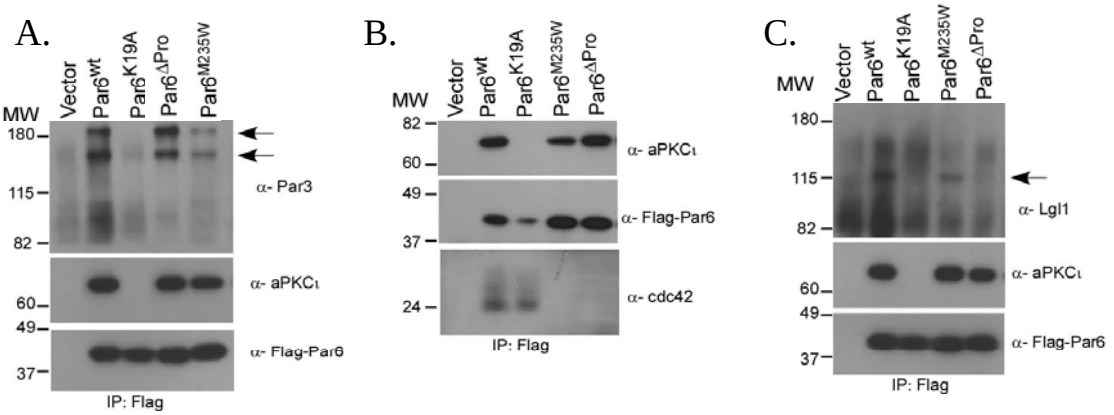

D.

Construct	Construct	Binds To:	Does Not Bind To:
F-Par6^{Wt}		aPKC, Par3, Lgl, Cdc42	
F- Par6 ^{K19A}		Cdc42	aPKC, Par3, Lgl
F-Par6 $^{\Delta Pro136}$		aPKC, Par3, Lgl	Cdc42
F-Par6 ^{M235W}		aPKC, [Par3]	Lgl, Cdc42, [Par3]

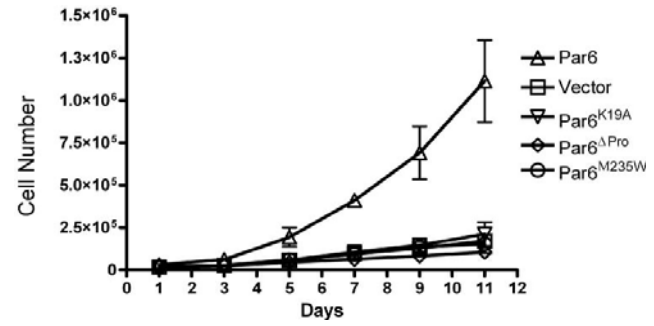

Figure 2.3 . Par6 induced cell proliferation requires interaction with aPKC and Cdc42.

(A,B,C) Extracts from MCF-10A cells expressing vector control, Flag-Par6α and mutants of Flag-Par6α were immunopreciptiated with anti-flag antibodies and analyzed for Par6 complex binding by immunoblotting with antibodies against aPKCι, Flag, **(A)** Par3, **(B)** Cdc42 and **(C)** Lgl. **(D)** Table summary of the Par6 mutants and their binding partners as determined by IP in **(A-C)**. **(E)** Growth curve of vector control cells compared to wild-type Par6 and mutant Par6 cells over a period of 11 days in EGF free media. Data are means +/- S.D. of estimated cell numbers from three independent experiments.

should be also disrupted by Par6^{M235W} mutant.

Par6 induced cell proliferation requires an increase in the aPKC concentration

Among the members of the Par6 complex, PKCι is overexpressed in ovarian and lung cancers (Eder et al. 2005; Regala et al. 2005b). In addition, we found that expression of two members of the atypical PKC family, PKCι and PKCζ was increased by ectopic expression of Par6 (Figure 2.4.A). The increased level of expression was specific to aPKC, because the levels of Par3 and Cdc42, the other members of Par complex, did not change in Par6 overexpressing cells (Figure 2.4.B and C). This is consistent with a previous report that overexpression of Par6 in myoblasts increased endogenous aPKC (Weyrich et al. 2004).

Together these observations suggest that the levels of Par6-aPKC may be co-regulated in cells and that Par6 induced cell proliferation may require regulation of aPKC levels. To directly determine if increased levels of aPKC plays a role during Par6 induced cell proliferation, we knocked down expression of aPKC in both control and Par6 expressing cell lines using two independent short-hairpin RNAs that target both PKCι and PKCζ (Figure 2.4.A). Decreased expression of aPKC significantly impaired the ability of Par6 overexpressing cells to proliferate in the absence of EGF (Figure 2.4.D). The data presented here show that Par6 overexpression has an effect in regulating cellular proliferation pathways probably mediated by its regulation of the activity of other Par complex members such as aPKC and Cdc42.

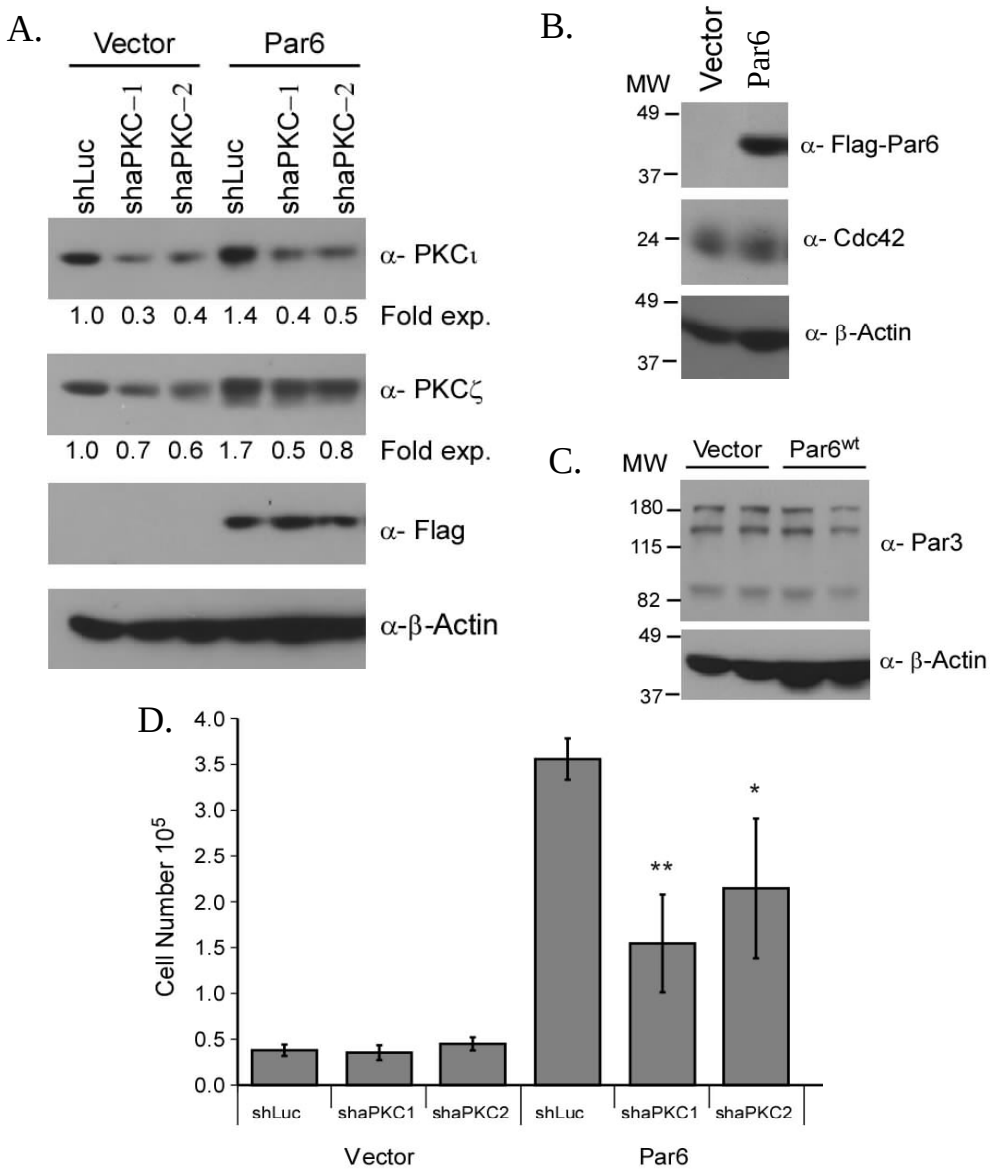

Figure 2.4 Par6 induced cell proliferation requires aPKC.

(A) MCF-10A cells expressing vector control and Flag-Par6α were infected with short-hairpins targeting PKC or Luciferase (Luc). Extracts from these cells were generated and analyzed for PKC silencing by immunoblotted with indicated antibodies. The numbers below the bands refer to fold change in PKCι and PKCζ protein expression normalized to β-actin as determined by densometric analysis. **(B-C)** Cell extracts from vector control and Flag-Par6α were analyzed for **(B)** Cdc42 and **(C)** Par3 expression by immunoblotting. **(D)** The indicated cells were grown in EGF free media for seven days and cell number was determined by counting. Data are means +/- S.D. of quantitated cell numbers from three independent experiments. Student t-test were performed showing statistical significance between Par6α-shLuc and Par6α–shaPKC1 (P=0.004) or Par6α–shaPKC2 (P=0.04).

Par6 overexpression promotes proliferation cell autonomously

In order to understand how Par6 expression promoted cell proliferation, we tested if Par6 induced autocrine production of growth factors or caused juxtacrine activation of cell-cell signaling. We first tested whether Par6 overexpressing cells secreted a growth factor. Conditioned media from Par6 expressing cells did not stimulate activation of phoshphotyrosine, MAPK (Figure 2.5 A and B) (see next section for information on MAPK) or promote proliferation of vector control MCF-10A cells (data not shown). In addition, co-culturing experiments demonstrated that Par6 expressing cells did not induce EGF-independent proliferation of control cells when separated by a porous membrane (Figure 2.5.C). To investigate if Par6 promoted juxtacrine signaling, cells were labeled with a cell permeable fluorescent dye (DiI) to monitor the proliferation of the control cells when co-cultured with unlabelled Par6 overexpressing cells in EGF free media. While the Par6 cells continued to proliferate (Figure 2.6, arrows), the control cells failed to proliferate in the absence of EGF even when intimately co-cultured with Par6 expressing cells (Figure 2.6, arrowheads). This demonstrated that Par6 does not promote proliferation by enhancing juxtacrine signaling. Together these observations suggested that Par6 promotes proliferation in a cell autonomous manner.

Par6 overexpression activates MAPK signaling

We investigated the possible cell autonomous pathways by which Par6 promotes proliferation. Activation of the EGFR pathway is an attractive possibility because our data showed that Par6 induces EGF independent proliferation of MCF-10A cells (Figure 2.2). However, we did not observe activation of EGFR without ligand stimulation in

Figure 2.5. Par6 overexpressing cells do not promote proliferation of vector control cells.

(A) Uninfected MCF-10A cells were stimulated with growth media that had been conditioned for 4 days with control, vector control or Par6α-Flag cells or stimulated with fresh growth media for 15 minutes. Cell extracts were analyzed for phosphorylated tyrosine and activation of ERK1/2 by immunoblotting with indicated phospho-specific antibodies. **(B)** MCF-10A cell extracts from **(A)** were immunoprecipitated with a antibody against phospho-tyrosine (P-tyr) and then immunoblotted with an anti-P-tyr antibody. **(C)** Vector and control cells were co-cultured in different combinations on or below a 8.0μm filter for 3 days in EGF free media. Cells were collected from the indicated position on the filter (top or bottom). The cells that were harvested for cell-cycle analysis from each condition are indicated in red. Data are S-phase of cells co-cultured with the indicated cell line are means +/- S.D. of three biological repeats.

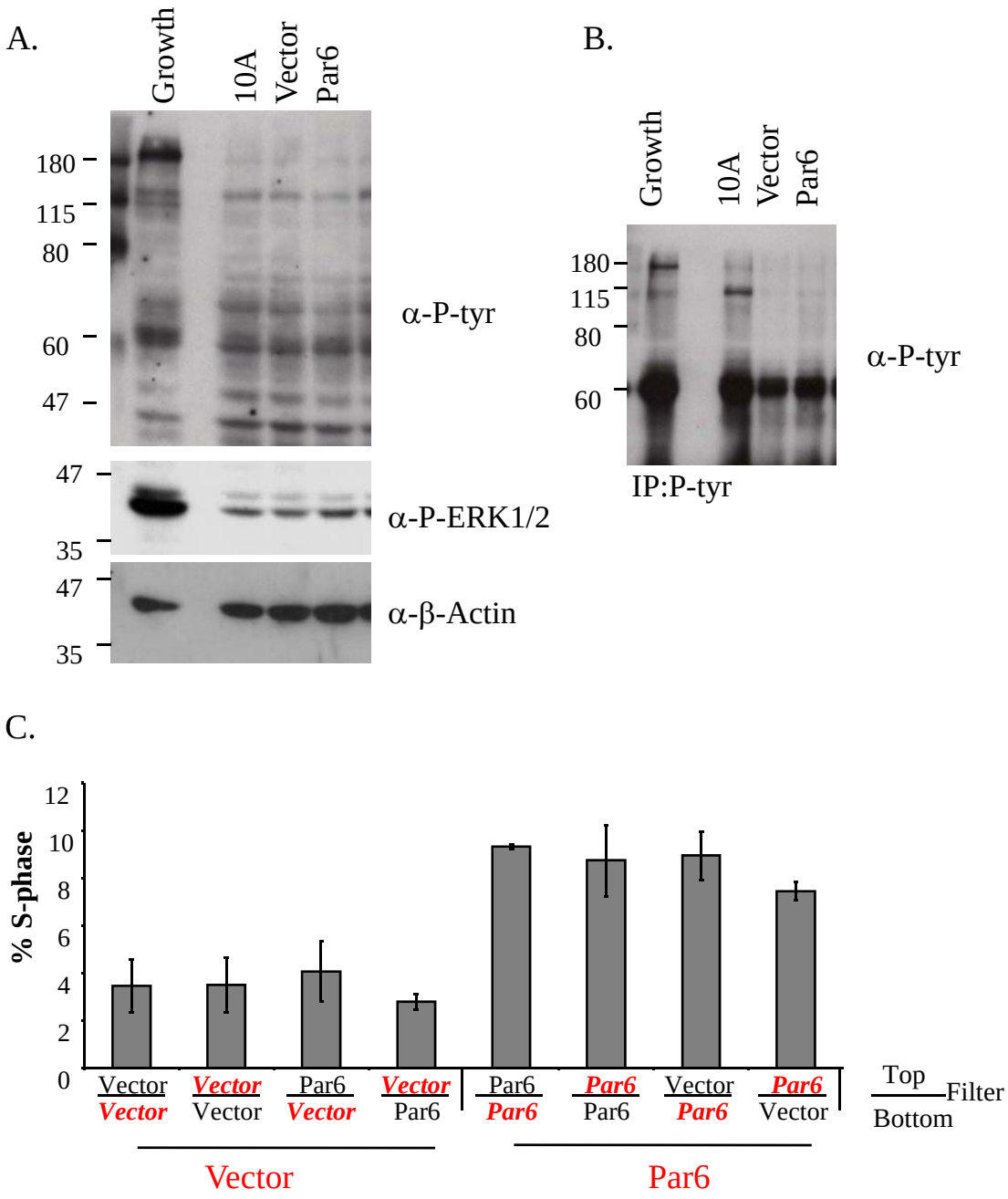

Figure 2.5. Par6 overexpressing cells do not promote proliferation of vector control cells.

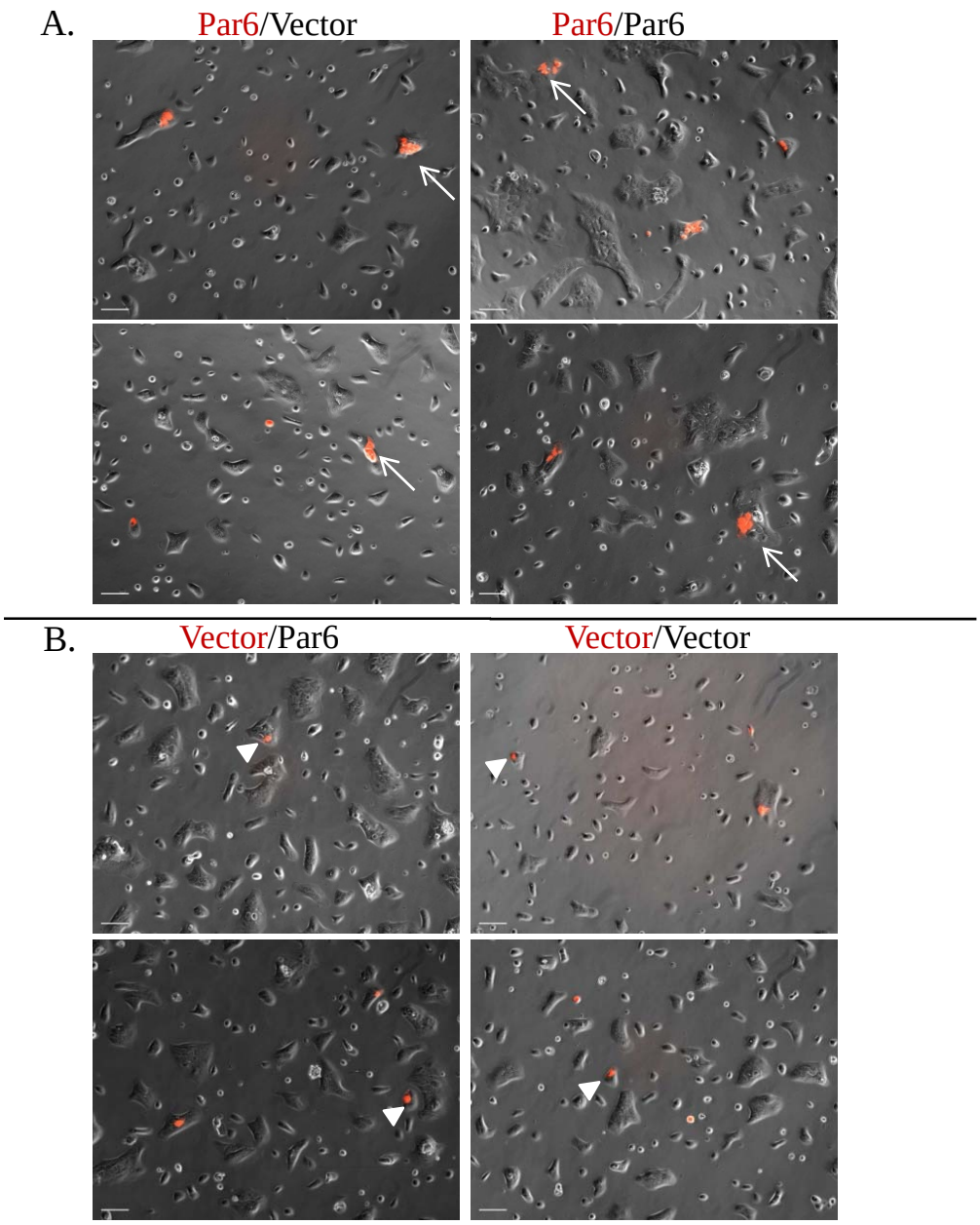

Figure 2.6. Overexpression of Par6 does not promote proliferation of juxtaposed control cells.

MCF-10A cells expressing vector control or Par6α-Flag were labeled with fluorescent DiI (red). **(A)** Labeled Par6 expressing cells (red) were co-cultured with unlabeled vector control or Par6 cells in EGF-free media. Fluorescent and phase images were taken after 30 hours, arrows point to proliferative Par6 expressing cells labeled cells. **(B)** Labeled vector control cells (red) were co-cultured with unlabeled vector control or Par6 cells in EGF-free media and imaged as in **(A)**. Arrowheads point to single labeled vector control cells. Scale bar represents100 μm.

Par6 overexpressing cells (This is extensively characterized in the Appendix, Figure A.2 and A.3). Therefore, we investigated pathways downstream of EGFR by examining activation of PLCγ, PI3K/AKT, Ras/MAPK and JNK, both in the presence and in the absence of EGF stimulation (Appendix, Figure A.1). Par6 overexpression did not activate AKT, PLCγ, or JNK pathways either in the presence or in the absence of EGF. (Figure 2.7.A, B and data not shown). However, Par6 overexpressing cells showed a significant increase in ERK phosphorylation in the absence of EGF stimulation. This activation of ERK was also evident in the presence of EGF stimulation. In these conditions control cells dowregulated ERK phosphorylation to basal levels 30 minutes after addition of EGF whereas in Par6 overexpressing cells ERK phosphorylation was prolonged for 60 (Figure 2.7.C) and 120 minutes (Figure 2.7.D). In contrast to wild-type Par6, the Par6 mutants neither induced phosphorylation of ERK in the absence of EGF nor promoted sustained ERK phosphorylation in the presence of EGF (Figure 2.7.C, E and data not shown).

To confirm that the effect of Par6 on proliferation is directly due to its effects on ERK activation, we inhibited ERK activation using the MEK kinase inhibitor U0126. Treatment of Par6 overexpressing cells with U0126 blocked both basal and EGF-induced sustained ERK phosphorylation (Figure 2.8.A). In addition, the MEK inhibitor also blocked EGF- independent cell proliferation (Figure 2.8.B) suggesting that Par6 is activating the MAP kinase pathway upstream of MEK kinase. Thus, Par6 overexpression promotes EGF independent cell proliferation by activating the MEK/ERK signaling pathway.

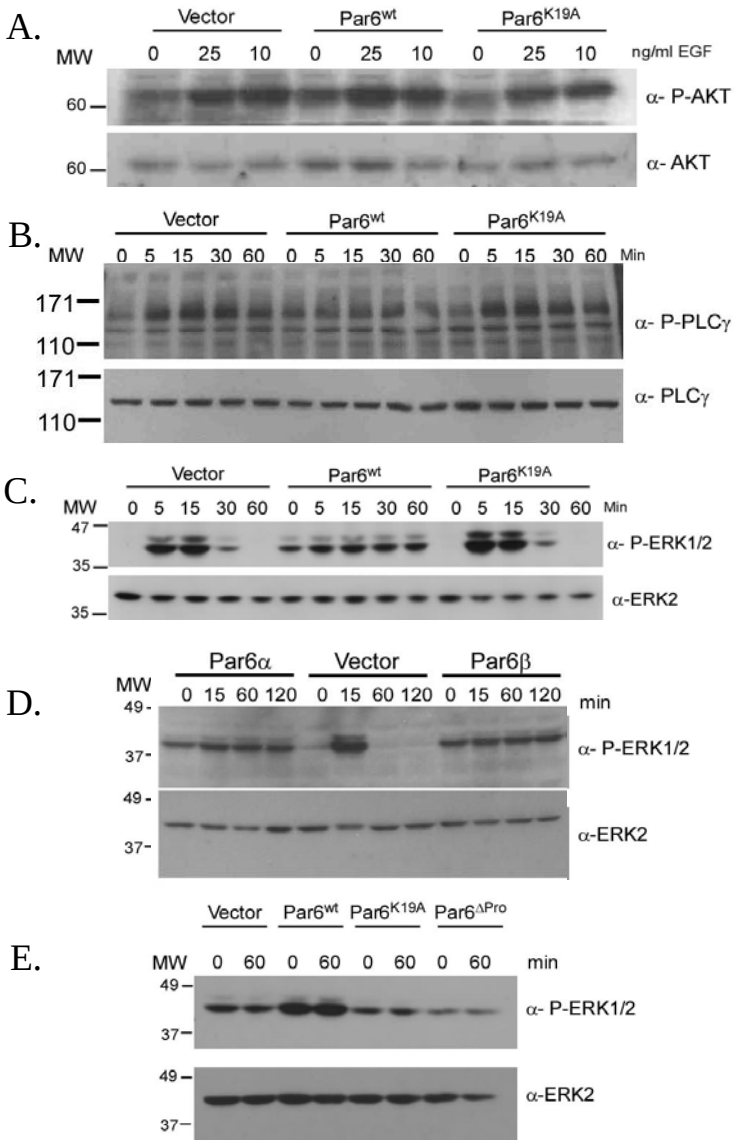

Figure 2.7. Par6 overexpression activates MAPK signaling.

(A) MCF-10A cells expressing vector control, Flag-Par6α or Flag-Par6^{K19A} were stimulated with 0, 10 and 25 ng/ml EGF for 15 minutes. Cell extracts were analyzed for activation of AKT by immunoblotting with a phospho-specific antibody. **(B)** Cells expressing vector control, Flag-Par6α or Flag-Par6^{K19A} were stimulated for 0,5,15, 30 and 60 minutes with 2 ng/ml EGF. Cell extracts were analyzed for activation of PLCγ by immunoblotting with a phospho-specific antibody **(C)** or for activation of phosphorylated ERK1/2 a phospho-specific antibody. **(D)** Cells expressing vector control, Flag-Par6α or Flag-Par6β were stimulated for 0, 15, 60 and 120 minutes. Cell extracts were analyzed for activation of ERK1/2 by immunoblotting **(E)** Cells expressing vector control, Flag-Par6α, Flag-Par6^{K19A} or Flag-Par6$^{\Delta pro}$ were stimulated for 0 and 60 min with 2 ng/ml EGF. Cell extracts were analyzed for activation of ERK1/2 by immunoblotting .

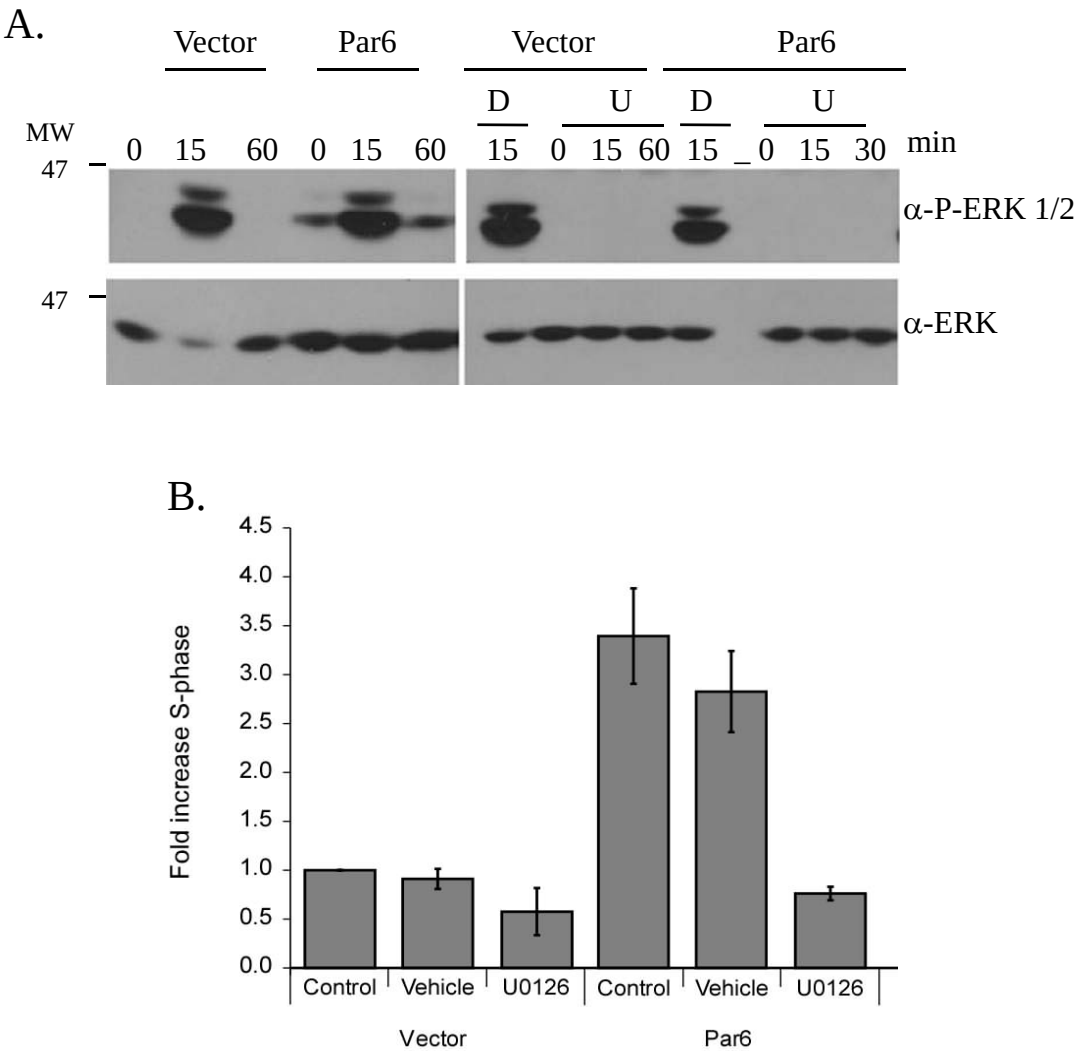

Figure 2.8. Par6 overexpression activation of MAPK signaling is dependent on MEK

(A) MCF-10A cells expressing vector control or Flag-Par6α were pretreated for 1 hr with (Control), DMSO (D) or Mek inhibitor (10 μM UO126) and then stimulated for 0,15,and 60 minutes with 2 ng/ml EGF. Cell extracts were analyzed for activation of ERK1/2 with antibodies phospho-specific antibodies. **(B)** Cells were grown in EGF free media for three days with no inhibitors (Control), DMSO (vehicle) or Mek inhibitor (10 μM UO126) and analyzed by flow cytometry. Data are fold increase in S-phase of Par6 expressing cells compared to control cells and are means +/- S.D. of three independent experiments.

Discussion:

We demonstrate that overexpression of Par6 in mammary epithelial cells promotes activation of MAPK and induces cell proliferation. Thus, our results identify a novel role for the polarity protein Par6 as an inducer of cell proliferation.

We show that the ability of Par6 to interact with aPKC and Cdc42 is required for stimulation of cell proliferation. The need for this interaction is consistent with the established role of aPKC and Cdc42 in Par6 mediated regulation of tight junction biogenesis, polarized cell migration and cell death (Yamanaka et al. 2001; Gao et al. 2002b; Etienne-Manneville and Hall 2003a; Kim et al. 2007). Previous studies have shown that Par6-aPKC-Cdc42 induced modulation of GSK3β activity is required for directed cell migration and apoptosis (Etienne-Manneville and Hall 2003a; Kim et al. 2007). We determined that modulation of GSK3β by the Par complex is unlikely to play a role in Par6 induced cell proliferation, because no difference in GSK3β activity was observed in Par6 overexpressing cells (data not shown). Here, we show that Par6 overexpression induces ERK phosphorylation in the absence of EGF, identifying MAPK pathway as an effector of the Par6-aPKC-Cdc42 complex. MAPK signaling can be activated by ligand-independent phosphorylation of EGFR (Miranti and Brugge 2002). Since we did not observe EGF independent phosphorylation of EGFR in Par6 overexpressing cells we can rule out activation of EGFR as a mechanism to activate MAPK in our cell system (Appendix).

Although Par6 overexpression did not activate EGF receptor directly, we observed a sustained activation of the Ras/MAP kinase pathway by monitoring

phosphorylated ERK1/2 under low EGF conditions. It has been shown that activation of B-Raf is one mechanism that sustains MAPK signaling (York et al. 1998). We did not see an increase in B-raf phosphorylation when Par6 was overexpressed suggesting that Par6 is using a different molecule to sustain this pathway.

Atypical PKC family members are known to activate ERK in a MEK dependent manner. Atypical PKC is not only sufficient but is also required for activation of ERK in response to serum stimulation (Berra et al. 1993; Berra et al. 1995; Bjorkoy et al. 1997; Schonwasser et al. 1998; Gao et al. 2002a). One possibility is that Par6/aPKC is binding to a scaffolding protein such as Kinase Suppressor of Ras (KSR), a known enhancer of MAPK signaling (Therrien et al. 1996; Morrison 2001). Par6 could localize active aPKC to a scaffold and promote activation of the MAPK pathway. Consistent with this hypothesis Par6 mutants that are unable to recruit a functional Par complex are unable to sustain activation of MAPK pathway. It is possible that the Par6-aPKC-Cdc42 complex uses a yet to be defined mechanism, such as a scaffold molecule to promote activation MEK-ERK signaling (Figure 2.3.9). It is also possible that Par6 is inhibiting with the activity of a serine/threonine phosphatase that normally inactivates MEK or ERK. This would mean that the MAPK pathway is not inactivated in the presence of Par6 and therefore result in sustained activation of ERK. Thus, in addition to its known effector interactions that regulate cell polarity, the Par6-aPKC-Cdc42 complex also regulates molecules that induce cell proliferation.

Par6 can cooperate with other factors such as oncogenes to promote transformation (Qiu et al. 2000; Aranda et al. 2006). One characteristic of cell transformation is the ability to grow in the absence of growth factors. We show that Par6

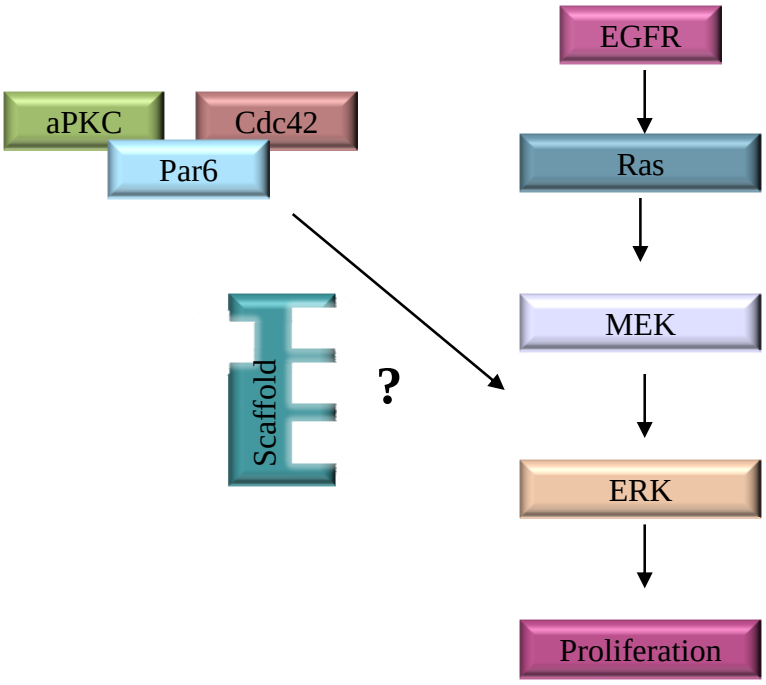

Figure 2.9 Model of how Par6 overexpression promotes activation of the MAPK pathway

We show that ectopic expression of Par6 activates the MAPK pathway and this activity is necessary for EGF-independent proliferation of MCF-10A cells. We postulate that Par6/aPKC/Cdc42 complex interacts with a scaffolding molecule that will bring together the complex and the MAPK signaling cascade. The interaction with a scaffolding molecule will facilitate the activation of the MAPK signaling pathway and bring the different components together for a more efficient interaction.

has a proliferative role by promoting growth factor independent activation of the MAPK pathway and proliferation. Therefore, deregulating a polarity protein in mammary epithelial cells can promote one property of cell transformation.

Chapter 3: The polarity Par6 protein promotes proliferation in mammary epithelial acini and is overexpressed in breast cancer

Introduction:

Overexpression of Par6 in various cell systems perturbs cell organization (Etienne-Manneville and Hall 2001; Ohno 2001; Gao et al. 2002a; Solecki et al. 2004). For example, in MDCK cells Par6 delays formation of tight junctions and disrupts their function (Gao et al. 2002a). In migrating astrocytes overexpression of Par6 blocks the microtubule organization center from polarizing towards the leading edge (Etienne-Manneville and Hall 2001). Furthermore, Par6 overexpression in granule neurons prevents migration and axon extension (Solecki et al. 2004).

Par6 is a known regulator of epithelial cell polarity and cooperates with oncogenes (Chapter 2). Interestingly, *Par6db* is located in a region of the genome that is frequently amplified in breast cancer and aPKC is overexpressed in non-small cell lung (NSCL) and ovarian carcinoma (Chapter 1). In addition, we also showed that overexpression of Par6 promotes EGF independent proliferation of mammary epithelial cells, one property of transformation (Chapter 2). Together, these data suggest a role for the Par6 polarity complex in progression to carcinoma.

Whether or not Par6 can contribute to breast cancer has not been studied. It is the aim of this chapter to determine if Par6 overexpression has an effect on the transformation of organized mammary epithelial cells. Therefore, we investigated if Par6

overexpression had an effect on the polarity of MCF-10A cells grown as acinar structures and if Par6 overexpression promoted proliferation in a similar manner as it did in two-dimensional cell culture in Chapter 2. Studying Par6 overexpression in the three-dimensional context generates a relevant system to human cancer progression.

In this chapter, we show that Par6 overexpression enhances proliferation of MCF-10A cells in three-dimensional cell culture and that this function is dependent on Par6's interaction with aPKC and Cdc42. Furthermore, we show that Par6 is overexpressed both in human precancerous breast lesions, and in estrogen receptor positive breast cancers suggesting that Par6 pathways are likely to play critical roles during initiation and progression of breast cancer. Thus, overexpression of the polarity protein Par6 can contribute to cell transformation by promoting cell proliferation.

Results:

Overexpression of Par6 does not disrupt 3D acini morphogenesis

Par6 overexpression has been shown to disrupt establishment of epithelial cell polarity in various cell systems. Therefore we wanted to investigate if overexpression of Par6 affects polarization and morphogenesis of MCF-10A cells in three-dimensional (3D) culture. We found that overexpression of Par6 did not affect the ability of MCF-10A cells to form acini with hollow lumens (Figure 3.1.A) or undergo apoptosis (Figure 3.1.B). In addition, these acini had no detectable loss of apical-basal polarity as determined by using the apical polarity marker GM130, a basal polarity marker Laminin V (Figure 3.1.B). We also found that there was no difference in localization of a basolateral marker E-cadherin (Figure 3.1.C), or in localization of the plasma membrane and apical marker Phospho-ERM (Figure 3.1.D). It is important to note that while MCF-10A cells do not form complete tight junctions (Chapter 1), one known marker of epithelial cell polarity, they do form an apical-basal axis of polarity. We found no difference in the apical-basal axis of polarity in structures derived from Par6 expressing cells. Thus, overexpression of Par6 did not affect polarization and morphogenesis of MCF-10A cells on Matrigel™.

Overexpression of Par6 promotes cell proliferation in 3D acini

Although there was no detectable difference in the organization of the acinar structures, Par6 expressing acini were larger than the control acini (Figure 3.1.A). To test the hypothesis that Par6 overexpression promotes acinar growth, acini size was quantitated by measuring the area occupied by each acinus. Par6α and β overexpressing

Figure 3.1. Overexpression of Par6 does not disrupt 3D acini morphogenesis

(A) MCF-10A cells expressing vector control, Par6α and Par6β were grown for 20 days on Matrigel in 0.5 ng/ml EGF. Phase contrast images show increased acinar size in Par6 expressing structures(top). Optical sections of acini stained with DAPI (bottom) images show a single layer of nuclei, arrows point to the hollow lumen in each acini (inset). Scale bar represents 50 μm. **(B)** MCF-10A cells expressing vector control, Par6α were grown for 7 days on Matrigel in 0.5 ng/ml EGF. Growing structures were stained with ethidium bromide (EtBr) to detect dead cells. Arrows point to the dead cells in the middle of the structure. This cell death will clear the middle of the structure to form the lumen. Scale bar represents 100 μm **(C)** MCF-10A cells expressing vector control and Par6α were grown for 12 days on Matrigel in 0.5 ng/ml EGF. Acinar structures were immunostained with the apical marker GM130 (green) and basal marker Laminin V (Red) and co-stained with DAPI (blue) nuclear stain. Arrowheads point to organized laminin and arrows point to the apical localization of the golgi apparatus above the nucleus. Scale bar represents 10 μm. **(D)** Acinar structures grown as in **(C)** and immunostained with the basolateral membrane marker E-Cadherin (Red, arrows) and the **(E)** plasma membrane (arrows) and apical marker P-ERM (Red, arrowhead) and co-stained with DAPI (blue) nuclear stain. **(C-E)** shows normal localization of the membranes and polarized markers in both Vector control and Par6 expressing acinar structures. Scale bar represents 50 μm.

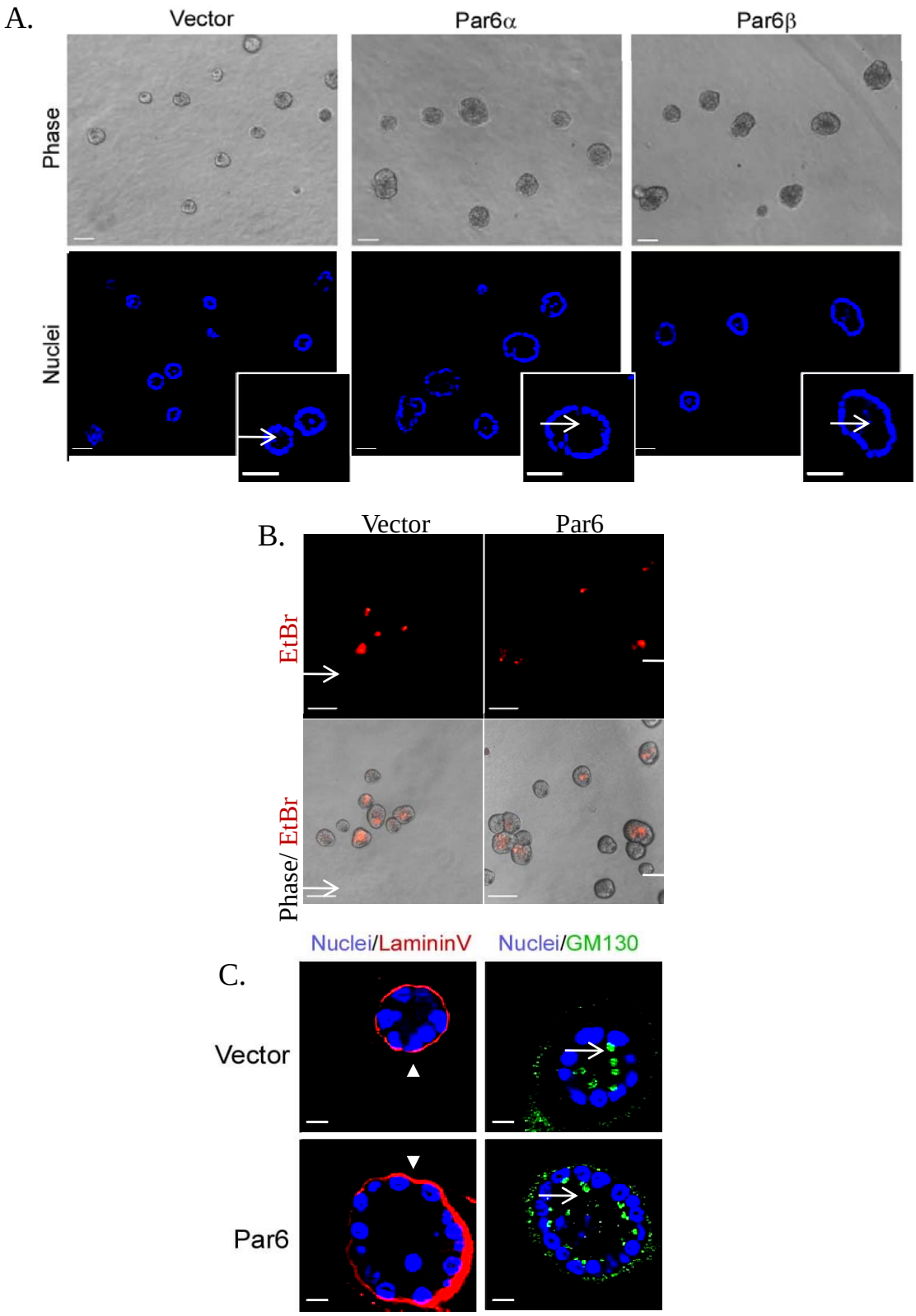

Figure 3.1. Overexpression of Par6 does not disrupt 3D acini morphogenesis

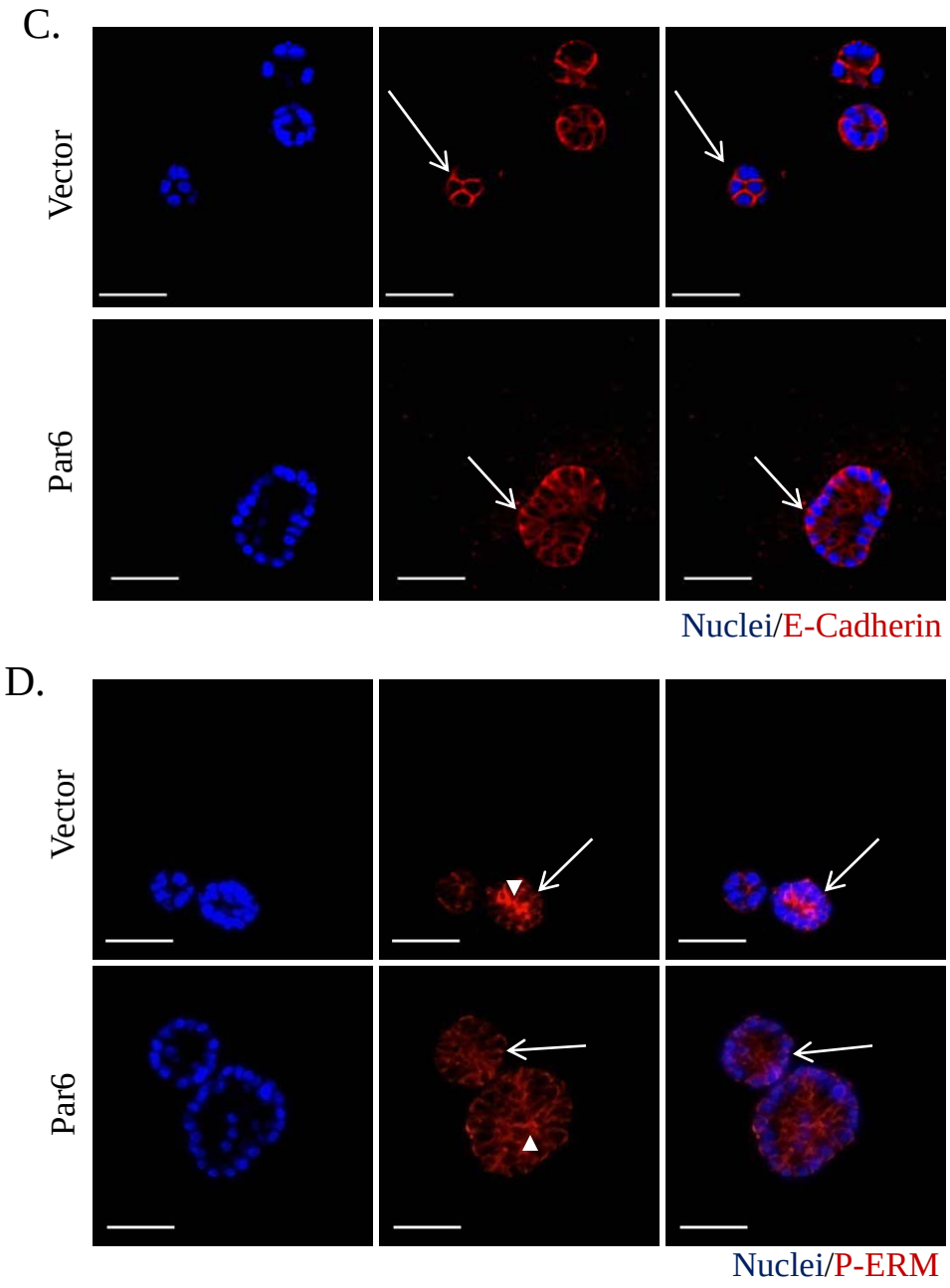

Figure 3.1. Overexpression of Par6 does not disrupt 3D acini morphogenesis

cells formed acini that were significantly larger than those formed by control cells, irrespective of the dose of EGF (Figure 3.2.A and B). To determine if the increase in size was due to an increase in cell number or cell size, we counted the number of cells per structure. Acini derived from Par6 overexpressing cells had significantly more cells than those derived from control cells (Figure 3.3.A). Furthermore, we did not observe an increase in cell size, as measured by forward scatter on the flow cytometer, suggesting that the increase in acinar size was due to an increase in proliferation (Figure 3.3.B), which is consistent with the findings we observed in monolayer culture (Chapter 2).

To determine if the increase in cell number is due to changes in cell proliferation rates, immunofluoresence was used to monitor the presence of the proliferation marker, Ki-67 during 3D morphogenesis. Consistent with previous reports (Muthuswamy et al. 2001), the majority of the acini derived from control cells reached proliferation arrest by day 12 (Figure 3.2.C). However, acini derived from Par6 expressing cells were over three-fold more proliferative on day 12 than control acini. The overall proliferation of Par6 expressing acinar structure decreased by day 16 and diminished even further to growth-arrested levels by day 20 (Figure 3.2.C). Thus, Par6 overexpression induces development of hyperplastic acini by delaying proliferation arrest during 3D morphogenesis without disrupting polarity.

This observation was not limited to MCF-10A cells. We observed that overexpression of Par6 promote acinar growth in a mouse mammary epithelial cell line, HC11, that form three-dimensional structures when plated on Matrigel (Figure 3.4.A)(Xian et al. 2005). HC11 structures derived from Par6 expressing cells were significantly larger that those derived from vector control cells (Figure 3.4.B). Thus, the

Figure 3.2 Overexpression of Par6 promotes cell proliferation in 3D acini structures

MCF-10A cells expressing vector control, Par6α and Par6β were grown for 12 days on Matrigel. **(A)** Graph represents the distribution of acinar size (circumferential area) of structures grown in 0, 0.1 and 0.5 ng/ml EGF and **(B)** 0.5 ng/ml. There is a significant size increase of the Par6 expressing acinar structures when compared to vector control. The area of each acini was measured using Zeiss Axiovision 4.5 software and plotted as box plots. The blue line represents the median value and the spread represents 1.5 times the inter-quartile range and outliers are shown as circles. Each condition represents approximately 800 acini structures from three dependent experiments. The P-value between Vector and Par6, for each EGF concentration was less than 0.0001 calculated by Mann-Whitney test. **(C)** Quantitation of proliferating day 12 acinar structures grown in 0.5ng/ml EGF from **(A),** acinar structures with at least one positive Ki-67 positive nuclei were counted as positive. Data are represented as percent Ki-67 positive structures +/- S.D. Each bar represents approximately 700 acini from three independent experiments **(D)** Quantitation of proliferating day 16 and day 20 acinar structures grown in 0.5ng/ml EGF. Data shows increased proliferation of acinar structures derived from Par6 expressing cells compared to vector control. For day 16 data represented % Ki-67 positive structures +/- S.D. Each bar represents approximately 700 acini from three independent experiments . For day 20 data represented % Ki-67 positive structures. Each bar represents approximately 1500 acini from one experiments.

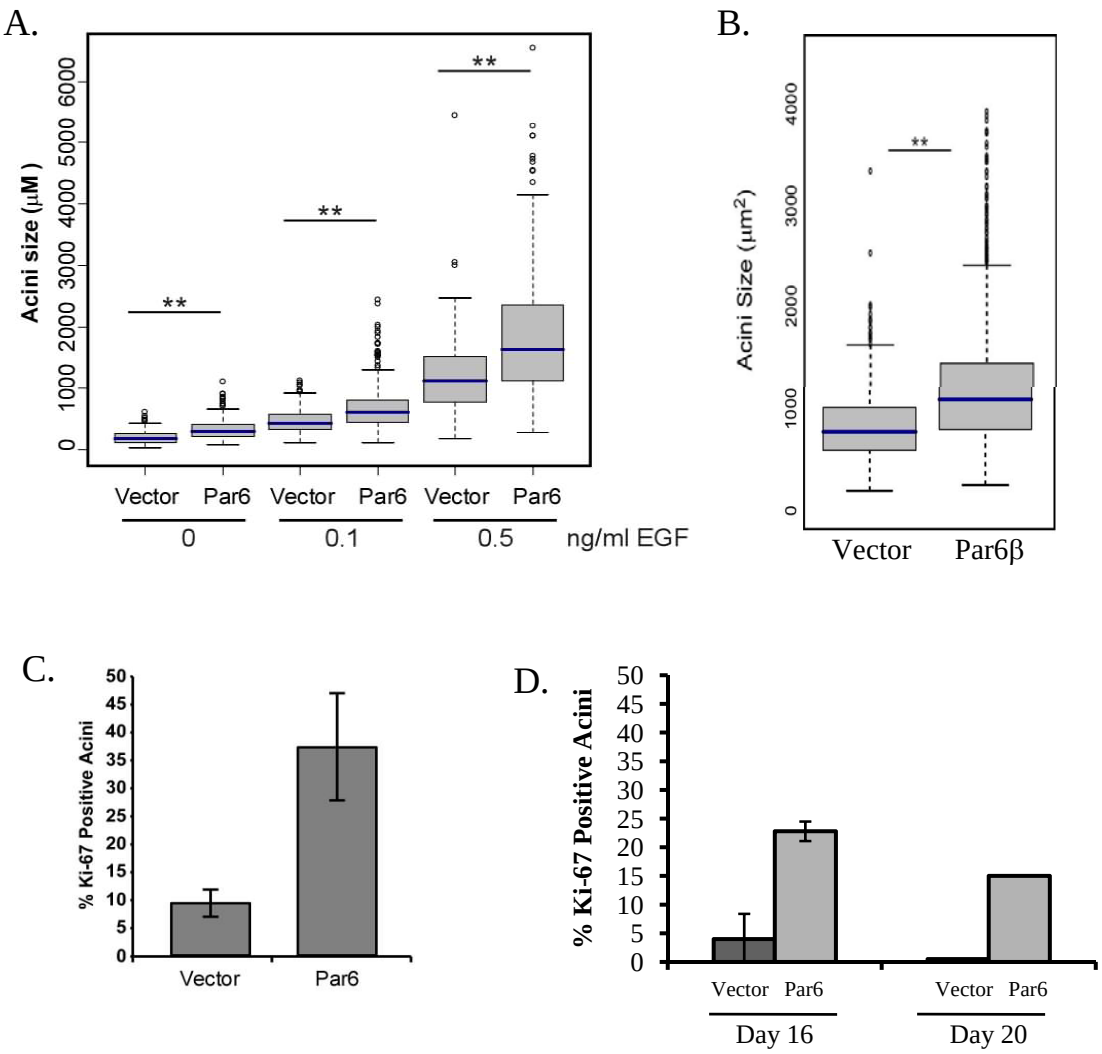

Figure 3.2 Overexpression of Par6 promotes cell proliferation in 3D acini structures

.

Figure 3.3 Par6 overexpression increases the cell number/acini and does not change the cell size

(A) MCF-10A cells expressing vector control and Par6α were grown for 4 days on Matrigel. Serial optical sections of DAPI nuclei stained acinar structures were taken and each nuclei within each acini was counted. Box plot shows the distribution of nuclei per acini structure and that Par6 acinar structures contain significantly more nuclei per structure than Vector control acini. The blue line represents the median value and the spread represents 1.5 times the inter-quartile range and outliers are shown as circles. The data represents approximately 300 acini. The P-value between Vector and Par6, was less than 0.0001 calculated by Mann-Whitney test. **(B)** Single cells from Day 4 acini structures were collected. There was no difference in cell size as measured by flow cytometry using forward scatter. Data are means +/- S.D. from three independent experiments.

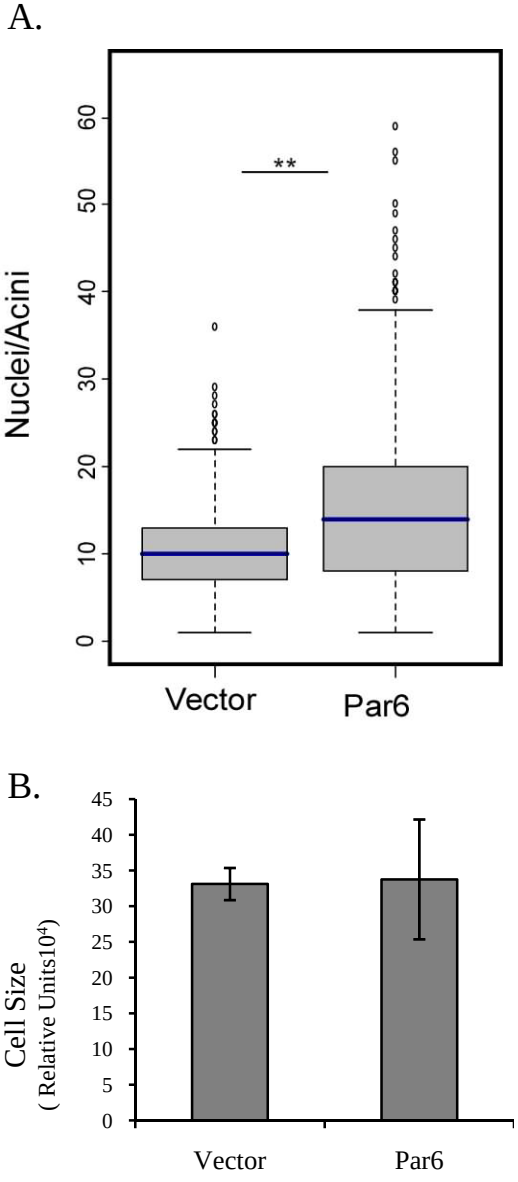

Figure 3.3 Par6 overexpression increases the cell number/acini and does not change the cell size

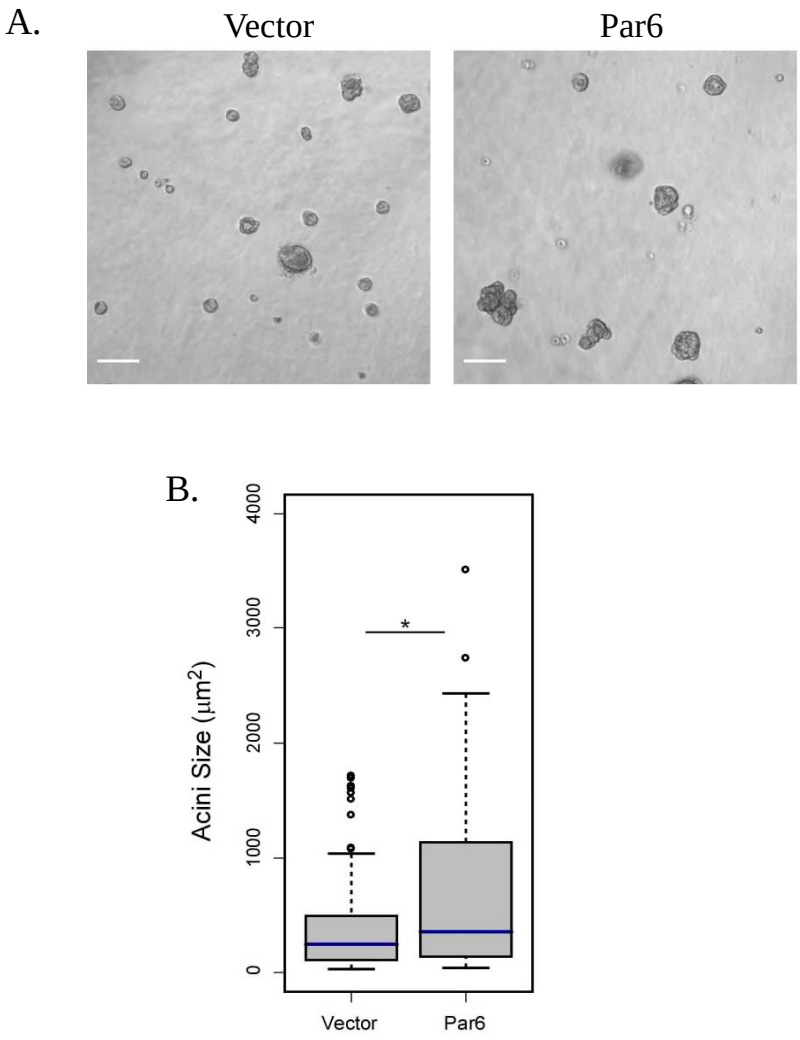

Figure 3.4 Par6 overexpression promotes HC11 acini growth

(A) HC11 cells expressing vector control and Par6α were grown for 12 days on Matrigel in 0.5 ng/ml EGF . Phase images of HC11 acini derived from cells overexpressing Par6 or vector control show an increase in acinar size in Par6 expressing acini. Scale bar represents 100 μm . **(B)** Graph represents the distribution of acinar size (circumferential area) of structures from **(A)**. There is a significant size increase of the Par6 expressing acinar structures when compared to vector control. The area of each acini was measured using Zeiss Axiovision 4.5 software and plotted as box plots. The blue line represents the median value and the spread represents 1.5 times the inter-quartile range and outliers are shown as circles. Data represents approximately 200 acini from one experiment. The P-value (P=0.03) between Vector and Par6, was calculated by Mann-Whitney test.

polarity protein Par6 promotes proliferation of multiple mammary epithelial cell lines both in 2D and 3D cell culture. In addition, MCF-10A cells expressing different mutants of Par6 that are defective in binding members of the Par complex (Figure 2.5) were plated on Matrigel. In contrast to Par6, none of the Par6 mutants tested were able to enhance acini cell proliferation (Figure 3.5.A and B), with no effect on morphogenesis. Therefore we determined that, similar to Par6 overexpression in monolayer culture (Chapter 2, Figure 2.3.E), Par6 requires interaction with aPKC and Cdc42 to enhance acinar cell proliferation.

Pard6b is overexpressed in estrogen receptor positive human breast tumor

Par6 overexpression promotes hyperplastic acinar structures and, *Pard6b* (Chr. 20q13.13) is located in a region of the genome that is frequently amplified in breast cancer (Bergamaschi et al. 2006; Chin et al. 2006; Ginestier et al. 2006; Hicks et al. 2006). Because two of these four studies correlated *Pard6b* genomic amplification of with *Pard6b* gene expression (Chin et al. 2006; Ginestier et al. 2006), we investigated if *Pard6b* gene expression was increased in primary human breast cancers. To directly test this, quantitative PCR analysis was performed on 25 primary breast cancer samples, two normal breast tissue samples, six breast cancer cell lines and MCF-10A cells. We found that 6/25 primary tumors and 2/6 breast cancer cells express mRNA at least two fold more than the levels observed in their respective controls (Figure 3.6.A and B). Thus, *Pard6b* is both amplified genomically and transcriptionally in breast cancer as found by multiple studies including my own. Both MCF-7 and T47D cell lines are estrogen receptor (ER) positive and overexpress Par6 (Fig 3.6A) (Lacroix and Leclercq 2004). To

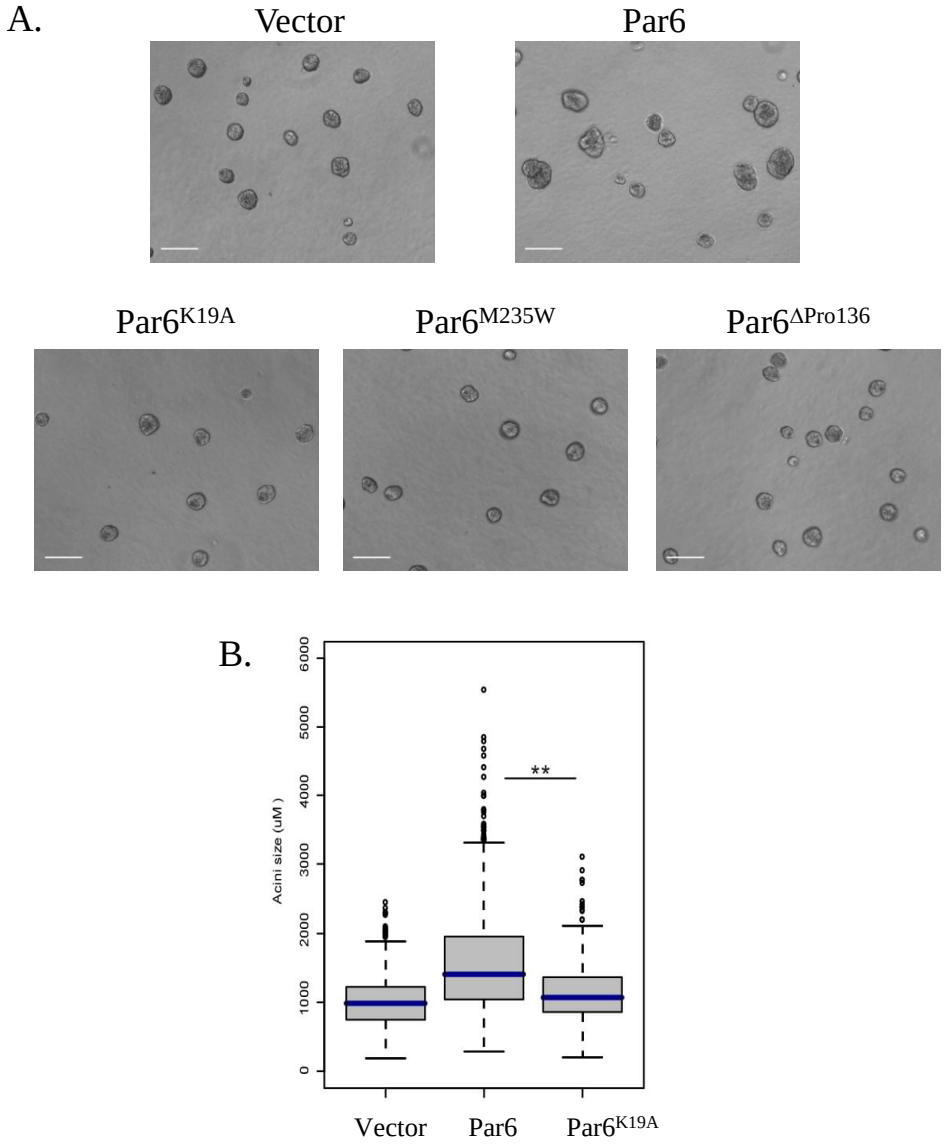

Figure 3.5 Par6 induced acini cell proliferation requires interaction with aPKC and Cdc42

(A) MCF-10A cells expressing vector control, Par6α and Par6^{K19A}, Par6^{M235W} and Par6$^{\Delta pro}$ were grown for 12 days on Matrigel in 0.5ng/ml EGF. Phase images of show that only wild-type Par6 promotes an increase in acinar size. **(B)** Box plot representation of the acinar size distribution (circumferential area) of vector control, Par6α and Par6^{K19A} . Data shows that only wild-type Par6 promotes an increase in acinar size. Each condition represents approximately 800 acini structures from three dependent experiments. The P-value between Vector and Par6 or Par6 and Par6^{K19A} is less than 0.0001 calculated by Mann-Whitney test.

A.

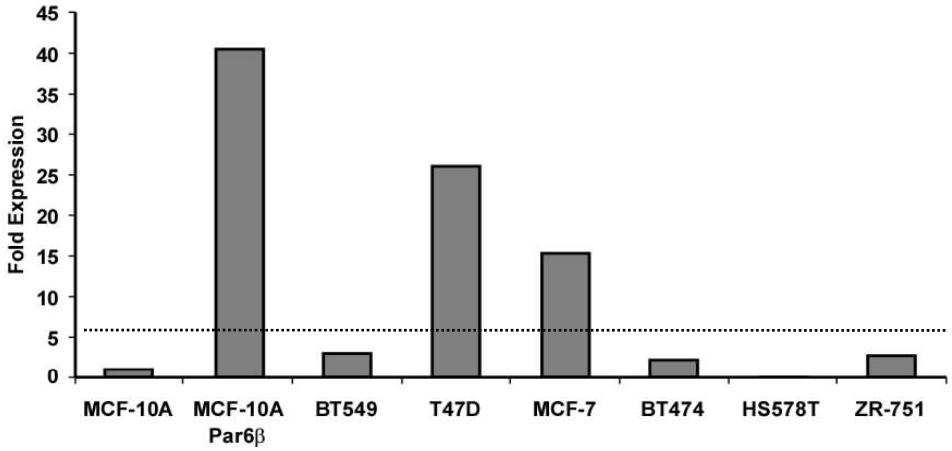

B.

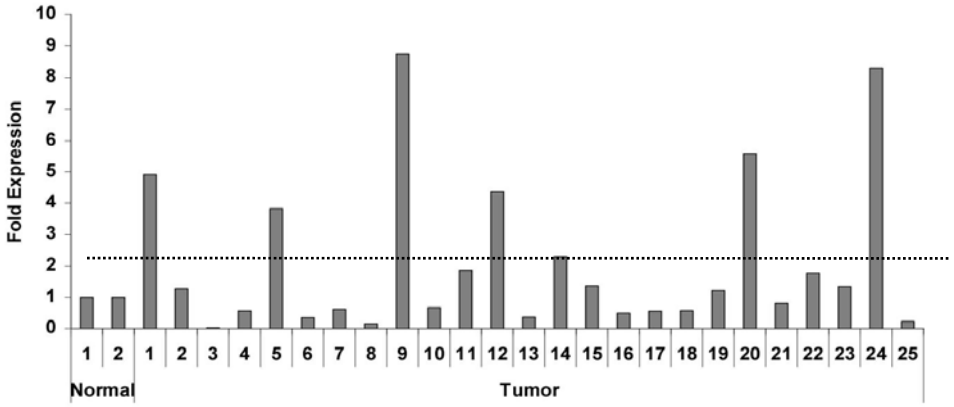

Figure 3.6 *Pard6b* is overexpressed in breast cancer

(A) Quantitative PCR analysis of *Pard6b* gene expression using cDNA from breast cancer cell lines and normalized to GAPDH gene expression. Data is represented as fold increase over MCF-10A control cells. Breast cancer cell lines with expression levels above the dotted line (5-Fold over MCF-10A) were considered to have *Pard6b* overexpressed. **(B)** Quantitative PCR analysis of *Pard6b* gene expression using cDNA generated from primary breast tumors and normalized to GAPDH gene expression. Data is represented as fold increase over the average levels expressed in normal breast tissue. Tumor samples with expression levels above the dotted line (2-fold over normal) were considered to have *Pard6b* overexpressed.

determine if there is a relationship between ER status and *Pard6b* expression, we compared *Pard6b* mRNA levels in 68 of ER positive and 44 of ER negative breast tumors. Overexpression of *Pard6b* showed a significant positive correlation with ER positive status (Figure 3.7.A). Analysis of a public gene expression database Oncomine (Rhodes et al. 2004), showed that *Pard6b* expression significantly correlated with ER positive status in four independent studies (Figure 3.7.B) (Perou et al. 1999; van de Vijver et al. 2002; Zhao et al. 2004; Ginestier et al. 2006). However, we did not observe any relationship between Par6 overexpression and ErbB2 amplification in human breast tumors (Figure 3.7.C), suggesting that *Par6db* overexpression is specific to the ER positive subtypes of breast cancer. Inhibition of ER signaling in MCF-7 cells by treatment with Tamoxifen did not result in a significant decrease in the levels of *Par6db* mRNA (Figure 3.7.D), suggesting that *Pard6b* levels may not be directly regulated by estrogen in MCF-7 cells. Since we do not see transcriptional regulation of *Pard6b* by tamoxifin, it is possible that Par6 cooperates with EGF to provide a proliferative advantage in ER positive breast cancers, but not for ErbB2 positive cancers. Precancerous breast lesions also overexpress ER (Lee et al. 2006). The earliest form of precancerous breast lesions are considered to be hyperplastic enlarged lobular units (HELUs). HELUs are hyperplastic structures that are derived from the normal terminal ductal lobular units (TDLU) where the acini are enlarged in size due to increase in cell number with no apparent loss of tissue architecture. HELUs are known to have high cell proliferation rates and increased expression of ER and EGF family of ligands (Lee et al. 2006; Lee et al. 2007). Since, MCF-10A cells overexpressing Par6 formed hyperplastic acini, with no loss of cell polarity, we tested if *Pard6b* was overexpressed in HELUs.

Figure 3.7 *Pard6b* is overexpressed in estrogen receptor positive human breast tumors

(A) A box plot of the microarray data comparing *Pard6b* gene expression in ER^- verses ER^+ tumor samples. A kolmogorov-Smirnov null hypothesis test was used to calculate the p-value ($P = 2.9 \times 10^{-7}$). A significant increase of *Pard6b* gene expression was seen in ER+ tumor samples when compared to ER negative tumor samples. **(B)** Meta-analysis of published databases using Oncomine an integrated data platform (Rhodes *et al*, 2004). Four independent breast tumor studies show that *Pard6b* gene expression was significantly increased in ER+ tumor samples compared to ER negative tumor samples. **(i)** Analysis of 69 ER^- and 226 ER^+ breast carcinoma, P-value = 2.4E-23 (van de Vijver *et al*, 2002). **(ii)** Analysis of 11 ER^- and 24 ER^+ breast carcinoma, P-value = 4.6E-7 (Zhao *et al*, 2004). **(iii)** Analysis of 28 ER^- and 27 ER^+ breast carcinoma, P-value = 9.5E-7 (Ginestier *et al*, 2006). **(iv)** Analysis of 9 ER^- and 26 ER^+ breast carcinoma, P-value = 7.1E-4 (Perou *et al*, 1999). **(C)** Meta-analysis of published databases using Oncomine an integrated data platform (Rhodes *et al*, 2004). Five independent breast tumor studies show that *Pard6b* gene expression was not significantly increased or decreased in ErbB2+ tumor samples when compared to ErbB2 negative tumor samples. **(i)** Analysis of 29 $ErbB2^-$ and 8 $ErbB2^+$ breast carcinoma, P-value = 0.019 (Richardson *et al*, 2006). **(ii)** Analysis of 52 $ErbB2^-$ and 3 $ErbB2^+$ breast carcinoma, P-value = 0.094 (Ma *et al*, 2004). **(iii)** Analysis of 62 $ErbB2^-$ and 26 $ErbB2^+$ breast carcinoma, P-value = 0.232 (Minn *et al*, 2005). **(iv)** Analysis of 78 $ErbB2^-$ and 24 $ErbB2^+$ breast carcinoma, P-value = 0.237 (Saal *et al*, 2007). **(v)** Analysis of 17 $ErbB2^-$ and 14 $ErbB2^+$ breast carcinoma, P-value = 0.47 (Zhao *et al*, 2004). **(D)** Inhibition of ER signaling with tamoxifen does not affect *Pard6b* levels in MCF-7 cells. Quantitative PCR analysis of *Par6b* gene expression using cDNA generated from MCF-7 cells. Data are represented as fold increase of treated MCF-7 cells over untreated control after normalization to β-actin gene expression. MCF-7 cells were grown for 3 days in media containing charcoal treated fetal bovine serum and treated with tamoxifen (0.5μm) for 3 hours before RNA extraction. Data are means +/- S.D. from three independent experiments. **(D)** Paired samples of normal TDLUs and HELUs were laser captured. Microarray gene expression analysis was performed. Heat map shows the hierarchical clustering from a supervised comparison between paired samples of normal TDLUs and HELUs. Colors represent gene expression, Green (low) or Red (high). *Pard6b* is expressed and average of 2.5 fold (P = 0.02) and *PKCZ* 1.46 fold (P = 0.029) in HELU compared to TDLU (Lee *et al*, 2006).

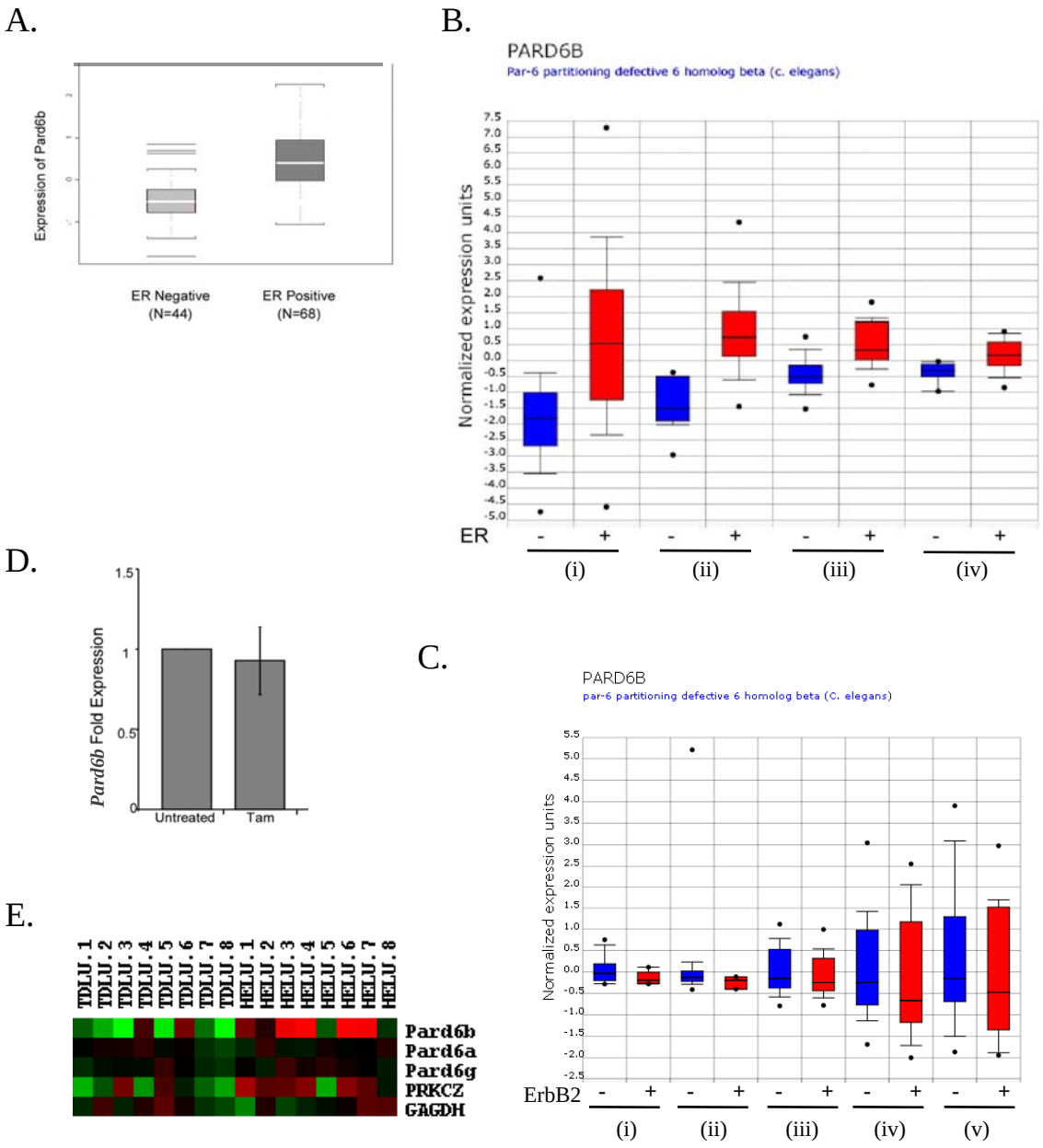

Figure 3.7 ***Pard6b*** **is overexpressed in estrogen receptor positive human breast tumors**

RNA isolated from microdissected HELUs and adjacent TDLUs were analyzed by microarray (Lee et al. 2007). *Pard6b* but not *Pard6a* or *Pard6g*, was overexpressed by 2.5 fold (p=0.002) in HELUs compared to adjacent TDLUs. Consistent with our observations in Par6 overexpressing MCF-10A cells where we found an increased levels of aPKC, the gene encoding for PKCζ (*PRKCZ*) was also upregulated by 1.46 fold (p=0.029) compared to TDLUs (Lee et al. 2007) (Figure 3.7.E). Thus, overexpression of the *Pard6b* is observed early in precancerous lesions and retained during development of ER positive cancers.

Discussion:

Our results show that overexpression of Par6α and β in non-transformed mammary epithelial cells does not affect establishment of apical-basal polarity during acinar morphogenesis. While several studies have reported that altered expression of both Par6α and β delays establishment of apical polarity (Yamanaka et al. 2001; Gao et al. 2002a), in almost all cases, they find that the cells recover from the effects of Par6 overexpression and eventually develop apical polarity. Since the cells eventually polarize, there must be compensatory mechanisms for apical polarity formation in the presence of altered Par6 expression. Since MCF-10A acinar morphogenesis takes several days, it is likely that Par6 overexpressing cells use these compensatory mechanisms to establish apical polarity. We found that ectopic expression of Par6 promotes proliferation of multiple epithelial cell lines in three-dimensional culture. Our results demonstrate that in addition to its known role as a polarity regulator, Par6 can also induce proliferation of organized mammary epithelial cells.

We demonstrate that Par6β is overexpressed in both HELUs and ER positive advanced carcinomas. HELUs are characterized by high rates of cell proliferation, ER positivity and increased expression of EGF family of growth factors. Considering that Par6 overexpression cooperated with EGF to promote hyperplastic acini, it is possible that these two factors could cooperate to promote the formation of HELUs. Since Par6 overexpression correlates with ER positivity in advanced breast carcinoma (Figure 3.7.A and B), Par6 could impart a proliferative advantage in this context. This means the cells overexpressing Par6 and ER could be selected for during tumor formation or be a driving force behind breast cancer formation.

How Par6 cooperates with ER has yet to be determined. Since we were unable to detect a change in Par6 expression upon inhibition of ER signaling with tamoxifin, not (Figure 3.7.D), it is possible that ER is not directly regulating Par6 expression. This would be consistent with the fact that Par6 is amplified genomically (Bergamaschi et al. 2006; Chin et al. 2006; Ginestier et al. 2006; Hicks et al. 2006). Therefore, Par6 overexpression could be cooperating with a downstream target of ER or the proliferative effects of both Par6 and ER could be additive. One system that could allow us to determine the importance of the ER/Par6 interaction would be to use ER positive breast cancer cell lines. We observed that Par6β was overexpressed in MCF-7 and T47D cells (Figure 3.6.A), therefore, we could determine if overexpression of Par6β is necessary for estrogen induced proliferation of these cell lines by reducing Par6β expression levels using RNA mediated interference.

Among the members of the Par complex, we found aPKC is also overexpressed in HELUs (Figure 3.7.E). Other studies have shown that aPKC is overexpressed in ovarian carcinoma and promotes aberrant proliferation in ovarian cells (Eder et al. 2005; Regala et al. 2005a; Regala et al. 2005b). Therefore, overexpression of multiple components of the Par complex plays a role in promoting proliferation in various cell systems. Whether this pathway is important in the formation of breast cancer has yet to be determined. It is possible that overexpression of Par6 or aPKC in carcinoma can play a role during cancer formation because overexpression promotes hyperproliferation, a necessary process in cancer formation. Not surprisingly, increased activation of MAPK, a known promoter of proliferation pathway, is associated with various types of cancer including breast cancer (Sivaraman et al. 1997; Hoshino et al. 1999; Sebolt-Leopold et al. 1999). Activation of

the MAPK pathway is an important event in cell proliferation. Therefore, overexpression Par6 and aPKC could be promoting proliferation of cells by activation of the MAPK pathway. This could be an important step in the progression to breast cancer.

Par6 is also known to cooperate with oncogenes associated with breast cancer progression. For example Par6 plays a critical role during ErbB2 induced transformation of organized epithelia (Chapter 4) and ErbB2 amplification is associated with the premalignant breast disease, DCIS (Allred et al. 1992). We did not observe either a positive or negative correlation between Par6 overexpression and ErbB2 status (Figure 3.7.C). Therefore, ErbB2 requires expression of Par6 but not overexpression. In addition, Par6 is required for TGFβ induced epithelial to mesenchymal transition, a cellular process that is associated with invasion. The ability of Par6 to interact with oncogenes in distinct cellular processes suggests that Par6 has multiple functions in different contexts. The results presented in this in this chapter, taken together with those above, suggest that the polarity signaling pathways regulated by Par6 plays a cooperative role during the initiation and progression to breast cancer. Thus, a further understanding of the alterations in the Par6 signaling pathways could identify both novel drug targets and predictive biomarkers for breast cancer progression.

Our data combined with other studies have shown that Par6 is amplified genomically, upregulated transcriptionally and Par6 overexpression correlates with ER positive advanced carcinoma. Therefore, it is likely that there is a genetic advantage to increased Par6 expression.

Chapter 4: The Par6–aPKC complex uncouples ErbB2 induced disruption of polarized epithelial organization from proliferation control

Preface:

The experiments presented in this chapter were done in collaboration with other members of the laboratory and published in Nature Cell Biology in 2006. I am including this chapter in my thesis because I have contributed significantly to this study by generating a number of reagents and assisting in experiments. Furthermore these studies were critical to the development of my own projects, both in terms of reagents and scientific ideas. The specific contributions that I made are as follows: generation of Par6 constructs and MCF-10A Par6 expressing cell lines, experimental assistance to first authors, development of the manuscript, and performed preliminary experiments that were followed by the first authors.

Introduction:

Glandular epithelia in organs such as the breast consists of cells that are organized around a central lumen and have an asymmetric distribution of proteins along the apical, lateral and basal surfaces referred to as apical-basal polarity (Drubin and Nelson 1996). In addition to the asymmetric localization of membrane proteins, polarized epithelia orient their Golgi stacks towards the apical membrane suggesting the presence of an intracellular apical-basal axis of polarity. This polarized, glandular organization is an evolutionarily conserved feature that regulates critical functions such as vectorial secretion of milk into the luminal space, in normal mammary glands.

Many oncogenes implicated in carcinoma, when overexpressed in cultured epithelial cells, induce changes in cell morphology and organization. For instance, we and others have previously shown that activation of oncogenes such as ErbB2 (Muthuswamy et al. 2001), K-ras (Schoenenberger et al. 1991), Raf (Li and Mrsny 2000), Fos (Reichmann et al. 1992), Jun (Fialka et al. 1996), Rho and Rac (Jou et al. 1998), Cdc42 (Rojas et al. 2001) and v-Src (Behrens et al. 1993) disrupt apical-basal polarity by altering the localization of apical membrane markers and tight junction proteins. However, the mechanism by which this occurs remains unknown.

Recently, alterations in polarity proteins, such as mutations in Dlg5, have been correlated with the disruption of epithelial organization observed in inflammatory bowel disease (Stoll et al. 2004). Although loss of epithelial organization is an early event in carcinoma development, the possible role of polarity regulators in oncogene-mediated transformation of epithelial cells has not been addressed.

We found that oncogenic signaling by ErbB2 (Chapter 1), disrupts epithelial organization. To model ErbB2 induced changes in epithelial organization, we used the, MCF-10A, in a three-dimensional (3D) culture system (Chapter 1). Activation of ErbB2 in these acini induces uncontrolled proliferation, protects from apoptosis and disrupts normal epithelial organization resulting in formation of large clusters of abnormal-acini (herein referred to as multi-acinar structures), which have luminal space filled with proliferating cells (Muthuswamy et al. 2001). Similar changes in epithelial organization, in particular the presence of multi-acinar structures, are seen in hyperplastic lesions induced by expression of ErbB2 in the mammary gland of transgenic mice (Andrechek et al. 2000). Thus, using the 3D culture model to understand how ErbB2 disrupts epithelial organization will provide critical insights into the development of ErbB2-positive tumors *in vivo*.

In this chapter we demonstrate that activation of ErbB2 disrupts polarized acini by directly interacting with components of the Par polarity complex. Interfering with this interaction blocked the ability of ErbB2 to disrupt polarized epithelial organization and protect cells from apoptosis but not cell proliferation. Thus inhibiting the interaction between ErbB2 and Par complex uncouples ErbB2-induced proliferation from disruption of polarized epithelial organization.

Results:

Activation of ErbB2 in polarized epithelia induces disruption of apical polarity and re-initiates proliferation

Madin-Darby Canine Kidney II (MDCK II) (Musch et al. 2002) cells expressing a synthetic ligand inducible form of ErbB2(Muthuswamy et al. 1999), provided an initial characterization of ErbB2 induced disruption of apical-basal polarity (Muthuswamy et al. 2001). These cells, when plated on a transwell filter form polarized, growth arrested monolayers with normal apical-basal polarity as determined by gp135, ZO-1 (Figure 4.1.A and 4.2.A) and E-cadherin staining (data not shown). I showed that activation of ErbB2 with a dimerizing ligand, AP1510 (Amara et al. 1997), induced re -localization of ZO-1 (Figure 4.1.A) and gp135 (Figure 4.2.A and B) and to the lateral membrane, where ErbB2 is located. In addition, I showed that active ErbB2 re-initiated proliferation as monitored by BrdU incorporation (Figure 4.1.B). We also showed that ErbB2 re-initiated proliferation by flow cytometery (Figure 4.2.D) and induced multilayering of the epithelial monolayer. In Figure 4.1, I show that disruption of polarity occurs within 3 hours of stimulation, whereas proliferation increases after 12 hours (Figure 4.1.B). These experiments suggest that ErbB2 disrupts epithelial cell polarity before and re-initiating cell proliferation. These observations were extensively characterized to determine how ErbB2 was initiating disruption of apical polarity.

Figure 4.1 ErbB2 initiates disruption of tight junction proteins prior to re-initiation of proliferation in polarized mammalian epithelial cells

(A) MDCK–ErbB2 cells grown on porous filters without dimerizer (unstimulated) of stimulated with dimerizer for 24 hr were immunostained for the tight junction marker ZO-1 (Red) and the nuclei (Blue) were co-stained with DAPI. The arrow points to the proper ring like localization of ZO-1 and the arrowheads point to the mislocalized or spotty ZO-1. The Scale bar represents 100 μm.**(B)** Quantitation of percent BrdU incorporation or ZO-1 mislocalization as defined in **(A)** in MDCK–ErbB2 cells grown on porous filters without dimerizer (unstimulated) of stimulated with dimerizer in the presence of BrdU for indicated times. BrdU incorporation was quantitated by visualization of immunofluoresence of BrdU positive cells. Mislocalization of ZO-1 was estimated by visualization of immunofluoresence of cell that contained mislocalized ZO-1. Bars represent average % BrdU incorporation or average % mislocalized ZO-1 +/- S.D. from 3 experiments for 0,6,8,12, and 24 hours and data for 3 and 15 hours was from two experiments. This graph shows that mislocalization of ZO-1 occurs before the re- initiation of proliferation in ErbB2 stimulated MDCK monolayers.

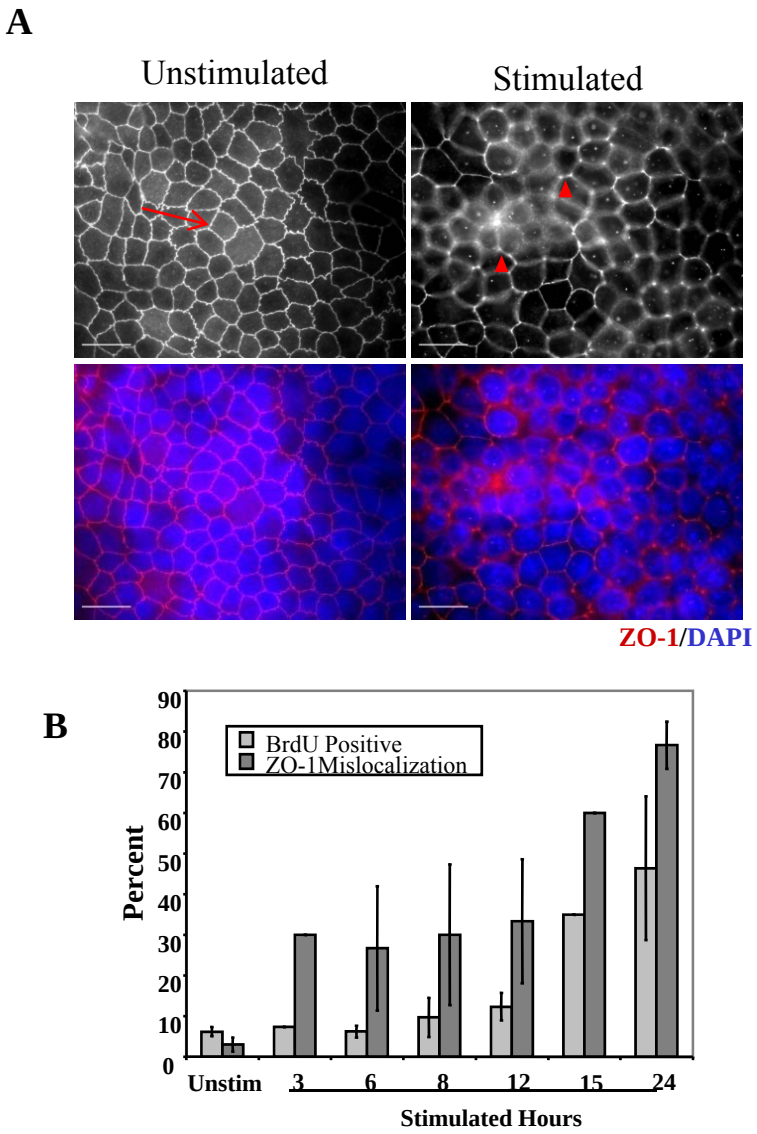

Figure 4.1 ErbB2 initiates disruption of tight junction proteins prior to re-initiation of proliferation in polarized mammalian epithelial cells

Figure 4.2. ErbB2 initiates disruption of apical–basal polarity at the apical–basal border.

(A) MDCK–ErbB2 cells grown on porous filters without dimerizer (unstimulated) of stimulated with dimerizer for 24 h were immunostained for polarized membrane markers: ZO-1 (tight junctions), gp135 (apical membrane); nuclei were costained with DAPI. Top and side boxes, *xz* axis; boxed area, *xy* axis; red arrow, point of plane in *xz* axis that was chosen for the *xy* image. The scale bar represents 10 μm. **(B)** Polarized MDCK–ErbB2 cells stimulated for the indicated times were immunostained with markers as stated above. Optical sections4 μm from the apex of the cell are shown. Schematic representation indicates the approximate position of the *xy* optical sections. **(C)** To quantitate ZO-1 mislocalization, optical sections below 3.0 μm from the apex were analyzed for ZO-1 staining. At least 200 junctions were analyzed and the values represent mean ± s.d. of three independent experiments (green). Red, multilayered regions measured (μm2) by image analysis as described in Methods. Data represent mean ± S.D. of three independent experiments. **(D)** Proliferation monitored by flow cytometry. Data represent mean ± S.D. of three independent experiments.

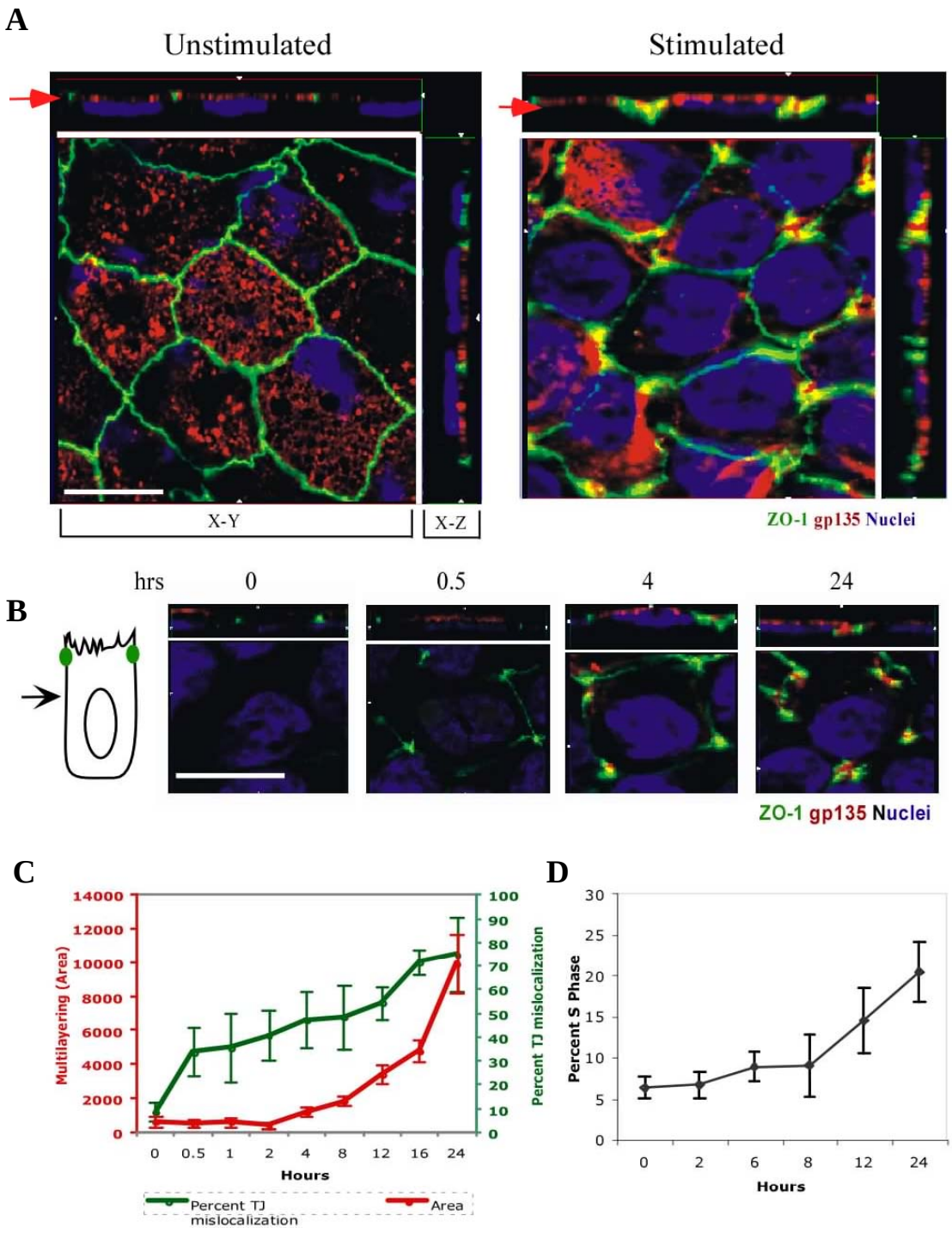

Figure 4.2. ErbB2 initiates disruption of apical–basal polarity at the apical–basal border.

ErbB2-induced disruption of polarity initiates at apical-lateral border

We determined how ErbB2 initiates disruption of apical polarity. In the absence of ErbB2 activation, the apical protein gp135 and the apical-lateral border marker, ZO-1, were restricted to a 3.0 μm region from the cell apex (Figure 4.2.B) in polarized monolayers. However, following 30 minutes of ErbB2 activation, ZO-1 staining was detected in optical sections 4.0 – 5.0 μm from the apex of the cell, without any detectable presence of the apical membrane protein gp135 (Figure 4.2.B). Prolonged activation (2 - 4 hrs) resulted in mislocalization of gp135 (Figure 4.2.B), which was followed by an initiation of the cell cycle (8 – 12 hrs) (Figure 4.2.D) and formation of multilayered epithelial sheets (10 - 18 hrs) (Figure 4.2.C). Thus, ErbB2 initiates disruption of cell polarity at apical-lateral border and progresses towards a loss of apical polarity.

ErbB2 activation disrupts Par complex

It is possible that ErbB2 directly affects the molecular machinery that regulates apical-basal polarity in epithelial cells. The Par complex that is implicated in the establishment and maintenance of the apical-lateral boarder (Chapter 1)(Etienne-Manneville and Hall 2003b; Macara 2004a; Fogg et al. 2005; Yamanaka et al. 2006). We analyzed the localization of exogenous Par6 in ErbB2 expressing MDCK cells by stably expressing flag-epitope Par6 that I generated. Par6 concentrated at the apical-lateral border membrane, and this localization is lost upon activation of ErbB2 (Figure 4.3.A). These data suggests that ErbB2 activation affects the Par complex because Par6 is no longer localized properly after ErbB2 activation.

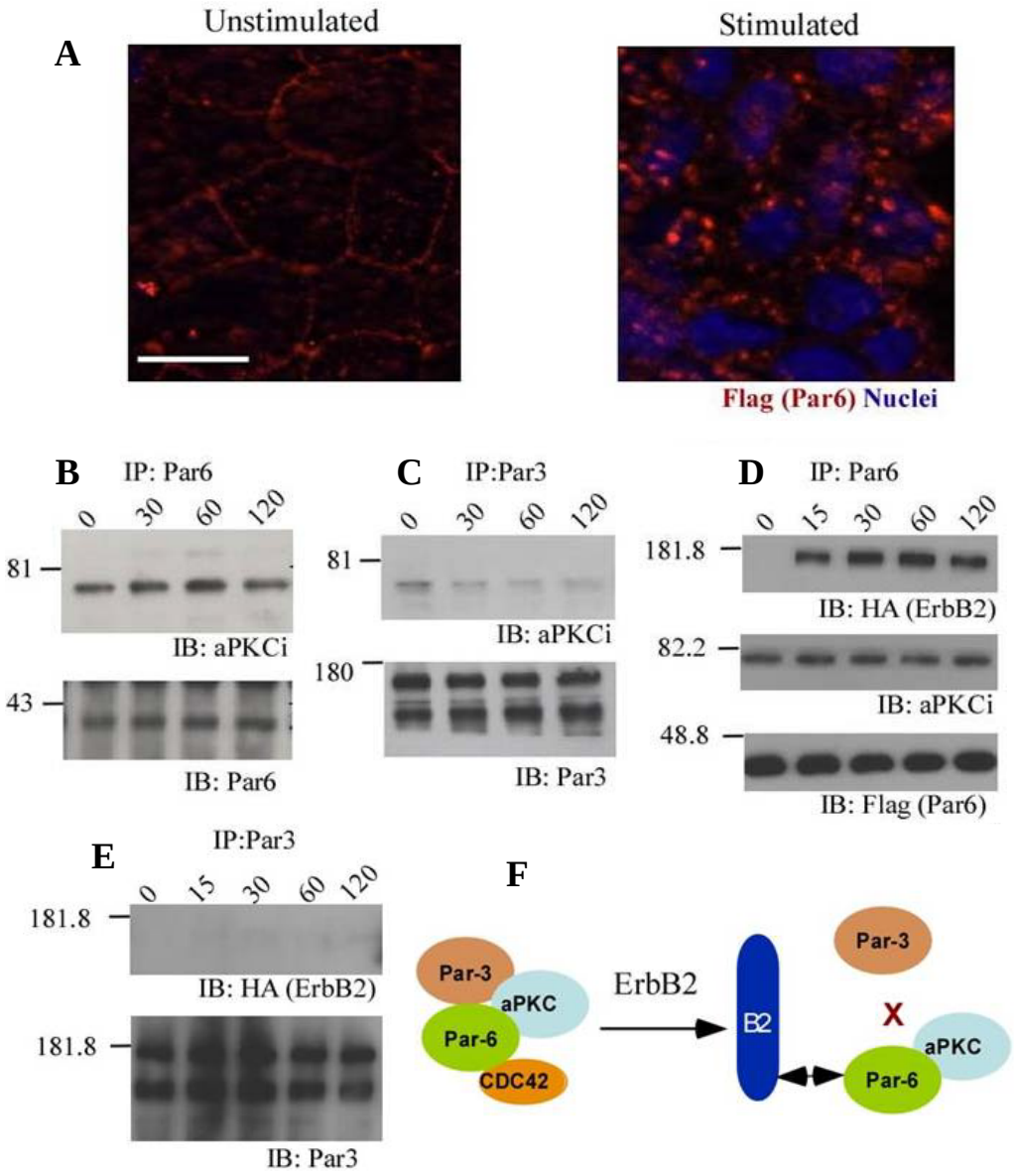

Figure 4.3 ErbB2 disrupts the Par complex and recruits Par6–aPKC

(A) Polarized monolayers of MDCK–ErbB2 cells expressing Flag-tagged Par6 left untreated (unstimulated) or treated with dimerizer (stimulated) for 1 h and immunostained for Flag-tagged Par6. Images were acquired by conventional fluorescence microscopy. The scale bar represents 10 μm. **(B–E)** Extracts from MDCK–ErbB2 **(B, C)** or MDCK–ErbB2 cells expressing Par6 **(D, E)** before and after activation of ErbB2 for the stated times were immunoprecipitated (IP) with anti-Par6 **(B, D)** or anti-Par3 **(C, E)** antibodies and immunoblotted (IB) with indicated antibodies. **(F)** Schematic representation of an active Par complex consisting of Par3–aPKC–Par-6–CDC42. Activation of ErbB2 disrupts the active Par complex by promoting disassociation of Par3 from rest of thecomplex and associating with Par6–aPKC.

In cells that have not formed cell-cell contacts, Par6-aPKC exists in a complex without Par3 binding. Cell-cell contact triggers recruitment of GTP-bound CDC42 and Par3 to form an active Par complex composed of Par-3/Par-6/aPKC/Cdc42-GTP (Yamanaka et al. 2001; Etienne-Manneville and Hall 2003b; Macara 2004a; Fogg et al. 2005; Yamanaka et al. 2006) (Figure 4.3.F). We asked whether ErbB2 affects the Par complex. Activation of ErbB2 induced a more than two-fold decrease in the levels of Par3-aPKC association but did not affect the interaction between aPKC and Par6 (Figure 4.3.B, C and F). Neither Par3 nor Par6 were tyrosine phosphorylated upon activation of ErbB2 (data not shown) suggesting that they were not direct substrates of ErbB2 kinase activity. Interestingly, ErbB1/EGFR, a related receptor tyrosine kinase lacking the ability to disrupt polarity (Muthuswamy et al. 2001), did not affect the interaction between the members of the Par complex (data not shown) suggesting that the ability to disrupt Par complex may be related to oncogene-induced disruption of apical-basal polarity.

ErbB2 associates with Par6-aPKC

A recent study demonstrated that Par6 associates with Transforming Growth Factor (TGF)β receptor type-1 and that this interaction is required for TGFβ-induced epithelial-mesenchymal transition (Ozdamar et al. 2005). We found that Par6-aPKC associated with ErbB2 within 15 minutes of receptor dimerization and the interaction was sustained thereafter (Figure 4.3.D and data not shown). However, we failed to detect association between Par3 and ErbB2 (Figure 4.3.E), suggesting ErbB2 associates with Par6-aPKC but not Par3 (Figure 4.3.F). Unlike the TGFβR1-Par6 interaction that does not require ligand binding, the ErbB2-Par6 interaction requires receptor dimerization

suggesting that Par6-aPKC may utilize distinct mechanisms to interact with cell surface receptors. Thus, ErbB2 recruits Par6-aPKC to its signaling complex.

ErbB2-Par6-aPKC association is required for disruption of apical-basal axis of polarity.

We have previously demonstrated that activation of ErbB2 induces the formation of multiaciniar structures with filled lumen in MCF-10A cells expressing ErbB2 (10A.ErbB2). Although MCF-10A cells lack tight junctions, they posses a distinct apical-basal axis of polarity as determined by localization of the *cis*-Golgi matrix protein GM130 (Debnath et al. 2002). Whereas epithelia in unstimulated acini localized GM130 on the side of the nuclei facing the lumen, activation of ErbB2 frequently relocalized GM130 to sides facing lateral or basal surface of the cells in acini with a luminal space (Figure 4.4.A). Moreover, cells within the filled lumens had no specific pattern to GM130 orientation (data not shown). Thus, activation of ErbB2 disrupts the apical-basal axis of polarity of MCF-10A cells in 3D organized acini.

To determine if ErbB2-Par6-aPKC interaction is required for ErbB2-induced disruption of apical-basal axis of polarity, I generated a Par6 mutant that is defective for binding to aPKC ($Par6^{K19A}$) and expressed this mutation and wildtype Par6 in 10A.ErbB2 cells (Chapter 2). As observed in MDCK cells, activation of ErbB2 induced recruitment of $Par6^{wt}$-aPKC complex to the receptor (Figure 4.4.B). As anticipated, the

Figure 4.4. Par6–aPKC is required for ErbB2-induced transformation of MCF10A three-dimensional (3D) acini.

(A) Day 20 acinar structures stimulated with dimerizer for four days were immunostained for a *cis*-Golgi matrix protein, GM130 (red). Nuclei were costained with DAPI. Arrows, mislocalization of GM130 to the lateral (L) or basal (B) surfaces. The scale bars represent 50 μm. **(B)** Extracts from 10A–ErbB2 cells expressing Par6 or Par6K19A immunoprecipitated with anti- ar6 antibodies and immunoblotted with anti-HA, anti-aPKCi, and anti-Flag–Par6 antibodies. **(C)** Phase images of unstimulated day 8 acinar structures or stimulated with dimerizer for four days. Inserts show details of acinar morphology. The scale bars represent 100 μm. **(D)** Number of multistructures quantified by image analysis. Data represent means ± S.D. from three different experiments. **(E)** Area of the acini was measured using Zeiss AxioVison 4.4 software and ata plotted as box plots. The median value (line within the box), inter-quartile range representing 50% of the data (boundaries of the box), the spread (vertical lines) representing 1.5 times the inter-quartile range and outliers (horizontal lines) are shown. Each condition represents area measurements from approximately 1200 acini from three independent experiments.

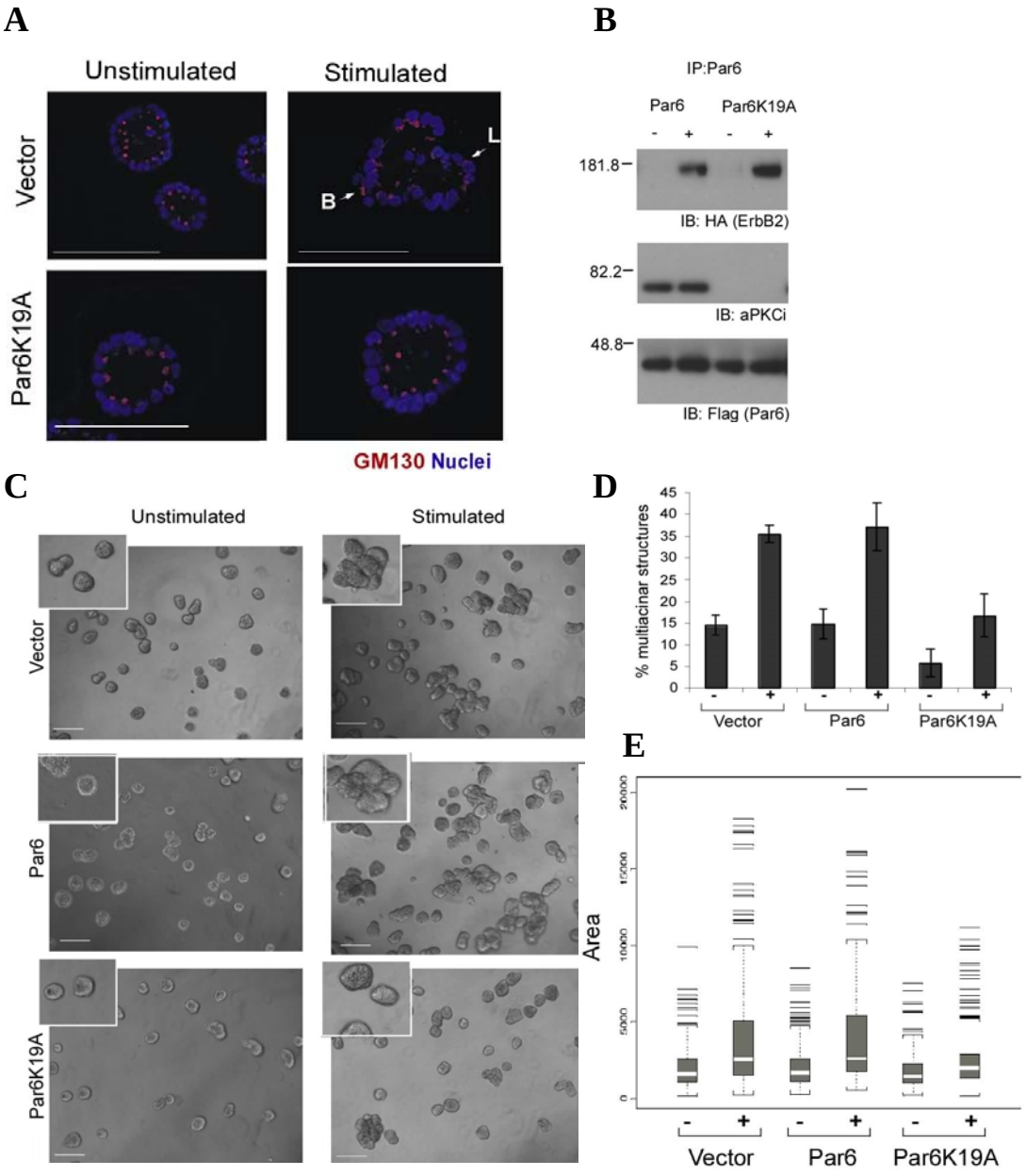

Figure 4.4. Par6–aPKC is required for ErbB2-induced transformation of MCF10A three-dimensional (3D) acini.

Par6^{K19A} failed to interact with aPKC but was still able to interact with ErbB2 (Figure 4.4.B). Interestingly, activation of ErbB2 in Par6^{K19A} expressing cells failed to mislocalize GM130 to lateral or basal surface of the nuclei (Figure 4.4.A) demonstrating that the interaction with Par6-aPKC complex is required for ErbB2 induced disruption of apical-basal axis of polarity.

ErbB2-Par6-aPKC pathway is required for formation of multi-acinar structures.

To investigate if the ErbB2-Par6-aPKC interaction is required for formation of multi-acinar structures, ErbB2 was activated in 3D acini derived from cells expressing Par6^{K19A} or Par6^{wt} or parental control. Activation of ErbB2 induced the formation of multi-acinar structures in parental and Par6^{wt} expressing cells. However, these structures were significantly reduced in cells expressing the Par6^{K19A} mutant (Figure 4.4.C and D). To avoid sampling bias, we measured the area of acini populations to analyze differences in their size (as performed in Chapter 3) (Figure 4.4.D). Activation of ErbB2 in parental or wild type Par6 expressing cells induced a significant change in the distribution of acini size (Figure 4.4.E) ($p<0.005$), whereas activation of ErbB2 in cells expressing Par6^{K19A} did not dramatically alter the size distribution (Figure 4.4.E) ($p<0.005$). The effect of expressing Par6^{K19A} was specific to ErbB2 induced changes because it did not affect epidermal growth factor (EGF)-induced normal morphogenesis (Figure 4.4.C and E) Thus, the association between ErbB2 and Par6-aPKC is critical for ErbB2-induced disruption of apical-basal axis of polarity and formation of multi-acinar structures.

ErbB2-Par6-aPKC pathway is not required for ErbB2-induced proliferation

In addition to disrupting 3D organized epithelia, ErbB2 is a potent inducer of cell proliferation (Figure 4.1 and 4.2). To investigate whether the ErbB2-Par6-aPKC pathway controls proliferation, we monitored ErbB2-induced changes in cell proliferation in control, $Par6^{wt}$ and $Par6^{K19A}$ expressing cells. Interestingly, ErbB2 induced proliferation in $Par6^{K19A}$ expressing cells was similar to that of control or $Par6^{wt}$ expressing cells grown in 3D cultures (Figure 4.5.A). In addition, the ability of ErbB2 to induce EGF-independent proliferation of MCF-10A cells grown as monolayer cultures was not affected by expression of $Par6^{wt}$ or $Par6^{K19A}$ (Figure 4.5.B). Thus, disrupting the ErbB2-Par6-aPKC complex uncouples the ability of ErbB2 to induce multi-acinar structures from inducing proliferation.

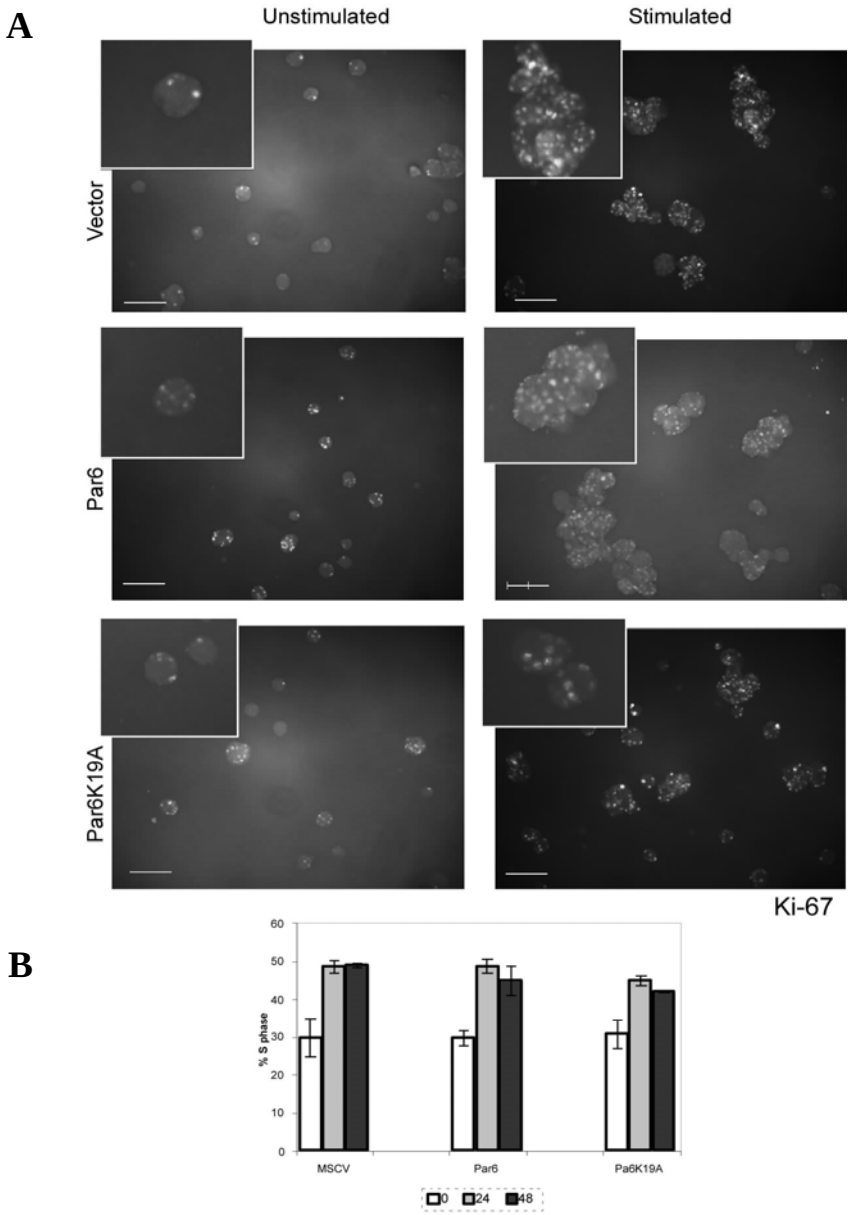

Figure 4.5. ErbB2–Par6–aPKC interaction is not required for ErbB2-induced proliferation.

(A) Ki67 staining of day 8 acinar structures from 10A–ErbB2–vector (vector), 10A–ErbB2–Par6 (Par6) or 10A–ErbB2–Par6^{K19A} (Par6K19A) cells grown with or without ErbB2 activation for four days. The scale bars represent 100 μm. **(B)** Proliferation analysis in normal culture conditions by flow cytometry. Data are means of S–G2 phase percentage ± S.D. from three independent experiments.

Discussion:

In this study we have demonstrated that polarity regulators are required for ErbB2 induced disruption of 3D acini. The interaction with polarity proteins uncouples the ability of ErbB2 to induce proliferation from its ability to induce formation of multi-acinar structures.

We have demonstrated that interaction with polarity genes is required for ErbB2 induced disruption of apical-basal axis of polarity and formation of multi-acinar structures. In addition to being downstream of oncogenes, it is possible that disruption of polarity regulators can initiate loss of tissue organization and increased growth. In *Drosophila*, loss-of-function mutation of polarity genes promotes uncontrolled proliferation and abnormal tissue architecture (Bilder 2004). In humans, genetic variations in Dlg5, a polarity regulator gene, are associated with inflammatory bowel disease, which increases the risk of gastric cancer (Dranoff 2004; Stoll et al. 2004). Thus, loss of cell polarity can either function as an initiating event or as a cooperating event during development of carcinoma.

Our observation of uncoupling of cell proliferation and disruption of cell polarity supports and advances previous studies. The GTP binding protein Rac1 is required for disruption of cell polarity and not for proliferation in transformed epithelia (Liu et al. 2004). Signal Transducer and Activator of Transcription 3 (STAT3) is required for ErbB2 induced disruption of epithelial cell polarity and not proliferation (Guo et al. 2006). It is unclear how Rac and STAT3 initiated pathways regulate epithelial cell polarity, independent of their ability to control proliferation (Downward 2003; Yu and Jove 2004). Our present study demonstrates that oncogenes disrupt cell and tissue

organization by directly regulating polarity proteins. Thus, while the well-established Ras-ERK pathway controls cell proliferation during ErbB2-induced oncogenesis (Hynes and Lane 2005; Citri and Yarden 2006), we identify the Par6-aPKC as mediators of changes in cell polarity.

Our observations have led us to a model for how regulators of apical-basal polarity can suppress transformation of polarized epithelial cells. Under normal conditions, polarity genes promote maintenance of glandular organization by acting as a 'checkpoint' and preventing survival of cells responding to unscheduled proliferation signals. Oncogenes that induce proliferation and disrupt polarity genes can overcome the checkpoint and disrupt 3D organization of epithelia by a loss of cell polarity and survival of the cell in the lumen

Par6-aPKC regulates phosphorylation of other polarity proteins such as Lgl, Par3, and members of the Crumbs polarity complex (Etienne-Manneville and Hall 2003b; Macara 2004a; Fogg et al. 2005; Yamanaka et al. 2006), during establishment of polarity. It will be of interest to identify direct and indirect targets of Par6-aPKC that are required for disruption of 3D organized epithelia.

It is likely that the targets of the Par6-aPKC will provide new opportunities for treating ErbB2 positive breast cancers. Atypical PKC targets may not be restricted to ErbB2 positive cancer because aPKC is overexpressed in ovarian and NSCL carcinoma, and correlates with poor clinical prognosis (Eder et al. 2005; Regala et al. 2005b). Thus, further analyses of Par6-aPKC pathway may identify novel targets for early stage carcinoma.

Chapter 5:

Activation of ErbB2 promotes invasion of dominant negative RhoA expressing MCF-10A acini

Introduction:

ErbB2 is amplified in up to 85% of comedo-type ductal carcinoma in-situ (DCIS), a pre-malignant human breast lesion. Genomic amplification of ErbB2 correlates with progression to invasive breast cancer and poor clinical prognosis (Slamon 1987; Hynes and Stern 1994; Harari and Yarden 2000).. Elucidation of the mechanisms responsible for the formation of DCIS and advancement to invasive breast cancer is critical to our understanding of disease progression. We have an established model system to study the effects of ErbB2 in normal breast epithelial acinar like structures. Activation of ErbB2 in MCF-10A acinar structures stimulates proliferation, inhibits apoptosis and induces the formation of multi-acinar structures (Muthuswamy et al. 2001). ErbB2 induced multi-acinar structures share properties DCIS. Specifically, both structures are hyperproliferative, non-invasive and have altered epithelial cell organization. This established DCIS model system is useful to study the mechanisms that ErbB2 uses to initiate transformation of human breast epithelial cells. This system can also be used to study alterations that promote invasion of the DCIS-like, ErbB2 transformed structures.

One family of proteins that is overexpressed in breast cancer is the Rho family of GTPases (Fritz et al. 1999; Fritz et al. 2002). RhoGTPases (RhoA, Rac1 and Cdc42) are small GTP binding proteins that cycle between active an inactive states (Chapter 1).

These proteins are known regulators of the cell cytoskeleton and more recently have been shown to be involved in various cell processes such as cell proliferation, cell polarity, and cell migration. RhoGTPase have also been shown to play a role in oncogenic transformation. For example, Rho, Rac and Cdc42 activity are required during the transformation of fibroblasts by oncogenic Ras, a small GTPase (Chapter 1) (Prendergast et al. 1995; Qiu et al. 1995a; Qiu et al. 1995b; Roux et al. 1997; Zohn et al. 1998). Interestingly, there have been no reports of mutant Rho proteins in human breast tumors. Therefore it is likely that the RhoGTPase contribution to tumorigenesis involves aberrant regulation of activity or expression. While the above studies have implicated the RhoGTPase proteins in established cancers, their role in tumorigenesis is not well understood.

The RhoGTPases are involved in regulating the cellular organization through protein-protein interactions. Both Rac1 and Cdc42 directly bind the Par6/aPKC polarity complex and these interactions are necessary for many different cell processes such as cell polarity, migration and transformation (Chapter 1). We have shown that the Par complex is important during ErbB2 induced transformation of epithelial acini. Activation of ErbB2 requires the interaction with the Par6/aPKC in order to disrupt acinar organization and form multi-acinar structures (Aranda et al. 2006). However, we do not know if RhoGTPase activity is required for ErbB2 induced transformation. One of the aims of this chapter is to determine if ErbB2 requires active Rac1 and Cdc42 to initiate transformation of human breast epithelial cells.

While both Rac1 and Cdc42 bind directly to the Par6/aPKC complex, RhoA has been indirectly linked to this complex. In migrating epithelial cells, Par6/aPKC is

localized to the leading edge and binds the the ubiqitin ligase Smurf1, which in turn targets RhoA for degradation via the proteasome (Wang et al. 2003). A subsequent study confirmed this interaction in a murine mammary epithelial cell system. This study showed that upon stimulation with transforming growth factor β (TGFβ), TGFβ type II receptor interacts and phosphorylates the polarity protein Par6. This phosphoryation event recruits Smurf-1 ubiquitin ligase which subsequently degrads RhoA leading to an epithelial to mesenchyml transition (Ozdamar et al. 2005). Elucidation of this mechanism is of particular interest to us because ErbB2 cooperates with transforming growth factor β (TGFβ) to promote invasion of MCF-10A acini in the DCIS model system described above (Seton-Rogers et al. 2004). Therefore it is plausible to think that TGFβ stimulation in MCF-10A acini could be degrading RhoA and together promoting invasion of acinar structures. RhoA downregulation has also been shown to be important in promoting the invasive potential of breast cancer cells (Simpson et al. 2004; Bellovin et al. 2006; Wu et al. 2007). The above studies suggest that downregulation of RhoA is important during invasion. Therefore the second aim of this chapter is to determine if downregulation of RhoA cooperates with ErbB2 to promote invasion of non-invasive transformed structures.

In this chapter, I will address whether the Rac1 and Cdc42 activity is required for ErbB2 induced transformation and I will also investigate how a non-invasive ErbB2 transformed structure could become invasive in the presence of downregulated RhoA activity. To address these questions, I will combine the inducible ErbB2 DCIS model system (Muthuswamy et al. 1999; Muthuswamy et al. 2001) and an adenoviral gene expression system to introduce dominant negative RhoGTPase protein expression in

acinar structures. The dominant negative mutations prevent the exchange of GDP to GTP by sequestering the guanine exchange factors (GEFs); thereby keeping the RhoGTPase in a constant inactive GDP bound state. This gene expression system has two advantages. First, adenovirus is capable of infecting non-dividing cells, and second, gene expression is under a tetracycline (Tet-Off) regulated promoter allowing for infection controls without protein expression. It is important to control for adenoviral infection because adenovirus has been shown to induce an interferon and apoptotic response (Russell 2000). These responses could confound the phenotype produced by ectopic protein expression. Therefore, all experiments performed will have an infection control. There are two additional disadvantages of this expression system. First, the adenoviral vector is not replicative within cells; therefore protein expression will be decreased as the infected cells proliferation. Second, adenovirus expresses high levels of protein which could negatively affect the cells. However, the high levels of ectopic expression could off-set the reduction of protein expression in proliferating cells. Despite these caveats, this system allows for precise regulation of RhoGTPase protein expression in MCF-10A acinar structures. Combining the DCIS model and the adenoviral gene expression system, will allow us to address the role of RhoGTPase activity in ErbB2 induced transformation.

Results:

Expression of RhoGTPase mutants effect MCF-10A acinar structures.

The focus of the chapter is to determine the effect of dominant negative RhoGTPase in ErbB2 transformed acinar structures. However, we were give reagents that contain a panel of both dominant negative (RacN17 and RhoN19) and dominant active (RacV12, RhoV14 and Cdc42L61) versions of the RhoGTPases. Unlike the dominant negative mutation that sequesters GEFs, the dominant active mutation prevents GTPase activity, therefore keeping the protein in an active state. The entire panel was tested in parental MCF-10A acini as a control before we tested the dominant negative proteins in ErbB2 expressing acini. First, we determined that the adenoviral system was able to express the RhoGTPase proteins in MCF-10A acinar structures. Polarized, growth arrested acinar structures were infected and protein expression was detected four days after infection by immunofluorescence (Figure 5.1). We determined that RacN17 and RhoN19 had no detectable effect on the acinar structures (Figure 5.2). However, expression of the dominant active versions of the RhoGTPase all disrupted acinar structures (Figure 5.2). Active Rac1 induced the most severe phenotype compared to RhoV14 and Cdc42L61. The cells within the acinar structures appeared to be protruding and blebbing from the main acini. Active Rho and Cdc42 also disrupted the structures and formed blebs of cells that were associated with the main acinar structure. The mechanism that these active mutants used to disrupt these organized acinar structures has yet to be determined. Further experiments need to be performed in order to determine how the active GTPase can disrupt acinar structures. Since we see different phenotypes

Figure 5.1. Expression of Cdc42L61, RacV12 and RacN17 in acinar structures

Day 12 MCF-10A acinar structures were infected with adenovirus (MOI 60) expressing either RacN17 or Cdc42L61. Tetracycline (Expression OFF) was added at the time of infection to prevent protein expression in control acinar structures. After 4 days, protein expression was detected by immunofluoresence with Rac or Cdc42 (Green) antibodies and co-stained with DAPI nuclei stain.

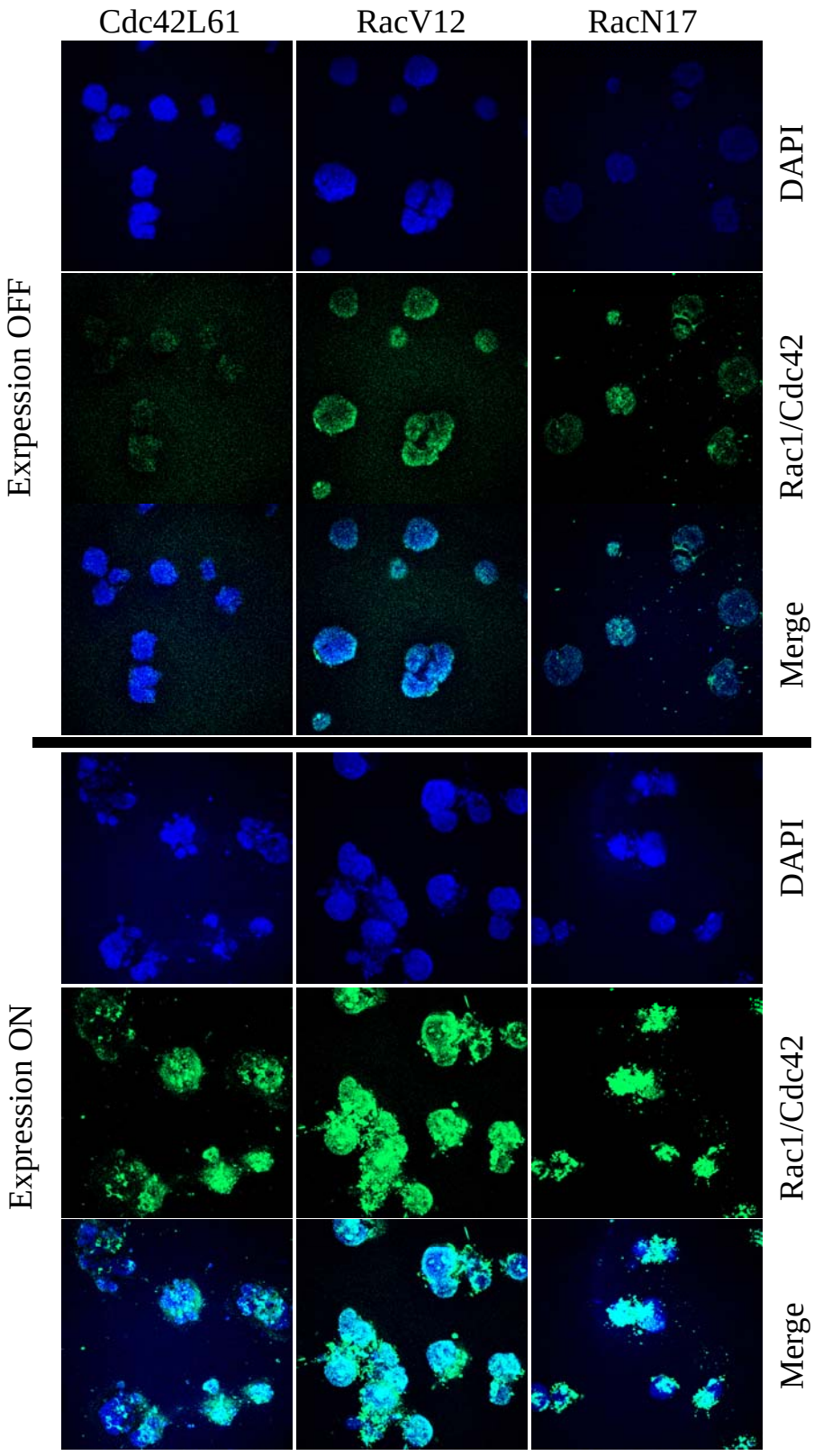

Figure 5.1. Expression of Cdc42L61, RacV12 and RacN17 in acinar structures

Figure 5.2. Expression of RacV12, RacN17, RhoV14, RhoN19 andCdc42L61 has different effects in acinar structures

Day 12 MCF-10A acinar structures were infected with adenovirus (MOI 60) expressing either RacN17 or Cdc42L61. Tetracycline (Expression OFF) was added at the time of infection to prevent protein expression in control acinar structures. Phase images show that expression of RacV12, RhoV14 and Cdc42L61 disrupts acinar structures. RacN17 and RhoN19 has no detectable effect on acinar morphology. Inserts show detail of the disruption. Arrows point to the blebbing cells and arrowhead points to the protrusions in RhoV14 expressing structures. Scale bar 100μM.

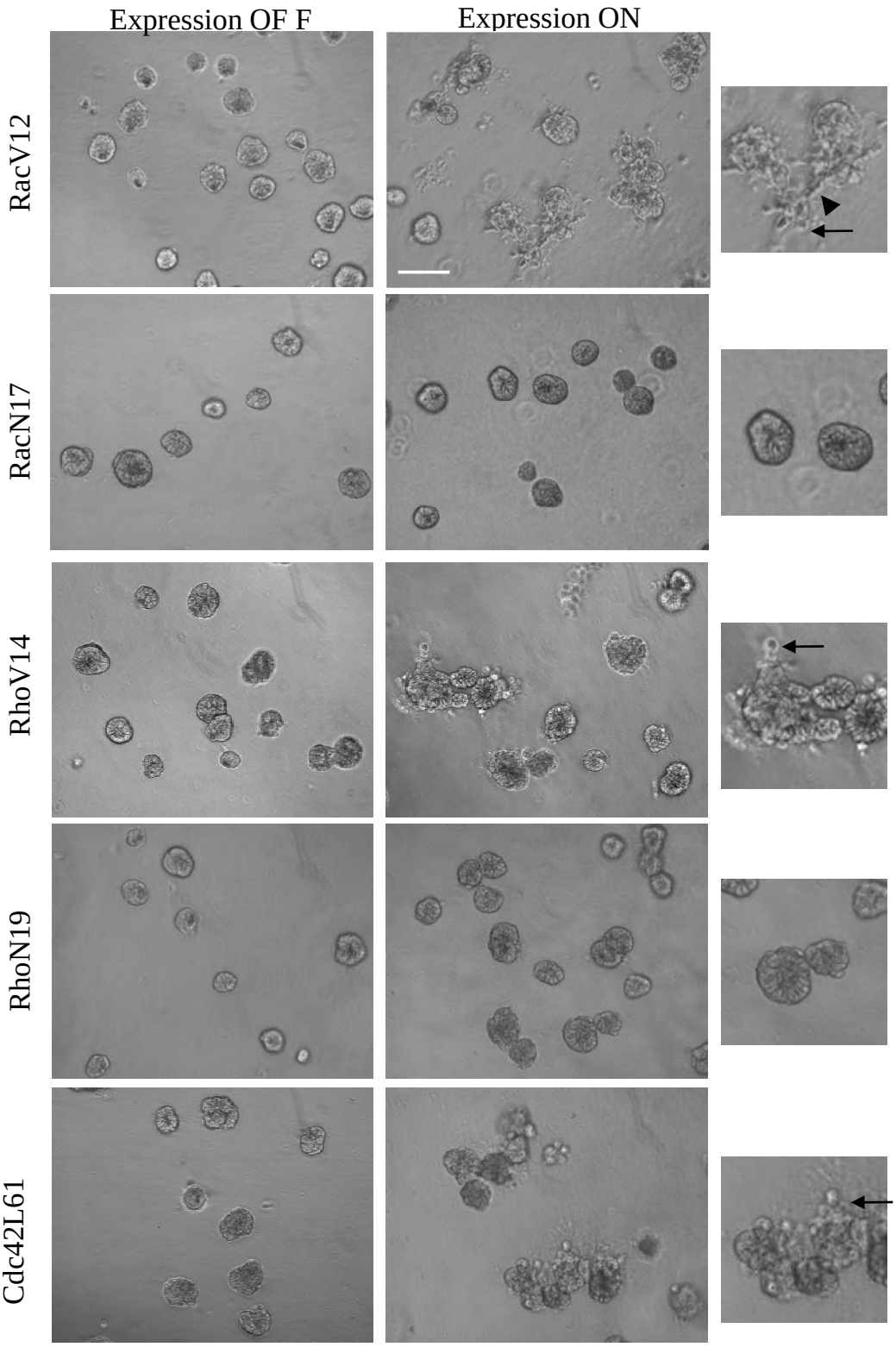

Figure 5.2. Expression of RacV12, RacN17, RhoV14, RhoN19 andCdc42L61 has different effects in acinar structures

between expression of the active mutations and the dominant negative mutations it was of great interest to determine if the dominant negative proteins will have an effect in activated ErbB2 acinar structures.

Expression of dominant negative Rac, Cdc42 did not affect ErbB2 induced multi-acinar structure formation.

To determine if downregulation of Rac1 or Cdc42 activity inhibited ErbB2 induced transformation, we infected growth arrested MCF-10A acinar structures expressing chimeric ErbB2 (10A.ErbB2) with Tet-Off RacN17 or Cdc42N17 expressing adenovirus. Tetracycline regulated RacN17 and Cdc42N17 protein expression was observed by western analysis (Figure 5.3.A and B). ErbB2 was activated 24 hours post-infection to allow for RhoGTPase protein expression in 10A.ErbB2 acinar structures. Consistent with previous results activation of ErbB2 transformed the cells and induced the formation of multi-acinar structures (Figure 5.4, arrowheads). Multi-acinar structures are defined as a structure containing three or more acini. This definition eliminated false negatives because it accounted for the random chance of two acinar structures that grew adjacent to other. Using this criterion, I determined that expression of RacN17 and Cdc42N17 had no affect on ErbB2 induced multi-structure formation (Figure 5.4-5.5). However, Cdc42N17 expressing acinar structures had many cells that were not contained within the main acinar body (Figure 5.5, arrows). This phenotype was in independent of ErbB2 activation which suggests that regulation of Cdc42 and not Rac1 activity is necessary to maintain the organization of MCF-10A acinar structures. Since, Cdc42 and Rac1 bind the same interacting domain of Par6, it is possible that Cdc42 is the more

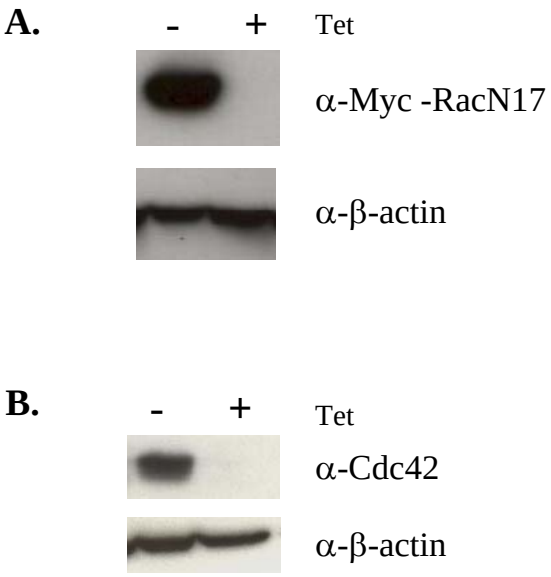

Figure 5.3. Expression of RacN17 and Cdc42N17 in acinar structures

Day 12 10A.ErbB2 acinar structures were infected with adenovirus (MOI 60) expressing either **(A)** RacN17 or **(B)** Cdc42. Tetracycline (Tet) was added at the time of infection to prevent protein expression in control acinar structures. After 5 days, cell extracts were generated and protein expression was detected by immunoblotting (IB) with 9E10 myc or Cdc42 antibodies.

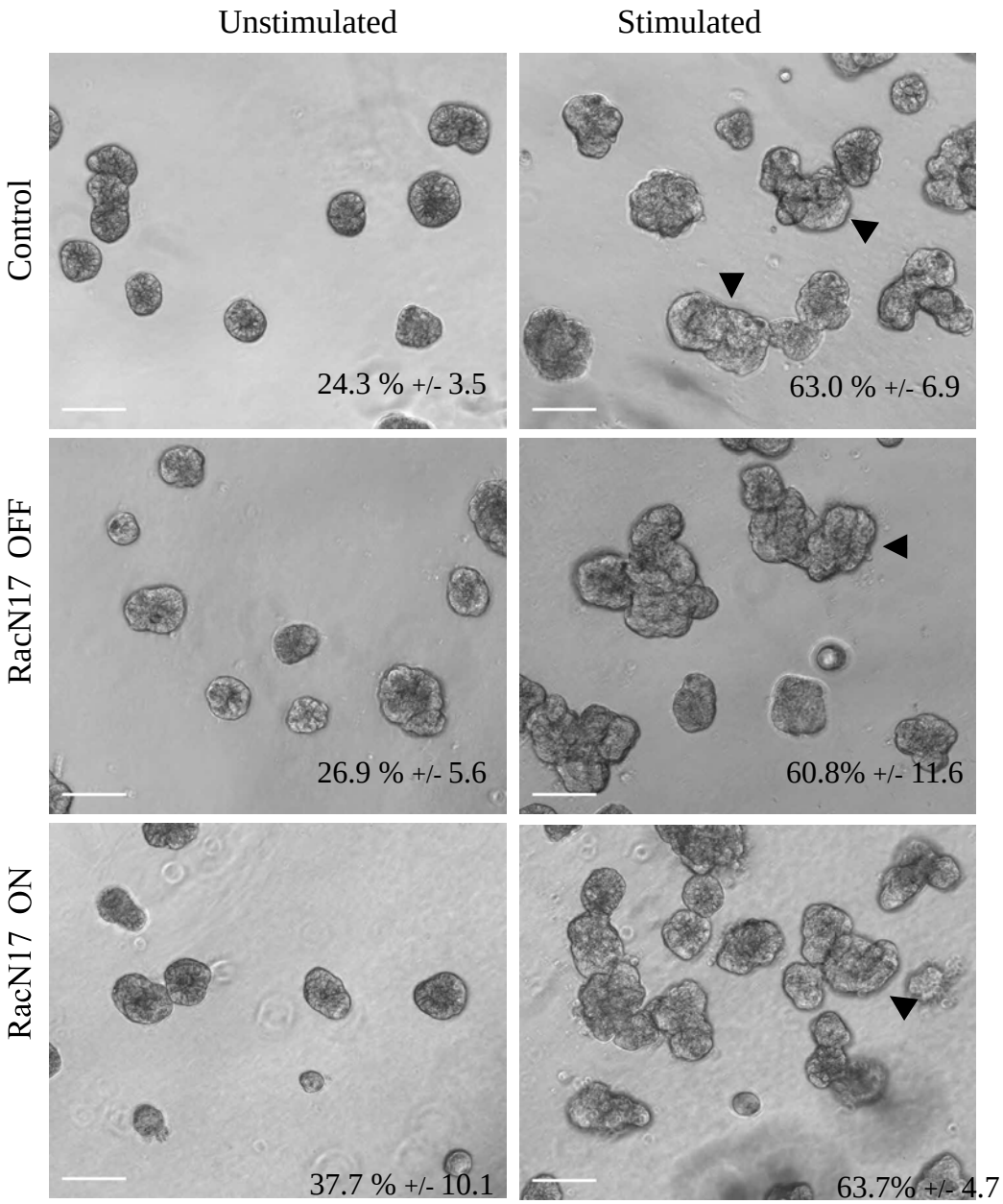

Figure 5.4. Expression of RacN17 does not affect ErbB2 induced multi-acinar structure formation

Day 12 10A.ErbB2 acinar structures were infected with adenovirus (MOI 60) expressing RacN17. Tetracycline (OFF) was added at the time of infection to prevent protein expression in control acinar structures. 24 hours post-infection ErbB2 was stimulated with dimerizer or left unstimulated for 4 days. Phase images show that expression of RacN17 had no affect on ErbB2 induced multi-acinar formation. The percent multi-acinar structures was quantitated. Data represent means ± S.D. of 600 structures from three independent experiments, scale bar 100μM.

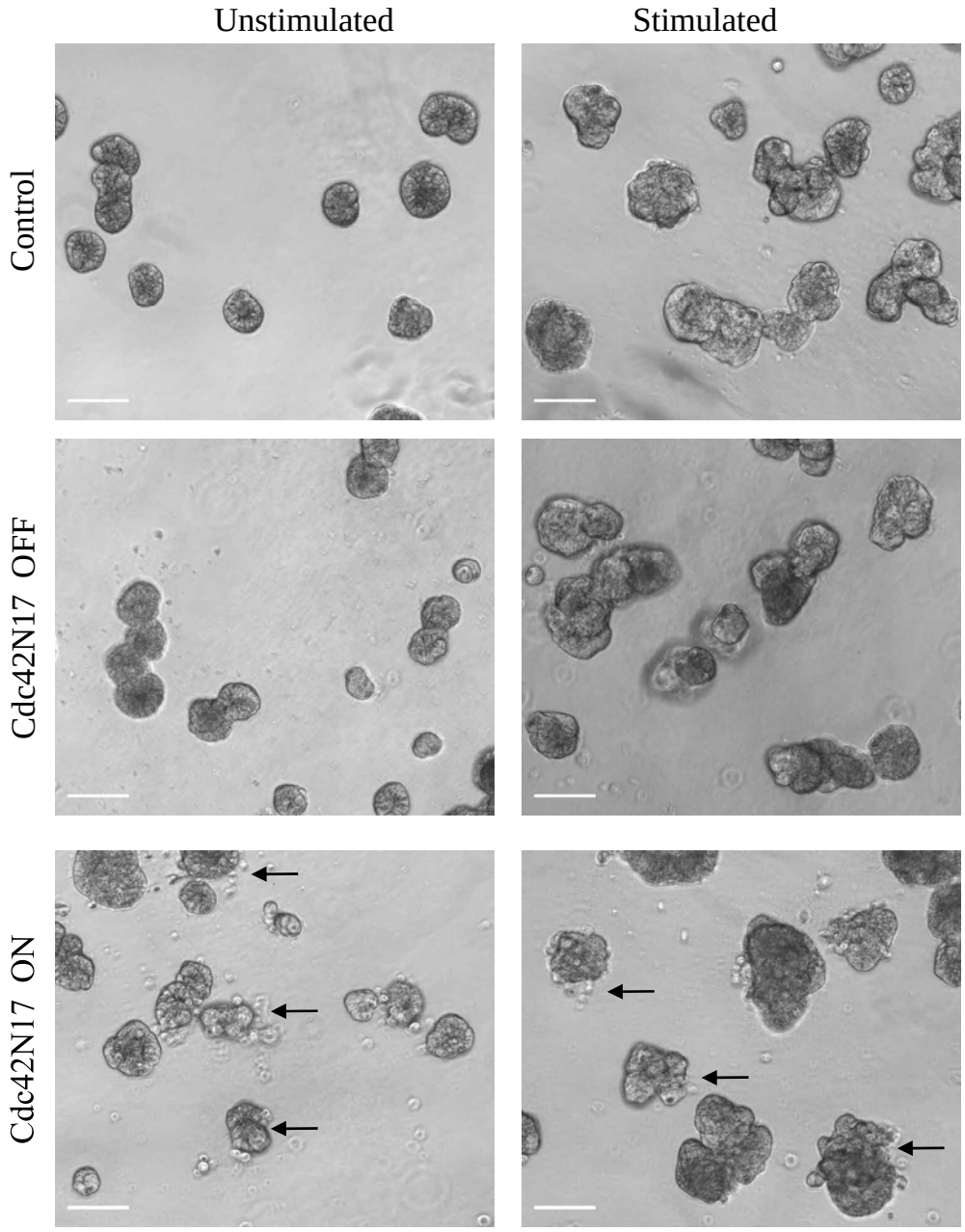

Figure 5.5. Expression of Cdc42N17 disrupts acinar structures

Day 12 10A.ErbB2 acinar structures were infected with adenovirus (MOI 60) expressing Cdc42N17. Tetracycline (OFF) was added at the time of infection to prevent protein expression in control acinar structures. 24 hours post-infection ErbB2 was stimulated with dimerizer or left unstimulated for 4 days. Phase images show that expression of Cdc42N7 has no effect on multi-acinar formation in the ErbB2 stimulated condition. However, arrows point to disrupted acinar (bottom left, unstimulated) or multi-acinar (bottom right, stimulated) structures that express Cdc42N17. Scale bar 100μM.

prominent RhoGTPase interaction in this cell system. This could explain why inhibition of Cdc42 and not Rac disrupts acinar organization. More experiments need to be performed to determine how expression of dominant negative Cdc42 disrupts preformed MCF-10A acinar structures.

Since neither Cdc42N17 nor RacN17 expression affected ErbB2 induced transformation as observed by multi-acinar structure formation (Figure 5.4-5), I focused on testing the hypothesis that expression of dominant negative RhoA will effect ErbB2 induced transformation by promoting invasion.

Activation of ErbB2 promoted blebbing protrusions in RhoN19 expressing acinar-structures

To determine if dominant negative RhoA (RhoN19) promoted invasion of ErbB2 activated acinar structures we infected 10A.ErbB2 acini with RhoN19 expressing adenovirus and activated ErbB2 (Figure 5.6.A). Expression of RhoN19 in the presence of activated ErbB2 generated a novel blebbing phenotype, without affecting the formation of multi-acinar structures (Figure 5.6.C). The cells within ErbB2 activated acinar structures appeared to be blebbing or protruding from the main multi-acinar structure (Figure 5.6.B, arrows). Figure 5.7.A shows a higher magnification of a multi-acinar structure that contains many blebbing protrusions. The percent of structures that contained blebs were quantitated and any multi-acinar structure that had at least one bleb was counted as positive for presence of blebs. The graph in Figure 5.7.B demonstrates that only activated ErbB2 and RhoN19 expressing structures formed blebbing

Figure 5.6. Expression of RhoN19 does not affect the formation of ErbB2 induced multi-acinar structures

Day 12 10A.ErbB2 acinar structures were infected with adenovirus (MOI 60) expressing RhoN19. Tetracycline (OFF) was added at the time of infection to prevent protein expression in control acinar structures. 24 hours post-infection ErbB2 was stimulated with dimerizer or left unstimulated for 4 days. **(A)** Cell extracts were generated and RhoN19 protein expression was detected by IB using a RhoA antibody. **(B)** Phase images show that expression of RhoN19 had no effect on ErbB2 induced multi-acinar formation. However, expression of RhoN19 in ErbB2 activated acinar structures form blebbing protrusions (arrows, bottom right). **(C)** The percent multi-acinar structures was quantitated. Data represent means ± S.D. of 600 structures from three independent experiments, scale bar 100μM.

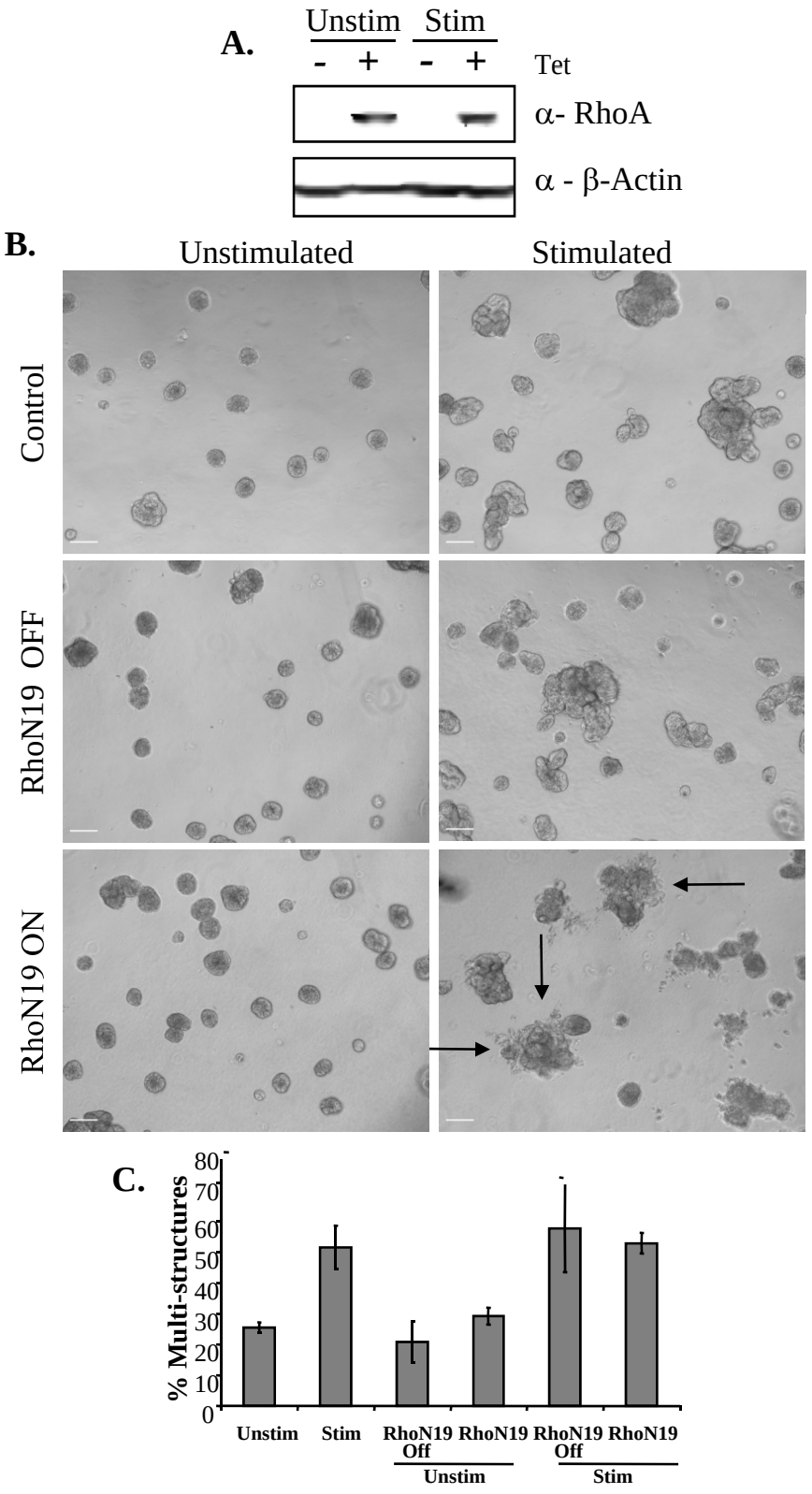

Figure 5.6. Expression of RhoN19 does not affect the formation of ErbB2 induced multi-acinar structures

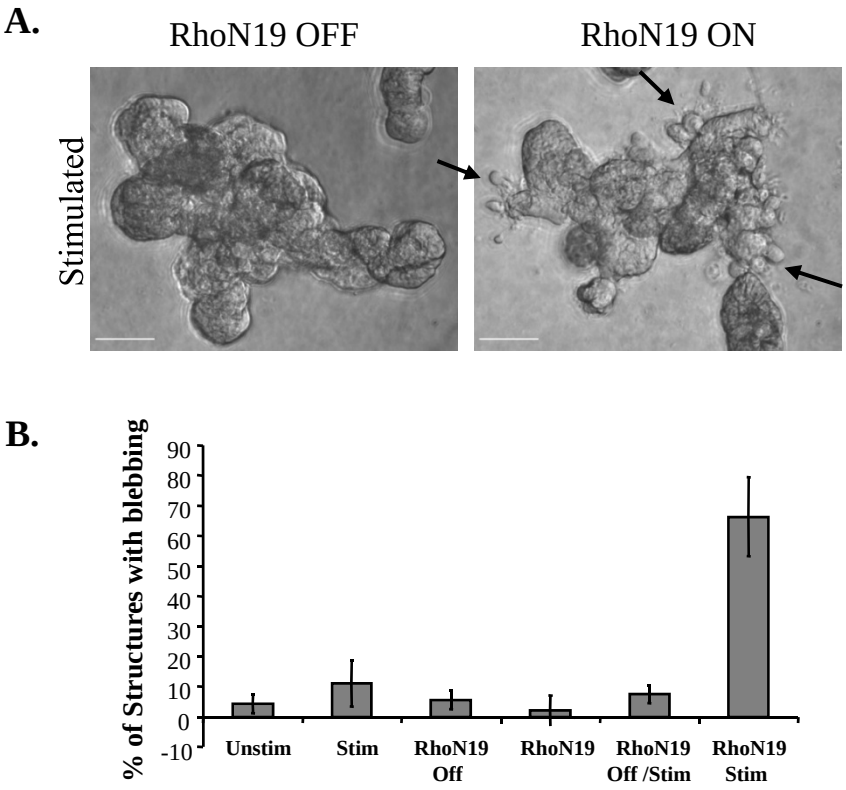

Figure 5.7. Activation of ErbB2 and expression of dominant negative RhoA induces blebbing protrusions.

(A) Day 12 10A.ErbB2 acinar structures were infected with adenovirus (MOI 60) expressing RhoN19. Tetracycline (OFF) was added at the time of infection to prevent protein expression in control acinar structures. 24 hours post-infection ErbB2 was stimulated with dimerizer or left unstimulated for 4 days. High magnification phase images of ErbB2 induced multi-acinar structures with (right) and without (left) RhoN19 expression. Arrows point to the blebbing protrusions, with multiple cells extending from main acinar body, scale bar 50μm. **(B)** The percentage of structures that contained one or more blebbing protrusion was quantified by image analysis. Data represent means ± S.D. of 600 structures from three different experiments.

protrusions. These results suggest that downregulation of the RhoA activity cooperates with ErbB2 activation to promote invasion of MCF-10A cells.

Activation of ErbB2 promoted proliferation and blocked apoptosis in RhoN19 expressing acinar-structures and in blebbing protrusions. Activation of ErbB2 in MCF-10A acini structures not only forms multi-acinar structures but also re-initiates proliferation and prevents apoptosis within these structures. Therefore we sought to determine the proliferation and apoptosis status of ErbB2 induced multi-structures and protrusions expressing RhoN19. We demonstrated that ErbB2 re-initiated proliferation in the presence of RhoN19 expression in acinar structures (Figure 5.8) and within the cells of the blebbing protrusions (Figure 5.8, arrows). In addition, we determined that activation of ErbB2 prevented apoptosis in the presence of RhoN19 expression (Figure 5.9). This experiment also demonstrated that the cells within the protrusions were not positive for the apoptosis marker, cleaved caspase-3 (Figure 5.9, insert). While these experiments need to be repeated with higher resolution microscopy, they do suggest that the protrusions contain proliferative and viable cells.

Blebbing protrusions lack organized laminin V.

Previous reports as well as our data (see Chapter 4) determined that ErbB2 induced multi-acinar structures are non-invasive (Muthuswamy et al. 2001; Aranda et al. 2006). The cells within each multi-acini structure that maintain contact with the basement membrane are able to secrete and organize laminin V, herein referred to as laminin, and collagen IV into a ring of fibers around the basal surface of the acini (Muthuswamy et al. 2001). One characteristic of invasion is the breakdown of the

Figure 5.8. ErbB2 activation induces proliferation in RhoN19 expressing acini structures.

Day 12 10A.ErbB2 acinar structures were infected with adenovirus (MOI 60) expressing RhoN19. Tetracycline (OFF) was added at the time of infection to prevent protein expression in control acinar structures. 24 hours post-infection ErbB2 was stimulated with dimerizer or left unstimulated for 4 days. Structures were then fixed and immunostained for Ki-67, a cell proliferation marker (red), RhoA (green) denoting expression of RhoN19, and DAPI (blue) nuclear stain. The percent of Ki-67 positive acini structures were quantitated (white numbers) from 200 structures per condition and one experiment. To account for basal ErbB2 activity a structure was considered positive for Ki-67 if it contained more than 3 Ki-67 positive cells. Insert in far right panel shows a detailed image of Ki-67 positive cells in an blebbing protrusion. Scale bar 50μm.

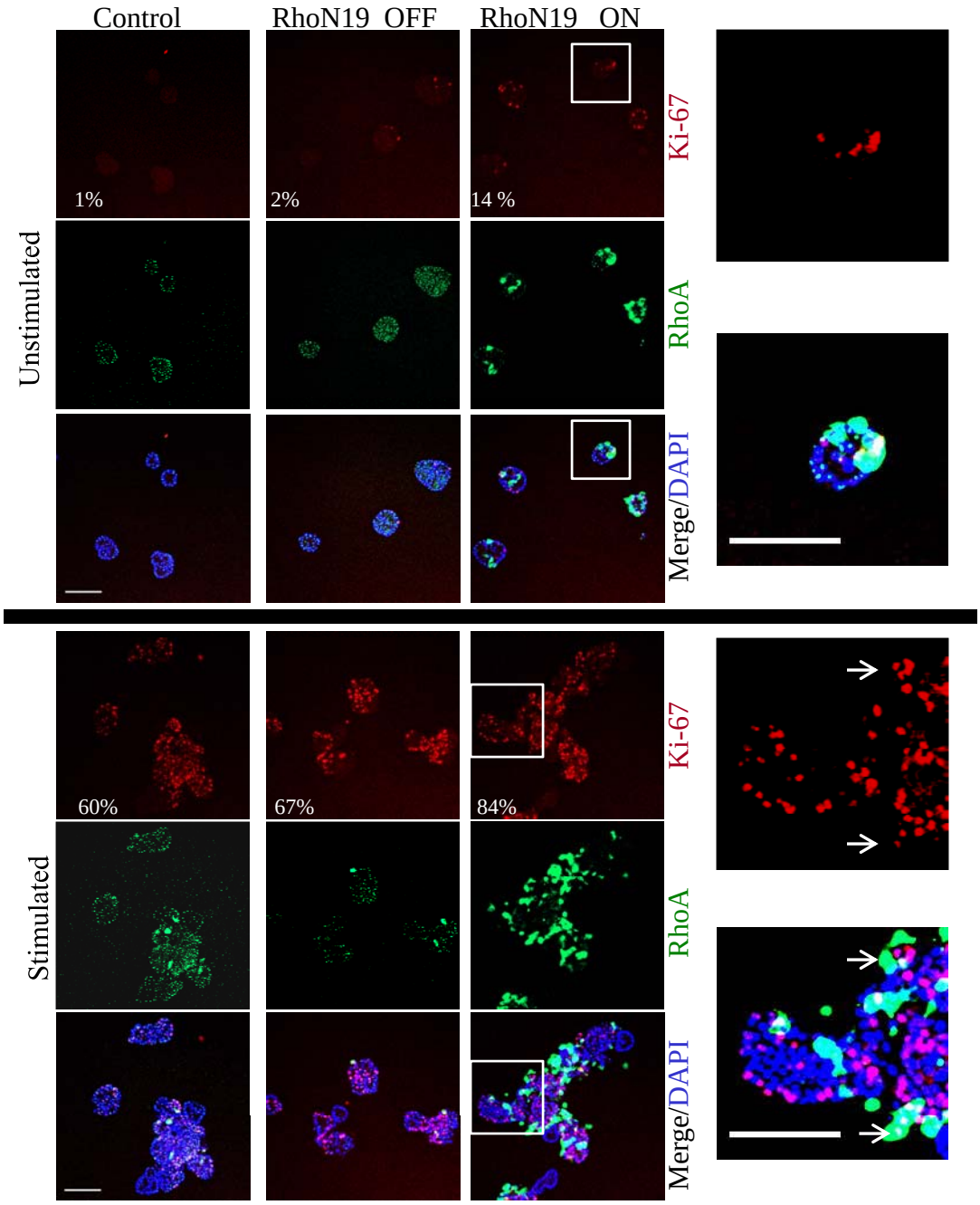

Figure 5.8. ErbB2 activation induces proliferation in RhoN19 expressing acini structures.

Figure 5.9. ErbB2 activation inhibits apoptosi in RhoN19 expressing acini structures.

Day 5 10A.ErbB2 acinar structures were infected with adenovirus (MOI 60) expressing RhoN19. Tetracycline (OFF) was added at the time of infection to prevent protein expression in control acinar structures. 24 hours post-infection ErbB2 was stimulated with dimerizer or left unstimulated for 3 days. Structures were then fixed and immunostained with the apoptotic marker activated cleaved caspase-3 (C3) (green), and DAPI (blue) nuclear stain. To reduce background a structure was considered positive for C3 if it contained more than 2 positive cells. The percent of C3 positive acini structures was quantitated (white numbers). Data represents the mean of 200 structures from two experiments and shows a 2-fold reduction in C3 staining upon ErbB2 stimulation. Arrows point to C3 positive cells. Insert and arrowhead show a protrusion without C3. Scale bar 50μm.

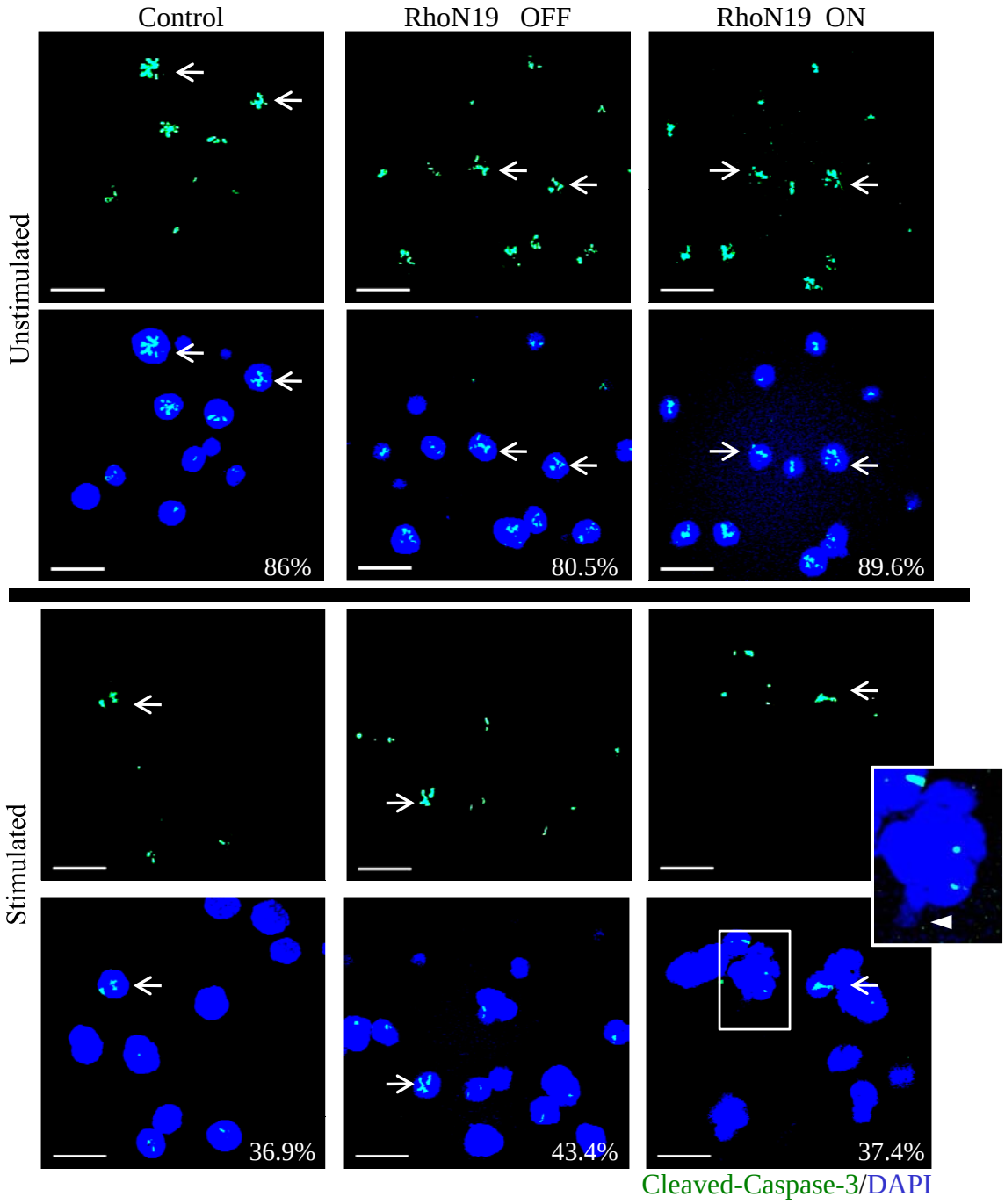

Figure 5.9. ErbB2 activation inhibits apoptosi in RhoN19 expressing acini structures.

extracellular matrix. Other characteristics include altered cell-cell adhesion, increased motility and changes to the cytoskeleton, reviewed in (Sahai and Marshall 2002). Therefore, I sought to determine if these blebbing protrusions retained ECM organization by immunofluoresence staining of the laminin. As expected, activated 10A.ErbB2 acini are encased in organized laminin. However, the protrusions observed after activation of ErbB2 in the presence of RhoAN19 expression lacked organized laminin (Figure 5.10.A). The number of blebbing protrusions that lack laminin were quantitated by visualization of serial z-stack images (See Materials and Methods). Optical sectioning was used to ensure that the laminin from acinar structures above or below the focal plane did not result in a false positive. A protrusion was classified devoid of laminin staining, if there was no laminin present in any focal plane of the acinar structure (Figure 5.10.A, arrow). There was a striking correlation between the presence of blebbing and the lack of organized laminin staining (Figure 5.7.B and 5.10.B), suggesting that the cells within the blebs had broken down the existing laminin. It is also possible that once the protruding cells had moved through the existing laminin border, they were no longer capable of secreting and organizing laminin. However, the existing laminin had to have been penetrated by the migrating cells regardless of the cells ability to secrete polarized laminin.

The lack of organized laminin suggests that the epithelial cells within the protrusion have the ability to move and invade into the surrounding basement membrane. Previous studies have shown downregulation of RhoA can promote both EMT and invasive phenotypes (Simpson et al. 2004; Bellovin et al. 2006). Therefore I sought to determine if RhoN19 and ErbB2 could cooperate to promote an EMT. One characteristic

Figure 5.10. ErbB2 activation cooperates with dominant negative RhoA to promote blebbing protrusions that lack organized laminin V.

(A) Day 5 10A.ErbB2 acinar structures were infected with adenovirus (MOI 60) expressing RhoN19. Tetracycline (OFF) was added at the time of infection to prevent protein expression in control acinar structures. 24 hours post-infection ErbB2 was stimulated with dimerizer or left unstimulated for 3 days. Structures were then fixed and immunostained for the ECM component laminin V (red), and DAPI (blue) nuclear stain. Arrowheads point to the organized laminin border surrounding the acinar structures and the arrow denotes lack of laminin stain, scale bar 20μm. **(B)** The number of blebbing protrusions that lack laminin staining was quantified by image analysis. A protrusion was considered devoid of laminin if there was no organized boarder in any focal plane. Data represent means ± S.D. of 500 structures from three different experiments.

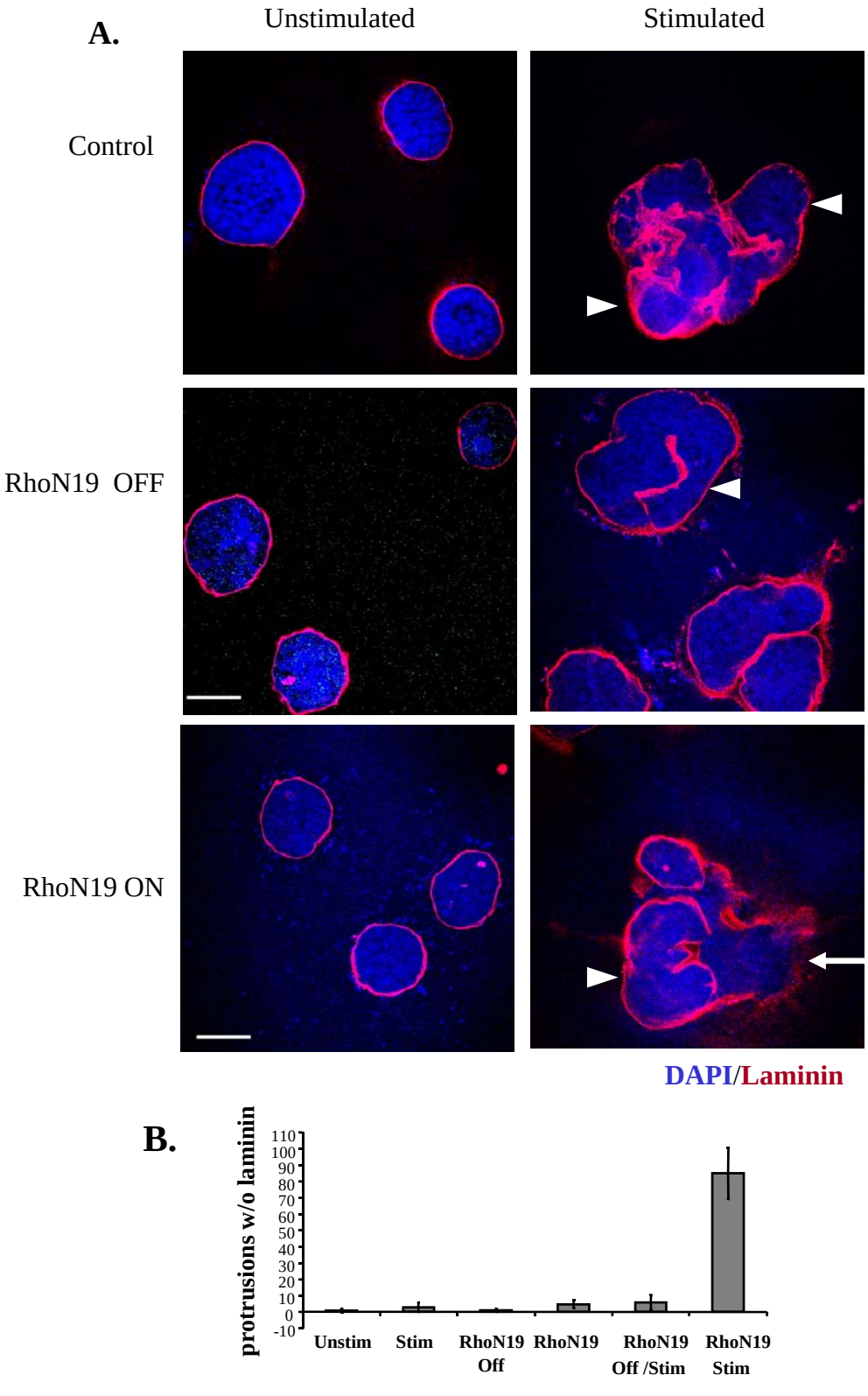

Figure 5.10. ErbB2 activation cooperates with dominant negative RhoA to promote blebbing protrusions that lack organized laminin V.

Figure 5.11. ErbB2 activation cooperates with dominant negative RhoA to promote blebbing protrusions that retain cell-cell contacts.

(A) Day 5 10A.ErbB2 acinar structures were infected with adenovirus (MOI 60) expressing RhoN19. Tetracycline (OFF) was added at the time of infection to prevent protein expression in control acinar structures. 24 hours post-infection ErbB2 was stimulated with dimerizer or left unstimulated for 3 days. Structures were then fixed and immunostained for laminin V (red), E-Cadherin (green), and DAPI (blue) nuclear stain. Arrowheads point to E-Cadherin localized to cell-cell junctions. The arrow points to a blebbing protrusion devoid of a laminin border yet retained cell-cell contacts visualized by E-Cadherin, scale bar 10μm.

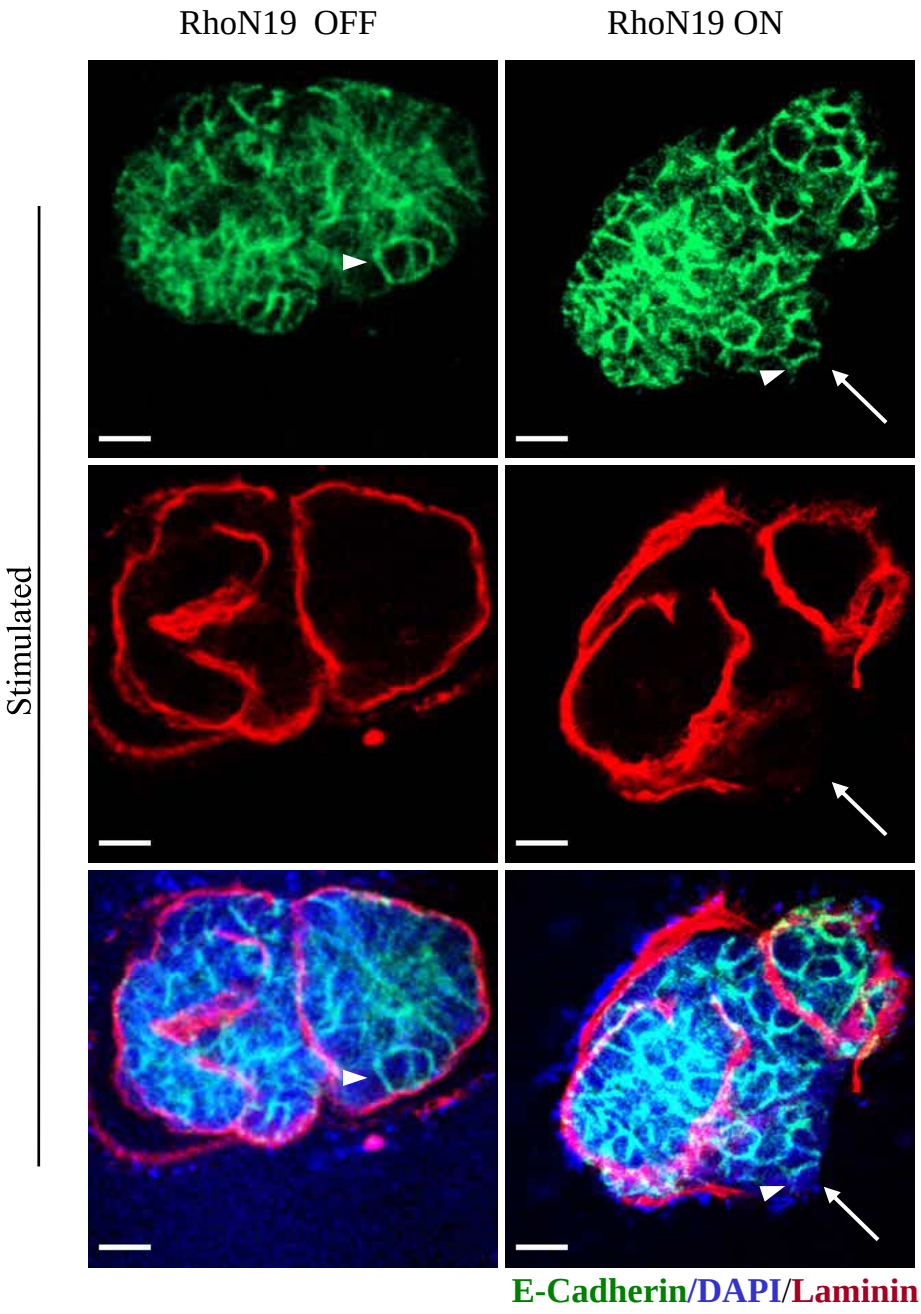

Figure 5.11. ErbB2 activation cooperates with dominant negative RhoA to promote blebbing protrusions that retain cell-cell contacts.

of EMT is loss of the cell adhesion molecule E-cadherin. I determined that the cells within the protrusions (Figure 5.11, arrow) retain their cell-cell contacts by immunofluorescence of E-cadherin (Figure 5.11, arrowhead). While the cells within the blebs do not have characteristics of EMT, epithelial cells can undergo invasion while maintaining cell-cell contacts (Friedl et al. 2004). Further experiments would need to be performed to determine what type of cell movement is occurring in these invasive protrusions.

Activation of ErbB2 promotes invasion of dominant negative RhoA expressing MCF-10A acini

The lack of laminin surrounding the blebbing protrusions, suggested that these cells are invasive. I performed two different invasion assays to further characterize these structures. The first invasion assay increased the stiffness or tension of the matrix by addition collagen I to Matrigel. It is important to mimic stiff ECM because an increase in ECM stiffness has been observed in tumors and this correlates with poor prognosis (Colpaert et al. 2003; Paszek and Weaver 2004; Paszek et al. 2005). In addition, studies have shown that increased tension of the ECM *in vitro* can increase the invasive potential of MCF-10A cells (Paszek et al. 2005). Therefore I used this assay to test for invasive potential of ErbB2 activated and RhoN19 expressing acinar structures.

10A.ErbB2 cells were plated on a matrix composed of 1:1 ratio of collagen I:Matrigel (See Materials and Methods). 10A.ErbB2 acini were infected with RhoN19 virus with and without activation of ErbB2. Upon activation the 10A.ErbB2/RhoN19 acinar structures formed invasive protrusions (Figure 5.12, arrows). Figure 5.12 (bottom

Figure 5.12. Activation of ErbB2 activation promotes invasion of RhoN19 expressing MCF-10A acini

Day 12 10A.ErbB2 acinar structures grown on Matrigel:CollagenIV were infected with adenovirus (MOI 60) expressing RhoN19. Tetracycline (OFF) was added at the time of infection to prevent protein expression in control acinar structures. 24 hours post-infection ErbB2 was stimulated with dimerizer or left unstimulated for 4 days. Phase images show invasive protrusions in the RhoN19/ErbB2 stimulated condition. blebbing protrusions, arrows. Arrowhead denotes the monolayer around a multi-acinar structure. Insert shows individual cells within the monolayer surrounding the main multi-acinar structure. Scale bar 100μm.

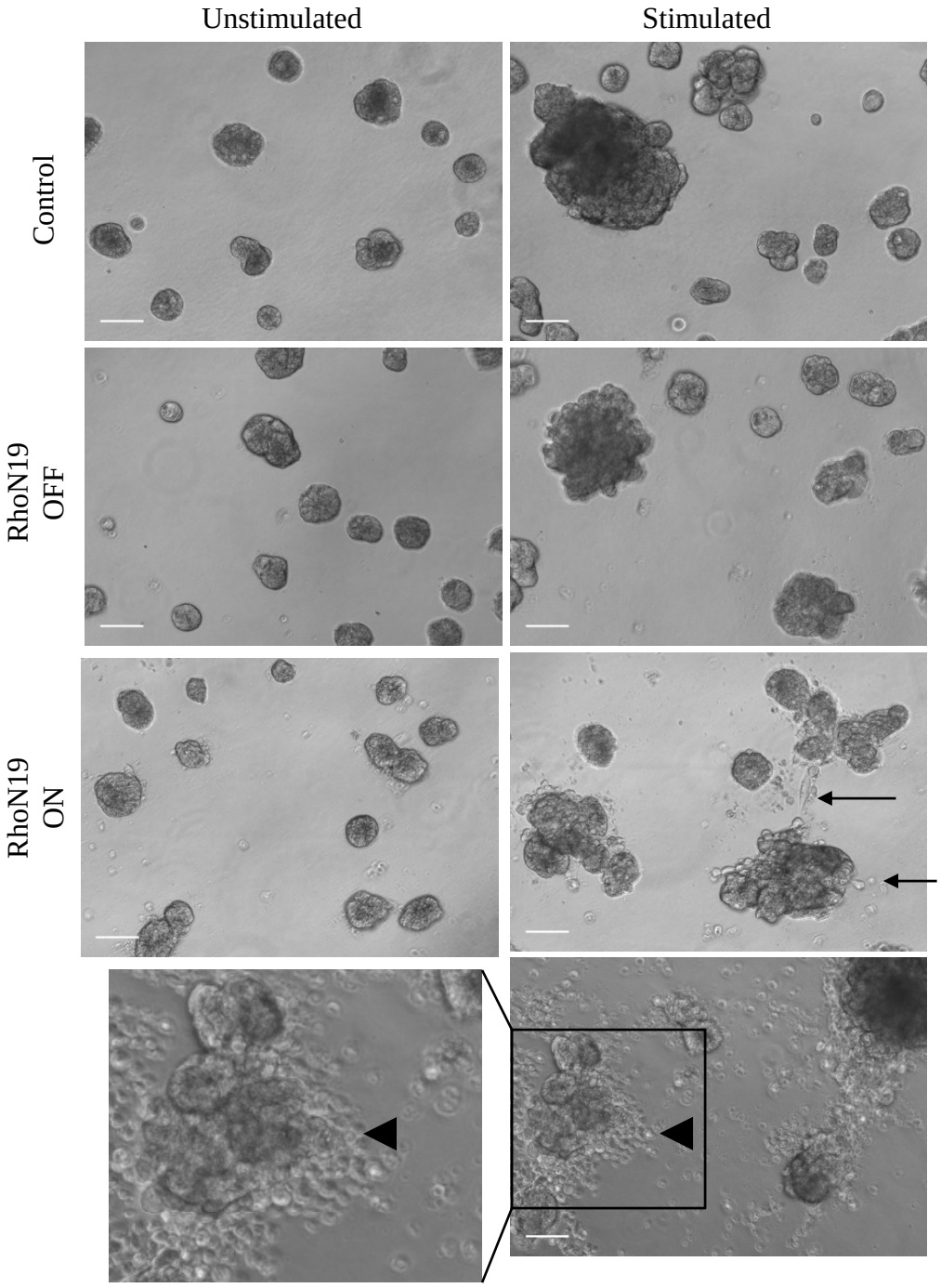

Figure 5.12. Activation of ErbB2 activation promotes invasion of RhoN19 expressing MCF-10A acini

panel), shows a multi-structure surrounded by a monolayer of cells (insert, arrow head), suggesting that the 10A.ErbB2/RhoN19 cells were migratory, invasive and have lost their ability to form organized acini structures. It is likely that the invasive cells are viable because activation of ErbB2 in the presence of RhoN19 expression did not induce apoptosis on Matrigel alone (Figure 5.9). Many of the invasive cells also retain proper E-Cadherin localization and therefore cell-cell contacts (Figure 5.13). Since loss of cell-cell contacts is a hallmark of cell death (Brancolini et al. 1997), it is unlikely that all the invasive cells are undergoing apoptosis. While these cells need to be further characterized with markers for apoptosis and proliferation, these data suggest that these cells are both viable and invasive.

To further prove that expression of RhoN19 and activation of ErbB2 promotes invasion, a modification of the 3D assay was used (See Materials and Methods). In contrast to the previous overlay method, 10A.ErbB2 cells were embedded in Matrigel. This assay tests for invasion by visualization of acinar protrusions that have penetrated the surrounding Matrigel. We first determined that embedded structures were able to be infected with a GFP reporter virus albeit a lower efficiency then overlaid acini structures (Figure 5.14.A and B). 10A.ErbB2 acini were then infected with RhoN19 virus with and without activation of ErbB2. After 4 days, protrusions radiated from multi-acinar structures (Figure 5.15, arrows). As expected the protrusions were smaller in the embedded acini when compared to either the collagen:Matrigel or Matrigel overlay assay. However, the acini still formed protrusions that invaded the surrounding matrix. Together, both the collagen:Matrigel overlay and embedded assays demonstrated that ErbB2 activation in RhoN19 expressing acinar structures promoted invasion.

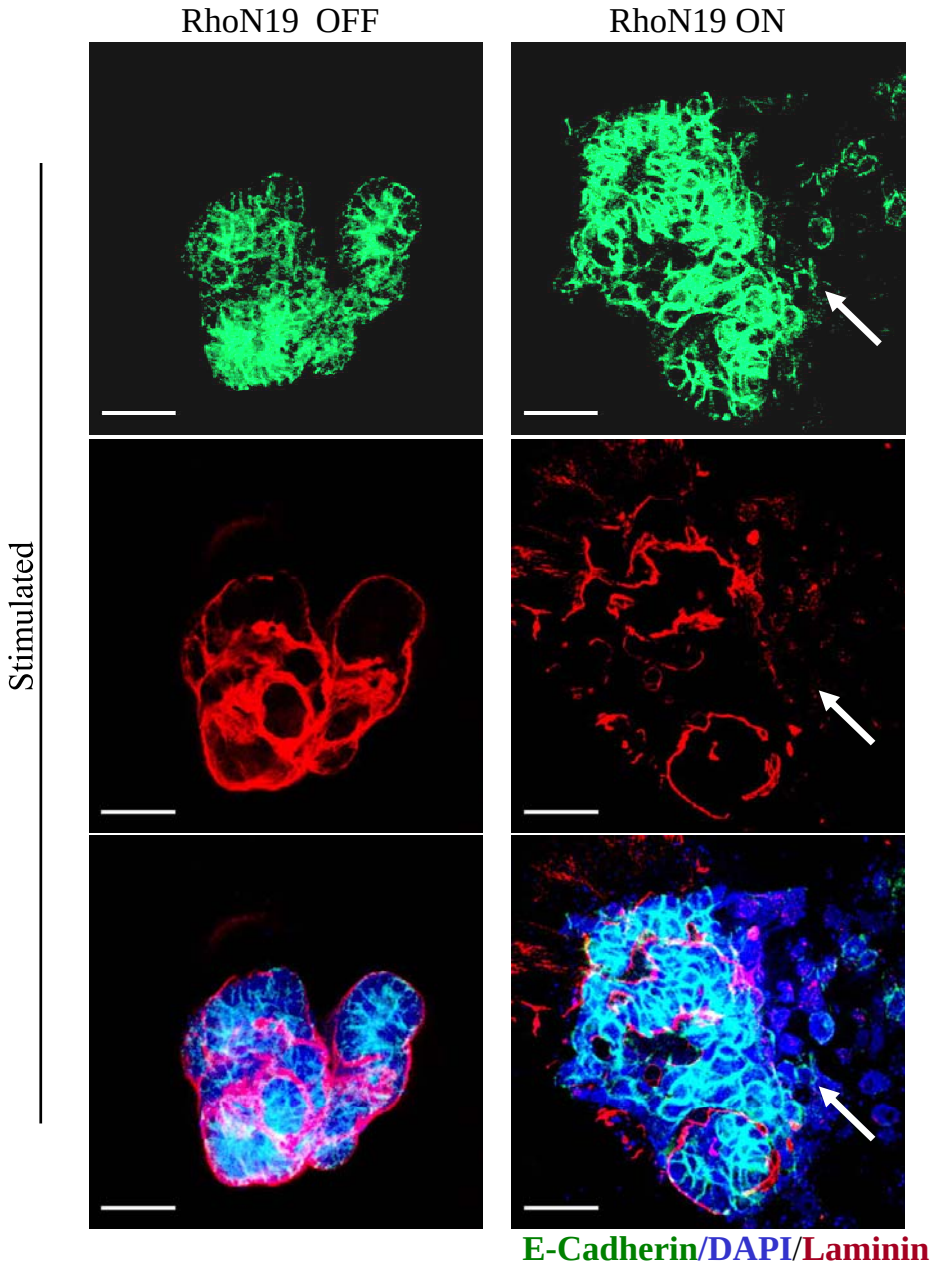

Figure 5.13. Invasive protrusions retain cell-cell contacts

Day 12 10A.ErbB2 acinar structures grown on Matrigel:CollagenIV were infected with adenovirus (MOI 60) expressing RhoN19. Tetracycline (OFF) was added at the time of infection to prevent protein expression in control acinar structures. 24 hours post-infection ErbB2 was stimulated with dimerizer or left unstimulated for 4 days. Structures were then fixed and immunostained for laminin (red), E-Cadherin (green), and DAPI (blue) nuclear stain. The arrow points to a group of cells protruding from the main multi-acinar structure. These cells have no laminin stain but they retain cell-cell contacts as monitored by E-Cadherin stain. Scale bar 50μm.

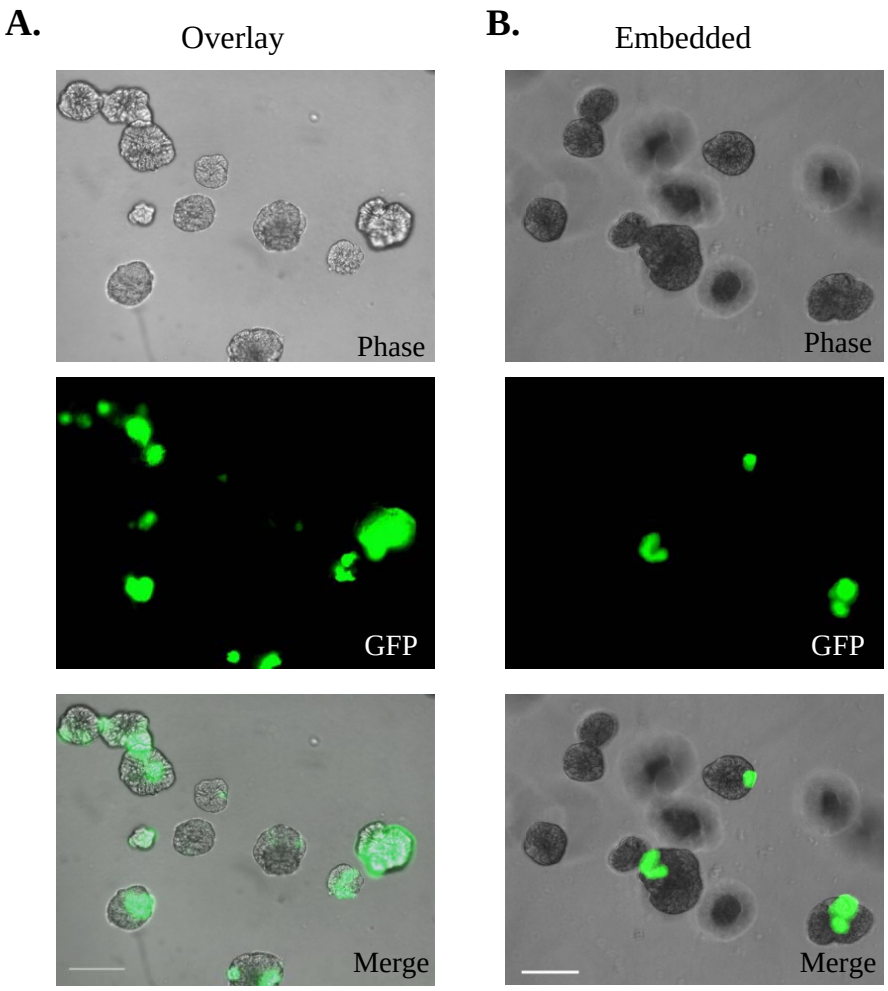

Figure 5.14. Adenovirus can infect acinar structures that are embedded in Matrigel

(A) MCF-10A cells were grown on Matrigel for 12 days. Acinar structures were then infected with adenovirus (MOI 60) expressing GFP. **(B)** MCF-10A cells were embedded in Matrigel and grown for 12 days. Acinar structures were then infected with adenovirus (MOI 120) expressing GFP. Fluorescence GFP and phase images from both **(A)** and **(B)** were taken after 4 days infection. Images show that embedded acinar structures **(B)** expressed GFP albeit lower than structures in **(A).**

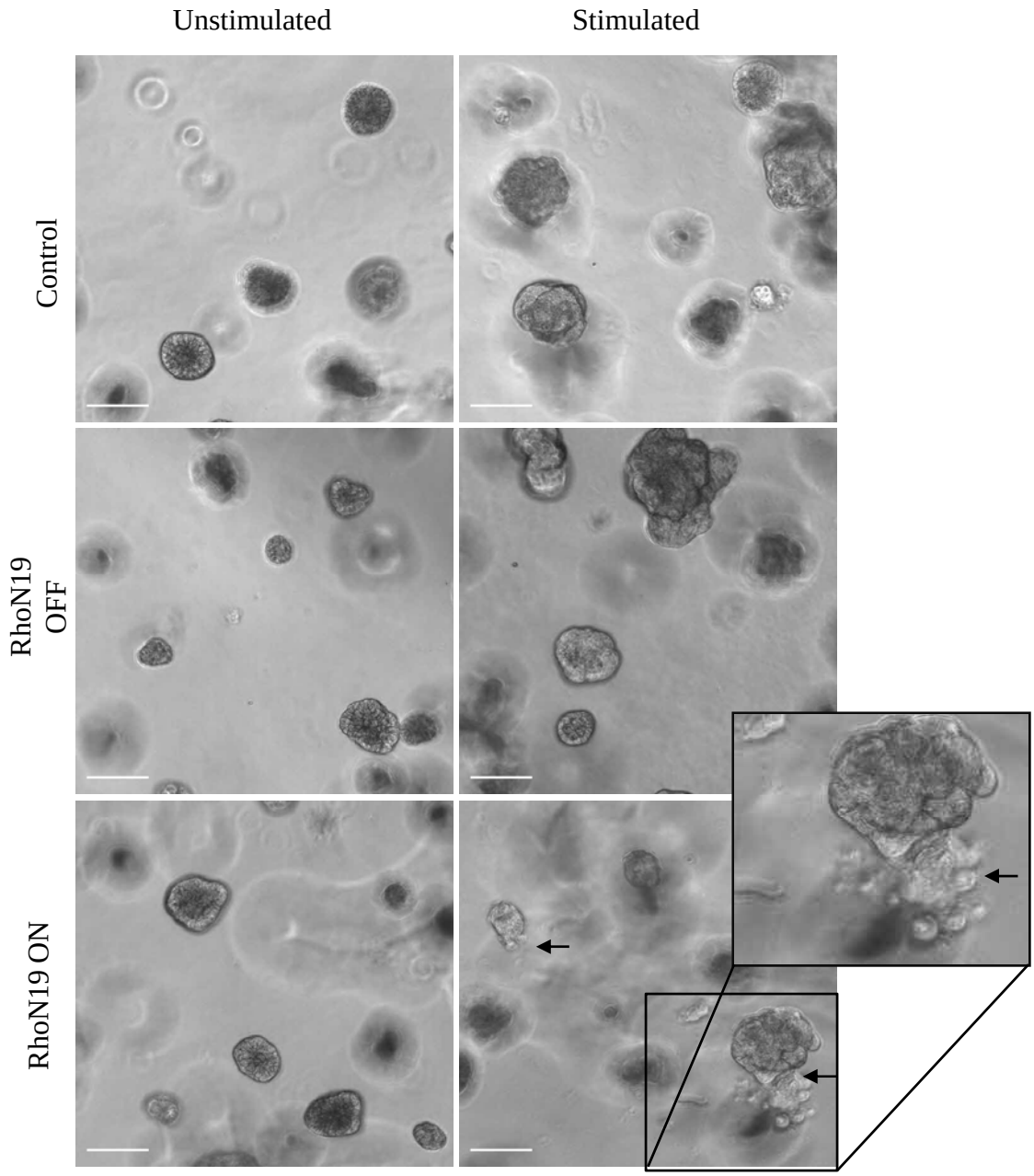

Figure 5.15 ErbB2 activation promotes invasion of RhoN19 expressing 10A.ErbB2 embedded acini structures

10A.ErbB2 cells were embedded in Matrigel for 12 days before infection with adenovirus expressing RhoN19 (MOI 120). 24 hours post-infection, ErbB2 was stimulated for 4 days and structures were imaged by phase microscopy. Arrows denote the invasive protrusions that formed after activation of ErbB2 in the presence of RhoN19 expression. Insert shows the cells that have invaded the surrounding Matrigel., scale bar 100μm.

RhoN19 expression is required to maintain invasive protrusions

The cooperative effect between activation of ErbB2 and expression of RhoN19 is a novel observation. In order to gain insight into the real-time formation of these protrusions, I performed two time-lapse experiments. In the first experiment I monitored the acinar structures after RhoN19 infection for 70 hours after ErbB2 activation. I found that RhoN19 expression increased the movement of the cells within the acini and frequently observed cells exiting the acinar structures. Figure 5.16 show the still images acquired from the time lapse experiment. The images show the formation of the invasive protrusions (Figure 5.16, arrows) within 50 hours of ErbB2 stimulation in RhoN19 expressing acini structures. This time-lapse imaging demonstrates that expression of dominant negative RhoA in the presence of activate ErbB2 promotes cell movement and invasion.

To determine if the invasive protrusions require RhoN19 expression to maintain protrusive activity, I performed a time-lapse experiment where I added tetracycline to turn off RhoN19 expression after 4 days of both RhoN19 expression and ErbB2 activation. The structures were monitored for 40 hours after addition of tetracycline (RhoN19 off) in the presence of stimulated ErbB2. After blocking RhoN19 expression with tetracycline for 10 hours the protrusions began to retract as shown in Figure 5.17 (arrows). The protrusions continued to regress to the main body of the multi-acini structure, which remained intact. The 40 hour image shows almost complete regression of the protrusion (Figure 5.17,arrows). This experiment showed that inhibition of RhoN19 expression caused the invasive cells to regress to the main multi-acinar structure. Therefore, downregulation of RhoA activity is necessary to sustain invasion of

Figure 5.16. ErbB2 activation in RhoN19 expressing acinar structures promotes invasive protrusion formation

Day 12 10A.ErbB2 acinar structures were infected with adenovirus (MOI 60) expressing RhoN19. Tetracycline (OFF) was added at the time of infection to prevent protein expression in control acinar structures (left column). 24 hours post-infection ErbB2 was stimulated with dimerizer or left unstimulated for 70 hours. Representative still images from 70 hours time lapse experiment are shown. The left column shows the formation of multi-acinar structures in ErbB2 stimulated RhoN19 OFF condition (arrowheads). Multi-acinar structure formation was seen within the first 40 hours and was more pronounced by 70 hours (arrowheads). The right two columns show the formation of invasive protrusions in ErbB2 stimulated RhoN19 ON structures. Invasive protrusion formation was seen within 50 hours (arrows). The black arrows point to the progression of protrusion formation throughout the 70 hour time course. Scale bar 100μm.

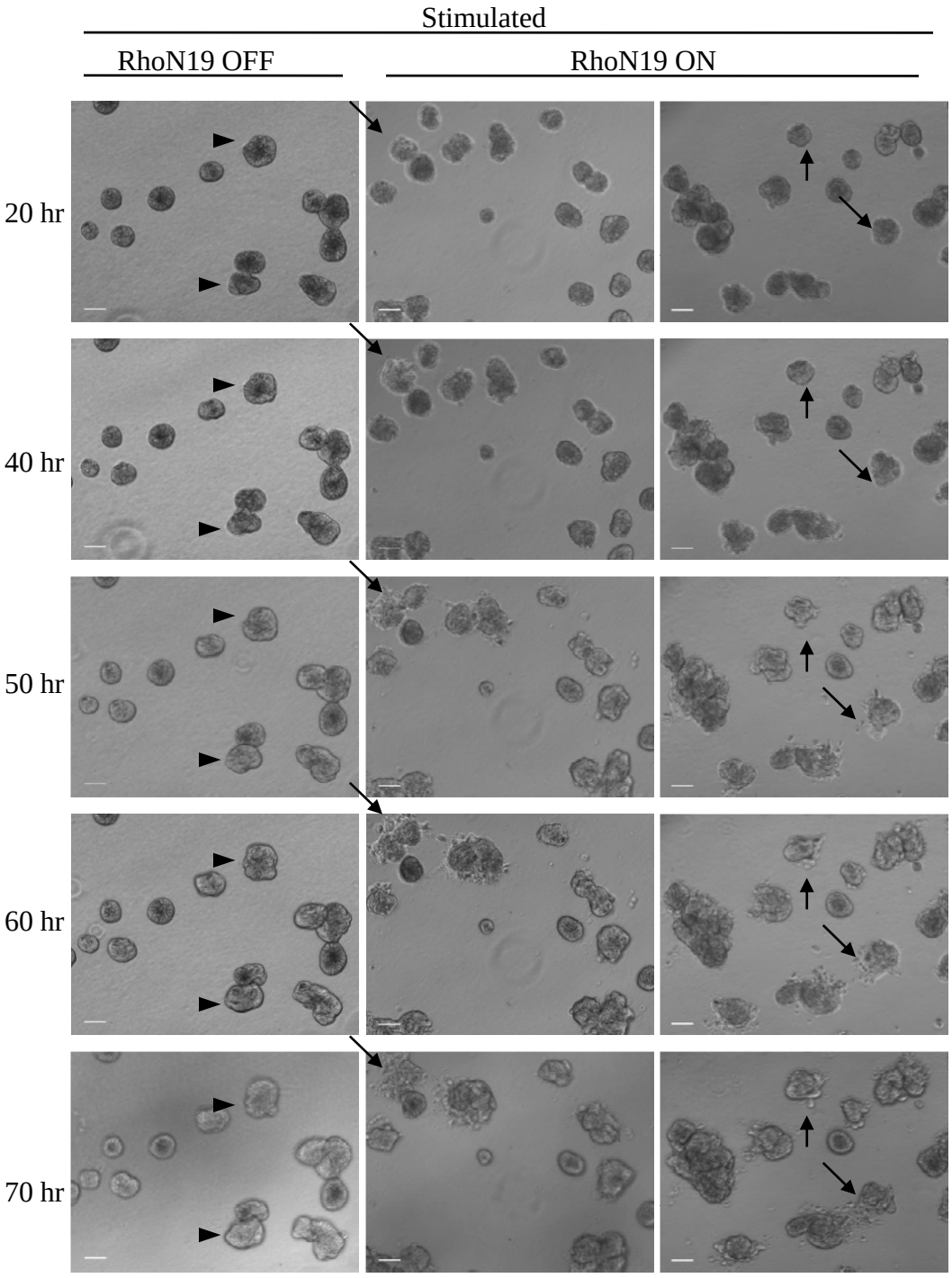

Figure 5.16. ErbB2 activation in RhoN19 expressing acinar structures promotes invasive protrusion formation

Figure 5.17. Invasive protrusion formation requires RhoN19 expression

10A.ErbB2 cells were grown on Matrigel for 12 days before infection with adenovirus expressing RhoN19 (MOI 60). Tetracycline (OFF) was added at the time of infection to prevent protein expression in control acinar structures (column A and B). 24 hours post-infection ErbB2 was stimulated with dimerizer or left unstimulated for 4 days. Tetracycline was then added to prevent RhoN19 expression (column C), and acini were imaged for 40 hours. **(A)** Unstimulated, RhoN19 OFF acini structures did not change throughout the time course. **(B)** The stimulated, RhoN19 OFF multi-acinar structure increased in size (arrowhead) throughout the time course. **(C)** The stimulated, RhoN19 ON mulit-acinar structure contains protrusions (arrows) that regressed within 10 hours post-tetracycline addition. Scale bar 100μm.

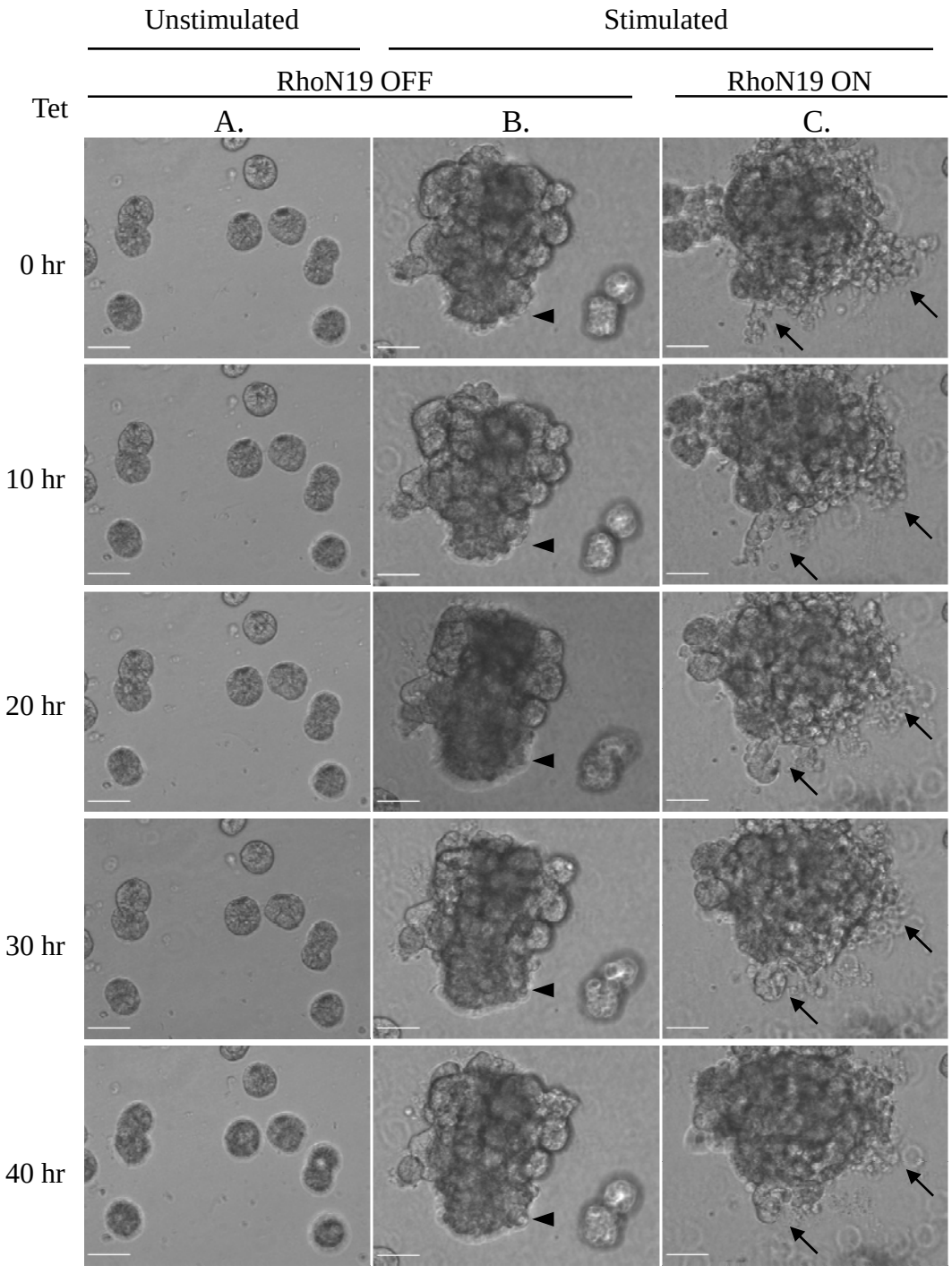

Figure 5.17. Invasive protrusion formation requires RhoN19 expression

.

ErbB2 activated MCF-10A cells. The mechanism by which inhibition of RhoA is cooperating with ErbB2 activation has to be determined. I speculate that by inhibiting RhoA activity with a dominant negative, the actin cytoskeleton becomes destabilizes by reduced stress fiber formation. This destabilization could be an event that cooperates with ErbB2 to promote invasion.

Inhibition of ROCK promotes protrusion formation in ErbB2 activated acinar structures

RhoA stabilizes the actin cytoskeleton through activation of downstream effectors molecules. One of these effectors is Rho-associated coiled-coiled kinases (ROCK). Activation of ROCK signals to downstream molecules that signal the formation of actomyosin and actin filament stabilization promote the formation of stress fibers. To determine if ErbB2 is cooperating with downregulation of RhoA activity through ROCK signaling, I inhibited ROCK in acinar structures and then activated ErbB2. My results show that activation of ErbB2 in the presence of ROCK inhibitor promoted protrusion formation (Figure 5.18). While this is only a correlation, these data suggest that ErbB2 cooperates with inhibition of the RhoA-ROCK pathway to promote invasion. Further experiments, such as using a dominant negative of ROCK, need to be performed to determine if the inhibition of the ROCK pathway cooperates with activated ErbB2 to promote invasion.

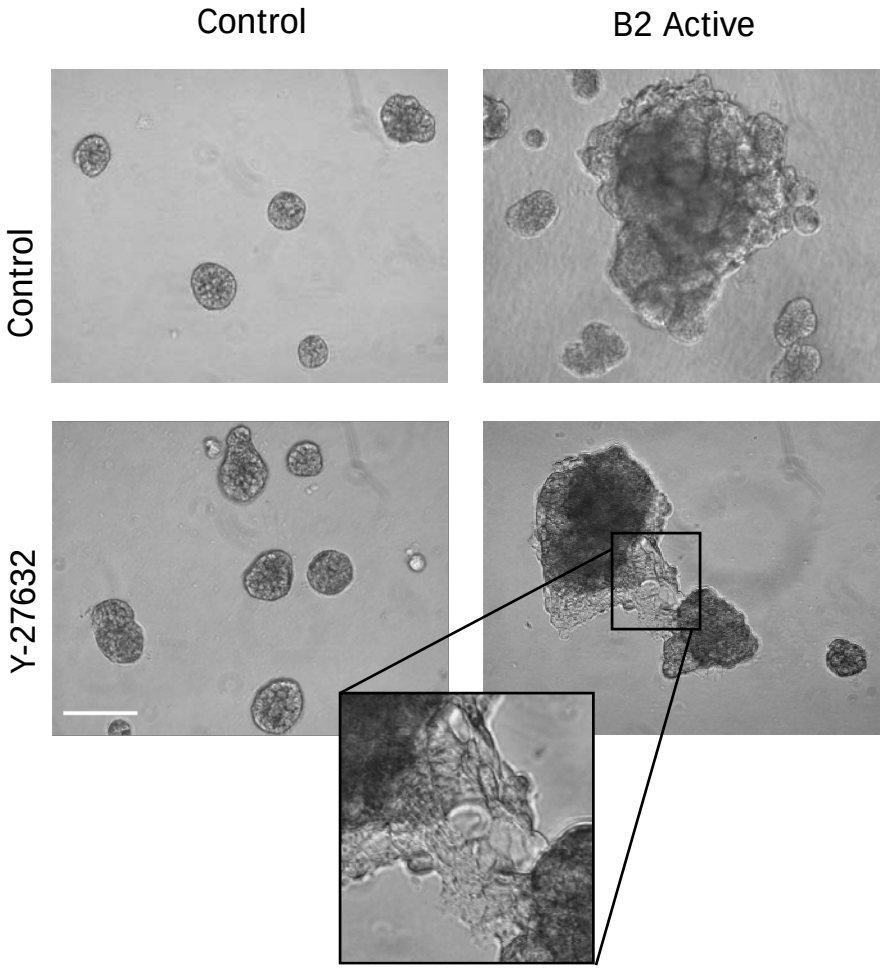

Figure 5.18. Inhibition of ROCK promotes protrusion formation in ErbB2 activated acinar structures

10A.ErbB2 cells were grown on Matrigel for 12 days. ROCK was inhibited with Y-27632 (20μm) for 24 hours before activation of ErbB2 for 4 days. Phase images show that inhibition of ROCK in combination with activated ErbB2 promotes the formation of protrusions in multi-acinar structures (bottom right). Insert shows a higher magnification of a protrusion in between two multi-acinar structures. This result was observed in two experiments. Scale bar 50μm.

Discussion

In this chapter, I determined that proper regulation of the RhoGTPases is important in MCF-10A acinar structures. First I determined that activation of the Rho, Rac and Cdc42 all disrupted organized, growth-arrested MCF-10A cells (Figure 5.2 and summarized in Figure 5.19). It is possible that RacV12, Cdc42L61 and RhoV14 disrupted the organized cytoskeleton by promoting the formation of lamelopodia, filipodia, and stress fibers, respectively. These cytoskeletal rearrangements could alter the way the cells interact with neighboring cells or the matrix thereby promoting aberrant organization. While we did not observe an effect of dominant negative Rho or Rac in preformed structures, we did observe disruption of acinar structures that were still undergoing programmed morphogenesis (Figure 5.20 and summarized in Figure 5.19). This observation is very interesting because it showed that forming acinar structures are dependent on Rac and Rho activation, whereas preformed structures are not. This suggests that organized epithelial cells are less vulnerable to disruptive signals than structure undergoing morphogenesis. It is possible that once the organization is established, the cells within the acinar structure no longer need the correct cycling of Rho and Rac to maintain organization of the cytoskeleton. The reason that dominant negative Cdc42 disrupts acinar organization (Figure 5.5) of preformed structures remains to be understood. Perhaps, since we see Cdc42 as the more prominent binding partner of Par6, over Rac, in MCF-10A cells (data not shown), that Cdc42 is necessary to maintain the active Par complex and thereby organization.

Rho GTPase	Expression in acinar structures	Expression + ErbB2 activation in acinar structures
RacV12	Disruption and blebbing	Not performed
RacN17	None	None
RhoV14	Disruption and blebbing	Not performed
RhoN19	None	Blebbing protrusions
Cdc42L61	Disruption and blebbing	Not performed
Cdc42N17	Disruption and blebbing	Disruption and blebbing

Figure 5.19. Summary table of the different effects RhoGTPase mutants generate in acinar structures.

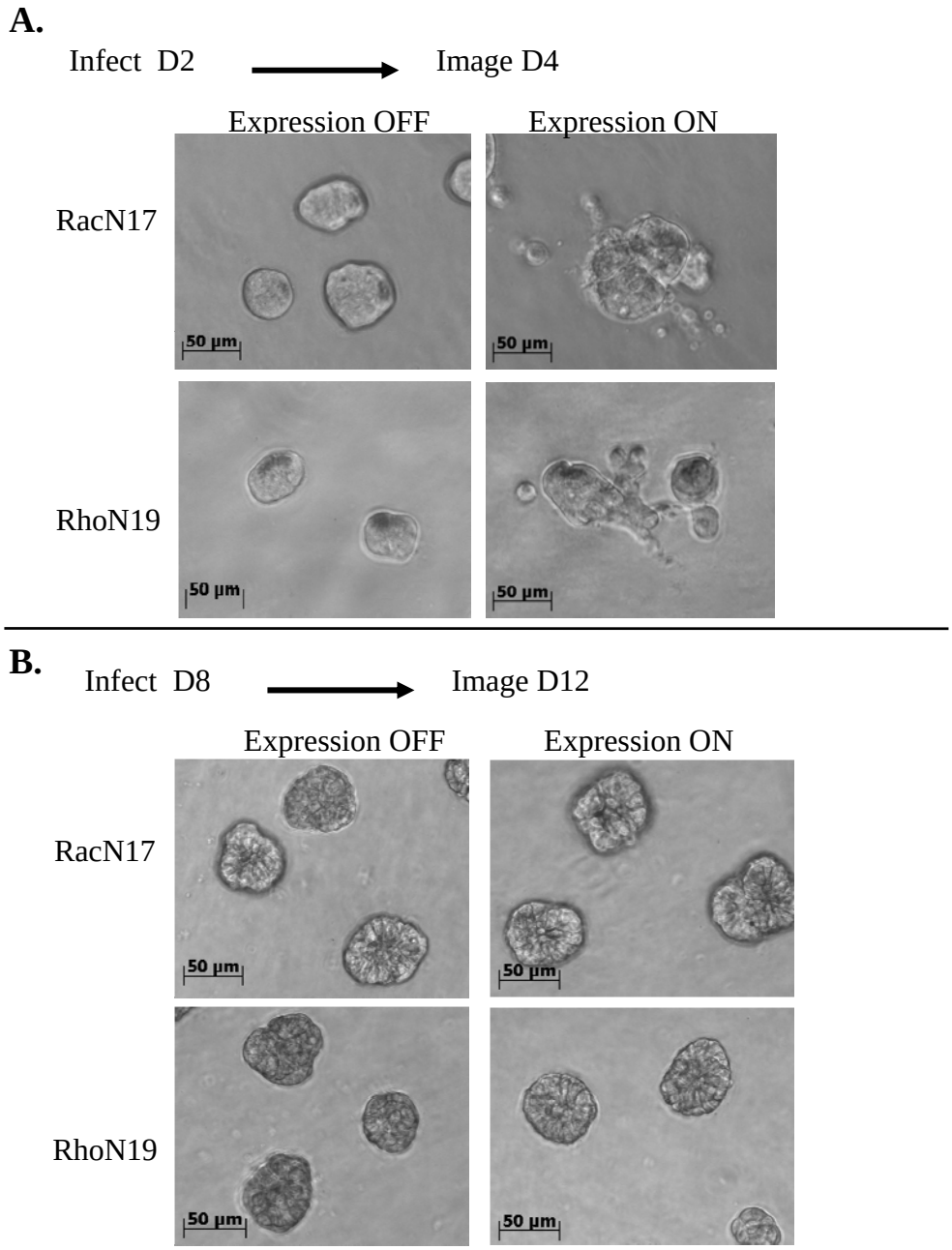

Figure 5.20. Expression of RacN17 and RhoN19 disrupts acinar formation but not maintenance.

(A) Day 2 MCF-10A acinar structures were infected with RacN17 or RhoN19 expressing adenovirus (MOI 60). Tetracycline was added at the time of infection to prevent protein expression in control structures. Protein was expressed for 2 days and phase images were taken that show disrupted acinar structures **(B)** Day 8 MCF-10A acinar structures were infected as above. Protein was expressed for 4 days and phase images were taken that show no disruption in preformed acinar structures.

We also found that interference with RhoGTPases activation had different effects on ErbB2 induced transformation. Expression of dominant negative Rac, Cdc42 and RhoA do not inhibit ErbB2 induced transformation (Figure 5.4-5.6 and summarized in Figure 5.19). However, activation of ErbB2 in the presence of dominant negative RhoA promoted a novel invasive phenotype (Figure 5.6 and summarized in Figure 5.19). These different phenotypes observed with the expression of the dominant negative RhoGTPases in ErbB2 transformed structures suggests that there is some specificity for RhoA in cooperation with ErbB2 to promote invasion of previously non-invasive structures. In addition RhoN19 alone does not have an effect on the organized acinar structures, suggesting that ErbB2 activation creates susceptibility. This chapter shows that alterations in epithelial cell organization and cytoarchitecture by activation of ErbB2 and RhoN19 are important in promoting and maintaining the invasion properties of organized acinar structures.

Among the three isoforms of Rho (RhoA, RhoB and RhoC), RhoA protein levels are overexpressed in breast cancer (Fritz et al. 1999; Fritz et al. 2002) and overexpression of RhoC protein and mRNA, is associated with inflammatory breast cancer (van Golen et al. 1999; Kleer et al. 2002; van Golen et al. 2002). The studies involving RhoA overexpression in breast cancer have been performed using antibodies that do not discriminate between the two isoforms (Fritz et al. 1999; Fritz et al. 2002). It was not until 2002 when an antibody that could distinguish RhoA from RhoC was published (Kleer et al. 2002), therefore it is possible that overexpression of "RhoA" could be both RhoA and RhoC. It becomes important to discriminate between the isoforms of Rho because recent reports support opposing roles for RhoA and RhoC in breast cancer

progression (Simpson et al. 2004; Bellovin et al. 2006; Wu et al. 2007). These studies show that overexpression of RhoC promotes invasive activity of breast cancer cells, while downregulation of RhoA and RhoA activity promotes a similar invasive and migratory phenotype (Simpson et al. 2004; Bellovin et al. 2006; Wu et al. 2007).

We see that expression of a dominant negative RhoA has a cooperative effect in promoting invasion of non-invasive acinar structures. This is similar to the aforementioned study where downregulation of RhoA in a non-invasive breast cancer cell line (MCF-7) promotes migration and invasion (Simpson et al. 2004). However, there are reports suggesting that downregulation of RhoA activity prevents metastatic progression (Bouzahzah et al. 2001; Denoyelle et al. 2001). These seemingly conflicting observations can be explained by the potential actions of the different isoforms of Rho that have been reported. The studies done showing increased invasion of cancer cells with downregulation RhoA, was specific to RhoA (Simpson et al. 2004). While the other studies showed that downregulation of RhoA prevents metastatic potential used a dominant negative RhoA and an inhibitor of Rho activity. Both the dominant negative and the inhibitor do not discriminate between the isoforms of Rho, which means that the activity of all three isoforms of Rho could be downregulated and this could confound the phenotype. Therefore, it becomes increasingly more important to know which isoform is being inhibited and/or expressed in a given cell system. Our study was done with a dominant negative RhoA construct and therefore our results need to be verified using RNAi that will specifically target RhoA. Importantly, we also need to verify that RhoA activity is indeed being inhibited in our cell system as predicted. Since our phenotype is in agreement with the studies showing downregulation of RhoA promotes invasion, it is

possible that RhoA is the predominant isoform in MCF-10A cells. This hypothesis needs to be verified using an antibody that discriminates between the different isoforms of Rho.

One model that could explain the RhoN19 invasive phenotype is that degradation of RhoA keeps the protrusions flexible for the activity of Rac or Cdc42 to induce lamelopodia and filipodia formation in migrating cells (Wang et al. 2003; Bose and Wrana 2006). A very recent study furthered our understanding of this model when it showed that RhoA activity prevents activation of Rac and lamelopodia formation in the rear of a migrating cell. However, at the leading edge, Rho/Rock activity is low. This allows for Rac activity to promote the formation of lamelopodia and membrane protrusions (Nakayama et al. 2008). Together these studies suggest that downregulation of RhoA could promote the formation of protrusions of invasive cells. We could test whether Rac activity is necessary for ErbB2/RhoN19 mediated invasion by co-expression of dominant negative RacN17A and RhoN19. If expression of RacN17 prevents the formation of invasive protrusions then we can speculate that Rac activity is necessary for the cells to form protrusions and invade in ErbB2 activated acinar structures.

We also need to consider the role that Par6 could play in ErbB2/RhoN19 induced invasion. We know that Par6/aPKC is necessary for ErbB2 induced transformation of MCF-10A acini (Figure 4.4.)(Aranda et al. 2006) and that Par6 is required in TGFβ induced downregulation of RhoA and epithelial to mesenchymal transition (Ozdamar et al. 2005). Along these same lines TGFβ cooperates with ErbB2 to promote invasion in acinar structures. Perhaps ErbB2 induced disruption of the Par complex cooperates with TGFβ induced degradation of RhoA and this is the mechanism that promotes invasion of acinar structures (Figure 5.21.A). Another recent study connected the Par complex with

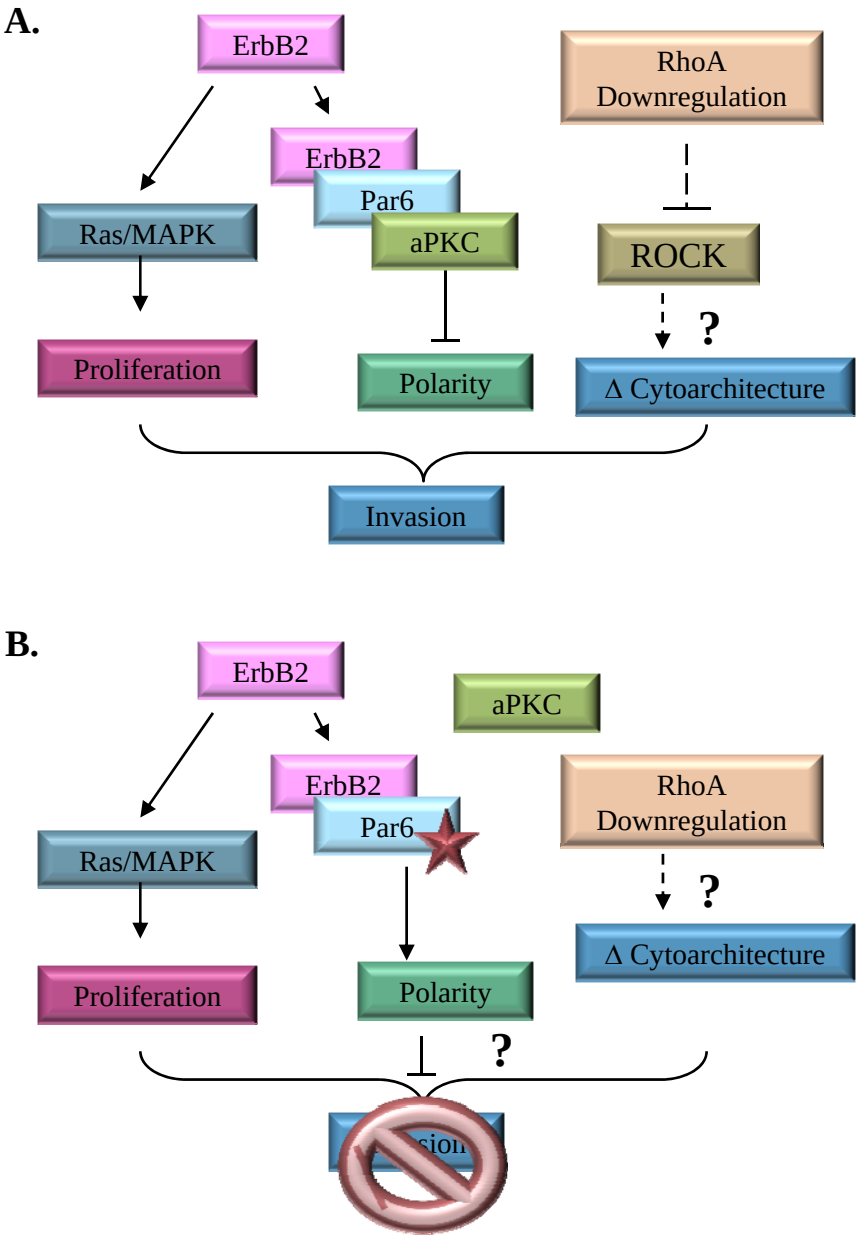

Figure 5.21. The Par polarity complex plays a central role in signaling pathways involved in proliferation and polarity.

(A) Model depicting the separate pathways of ErbB2 induced transformation. Downregulation of RhoA activity is know to promote changes to the cytoskeleton and promote formation of protrusion. Model shows the possible cooperative effect between downregulation of RhoA/ROCK activity and ErbB2 induced transformation. **(B)** Interference with Par6/aPKC complex using a Par6 mutant that does not bind aPKC prevents ErbB2 induced disruption of cell polarity and transformation . This mutation could also block RhoN19 induced invasion.

regulation of RhoA. It was shown that the Par6/aPKC complex downregulates RhoA/ROCK activity and this promotes spine morphogenesis in dendrites. This study further supports the connection between Par6 and RhoA regulation and allows us to speculate about what is happening to the cytoskeleton in the invasive protrusions. Perhaps activation of ErbB2 disrupts the Par complex and the polarity of the cells. This disrupted organization could cooperate with downregulation of RhoA, facilitating the dynamic reorganization of the cytoskeleton in the invasive protrusions.

To determine if the disruption of the Par complex is involved in the cooperation between ErbB2 and RhoN19 we could express mutant $Par6^{K19A}$ (ΔaPKC). Since Par6 requires aPKC activity for many of its functions, disturbing this complex would allow us to determine if this complex is necessary for invasive protrusion formation. Figure 5.21.B depicts a model where, expression of $Par6^{K19A}$ blocks disruption of acinar organization, even in the presence of active ErbB2. If in the presence of RhoN19 and active ErbB2, $Par6^{K19A}$ also blocks invasion, we can hypothesize that acinar organization is preventing the invasive phenotype. In further support of this model is the fact that activation of the MAPK proliferation pathway in MCF-10A acini structures did not cooperate with TGFβ to induced invasion. This suggests that ErbB2 induced proliferation is not the event that cooperates with RhoN19 to induce invasion. Although this model needs to be tested, I hypothesize that acini structures rely on organizational regulation to restrict blebbing formation and only upon disruption of organization can RhoN19 facilitate remodeling of the actin cytoskeleton and subsequent invasion.

Chapter 6: Conclusions and Perspectives

Breast cancer is thought to arise from normal breast epithelial cells that acquire the ability to proliferate uncontrollably and disrupt normal acinar organization. In precancerous breast lesions called hyperplastic enlarged lobular units (HELUs), the cells within these structures distend the acini to form lesions that are up to 100 times the size of a their normal counterpart, terminal ductal lobular units (TDLU) (Lee et al. 2006). HELUs are considered the earliest histologically identifiable precancerous breast lesion and are surprisingly common among women (Nasser 2004; Lee et al. 2006). The next stages on the histological continuum represented in the modified Wellings-Jensen model (Figure 6.1) is atypical ductal hyperplasia (ADH) and ductal carcinoma in situ (DCIS). These benign lesions are characterized by alterations to cell-cell adhesion and acinar organization. The cells within these structures begin to multilayer and fill the lumen. DCIS can be considered precursors of invasive breast cancer (IBC) because of their similar gene expression profiles (O'Connell et al. 1998; Ma et al. 2003; Seth et al. 2003; Simpson et al. 2005). In order for progression to IBC to occur, the cells within the benign lesion must break through the encompassing basement membrane and invade the surrounding breast tissue. Our studies have shown that the regulators of cell polarity and cytoarchitecture are involved with these different stages of breast cancer initiation and progression (Figure 6.1)

In collaboration with D.C. Allred, we found that that the polarity gene *Pard6b* was transcriptionally upregulated in HELUs when compared to adjacent TDLUs (Figure 6.1.A). HELUs are characterized by high proliferation rates, estrogen receptor (ERα)

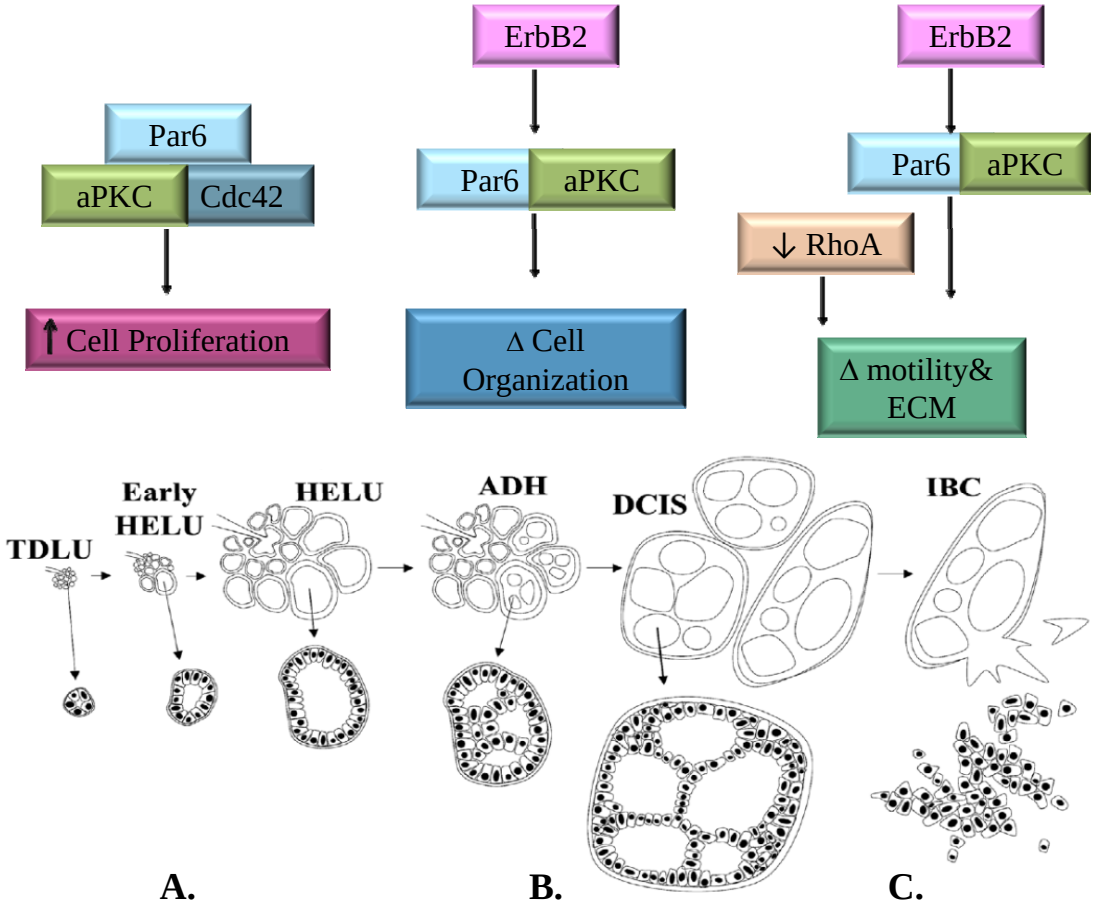

Figure 6.1 The proposed role of polarity regulators in breast cancer progression

(A) Par6 overexpression promotes proliferation and *Pard6b* is overexpressed in HELUs. **(B)** Par6/aPKC is necessary for ErbB2 to disrupt the organization of human mammary epithelial cells. ErbB2 is amplified in 30% of DCIS which are characterized by changes in cell adhesion and organization. In addition *Pard6b* overexpression is associated with ER positive breast tumors. ER is overexpressed in 70% of DCIS (Burstein et al, 2004). **(C)** ErbB2 cooperates with downregulation of RhoA to promote invasion of organized human mammary epithelial cells. IBC is characterized by breakdown of ECM and increased motility of cancer cells**.** (Modified from D.C. Allred)

positivity, low rates of apoptosis increased expression of EGF family of growth factors (Lee et al. 2006; Lee et al. 2007). Indeed, when we overexpressed Par6 in the non-transformed breast epithelial cell line, MCF-10A we observed that Par6 promoted proliferation. We determined that the proliferative effect was dependent on Par6 activating the MAPK proliferation pathway and on Par6 interactions with aPKC and Cdc42. When we plated Par6 overexpressing MCF-10A cells on basement membrane to recapitulate the organization of normal human breast acini structures *in vivo*, we found that Par6 cooperated with EGF to promote the formation of hyperplastic acinar structures. These hyperplastic structures resembled the precancerous HELUs observed *in vivo*, because they both have an increase in proliferation and an enlargement of the acinar structure. Considering that Par6 overexpression cooperated with EGF to promote hyperplastic acini, it is possible that Par6 is cooperating with EGF family of ligands to promote proliferation of HELUs.

The fact that Par6 promotes proliferation and is overexpressed in early precancerous lesions is very intriguing, because previous studies have linked Par6 to cancer progression. Par6 is required for TGFβ induced EMT (Ozdamar et al. 2005) and it cooperates with Rac/Cdc42 to promote transformation (Qiu et al. 2000). In addition, *Pard6b* is located within a frequently amplified genomic region in advanced breast cancer (Bergamaschi et al. 2006; Chin et al. 2006; Ginestier et al. 2006; Hicks et al. 2006) and this correlates with amplification of *Pard6b* mRNA (Chin et al. 2006; Ginestier et al. 2006). We found that *Pard6b* was overexpressed in 25% of breast tumors and breast cancer cell lines. Upon further experimentation we also found that Par6 overexpression correlates with ER positive breast cancers. We determined this in our

own analysis of a microarray data base as well as through a meta-analysis of published microarray databases. Since Par6 overexpression is found in precancerous breast lesions and correlates with ER positivity in advanced breast carcinoma, Par6 could impart a proliferative advantage in this context. An excess in proliferation provides a cell the opportunity to acquire genetic changes that could be beneficial for cell survival. Therefore Par6 and ER expressing hyperproliferative cells could promote genetic instability and be a driving force behind cancer formation.

Since HELUs and a subset of breast tumors have an increase in ERα expression and that a major function of estrogen is to promote proliferation through the activation of ERα (Anderson and Clarke 2004), it is likely that estrogen exposure is contributing to proliferation in HELUs and breast cancer. A recent study performed in mice supports this theory. The authors show that an increase in ERα expression in the mammary gland increased rates of cell proliferation and promoted the formation of hyperplasia that occasionally gave rise to DCIS (Frech et al. 2005). How Par6 and ER could be cooperating is not known. Since we were unable to detect a change in Par6 gene expression in the present of the ER antagonist tamoxifin, it is possible that ER does not directly regulate *Par6b* transcription in MCF-7 cells. However, the correlation between ER positivity and Par6 overexpression is observed *in vivo,* where breast tumors are surrounded by stroma and extracellular matrix, and the MCF-7 assay was not performed in the context of any microenvironment. Therefore, we either do not have the correct conditions or another mechanism is promoting the hypothesized cooperation, such as cooperation between a downstream target of ER signaling and Par6 overexpression.

While these studies and ours suggest a role for ER and Par6 in the development of hyperplasias and breast cancer, the underlying mechanism remains to be elucidated.

ER positive tumors are treated with endocrine therapy, such as tamoxifin, to antagonize ER signaling. While many patients respond to this therapy, many other do not (Osborne 1998). This could be due in part to tumor heterogeneity, therefore, we need to discover other biomarker that could be correlated with the different subtypes of breast cancer to better predict and treat the specific types of breast cancer. Perhaps overexpression of Par6 could be used as a predicative biomarker to determine which tumors will progress to malignancy and which one will remain benign.

A hallmark of cancer progression is the disruption of epithelial cell architecture. DCIS is characterized by hyperproliferation, and disorganization of the epithelium (Allred et al. 2001). The epithelial cells within these lesions display an improper architecture and fill the lumen to form abnormal structures. These multiple layers of cells that lack proper apical-basal polarity and organization (Corn and El-Deiry 2002). Since the acinar organization is disrupted during the progression of cancer, it is possible that the mechanisms that regulate normal epithelial cell polarity are disrupted and incapable of maintaining proper acinar organization. Recent studies have shown that this may be the case and that viral oncoproteins do target polarity regulators (Kiyono et al. 1997; Lee et al. 1997; Suzuki et al. 1999; Nakagawa and Huibregtse 2000; Pim et al. 2000) and others studies have correlated alterations in the polarity proteins to human cancer progression (Cavatorta et al. 2004; Schimanski et al. 2005; Gardiol et al. 2006; Kuphal et al. 2006). However, the precise mechanisms by which these alterations are involved cancer are not known.

Our studies have determined an oncogene, ErbB2 can disrupt acinar organization by targeting a regulator of cell organization, the Par polarity complex We have shown that Par6/aPKC is required for ErbB2 induced transformation of three-dimensional mammary epithelial cells (Chapter 4)(Aranda et al. 2006). Using a Par6 mutant that can no longer bind to aPKC, we determined that ErbB2 requires an interaction with Par6/aPKC in order to disrupt epithelial cell polarity and inhibit apoptosis. However, the interaction with Par6/aPKC is not required for ErbB2 to induce cell proliferation. Our study suggests that ErbB2 induced transformation uses two different arms, one that activates the well-established Ras-MAPK proliferation pathway (Hynes and Lane 2005; Citri and Yarden 2006) and the other that interacts with Par6/aPKC and disrupts epithelial cell polarity (Figure 6.2). Therefore, polarity regulators can be targeted by oncogenes during transformation of three-dimensional organized epithelial structures.

We hypothesize that the regulators of normal epithelial cell organization need to be targeted or disrupted in order for tumor formation to progress. Therefore maintenance of normal epithelial cell organization can serve as a 'checkpoint' for tumorigenesis preventing the survival of cells that respond to aberrant proliferative signals. Oncogenes such as ErbB2 have the ability to overcome this checkpoint by targeting the regulators of cell polarity in addition to promoting aberrant proliferation. This hypothesis fits into our model of breast cancer progression (Figure 6.1). ErbB2 is amplified in DCIS and these lesions not only have an increase in proliferation as seen in hyperplasic lesion, but they also have a disruption in organization (Figure 6.1.B). This work has identified a role for the polarity regulators in the progression of breast cancer by placing the Par6/aPKC module downstream of oncogenic ErbB2.

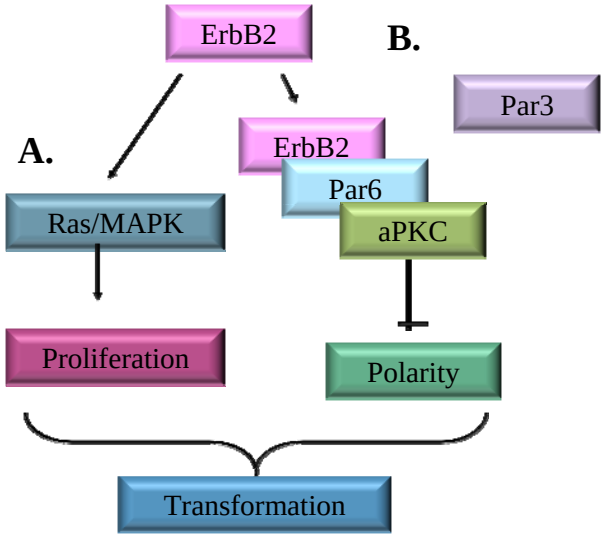

Figure 6.2. ErbB2 induced transformation

Model depicting the separate pathways of ErbB2 induced transformation. **(A)** Activation of ErbB2 stimulates the Ras/MAPK proliferation pathway. **(B)** Activation of ErbB2 disrupts the Par complex by recruiting Par6/aPKC. This interaction is necessary in order for ErbB2 to disrupt acinar organization. Both arms of ErbB2 signaling are necessary to transform acinar structures.

The genetic features that distinguish pre-malignant lesions such as DCIS from IBC are not known (Burstein et al. 2004). Therefore it is important to identify the mechanisms that promote invasion of breast cancer cells. IBC is characterized by changes in cell adhesion, ECM, and the presence of motile cells that are no longer associated with the primary tumor site (Ronnov-Jessen et al. 1996). ErbB2 transformed multi-acinar structures share properties of pre-malignant breast cancer and can be considered a model this type of breast cancer. Therefore we used the MCF-10A, inducible ErbB2 model system to study alterations that can cooperate with ErbB2 to promote invasion acinar structures. Our studies have shown that downregulation of the cytoarchitecture regulator RhoA in cooperates with ErbB2 to promote invasion of multi-acinar structures. This study demonstrates that re-initiation of proliferation, disruption of apical-basal polarity and deregulation of cytoarchitectural proteins together can promote invasion of previously non-invasive structures (Figure 6.1.C). In order for the cells to become invasive the cytoarchitecture needs to be altered to facilitate the formation of protrusions commonly observed in migratory cells (Wang et al. 2003; Bose and Wrana 2006; Nakayama et al. 2008). These data lend further support to our theory that cell organization is a checkpoint for the progression to cancer because alterations to the cell cytoskeleton, which is necessary to maintain proper cell organization, could promote invasion and therefore progression to malignancy.

The studies outlined in this thesis identify a role for the regulators of cell organization in oncogenic signaling and transformation. We have found that Par6 is overexpressed in precancerous breast lesion and that its overexpression is maintained in advanced ER positive breast cancers (Figure 6.1.A). In addition we have placed

Par6/aPKC downstream of ErbB2 induced transformation (Figure 6.1.B) and we have shown cooperation between ErbB2 and downregulation of RhoA to promote invasion in breast epithelial acinar structures (Figure 6.1.C). Our studies exemplify the need to understand the mechanisms that regulate epithelial cell organization because disruption of these mechanisms promotes breast cancer progression. Since we have observed the Par6/aPKC module as a player in the different stages of breast cancer, it is possible that Par6 could be a predictive biomarker for cancers that will progress to malignancy. Further analyses of Par6-aPKC pathway allow for the discovery of novel targets for early stage precancerous breast lesions.

Materials and methods

Cell culture and stable cell line generation

MCF-10A cells were maintained in DMEM/F12 supplemented with 5% horse serum, 10 μg/mL insulin, 20 ng/mL EGF, 500 ng/ml hydrocortisone and 100 ng/ml Cholera toxin as previously described in (Debnath et al. 2003a). Comma-1D β geo cells were kindly provided by Daniel Medina (Baylor College of Medicine) and were maintained in DMEM/F12 supplemented with 2% FBS, 10 μg/mL insulin and 5 ng/mL EGF (Danielson et al. 1984). HC11 cells were obtained from the Rosen laboratory and cultured according to (Xian et al. 2005). Preparation of virus was performed as previously described (Ory et al. 1996). Briefly, 10 μg plasmid DNA was transfected into the VSV-GPG retrovirus packaging cell line by standard liposome mediate transfection (Lipofectamine). Media containing virus were collected at day 4, 5 and 6 after transfection, and passed through a 0.45-μm filter. Infection was preformed as previously described (Debnath et al. 2003a). Briefly, 1 X 10^5 cells were plated on a 10 cm dish and incubated for 16 hours. Cells were then infected with 1 ml of virus in media containing 4 μg/ml polybrene for 6 hours. 24 hours post-infection cells were selected with fresh media containing 1μg/ml of puromyocin. MCF-7 cells were maintained in DMEM supplemtented with 10% FBS. MDCK cells were grown in Minimal Essential Medium (MEM, GibcoBRL, Grand Island, NE) supplemented with 10% fetal bovine serum, 50U/ml penicillin, 50U/ml streptomycin, and 50U/ml non-essential amino acids. Populations of Madin Darby Canine Kidney II cells expressing ErbB2 chimera (MDCK-

ErbB2) were previously described (Muthuswamy et al. 2001). Clones expressing equal levels of the ErbB2 chimera were selected by anti-HA immunoblots, and their ability to undergo dimerizer (AP1510)-inducible phosphorylation was determined by performing phosphosphotyrosine immunoblots (Muthuswamy et al. 1999). MDCK-ErbB2 cells overexpressing mPar6 (MDCK-ErbB2-Par6) were also generated by infection.

DNA constructs

Carboxy or amino-terminal Flag-epitope tag mouse par6C (Par6α) was generated by PCR amplification of *mPar6C* from pFlag-CMV-mpar6C (Lin et al. 2000) and cloned into MSCV-PURO-IRES-GFP (kindly provided by S. Lowe, Cold Spring Harbor Laboratory, Cold Spring Harbor, NY). Point mutations of mPar6C (Par6α) were generated using site directed mutagenesis. Amino-terminal Flag-epitope tag human Par6β was generated by PCR amplification from pBluescriptR-hPar6β (ATCC) and cloned in to MSCV-PURO-IRES-GFP. Two aPCK short-hairpin vectors were obtained from Open Biosystems, Huntsville, AL and subcloned into MSCV-LTR-PURO-IRES-GFP (Dickins et al. 2005). The targeting sequence of the shPKC1: CACAGACAGTAATTCCATATTAG and shPKC2: GATTATCTCTTCCAAGTTATTAG. Construction and characterization of chimeric ErbB2 receptor that can be activated by addition of a small molecule ligand, AP1510 (ARIAD Pharmaceuticals, Cambridge, MA) was previously described (Muthuswamy et al. 1999).

Antibodies and Materials

MG-132, Lactocystin, Bafilomycin A1, U0126 (Calbiochem), Filipin III, Tamoxifin Propidium Iodide (Sigma, St Louis, MO), ap1510 (ARIAD Pharmaceuticals, Cambridge, MA), Growth factor reduced Matrigel^{TM} (BD Biosciences, San Jose, C). Antibodies used in this study were against: Ki67, ZO1 (Zymed, San Francisco, CA); PKCι, GM130, Ccdc42, Erk2, P-tyr, E-cadherin (BD Biosciences, San Jose, CA); hPar6c antibody hPar6c antibody was generated against a N-terminal peptide sequence (MARPQRTPARSPDSI) in rabbits (Aranda et al. 2006); mPar3, EGFR (Upstate Biotechnology, Lake Placid, NY); HA (Covance, Princeton, NJ); gp135 (gift from James Nelson); PKCζ (Santa Cruz Biotechnology, Santa Cruz, CA) cleaved caspase-3, p-ERM, p-AKT (Cell Signaling Technology, Danvers, MA); Flag M2, β-Actin (Sigma, St Louis, MO); Laminin (Chemicon, Temecula, CA); p-ERK 1 and 2, p-PKCι, Alexa-Fluor-conjugated secondary antibodies (Invitrogen, Carlsbad, CA) were used.

Cell growth and S-phase assays

MCF-10A (Vector, Par6α, K19A, ΔPro136, M235W and Par6β) cells were grown to confluency under normal growth conditions and placed in assay medium (DMEM/F12 supplemented with 2% horse serum, mg/ml Insulin, mg/ml hydrocortisone and mg/ml cholera toxin) for 16 hours. Cells were then trypsinized and $5X10^4$ (growth curve) or $2.5X10^5$ (S-phase) cells were plated in assay medium. For growth curve assays cells were trypsinized and counted by hemacytometer on day 1,3,5,7,9 and 11. For S-phase assay 30% of the assay media was changed on day 1 and cells were imaged by phase micrscopy before harvesting on day 3. Cells were collected for flow cytometery by

trypsinization and subsequent ethanol (70%) fixation. Cells were rehydrated in PBS with 1% Calf serum and stained with 20mg/ml Propidium Iodide (Sigma) containing 100ug/ml RNAseA. Samples were analyzed using an LSRII flow cytometer (Becton Dickinson, San Jose, CA), at least 10,000 cells per sample were collected. The Data from three independent experiments were analyzed using ModFit software (Verity, Topsham, ME). Comma1D cells (Vector, Par6α) were grown to confluency under normal growth conditions and then placed in assay medium (DMEM/F12 supplemented with 0.5% Fetal Bovine Serum, 5μg/ml Insulin). $1X10^5$ cells were plated and cells numbers were counted on day 3 using a hemacytometer.

For morphological and cell cycle studies, all MDCK derived cell lines were platted at density of 0.5×10^6 cells per well in a 12 well plate on 0.4μ pore size Transwell inserts (Corning, Corning, NY) and allowed to polarize for four days. ErbB2 was activated in these polarized monolayers by addition of Dimerizer (1.0 μM) for indicated length of time and the filters were further processed as described below.

Co-culture growth assays

Vector or Par6 (C-terminal Flag) expressing cells were plated on 8.0um pore size Transwell inserts (Corning, Corning, NY). The inserts were placed in tissue culture plates that contain either vector or Par6 expressing cells. Co-cultures were maintained for 3 days in assay medium and then collected for cell cycle analysis as described in the previous section.

Vector or Par6 (C-terminal Flag) expressing cells were labeled with a cell permeable DiI derivative (DiI C_{18}(3)-DS) (Molecular Probes) at a concentration of

2ug/ml. Labeled cells were plated with unlabeled vector or Par6 expressing cells at a ratio of 1:250. The cells were plated on tissue culture dishes and imaged by phase and fluorescent microscopy after 30 hours.

3D morphogeneis Matrigel^{TM} overlay assay

Chapters 2 and 3

MCF-10A stable cell lines (Vector, Par6α, K19A, and Par6β) were trypsinized and 4,000 single cells/well in an 8 well chamber slide (BD) coated with Matrigel. Cells were grown in assay medium with various amount of EGF (5, 0.5, 0.1 and 0 ng/ml). Media was changed and acini were imaged every four days. Day 12 acini structures were analyzed using using AxioVison 4.5 (Zeiss, Thornwood, NY). The acini size distribution of ~600 acini from 3 independent experiments were represented in a box plot. Each box represents 50% of the data within the inter-quartile range. The blue line represents the median value and the spread represents 1.5 times the inter-quartile range and outliers are shown as circles. Statistical analyses were performed using GraphPad Prism software and Mann-Whitney test. HC11 stable cell lines (Vector, Par6α) were grown on Matrigel with 0.5ng/ml EGF and day 12 structures were analyzed as done for MCF-10A cells.

Chapters 4 and 5

10A.ErbB2 cell lines overexpressing control vector, Par6α, or Par6^{K19A} were plated on Matrigel. Day 4 or day 16 acinar structures were stimulated with 1.0 μM AP1510 or left untreated for 4 days. At day 8 or day20, morphology was assessed by phase microscopy and cells were fixed and processed for immunoflourescence analysis as described elsewhere(Debnath et al. 2003a). Structure area was measured using

Axiovision 4.4 software (Zeiss) and the number of multistructures was counted. At least 400 structures from three different experiments were studied for each experimental condition, and areas were subjected to statistical analysis (see above) and plotted as box plots showing a box with the median and the 25 to 75 quartiles and lines for atypical values. 10A. ErbB2.

10A.ErbB2 cells were plated on Matrigel. On Day 12 of morphogenesis acini were infected with RhoN19 expressing and a tetracycline regulator virus. Acini structures were infected in the presence or absence of tetracycline. 24 hours post-infection ErbB2 was activated by AP1510. Acini structure were monitored for 4 day post-activation and imaged by phase microscopy and subsequent biochemical and immunofluoresecent analysis.

Invasion overlay and embedded assay

10A.ErbB2 cells were cultured on a mixture of collagen:Matrigel using the overlay method as described in (Seton-Rogers et al. 2004). Briefly, a mixture of bovine dermal collagen I (Vitrogen; Cohesion Technologies, Palo Alto, CA) and growth factor-reduced Matrigel, was used as the underlay. Collagen I was neutralized by NaOH and PBS to final concentrations of 10 mM and 1X, respectively, and the pH was adjusted to 7.5 with 0.1 M HCl. After plating the cultures were treated the same as Matrigel overlay alone.

For the embedded assay, chamber slides were first coated with a layer of Matrigel (50µl), after solidification 40,000 cells were resuspended in 100 µl of cold Matrigel and added to each well and incubated for 20 min at 37°C. Then another layer of 100 µl

Matrigel was added to the layer of cells. After plating the cultures were treated the same as the Matrigel overlay assay.

Time lapse imaging

10A.ErbB2 cells were plated, infected and stimulated as stated above in the Matrigel overlay assay. Microscopy was performed on Zeiss Axiovert 200M using AxioVison 4.1. Live acini structures were placed in a temperature controlled humidified chamber with 5% CO2. (Temp control 37.2 digital and CT1 controller 3700 digital, Zeiss, Thornwood, NY). Phase images were collected every 30 minutes from multiple points of interest within each well/condition for a period of 70 hours. The images were compiled in AxioVision 4.1. For the tetracycline repression time course, 10A. ErbB2 acini are infected and plated as above and on day 4 of stimulation, tetracycline was added to the media. The acinar response was monitored for a period of 40 hours post addition of tetracycline. The phase images were collected and compiled as explained above.

Immunofluorescence

All Immunofluorescence procedures were performed as previously described (Debnath et al. 2003a). Microscopy was performed on Zeiss Axiovert 200M using AxioVison 4.5 and ApoTome imaging system (Zeiss, Thornwood, NY). A quantitative image analysis method was designed to estimate the disruption of apical basal polarity caused by ErbB2 activation. First, boundaries between the different membrane domains were defined in non-stimulated fully polarized monolayers by addressing the localization of different membrane markers in 0.5 μm non-overlapping X-Z optical sections. The apical domain was defined as a 1.0 μm region from the apex of the monolayer and the

apical-lateral border was defined as the 2.0 – 3.0 μm region from the apex and the remainder (4.0 – 8.0 μm) was defined as the lateral membrane by analyzing more than 2000 cell junctions. The presence of markers outside this standardized boundary was analyzed then in ErbB2 activated filters as an indicator of polarity disruption. For each time point considered, over 200 junctions were analyzed. Multilayering was estimated as follows: For each condition, fluorescence images were collected for five fields. Total area with more than one layer of nuclei was estimated using image analysis using Axiovision 4.4 software (Zeiss). Data from three independent experiments were plotted as mean ±SD.

The number of blebbing protrusions that lack laminin were quantitated by visualization of serial z-stack images taken on a microscope capable of optical sectioning. This aspect of microscopy was crucial to ensure that the laminin from acini structures above or below the focal plane did not result in a false positive. A protrusion was classified devoid of laminin staining, if there was no laminin present in any focal plane of the acinar structure

Par complex immunoprecipitation

MDCK-ErbB2 or 10A.ErbB2 cells were grown to confluency in 10 cm plates. ErbB2 signaling was activated by adding AP1510 (Dimerizer) (1.0 μM). For immunoprecipitation studies, cells were lysed and anti-mPar3, anti-mPar6, anti-Ha.11, and anti-Flag immunoprecipitations and immunoblots were carried out as described earlier (Muthuswamy et al. 2001).

Biochemistry and immunoprecipitation

MCF-10A cells (Vector, Par6α, K19A, ΔPro136, M235W and Par6β) were plated $2x10^6$ in growth media and cells were stimulated on day 5 with 2ug/ml EGF. Cells were lysed in TNE buffer, (50mM Tris, 150mM NaCl, 1% NP-40, 10mM NaF, pH 8.0) and immunoprecipitation of with Flag antibodies or immunoblotted with indicated antibodies. For cells lysed in RIPA: (20mM Tris, 150mM NaCl, 1% NP-40, 0.1% SDS, 10mM NaF, pH 8.0)

Densometric analysis of short-hairpin RNA knock down of aPKC was performed using image J software. The intensity of each band we quantitated and normalized to b-actin. Expression was normalized to vector shLuc expressing MCF-10A cells and represented as fold overexpression.

Quantitative PCR

25 breast tumor samples were obtained from the Wigler laboratory (CSHL). RNA was isolated using a Versagene RNA tissue kit (Gentra Systems) (Min Yu). Normal breast tissue RNA was a gift from David Mu (CSHL). Breast cancer cell line RNA was a gift from Adrian Krainer (CSHL). MCF-10A control and Par6β overexpressing RNA were obtained from trizol lysis (Invitrogen, Carlsbad, CA) according to the manufactures protocol. MCF-7 cells were grown to 70% confleuncey in charcoal treated FBS and inhibited with Tamoxifin for 3 hours and harvested the same as MCF-10A RNA preparation. cDNA was generated using a Taqman reverse transcriptase kit (Roche). Quantitative real-time PCR was performed using SYBR® green master mix (Applied Biosystems). The following primer sequences were used for Par6β, 5'-

GTGAAGAGCAAGTTTGGAGC-3', and 5'-GATGTCTGATAGCCTACCA-3' and, for GAPHDH, 5'-CGACAGTCAGCCGCATCTT-3' and 5'-CGTTGACTCCGA CCTTCA-3'. Samples were run on a Peltier thermalcycler (PTC-200) from MJ Research and data was collected using an Opticon monitor chromo4 continuous fluorescence detector. Cycles were normalized to GAPDH and compared to MCF-10A or normal breast tissue Par6β levels.

Analysis of human breast cancers

Gene expression was performed on 112 breast tumors samples and data was generously provided by Therese Sorlei and colleagues by Lakshmi Muthuswamy. Laser capture and subsequent gene expression analysis was performed by Sanjun Lee and previously published (Lee *et al*, 2006). A meta-analysis was performed of of published gene expression databases using the integrated data platform Oncomine (Rhodes *et al*, 2004).

Analysis of 69 ER^- and 226 ER^+ breast carcinoma, P-value = 2.4E-23 (van deVijver *et al*, 2002). Analysis of 11 ER^- and 24 ER^+ breast carcinoma, P-value = 4.6E-7(Zhao *et al*, 2004). Analysis of 28 ER^- and 27 ER^+ breast carcinoma, P-value = 9.5E-7 (Ginestetier *et al*, 2006). Analysis of 9 ER^- and 26 ER^+ breast carcinoma, P-value = 7.1E-4 (Perou *et al*, 1999).

Adenovirus:

pADTet adenovirus expressing RhoN19 and was generously provided by Jonathan Chernoff (FCCC). Virus was amplified in 293T cells. The cells were infected with 3 μl of stock virus and 3 ul of pAdTet virus expressing tet repressor. Cells were

harvested by scraping once 70% of the cells had rounded off the dish. The cells were then resuspended in 5 ml of media and subjected to 3 rounds of freeze thaw cycles to break open the cells. The cell debris was spun down and the viral supernatant was used for subsequent infections. Viral titer was determined by OD at 260 nm. One A260 unit contains ~10^{12} viral particles (particles:infectious particles=~20:1).

Bibliography:

Abd El-Rehim, D.M., Ball, G., Pinder, S.E., Rakha, E., Paish, C., Robertson, J.F., Macmillan, D., Blamey, R.W., and Ellis, I.O. 2005. High-throughput protein expression analysis using tissue microarray technology of a large well-characterised series identifies biologically distinct classes of breast cancer confirming recent cDNA expression analyses. *Int J Cancer* **116**(3): 340-350.

ACS. 2008. American Cancer Society. Cancer facts and figures 2008.

Aldaz, C.M., Chen, T., Sahin, A., Cunningham, J., and Bondy, M. 1995. Comparative allelotype of in situ and invasive human breast cancer: high frequency of microsatellite instability in lobular breast carcinomas. *Cancer Res* **55**(18): 3976-3981.

Allred, D.C., Clark, G.M., Molina, R., Tandon, A.K., Schnitt, S.J., Gilchrist, K.W., Osborne, C.K., Tormey, D.C., and McGuire, W.L. 1992. Overexpression of HER-2/neu and its relationship with other prognostic factors change during the progression of in situ to invasive breast cancer. *Hum Pathol* **23**(9): 974-979.

Allred, D.C., Mohsin, S.K., and Fuqua, S.A. 2001. Histological and biological evolution of human premalignant breast disease. *Endocr Relat Cancer* **8**(1): 47-61.

Amara, J.F., Clackson, T., Rivera, V.M., Guo, T., Keenan, T., Natesan, S., Pollock, R., Yang, W., Courage, N.L., Holt, D.A., and Gilman, M. 1997. A versatile synthetic dimerizer for the regulation of protein-protein interactions. *Proc Natl Acad Sci U S A* **94**(20): 10618-10623.

Anderson, E. and Clarke, R.B. 2004. Steroid receptors and cell cycle in normal mammary epithelium. *J Mammary Gland Biol Neoplasia* **9**(1): 3-13.

Andrechek, E.R., Hardy, W.R., Siegel, P.M., Rudnicki, M.A., Cardiff, R.D., and Muller, W.J. 2000. Amplification of the neu/erbB-2 oncogene in a mouse model of mammary tumorigenesis. *Proc Natl Acad Sci U S A* **97**(7): 3444-3449.

Aranda, V., Haire, T., Nolan, M.E., Calarco, J.P., Rosenberg, A.Z., Fawcett, J.P., Pawson, T., and Muthuswamy, S.K. 2006. Par6-aPKC uncouples ErbB2 induced disruption of polarized epithelial organization from proliferation control. *Nat Cell Biol* **8**(11): 1235-1245.

Battersby, S. and Anderson, T.J. 1988. Proliferative and secretory activity in the pregnant and lactating human breast. *Virchows Arch A Pathol Anat Histopathol* **413**(3): 189-196.

Behrens, J., Vakaet, L., Friis, R., Winterhager, E., Van Roy, F., Mareel, M.M., and Birchmeier, W. 1993. Loss of epithelial differentiation and gain of invasiveness correlates with tyrosine phosphorylation of the E-cadherin/beta-catenin complex in cells transformed with a temperature-sensitive v-SRC gene. *J Cell Biol* **120**(3): 757-766.

Bellovin, D.I., Simpson, K.J., Danilov, T., Maynard, E., Rimm, D.L., Oettgen, P., and Mercurio, A.M. 2006. Reciprocal regulation of RhoA and RhoC characterizes the EMT and identifies RhoC as a prognostic marker of colon carcinoma. **25**(52): 6959-6967.

Bergamaschi, A., Kim, Y.H., Wang, P., Sorlie, T., Hernandez-Boussard, T., Lonning, P.E., Tibshirani, R., Borresen-Dale, A.L., and Pollack, J.R. 2006. Distinct patterns of DNA copy number alteration are associated with different clinicopathological features and gene-expression subtypes of breast cancer. *Genes Chromosomes Cancer* **45**(11): 1033-1040.

Berra, E., Diaz-Meco, M.T., Dominguez, I., Municio, M.M., Sanz, L., Lozano, J., Chapkin, R.S., and Moscat, J. 1993. Protein kinase C ? isoform is critical for mitogenic signal transduction. *Cell* **74**(3): 555-563.

Berra, E., Diaz-Meco, M.T., Lozano, J., Frutos, S., Municio, M.M., Sanchez, P., Sanz, L., and Moscat, J. 1995. Evidence for a role of MEK and MAPK during signal transduction by protein kinase C zeta. *Embo J* **14**(24): 6157-6163.

Betschinger, J., Mechtler, K., and Knoblich, J.A. 2003. The Par complex directs asymmetric cell division by phosphorylating the cytoskeletal protein Lgl. *Nature* **422**(6929): 326-330.

Bilder, D. 2004. Epithelial polarity and proliferation control: links from the Drosophila neoplastic tumor suppressors. *Genes Dev* **18**(16): 1909-1925.

Bilder, D., Li, M., and Perrimon, N. 2000. Cooperative regulation of cell polarity and growth by Drosophila tumor suppressors. *Science* **289**(5476): 113-116.

Bjorkoy, G., Perander, M., Overvatn, A., and Johansen, T. 1997. Reversion of Ras- and phosphatidylcholine-hydrolyzing phospholipase C-mediated transformation of NIH 3T3 cells by a dominant interfering mutant of protein kinase C lambda is accompanied by the loss of constitutive nuclear mitogen-activated protein kinase/extracellular signal-regulated kinase activity. *J Biol Chem* **272**(17): 11557-11565.

Bodian, C.A., Perzin, K.H., Lattes, R., Hoffmann, P., and Abernathy, T.G. 1993. Prognostic significance of benign proliferative breast disease. *Cancer* **71**(12): 3896-3907.

Bose, R. and Wrana, J.L. 2006. Regulation of Par6 by extracellular signals. *Current Opinion in Cell Biology*

Cell regulation **18**(2): 206-212.

Bouzahzah, B., Albanese, C., Ahmed, F., Pixley, F., Lisanti, M.P., Segall, J.D., Condeelis, J., Joyce, D., Minden, A., Der, C.J., Chan, A., Symons, M., and Pestell, R.G. 2001. Rho family GTPases regulate mammary epithelium cell growth and metastasis through distinguishable pathways. *Mol Med* **7**(12): 816-830.

Brajenovic, M., Joberty, G., Kuster, B., Bouwmeester, T., and Drewes, G. 2004. Comprehensive proteomic analysis of human Par protein complexes reveals an interconnected protein network. *J Biol Chem* **279**(13): 12804-12811.

Brancolini, C., Lazarevic, D., Rodriguez, J., and Schneider, C. 1997. Dismantling Cell-Cell Contacts during Apoptosis Is Coupled to a Caspase-dependent Proteolytic Cleavage of beta -Catenin. *J Cell Biol* **139**(3): 759-771.

Brumby, A.M. and Richardson, H.E. 2003. scribble mutants cooperate with oncogenic Ras or Notch to cause neoplastic overgrowth in Drosophila. *Embo J* **22**(21): 5769-5779.

Burstein, H.J., Polyak, K., Wong, J.S., Lester, S.C., and Kaelin, C.M. 2004. Ductal carcinoma in situ of the breast. *N Engl J Med* **350**(14): 1430-1441.

Carter, P., Presta, L., Gorman, C.M., Ridgway, J.B., Henner, D., Wong, W.L., Rowland, A.M., Kotts, C., Carver, M.E., and Shepard, H.M. 1992. Humanization of an anti-p185HER2 antibody for human cancer therapy. *Proc Natl Acad Sci U S A* **89**(10): 4285-4289.

Cavatorta, A.L., Fumero, G., Chouhy, D., Aguirre, R., Nocito, A.L., Giri, A.A., Banks, L., and Gardiol, D. 2004. Differential expression of the human homologue of drosophila discs large oncosuppressor in histologic samples from human papillomavirus-associated lesions as a marker for progression to malignancy. *Int J Cancer* **111**(3): 373-380.

Chalmers, A.D., Pambos, M., Mason, J., Lang, S., Wylie, C., and Papalopulu, N. 2005. aPKC, Crumbs3 and Lgl2 control apicobasal polarity in early vertebrate development. *Development* **132**(5): 977-986.

Chin, K., DeVries, S., Fridlyand, J., Spellman, P.T., Roydasgupta, R., Kuo, W.L., Lapuk, A., Neve, R.M., Qian, Z., Ryder, T., Chen, F., Feiler, H., Tokuyasu, T., Kingsley, C., Dairkee, S., Meng, Z., Chew, K., Pinkel, D., Jain, A., Ljung, B.M., Esserman, L., Albertson, D.G., Waldman, F.M., and Gray, J.W. 2006. Genomic and transcriptional aberrations linked to breast cancer pathophysiologies. *Cancer Cell* **10**(6): 529-541.

Citri, A. and Yarden, Y. 2006. EGF-ERBB signalling: towards the systems level. *Nat Rev Mol Cell Biol* **7**(7): 505-516.

Corn, P.G. and El-Deiry, W.S. 2002. Derangement of growth and differentiation control in oncogenesis. *Bioessays* **24**(1): 83-90.

Cotran, R.S., Kumar, V., and Robbins, S.L. 1989. *Robbins pathologic basis of disease*. Saunders, Philadelphia.

Danielson, K.G., Oborn, C.J., Durban, E.M., Butel, J.S., and Medina, D. 1984. Epithelial Mouse Mammary Cell Line Exhibiting Normal Morphogenesis in vivo and Functional Differentiation in vitro

10.1073/pnas.81.12.3756. *PNAS* **81**(12): 3756-3760.

Debnath, J., Mills, K.R., Collins, N.L., Reginato, M.J., Muthuswamy, S.K., and Brugge, J.S. 2002. The role of apoptosis in creating and maintaining luminal space within normal and oncogene-expressing mammary acini. *Cell* **111**(1): 29-40.

Debnath, J., Muthuswamy, S.K., and Brugge, J.S. 2003a. Morphogenesis and oncogenesis of MCF-10A mammary epithelial acini grown in three-dimensional basement membrane cultures. *Methods* **30**(3): 256-268.

Debnath, J., Walker, S.J., and Brugge, J.S. 2003b. Akt activation disrupts mammary acinar architecture and enhances proliferation in an mTOR-dependent manner. *J Cell Biol* **163**(2): 315-326.

Denoyelle, C., Vasse, M., Korner, M., Mishal, Z., Ganne, F., Vannier, J.P., Soria, J., and Soria, C. 2001. Cerivastatin, an inhibitor of HMG-CoA reductase, inhibits the signaling pathways involved in the invasiveness and metastatic properties of highly invasive breast cancer cell lines: an in vitro study. *Carcinogenesis* **22**(8): 1139-1148.

Devi, G.R., Beer, T.M., Corless, C.L., Arora, V., Weller, D.L., and Iversen, P.L. 2005. In vivo bioavailability and pharmacokinetics of a c-MYC antisense phosphorodiamidate morpholino oligomer, AVI-4126, in solid tumors. *Clin Cancer Res* **11**(10): 3930-3938.

Di Guglielmo, G.M., Baass, P.C., Ou, W.J., Posner, B.I., and Bergeron, J.J. 1994. Compartmentalization of SHC, GRB2 and mSOS, and hyperphosphorylation of Raf-1 by EGF but not insulin in liver parenchyma. *Embo J* **13**(18): 4269-4277.

Dickins, R.A., Hemann, M.T., Zilfou, J.T., Simpson, D.R., Ibarra, I., Hannon, G.J., and Lowe, S.W. 2005. Probing tumor phenotypes using stable and regulated synthetic microRNA precursors. *Nat Genet* **37**(11): 1289-1295.

Downward, J. 2003. Targeting RAS signalling pathways in cancer therapy. *Nat Rev Cancer* **3**(1): 11-22.

Dranoff, G. 2004. Cytokines in cancer pathogenesis and cancer therapy. *Nat Rev Cancer* **4**(1): 11-22.

Drubin, D.G. and Nelson, W.J. 1996. Origins of cell polarity. *Cell* **84**(3): 335-344.

Dupont, W.D., Parl, F.F., Hartmann, W.H., Brinton, L.A., Winfield, A.C., Worrell, J.A., Schuyler, P.A., and Plummer, W.D. 1993. Breast cancer risk associated with proliferative breast disease and atypical hyperplasia. *Cancer* **71**(4): 1258-1265.

Eder, A.M., Sui, X., Rosen, D.G., Nolden, L.K., Cheng, K.W., Lahad, J.P., Kango-Singh, M., Lu, K.H., Warneke, C.L., Atkinson, E.N., Bedrosian, I., Keyomarsi, K., Kuo, W.L., Gray, J.W., Yin, J.C., Liu, J., Halder, G., and Mills, G.B. 2005. Atypical PKCiota contributes to poor prognosis through loss of apical-basal polarity and cyclin E overexpression in ovarian cancer. *Proc Natl Acad Sci U S A* **102**(35): 12519-12524.

Etienne-Manneville, S. and Hall, A. 2001. Integrin-mediated activation of Cdc42 controls cell polarity in migrating astrocytes through PKCzeta. *Cell* **106**(4): 489-498.

-. 2003a. Cdc42 regulates GSK-3beta and adenomatous polyposis coli to control cell polarity. *Nature* **421**(6924): 753-756.

-. 2003b. Cell polarity: Par6, aPKC and cytoskeletal crosstalk. *Curr Opin Cell Biol* **15**(1): 67-72.

Fata, J.E., Werb, Z., and Bissell, M.J. 2004. Regulation of mammary gland branching morphogenesis by the extracellular matrix and its remodeling enzymes. *Breast Cancer Res* **6**(1): 1-11.

Ferlay, J., Autier, P., Boniol, M., Heanue, M., Colombet, M., and Boyle, P. 2007. Estimates of the cancer incidence and mortality in Europe in 2006. *Ann Oncol* **18**(3): 581-592.

Fialka, I., Schwarz, H., Reichmann, E., Oft, M., Busslinger, M., and Beug, H. 1996. The estrogen-dependent c-JunER protein causes a reversible loss of mammary epithelial cell polarity involving a destabilization of adherens junctions. *J Cell Biol* **132**(6): 1115-1132.

Fitzgibbons, P.L., Page, D.L., Weaver, D., Thor, A.D., Allred, D.C., Clark, G.M., Ruby, S.G., O'Malley, F., Simpson, J.F., Connolly, J.L., Hayes, D.F., Edge, S.B., Lichter, A., and Schnitt, S.J. 2000. Prognostic factors in breast cancer. College of American Pathologists Consensus Statement 1999. *Arch Pathol Lab Med* **124**(7): 966-978.

Fogg, V.C., Liu, C.J., and Margolis, B. 2005. Multiple regions of Crumbs3 are required for tight junction formation in MCF10A cells. *J Cell Sci* **118**(Pt 13): 2859-2869.

Forcet, C., Etienne-Manneville, S., Gaude, H., Fournier, L., Debilly, S., Salmi, M., Baas, A., Olschwang, S., Clevers, H., and Billaud, M. 2005. Functional analysis of Peutz-Jeghers mutations reveals that the LKB1 C-terminal region exerts a crucial role in regulating both the AMPK pathway and the cell polarity. *Hum Mol Genet* **14**(10): 1283-1292.

Frech, M.S., Halama, E.D., Tilli, M.T., Singh, B., Gunther, E.J., Chodosh, L.A., Flaws, J.A., and Furth, P.A. 2005. Deregulated estrogen receptor alpha expression in mammary epithelial cells of transgenic mice results in the development of ductal carcinoma in situ. *Cancer Res* **65**(3): 681-685.

Friedl, P., Hegerfeldt, Y., and Tusch, M. 2004. Collective cell migration in morphogenesis and cancer. *Int J Dev Biol* **48**(5-6): 441-449.

Fritz, G., Brachetti, C., Bahlmann, F., Schmidt, M., and Kaina, B. 2002. Rho GTPases in human breast tumours: expression and mutation analyses and correlation with clinical parameters. *Br J Cancer* **87**(6): 635-644.

Fritz, G., Just, I., and Kaina, B. 1999. Rho GTPases are over-expressed in human tumors. *Int J Cancer* **81**(5): 682-687.

Fukata, M. and Kaibuchi, K. 2001. Rho-family GTPases in cadherin-mediated cell-cell adhesion. *Nat Rev Mol Cell Biol* **2**(12): 887-897.

Gao, L., Joberty, G., and Macara, I.G. 2002a. Assembly of epithelial tight junctions is negatively regulated by Par6. *Curr Biol* **12**(3): 221-225.

Gao, L., Macara, I.G., and Joberty, G. 2002b. Multiple splice variants of Par3 and of a novel related gene, Par3L, produce proteins with different binding properties. *Gene* **294**(1-2): 99-107.

Gardiol, D., Zacchi, A., Petrera, F., Stanta, G., and Banks, L. 2006. Human discs large and scrib are localized at the same regions in colon mucosa and changes in their expression patterns are correlated with loss of tissue architecture during malignant progression. *Int J Cancer* **119**(6): 1285-1290.

Ginestier, C., Cervera, N., Finetti, P., Esteyries, S., Esterni, B., Adelaide, J., Xerri, L., Viens, P., Jacquemier, J., Charafe-Jauffret, E., Chaffanet, M., Birnbaum, D., and Bertucci, F. 2006. Prognosis and Gene Expression Profiling of 20q13-Amplified Breast Cancers

10.1158/1078-0432.CCR-05-2339. *Clin Cancer Res* **12**(15): 4533-4544.

Guo, W., Pylayeva, Y., Pepe, A., Yoshioka, T., Muller, W.J., Inghirami, G., and Giancotti, F.G. 2006. Beta 4 integrin amplifies ErbB2 signaling to promote mammary tumorigenesis. *Cell* **126**(3): 489-502.

Hansen, S.H., Zegers, M.M., Woodrow, M., Rodriguez-Viciana, P., Chardin, P., Mostov, K.E., and McMahon, M. 2000. Induced expression of Rnd3 is associated with transformation of polarized epithelial cells by the Raf-MEK-extracellular signal-regulated kinase pathway. *Mol Cell Biol* **20**(24): 9364-9375.

Harari, D. and Yarden, Y. 2000. Molecular mechanisms underlying ErbB2/HER2 action in breast cancer. *Oncogene* **19**(53): 6102-6114.

Hicks, J., Krasnitz, A., Lakshmi, B., Navin, N.E., Riggs, M., Leibu, E., Esposito, D., Alexander, J., Troge, J., Grubor, V., Yoon, S., Wigler, M., Ye, K., Borresen-Dale,

A.L., Naume, B., Schlicting, E., Norton, L., Hagerstrom, T., Skoog, L., Auer, G., Maner, S., Lundin, P., and Zetterberg, A. 2006. Novel patterns of genome rearrangement and their association with survival in breast cancer. *Genome Res* **16**(12): 1465-1479.

Hilkens, J., Buijs, F., Hilgers, J., Hageman, P., Calafat, J., Sonnenberg, A., and van der Valk, M. 1984. Monoclonal antibodies against human milk-fat globule membranes detecting differentiation antigens of the mammary gland and its tumors. *Int J Cancer* **34**(2): 197-206.

Hollstein, M., Sidransky, D., Vogelstein, B., and Harris, C.C. 1991. p53 mutations in human cancers. *Science* **253**(5015): 49-53.

Hoshino, R., Chatani, Y., Yamori, T., Tsuruo, T., Oka, H., Yoshida, O., Shimada, Y., Ari-i, S., Wada, H., Fujimoto, J., and Kohno, M. 1999. Constitutive activation of the 41-/43-kDa mitogen-activated protein kinase signaling pathway in human tumors. *Oncogene* **18**(3): 813-822.

Humbert, P., Russell, S., and Richardson, H. 2003. Dlg, Scribble and Lgl in cell polarity, cell proliferation and cancer. *Bioessays* **25**(6): 542-553.

Hurd, T.W., Gao, L., Roh, M.H., Macara, I.G., and Margolis, B. 2003. Direct interaction of two polarity complexes implicated in epithelial tight junction assembly. *Nat Cell Biol* **5**(2): 137-142.

Hynes, N.E. and Lane, H.A. 2005. ERBB receptors and cancer: the complexity of targeted inhibitors. *Nat Rev Cancer* **5**(5): 341-354.

Hynes, N.E. and Stern, D.F. 1994. The biology of erbB-2/neu/HER-2 and its role in cancer. *Biochim Biophys Acta* **1198**(2-3): 165-184.

Ioakim-Liossi, A., Karakitsos, P., Markopoulos, C., Aroni, K., Athanassiadou, P., Delivelioti, K., Athanassiades, P., and Vaiopoulos, G. 2001. p53 protein expression and oestrogen and progesterone receptor status in invasive ductal breast carcinomas. *Cytopathology* **12**(3): 197-202.

Jenne, D.E., Reimann, H., Nezu, J., Friedel, W., Loff, S., Jeschke, R., Muller, O., Back, W., and Zimmer, M. 1998. Peutz-Jeghers syndrome is caused by mutations in a novel serine threonine kinase. *Nat Genet* **18**(1): 38-43.

Jiang, X. and Sorkin, A. 2002. Coordinated traffic of Grb2 and Ras during epidermal growth factor receptor endocytosis visualized in living cells. *Mol Biol Cell* **13**(5): 1522-1535.

Joberty, G., Petersen, C., Gao, L., and Macara, I.G. 2000. The cell-polarity protein Par6 links Par3 and atypical protein kinase C to Cdc42. *Nat Cell Biol* **2**(8): 531-539.

Johansson, A., Driessens, M., and Aspenstrom, P. 2000. The mammalian homologue of the Caenorhabditis elegans polarity protein PAR-6 is a binding partner for the Rho GTPases Cdc42 and Rac1. *J Cell Sci* **113 (Pt 18)**: 3267-3275.

Johnston, S.R., Hickish, T., Ellis, P., Houston, S., Kelland, L., Dowsett, M., Salter, J., Michiels, B., Perez-Ruixo, J.J., Palmer, P., and Howes, A. 2003. Phase II study of the efficacy and tolerability of two dosing regimens of the farnesyl transferase inhibitor, R115777, in advanced breast cancer. *J Clin Oncol* **21**(13): 2492-2499.

Jou, T.S. and Nelson, W.J. 1998. Effects of regulated expression of mutant RhoA and Rac1 small GTPases on the development of epithelial (MDCK) cell polarity. *J Cell Biol* **142**(1): 85-100.

Jou, T.S., Schneeberger, E.E., and Nelson, W.J. 1998. Structural and functional regulation of tight junctions by RhoA and Rac1 small GTPases. *J Cell Biol* **142**(1): 101-115.

Kemphues, K.J., Priess, J.R., Morton, D.G., and Cheng, N.S. 1988. Identification of genes required for cytoplasmic localization in early C. elegans embryos. *Cell* **52**(3): 311-320.

Keyomarsi, K., Tucker, S.L., Buchholz, T.A., Callister, M., Ding, Y., Hortobagyi, G.N., Bedrosian, I., Knickerbocker, C., Toyofuku, W., Lowe, M., Herliczek, T.W., and Bacus, S.S. 2002. Cyclin E and survival in patients with breast cancer. *N Engl J Med* **347**(20): 1566-1575.

Kim, M., Datta, A., Brakeman, P., Yu, W., and Mostov, K.E. 2007. Polarity proteins PAR6 and aPKC regulate cell death through GSK-3beta in 3D epithelial morphogenesis. *J Cell Sci* **120**(Pt 14): 2309-2317.

Kiyono, T., Hiraiwa, A., Fujita, M., Hayashi, Y., Akiyama, T., and Ishibashi, M. 1997. Binding of high-risk human papillomavirus E6 oncoproteins to the human homologue of the Drosophila discs large tumor suppressor protein. *Proc Natl Acad Sci U S A* **94**(21): 11612-11616.

Kleer, C.G., van Golen, K.L., Zhang, Y., Wu, Z.F., Rubin, M.A., and Merajver, S.D. 2002. Characterization of RhoC expression in benign and malignant breast disease: a potential new marker for small breast carcinomas with metastatic ability. *Am J Pathol* **160**(2): 579-584.

Kleinman, H.K., McGarvey, M.L., Hassell, J.R., Star, V.L., Cannon, F.B., Laurie, G.W., and Martin, G.R. 1986. Basement membrane complexes with biological activity. *Biochemistry* **25**(2): 312-318.

Kleinman, H.K., McGarvey, M.L., Liotta, L.A., Robey, P.G., Tryggvason, K., and Martin, G.R. 1982. Isolation and characterization of type IV procollagen, laminin, and heparan sulfate proteoglycan from the EHS sarcoma. *Biochemistry* **21**(24): 6188-6193.

Knust, E. and Bossinger, O. 2002. Composition and formation of intercellular junctions in epithelial cells. *Science* **298**(5600): 1955-1959.

Kodama, A., Karakesisoglou, I., Wong, E., Vaezi, A., and Fuchs, E. 2003. ACF7: an essential integrator of microtubule dynamics. *Cell* **115**(3): 343-354.

Kuphal, S., Wallner, S., Schimanski, C.C., Bataille, F., Hofer, P., Strand, S., Strand, D., and Bosserhoff, A.K. 2006. Expression of Hugl-1 is strongly reduced in malignant melanoma. *Oncogene* **25**(1): 103-110.

Lacroix, M. and Leclercq, G. 2004. Relevance of breast cancer cell lines as models for breast tumours: an update. *Breast Cancer Res Treat* **83**(3): 249-289.

Lee, D.H. and Goldberg, A.L. 1998. Proteasome inhibitors: valuable new tools for cell biologists. *Trends in Cell Biology* **8**(10): 397-403.

Lee, S., Medina, D., Tsimelzon, A., Mohsin, S.K., Mao, S., Wu, Y., and Allred, D.C. 2007. Alterations of Gene Expression in the Development of Early Hyperplastic Precursors of Breast Cancer. *Am J Pathol*.

Lee, S., Mohsin, S.K., Mao, S., Hilsenbeck, S.G., Medina, D., and Allred, D.C. 2006. Hormones, receptors, and growth in hyperplastic enlarged lobular units: early potential precursors of breast cancer. *Breast Cancer Res* **8**(1): R6.

Lee, S.S., Weiss, R.S., and Javier, R.T. 1997. Binding of human virus oncoproteins to hDlg/SAP97, a mammalian homolog of the Drosophila discs large tumor suppressor protein. *Proc Natl Acad Sci U S A* **94**(13): 6670-6675.

Lemmers, C., Medina, E., Delgrossi, M.H., Michel, D., Arsanto, J.P., and Le Bivic, A. 2002. hINADl/PATJ, a homolog of discs lost, interacts with crumbs and localizes to tight junctions in human epithelial cells. *J Biol Chem* **277**(28): 25408-25415.

Li, D. and Mrsny, R.J. 2000. Oncogenic Raf-1 disrupts epithelial tight junctions via downregulation of occludin. *J Cell Biol* **148**(4): 791-800.

Li, Y.Y., Wang, R., Zhang, G.L., Zheng, Y.J., Zhu, P., Zhang, Z.M., Fang, X.X., and Feng, Y. 2007. An archaeal histone-like protein mediates efficient p53 gene transfer and facilitates its anti-cancer effect in vitro and in vivo. *Cancer Gene Ther* **14**(12): 968-975.

Lin, D., Edwards, A.S., Fawcett, J.P., Mbamalu, G., Scott, J.D., and Pawson, T. 2000. A mammalian PAR-3-PAR-6 complex implicated in Cdc42/Rac1 and aPKC signalling and cell polarity. *Nat Cell Biol* **2**(8): 540-547.

Liu, H., Radisky, D.C., Wang, F., and Bissell, M.J. 2004. Polarity and proliferation are controlled by distinct signaling pathways downstream of PI3-kinase in breast epithelial tumor cells. *J Cell Biol* **164**(4): 603-612.

Ma, X.J., Salunga, R., Tuggle, J.T., Gaudet, J., Enright, E., McQuary, P., Payette, T., Pistone, M., Stecker, K., Zhang, B.M., Zhou, Y.X., Varnholt, H., Smith, B., Gadd, M., Chatfield, E., Kessler, J., Baer, T.M., Erlander, M.G., and Sgroi, D.C. 2003. Gene expression profiles of human breast cancer progression. *Proc Natl Acad Sci U S A* **100**(10): 5974-5979.

Macara, I.G. 2004a. Par proteins: partners in polarization. *Curr Biol* **14**(4): R160-162.

-. 2004b. Parsing the polarity code. *Nat Rev Mol Cell Biol* **5**(3): 220-231.

Miranti, C.K. and Brugge, J.S. 2002. Sensing the environment: a historical perspective on integrin signal transduction. **4**(4): E83-E90.

Mita, M.M., Mita, A., and Rowinsky, E.K. 2003. Mammalian target of rapamycin: a new molecular target for breast cancer. *Clin Breast Cancer* **4**(2): 126-137.

Mori, S., Claessonwelsh, L., Okuyama, Y., and Saito, Y. 1995. Ligand-Induced Polyubiquitination of Receptor Tyrosine Kinases. *Biochemical and Biophysical Research Communications* **213**(1): 32-39.

Morrison, D.K. 2001. KSR: a MAPK scaffold of the Ras pathway? *J Cell Sci* **114**(Pt 9): 1609-1612.

Musch, A., Cohen, D., Yeaman, C., Nelson, W.J., Rodriguez-Boulan, E., and Brennwald, P.J. 2002. Mammalian homolog of Drosophila tumor suppressor lethal (2) giant larvae interacts with basolateral exocytic machinery in Madin-Darby canine kidney cells. *Mol Biol Cell* **13**(1): 158-168.

Muthuswamy, S.K., Gilman, M., and Brugge, J.S. 1999. Controlled dimerization of ErbB receptors provides evidence for differential signaling by homo- and heterodimers. *Mol Cell Biol* **19**(10): 6845-6857.

Muthuswamy, S.K., Li, D., Lelievre, S., Bissell, M.J., and Brugge, J.S. 2001. ErbB2, but not ErbB1, reinitiates proliferation and induces luminal repopulation in epithelial acini. *Nat Cell Biol* **3**(9): 785-792.

Nakagawa, S. and Huibregtse, J.M. 2000. Human scribble (Vartul) is targeted for ubiquitin-mediated degradation by the high-risk papillomavirus E6 proteins and the E6AP ubiquitin-protein ligase. *Mol Cell Biol* **20**(21): 8244-8253.

Nakayama, M., Goto, T.M., Sugimoto, M., Nishimura, T., Shinagawa, T., Ohno, S., Amano, M., and Kaibuchi, K. 2008. Rho-Kinase Phosphorylates PAR-3 and Disrupts PAR Complex Formation. *Dev Cell* **14**(2): 205-215.

Nakopoulou, L., Tsirmpa, I., Alexandrou, P., Louvrou, A., Ampela, C., Markaki, S., and Davaris, P.S. 2003. MMP-2 protein in invasive breast cancer and the impact of MMP-2/TIMP-2 phenotype on overall survival. *Breast Cancer Res Treat* **77**(2): 145-155.

Nass, S.J. and Dickson, R.B. 1997. Defining a role for c-Myc in breast tumorigenesis. *Breast Cancer Res Treat* **44**(1): 1-22.

Nasser, S.M. 2004. Columnar cell lesions: current classification and controversies. *Semin Diagn Pathol* **21**(1): 18-24.

Nelson, W.J. 2003. Adaptation of core mechanisms to generate cell polarity. *Nature* **422**(6933): 766-774.

Noda, Y., Kohjima, M., Izaki, T., Ota, K., Yoshinaga, S., Inagaki, F., Ito, T., and Sumimoto, H. 2003. Molecular recognition in dimerization between PB1 domains. *J Biol Chem* **278**(44): 43516-43524.

O'Brien, L.E., Zegers, M.M., and Mostov, K.E. 2002. Opinion: Building epithelial architecture: insights from three-dimensional culture models. *Nat Rev Mol Cell Biol* **3**(7): 531-537.

O'Connell, P., Pekkel, V., Fuqua, S.A., Osborne, C.K., Clark, G.M., and Allred, D.C. 1998. Analysis of loss of heterozygosity in 399 premalignant breast lesions at 15 genetic loci. *J Natl Cancer Inst* **90**(9): 697-703.

Ohno, S. 2001. Intercellular junctions and cellular polarity: the PAR-aPKC complex, a conserved core cassette playing fundamental roles in cell polarity. *Curr Opin Cell Biol* **13**(5): 641-648.

Ory, D.S., Neugeboren, B.A., and Mulligan, R.C. 1996. A stable human-derived packaging cell line for production of high titer retrovirus/vesicular stomatitis virus G pseudotypes. *Proc Natl Acad Sci U S A* **93**(21): 11400-11406.

Osborne, C., Wilson, P., and Tripathy, D. 2004. Oncogenes and tumor suppressor genes in breast cancer: potential diagnostic and therapeutic applications. *Oncologist* **9**(4): 361-377.

Osborne, C.K. 1998. Tamoxifen in the treatment of breast cancer. *N Engl J Med* **339**(22): 1609-1618.

Ozdamar, B., Bose, R., Barrios-Rodiles, M., Wang, H.R., Zhang, Y., and Wrana, J.L. 2005. Regulation of the polarity protein Par6 by TGFbeta receptors controls epithelial cell plasticity. *Science* **307**(5715): 1603-1609.

Pagliarini, R.A. and Xu, T. 2003. A genetic screen in Drosophila for metastatic behavior. *Science* **302**(5648): 1227-1231.

Paszek, M.J., Zahir, N., Johnson, K.R., Lakins, J.N., Rozenberg, G.I., Gefen, A., Reinhart-King, C.A., Margulies, S.S., Dembo, M., Boettiger, D., Hammer, D.A., and Weaver, V.M. 2005. Tensional homeostasis and the malignant phenotype. *Cancer Cell* **8**(3): 241-254.

Peppercorn, J., Perou, C.M., and Carey, L.A. 2008. Molecular subtypes in breast cancer evaluation and management: divide and conquer. *Cancer Invest* **26**(1): 1-10.

Perou, C.M., Jeffrey, S.S., van de Rijn, M., Rees, C.A., Eisen, M.B., Ross, D.T., Pergamenschikov, A., Williams, C.F., Zhu, S.X., Lee, J.C.F., Lashkari, D., Shalon, D., Brown, P.O., and Botstein, D. 1999. Distinctive gene expression patterns in human mammary epithelial cells and breast cancers

10.1073/pnas.96.16.9212. *Proceedings of the National Academy of Sciences* **96**(16): 9212-9217.

Perou, C.M., Sorlie, T., Eisen, M.B., van de Rijn, M., Jeffrey, S.S., Rees, C.A., Pollack, J.R., Ross, D.T., Johnsen, H., Akslen, L.A., Fluge, O., Pergamenschikov, A., Williams, C., Zhu, S.X., Lonning, P.E., Borresen-Dale, A.-L., Brown, P.O., and Botstein, D. 2000. Molecular portraits of human breast tumours. **406**(6797): 747-752.

Petersen, O.W., Ronnov-Jessen, L., Howlett, A.R., and Bissell, M.J. 1992. Interaction with basement membrane serves to rapidly distinguish growth and differentiation pattern of normal and malignant human breast epithelial cells. *Proc Natl Acad Sci U S A* **89**(19): 9064-9068.

Petersen, O.W. and van Deurs, B. 1986. Characterization of epithelial membrane antigen expression in human mammary epithelium by ultrastructural immunoperoxidase cytochemistry. *J Histochem Cytochem* **34**(6): 801-809.

Pim, D., Thomas, M., Javier, R., Gardiol, D., and Banks, L. 2000. HPV E6 targeted degradation of the discs large protein: evidence for the involvement of a novel ubiquitin ligase. *Oncogene* **19**(6): 719-725.

Plant, P.J., Fawcett, J.P., Lin, D.C., Holdorf, A.D., Binns, K., Kulkarni, S., and Pawson, T. 2003. A polarity complex of mPar-6 and atypical PKC binds, phosphorylates and regulates mammalian Lgl. *Nat Cell Biol* **5**(4): 301-308.

Porter, D., Lahti-Domenici, J., Keshaviah, A., Bae, Y.K., Argani, P., Marks, J., Richardson, A., Cooper, A., Strausberg, R., Riggins, G.J., Schnitt, S., Gabrielson, E., Gelman, R., and Polyak, K. 2003. Molecular markers in ductal carcinoma in situ of the breast. *Mol Cancer Res* **1**(5): 362-375.

Prendergast, G.C., Khosravi-Far, R., Solski, P.A., Kurzawa, H., Lebowitz, P.F., and Der, C.J. 1995. Critical role of Rho in cell transformation by oncogenic Ras. *Oncogene* **10**(12): 2289-2296.

Qiu, R.G., Abo, A., and Steven Martin, G. 2000. A human homolog of the C. elegans polarity determinant Par-6 links Rac and Cdc42 to PKCzeta signaling and cell transformation. *Curr Biol* **10**(12): 697-707.

Qiu, R.G., Chen, J., Kirn, D., McCormick, F., and Symons, M. 1995a. An essential role for Rac in Ras transformation. *Nature* **374**(6521): 457-459.

Qiu, R.G., Chen, J., McCormick, F., and Symons, M. 1995b. A role for Rho in Ras transformation. *Proc Natl Acad Sci U S A* **92**(25): 11781-11785.

Regala, R.P., Weems, C., Jamieson, L., Copland, J.A., Thompson, E.A., and Fields, A.P. 2005a. Atypical protein kinase Ciota plays a critical role in human lung cancer cell growth and tumorigenicity. *J Biol Chem* **280**(35): 31109-31115.

Regala, R.P., Weems, C., Jamieson, L., Khoor, A., Edell, E.S., Lohse, C.M., and Fields, A.P. 2005b. Atypical protein kinase C iota is an oncogene in human non-small cell lung cancer. *Cancer Res* **65**(19): 8905-8911.

Reginato, M.J., Mills, K.R., Becker, E.B., Lynch, D.K., Bonni, A., Muthuswamy, S.K., and Brugge, J.S. 2005. Bim regulation of lumen formation in cultured mammary epithelial acini is targeted by oncogenes. *Mol Cell Biol* **25**(11): 4591-4601.

Reichmann, E., Schwarz, H., Deiner, E.M., Leitner, I., Eilers, M., Berger, J., Busslinger, M., and Beug, H. 1992. Activation of an inducible c-FosER fusion protein causes loss of epithelial polarity and triggers epithelial-fibroblastoid cell conversion. *Cell* **71**(7): 1103-1116.

Rhodes, D.R., Yu, J., Shanker, K., Deshpande, N., Varambally, R., Ghosh, D., Barrette, T., Pandey, A., and Chinnaiyan, A.M. 2004. ONCOMINE: a cancer microarray database and integrated data-mining platform. *Neoplasia* **6**(1): 1-6.

Rojas, R., Ruiz, W.G., Leung, S.M., Jou, T.S., and Apodaca, G. 2001. Cdc42-dependent modulation of tight junctions and membrane protein traffic in polarized Madin-Darby canine kidney cells. *Mol Biol Cell* **12**(8): 2257-2274.

Ronnov-Jessen, L., Petersen, O.W., and Bissell, M.J. 1996. Cellular changes involved in conversion of normal to malignant breast: importance of the stromal reaction. *Physiol Rev* **76**(1): 69-125.

Rousset, R., Fabre, S., Desbois, C., Bantignies, F., and Jalinot, P. 1998. The C-terminus of the HTLV-1 Tax oncoprotein mediates interaction with the PDZ domain of cellular proteins. *Oncogene* **16**(5): 643-654.

Roux, P., Gauthier-Rouviere, C., Doucet-Brutin, S., and Fort, P. 1997. The small GTPases Cdc42Hs, Rac1 and RhoG delineate Raf-independent pathways that cooperate to transform NIH3T3 cells. *Curr Biol* **7**(9): 629-637.

Roy, R., Wewer, U.M., Zurakowski, D., Pories, S.E., and Moses, M.A. 2004. ADAM 12 cleaves extracellular matrix proteins and correlates with cancer status and stage. *J Biol Chem* **279**(49): 51323-51330.

Rudas, M., Neumayer, R., Gnant, M.F., Mittelbock, M., Jakesz, R., and Reiner, A. 1997. p53 protein expression, cell proliferation and steroid hormone receptors in ductal and lobular in situ carcinomas of the breast. *Eur J Cancer* **33**(1): 39-44.

Russell, W.C. 2000. Update on adenovirus and its vectors. *J Gen Virol* **81**(Pt 11): 2573-2604.

Sahai, E. and Marshall, C.J. 2002. RHO-GTPases and cancer. *Nat Rev Cancer* **2**(2): 133-142.

Schimanski, C.C., Schmitz, G., Kashyap, A., Bosserhoff, A.K., Bataille, F., Schafer, S.C., Lehr, H.A., Berger, M.R., Galle, P.R., Strand, S., and Strand, D. 2005. Reduced expression of Hugl-1, the human homologue of Drosophila tumour suppressor gene lgl, contributes to progression of colorectal cancer. *Oncogene* **24**(19): 3100-3109.

Schnitzer, J., Oh, P., Pinney, E., and Allard, J. 1994. Filipin-sensitive caveolae-mediated transport in endothelium: reduced transcytosis, scavenger endocytosis, and capillary permeability of select macromolecules

10.1083/jcb.127.5.1217. *J Cell Biol* **127**(5): 1217-1232.

Schoenenberger, C.A., Zuk, A., Kendall, D., and Matlin, K.S. 1991. Multilayering and loss of apical polarity in MDCK cells transformed with viral K-ras. *J Cell Biol* **112**(5): 873-889.

Schonegg, S. and Hyman, A.A. 2006. CDC-42 and RHO-1 coordinate acto-myosin contractility and PAR protein localization during polarity establishment in C. elegans embryos. *Development* **133**(18): 3507-3516.

Schonwasser, D.C., Marais, R.M., Marshall, C.J., and Parker, P.J. 1998. Activation of the mitogen-activated protein kinase/extracellular signal-regulated kinase pathway by conventional, novel, and atypical protein kinase C isotypes. *Mol Cell Biol* **18**(2): 790-798.

Sebolt-Leopold, J.S., Dudley, D.T., Herrera, R., Van Becelaere, K., Wiland, A., Gowan, R.C., Tecle, H., Barrett, S.D., Bridges, A., Przybranowski, S., Leopold, W.R., and Saltiel, A.R. 1999. Blockade of the MAP kinase pathway suppresses growth of colon tumors in vivo. *Nat Med* **5**(7): 810-816.

Seth, A., Kitching, R., Landberg, G., Xu, J., Zubovits, J., and Burger, A.M. 2003. Gene expression profiling of ductal carcinomas in situ and invasive breast tumors. *Anticancer Res* **23**(3A): 2043-2051.

Seton-Rogers, S.E., Lu, Y., Hines, L.M., Koundinya, M., LaBaer, J., Muthuswamy, S.K., and Brugge, J.S. 2004. Cooperation of the ErbB2 receptor and transforming growth factor {beta} in induction of migration and invasion in mammary epithelial cells. *Proc Natl Acad Sci U S A* **101**(5): 1257-1262.

Shaaban, A.M., Sloane, J.P., West, C.R., Moore, F.R., Jarvis, C., Williams, E.M., and Foster, C.S. 2002. Histopathologic types of benign breast lesions and the risk of breast cancer: case-control study. *Am J Surg Pathol* **26**(4): 421-430.

Shi, S.H., Jan, L.Y., and Jan, Y.N. 2003. Hippocampal neuronal polarity specified by spatially localized mPar3/mPar6 and PI 3-kinase activity. *Cell* **112**(1): 63-75.

Sigismund, S., Woelk, T., Puri, C., Maspero, E., Tacchetti, C., Transidico, P., Di Fiore, P.P., and Polo, S. 2005. From the Cover: Clathrin-independent endocytosis of ubiquitinated cargos

10.1073/pnas.0409817102. *Proceedings of the National Academy of Sciences* **102**(8): 2760-2765.

Simpson, K.J., Dugan, A.S., and Mercurio, A.M. 2004. Functional analysis of the contribution of RhoA and RhoC GTPases to invasive breast carcinoma. *Cancer Res* **64**(23): 8694-8701.

Simpson, P.T., Reis-Filho, J.S., Gale, T., and Lakhani, S.R. 2005. Molecular evolution of breast cancer. *J Pathol* **205**(2): 248-254.

Sivaraman, V.S., Wang, H., Nuovo, G.J., and Malbon, C.C. 1997. Hyperexpression of mitogen-activated protein kinase in human breast cancer. *J Clin Invest* **99**(7): 1478-1483.

Slamon, D.J. 1987. Proto-oncogenes and human cancers. *N Engl J Med* **317**(15): 955-957.

Smith, C.A., Lau, K.M., Rahmani, Z., Dho, S.E., Brothers, G., She, Y.M., Berry, D.M., Bonneil, E., Thibault, P., Schweisguth, F., Le Borgne, R., and McGlade, C.J. 2007. aPKC-mediated phosphorylation regulates asymmetric membrane localization of the cell fate determinant Numb. *EMBO Journal* **26**(2): 468-480.

Solecki, D.J., Model, L., Gaetz, J., Kapoor, T.M., and Hatten, M.E. 2004. Par6alpha signaling controls glial-guided neuronal migration. *Nat Neurosci* **7**(11): 1195-1203.

Sorkin, A. and Waters, C.M. 1993. Endocytosis of growth factor receptors. *Bioessays* **15**(6): 375-382.

Sorlie, T., Perou, C.M., Tibshirani, R., Aas, T., Geisler, S., Johnsen, H., Hastie, T., Eisen, M.B., van de Rijn, M., Jeffrey, S.S., Thorsen, T., Quist, H., Matese, J.C., Brown, P.O., Botstein, D., Eystein Lonning, P., and Borresen-Dale, A.L. 2001. Gene expression patterns of breast carcinomas distinguish tumor subclasses with clinical implications. *Proc Natl Acad Sci U S A* **98**(19): 10869-10874.

Sorlie, T., Tibshirani, R., Parker, J., Hastie, T., Marron, J.S., Nobel, A., Deng, S., Johnsen, H., Pesich, R., Geisler, S., Demeter, J., Perou, C.M., Lonning, P.E., Brown, P.O., Borresen-Dale, A.L., and Botstein, D. 2003. Repeated observation of breast tumor subtypes in independent gene expression data sets. *Proc Natl Acad Sci U S A* **100**(14): 8418-8423.

Soule, H.D., Maloney, T.M., Wolman, S.R., Peterson, W.D., Jr., Brenz, R., McGrath, C.M., Russo, J., Pauley, R.J., Jones, R.F., and Brooks, S.C. 1990. Isolation and characterization of a spontaneously immortalized human breast epithelial cell line, MCF-10. *Cancer Res* **50**(18): 6075-6086.

Sternlicht, M. 2006. Key stages in mammary gland development: The cues that regulate ductal branching morphogenesis. *Breast Cancer Research* **8**(1): 201.

Stoll, M., Corneliussen, B., Costello, C.M., Waetzig, G.H., Mellgard, B., Koch, W.A., Rosenstiel, P., Albrecht, M., Croucher, P.J., Seegert, D., Nikolaus, S., Hampe, J., Lengauer, T., Pierrou, S., Foelsch, U.R., Mathew, C.G., Lagerstrom-Fermer, M., and Schreiber, S. 2004. Genetic variation in DLG5 is associated with inflammatory bowel disease. *Nat Genet* **36**(5): 476-480.

Straight, S.W., Shin, K., Fogg, V.C., Fan, S., Liu, C.J., Roh, M., and Margolis, B. 2004. Loss of PALS1 expression leads to tight junction and polarity defects. *Mol Biol Cell* **15**(4): 1981-1990.

Suzuki, A., Hirata, M., Kamimura, K., Maniwa, R., Yamanaka, T., Mizuno, K., Kishikawa, M., Hirose, H., Amano, Y., Izumi, N., Miwa, Y., and Ohno, S. 2004. aPKC Acts Upstream of PAR-1b in Both the Establishment and Maintenance of Mammalian Epithelial Polarity. *Current Biology* **14**(16): 1425-1435.

Suzuki, R., Atherton, A.J., O'Hare, M.J., Entwistle, A., Lakhani, S.R., and Clarke, C. 2000. Proliferation and differentiation in the human breast during pregnancy. *Differentiation* **66**(2-3): 106-115.

Suzuki, T., Ohsugi, Y., Uchida-Toita, M., Akiyama, T., and Yoshida, M. 1999. Tax oncoprotein of HTLV-1 binds to the human homologue of Drosophila discs large tumor suppressor protein, hDLG, and perturbs its function in cell growth control. *Oncogene* **18**(44): 5967-5972.

Tanentzapf, G. and Tepass, U. 2003. Interactions between the crumbs, lethal giant larvae and bazooka pathways in epithelial polarization. *Nat Cell Biol* **5**(1): 46-52.

Therrien, M., Michaud, N.R., Rubin, G.M., and Morrison, D.K. 1996. KSR modulates signal propagation within the MAPK cascade. *Genes Dev* **10**(21): 2684-2695.

Tsukita, S., Furuse, M., and Itoh, M. 1999. Structural and signalling molecules come together at tight junctions. *Curr Opin Cell Biol* **11**(5): 628-633.

van de Vijver, M.J., He, Y.D., van 't Veer, L.J., Dai, H., Hart, A.A.M., Voskuil, D.W., Schreiber, G.J., Peterse, J.L., Roberts, C., Marton, M.J., Parrish, M., Atsma, D., Witteveen, A., Glas, A., Delahaye, L., van der Velde, T., Bartelink, H., Rodenhuis, S., Rutgers, E.T., Friend, S.H., and Bernards, R. 2002. A Gene-Expression Signature as a Predictor of Survival in Breast Cancer
10.1056/NEJMoa021967. *N Engl J Med* **347**(25): 1999-2009.

van Golen, K.L., Bao, L.W., Pan, Q., Miller, F.R., Wu, Z.F., and Merajver, S.D. 2002. Mitogen activated protein kinase pathway is involved in RhoC GTPase induced motility, invasion and angiogenesis in inflammatory breast cancer. *Clin Exp Metastasis* **19**(4): 301-311.

van Golen, K.L., Davies, S., Wu, Z.F., Wang, Y., Bucana, C.D., Root, H., Chandrasekharappa, S., Strawderman, M., Ethier, S.P., and Merajver, S.D. 1999. A novel putative low-affinity insulin-like growth factor-binding protein, LIBC (lost in inflammatory breast cancer), and RhoC GTPase correlate with the inflammatory breast cancer phenotype. *Clin Cancer Res* **5**(9): 2511-2519.

Van Laere, S.J., Van den Eynden, G.G., Van der Auwera, I., Vandenberghe, M., van Dam, P., Van Marck, E.A., van Golen, K.L., Vermeulen, P.B., and Dirix, L.Y. 2006. Identification of cell-of-origin breast tumor subtypes in inflammatory breast cancer by gene expression profiling. *Breast Cancer Res Treat* **95**(3): 243-255.

Varley, J.M., Swallow, J.E., Brammar, W.J., Whittaker, J.L., and Walker, R.A. 1987. Alterations to either c-erbB-2(neu) or c-myc proto-oncogenes in breast carcinomas correlate with poor short-term prognosis. *Oncogene* **1**(4): 423-430.

Vieira, A.V., Lamaze, C., and Schmid, S.L. 1996. Control of EGF receptor signaling by clathrin-mediated endocytosis. *Science* **274**(5295): 2086-2089.

Waldman, F.M., DeVries, S., Chew, K.L., Moore, D.H., 2nd, Kerlikowske, K., and Ljung, B.M. 2000. Chromosomal alterations in ductal carcinomas in situ and their in situ recurrences. *J Natl Cancer Inst* **92**(4): 313-320.

Wang, A.Z., Ojakian, G.K., and Nelson, W.J. 1990. Steps in the morphogenesis of a polarized epithelium. II. Disassembly and assembly of plasma membrane domains during reversal of epithelial cell polarity in multicellular epithelial (MDCK) cysts. *J Cell Sci* **95 (Pt 1)**: 153-165.

Wang, H.R., Zhang, Y., Ozdamar, B., Ogunjimi, A.A., Alexandrova, E., Thomsen, G.H., and Wrana, J.L. 2003. Regulation of cell polarity and protrusion formation by targeting RhoA for degradation. *Science* **302**(5651): 1775-1779.

Wang, Q., Hurd, T.W., and Margolis, B. 2004. Tight junction protein Par6 interacts with an evolutionarily conserved region in the amino terminus of PALS1/stardust. *J Biol Chem* **279**(29): 30715-30721.

Wellings, S.R. and Jensen, H.M. 1973. On the origin and progression of ductal carcinoma in the human breast. *J Natl Cancer Inst* **50**(5): 1111-1118.

Wellings, S.R., Jensen, H.M., and Marcum, R.G. 1975. An atlas of subgross pathology of the human breast with special reference to possible precancerous lesions. *J Natl Cancer Inst* **55**(2): 231-273.

Weyrich, P., Kapp, K., Niederfellner, G., Melzer, M., Lehmann, R., Haring, H.U., and Lammers, R. 2004. Partitioning-defective protein 6 regulates insulin-dependent glycogen synthesis via atypical protein kinase C. *Mol Endocrinol* **18**(5): 1287-1300.

Wiley, H.S. 2003. Trafficking of the ErbB receptors and its influence on signaling. *Exp Cell Res* **284**(1): 78-88.

Wilson, M.I., Gill, D.J., Perisic, O., Quinn, M.T., and Williams, R.L. 2003. PB1 domain-mediated heterodimerization in NADPH oxidase and signaling complexes of atypical protein kinase C with Par6 and p62. *Mol Cell* **12**(1): 39-50.

Wrobel, C.N., Debnath, J., Lin, E., Beausoleil, S., Roussel, M.F., and Brugge, J.S. 2004. Autocrine CSF-1R activation promotes Src-dependent disruption of mammary epithelial architecture. *J Cell Biol* **165**(2): 263-273.

Wu, M., Wu, Z.F., and Merajver, S.D. 2007. Rho proteins and cell-matrix interactions in cancer. *Cells Tissues Organs* **185**(1-3): 100-103.

Xian, W., Schwertfeger, K.L., Vargo-Gogola, T., and Rosen, J.M. 2005. Pleiotropic effects of FGFR1 on cell proliferation, survival, and migration in a 3D mammary epithelial cell model. *J Cell Biol* **171**(4): 663-673.

Yamanaka, T., Horikoshi, Y., Izumi, N., Suzuki, A., Mizuno, K., and Ohno, S. 2006. Lgl mediates apical domain disassembly by suppressing the PAR-3-aPKC-PAR-6 complex to orient apical membrane polarity. *J Cell Sci* **119**(Pt 10): 2107-2118.

Yamanaka, T., Horikoshi, Y., Sugiyama, Y., Ishiyama, C., Suzuki, A., Hirose, T., Iwamatsu, A., Shinohara, A., and Ohno, S. 2003. Mammalian Lgl forms a protein complex with PAR-6 and aPKC independently of PAR-3 to regulate epithelial cell polarity. *Curr Biol* **13**(9): 734-743.

Yamanaka, T., Horikoshi, Y., Suzuki, A., Sugiyama, Y., Kitamura, K., Maniwa, R., Nagai, Y., Yamashita, A., Hirose, T., Ishikawa, H., and Ohno, S. 2001. PAR-6 regulates aPKC activity in a novel way and mediates cell-cell contact-induced formation of the epithelial junctional complex. *Genes Cells* **6**(8): 721-731.

Yarden, Y. and Sliwkowski, M.X. 2001. Untangling the ErbB signalling network. *Nat Rev Mol Cell Biol* **2**(2): 127-137.

York, R.D., Yao, H., Dillon, T., Ellig, C.L., Eckert, S.P., McCleskey, E.W., and Stork, P.J.S. 1998. Rap1 mediates sustained MAP kinase activation induced by nerve growth factor. **392**(6676): 622-626.

Yu, H. and Jove, R. 2004. The STATs of cancer--new molecular targets come of age. *Nat Rev Cancer* **4**(2): 97-105.

Yu, K., Lee, C.H., Tan, P.H., and Tan, P. 2004. Conservation of breast cancer molecular subtypes and transcriptional patterns of tumor progression across distinct ethnic populations. *Clin Cancer Res* **10**(16): 5508-5517.

Zhao, H., Langerod, A., Ji, Y., Nowels, K.W., Nesland, J.M., Tibshirani, R., Bukholm, I.K., Karesen, R., Botstein, D., Borresen-Dale, A.-L., and Jeffrey, S.S. 2004. Different Gene Expression Patterns in Invasive Lobular and Ductal Carcinomas of the Breast

10.1091/mbc.E03-11-0786. *Mol Biol Cell* **15**(6): 2523-2536.

Zohn, I.M., Campbell, S.L., Khosravi-Far, R., Rossman, K.L., and Der, C.J. 1998. Rho family proteins and Ras transformation: the RHOad less traveled gets congested. *Oncogene* **17**(11 Reviews): 1415-1438.

Appendix: Par6 overexpression does not activate EGFR

Introduction:

I determined that Par6 overexpression promotes EGF independent proliferation of mammary epithelial cells (Chapter 2). In addition I showed that Par6 induced proliferation was dependent on activation of ERK. Therefore, I reasoned that Par6 could be inducing ERK phosphorylation by promoting activation of EGFR. Activation of EGFR stimulates many downstream signaling pathways such as PI3K, PLCγ and JNK and Ras/MAPK (Figure A.1). Activation of these pathways results in multiple cell biological effects such as cell proliferation, cell survival, and cell growth reviewed in (Yarden and Sliwkowski 2001). In this appendix, I will discuss the experiments that were performed to investigate if overexpression of Par6 is activating EGFR and therefore promoting activation of MAPK and cell proliferation as observed in Chapter 2.

Activation of EGFR occurs upon ligand stimulation. Once stimulated the receptor becomes tyrosine phosphorlyated and mediates downstream signals. The active receptor is then regulated through various mechanisms such as receptor-mediated endocytosis (Sorkin and Waters 1993) and proteosomal degradation (Mori et al. 1995). During receptor-mediated endocytosis, the ligand bound receptor is internalized via clathrin coated pits and then either recycled back to the plasma membrane or targeted for degradation via the proteasome or the lysosomal pathways (Sorkin and Waters 1993). In addition to the EGFR signaling complexes that form at the membrane, active EGFR can be detected in endosomal membranes, associated with downstream effectors such as, GRB2 and Ras (Di Guglielmo et al. 1994; Jiang and Sorkin 2002). Thus active EGFR

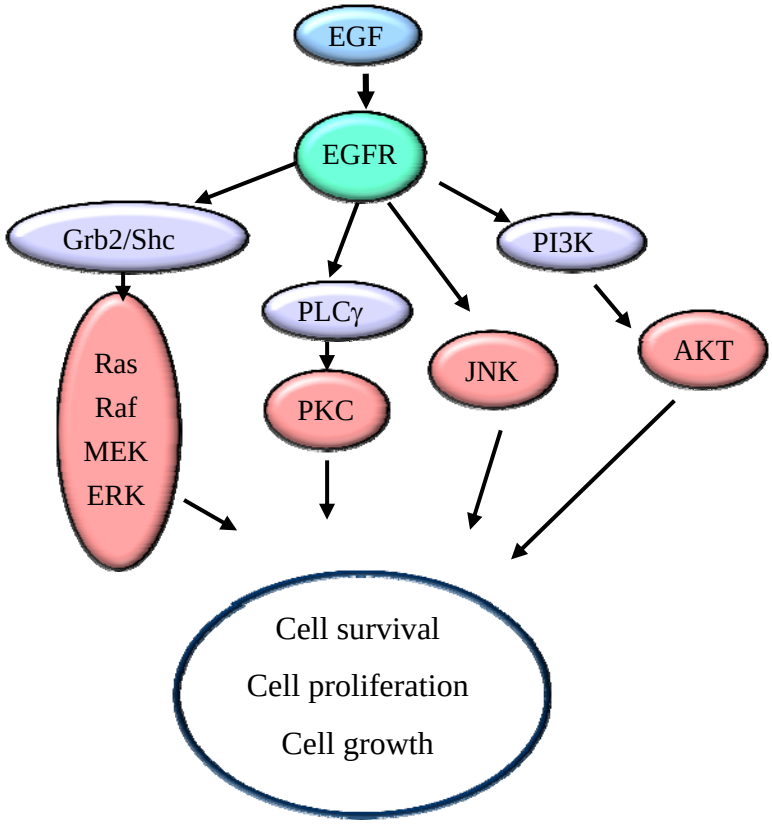

Figure A.1. Signal transduction pathways downstream of EGFR activation.

Activation of the EGFR pathway by EGF ligand. EGFR receptors dimerize and become phosphorlyated on the cytoplasmic tail. This receptor can stimulate the Ras/MAPK, PLCγ, JNK and PI3K pathways that lead to cell growth, proliferation and survival.

signals can be found in endosomes, prior to recycling or degradation. In this appendix I will address my hypothesis that Par6 overexpression promotes activation of EGFR which leads to receptor-mediated endocytosis and Ras/MAPK pathway activation. To test this hypothesis, I investigated if EGFR was activated in Par6 overexpressing cells independent of EGF stimulation.

Results*:*

Par6 overexpression did not promote phosphorylation of EGFR

To determine if Par6 overexpression induced EGFR activation, I first examined if EGFR was tyrosine phosphorylated in growth-arrested quiescent MCF-10A cells expressing Par6 or vector control (Figure A.2). This experiment showed that Par6 overexpression did not phosphorylate EGFR under these conditions. However, the levels of EGFR in Par6 overexpressing cells (Figure A.2 [lane 3]) were similar to the levels in MCF-10A cells that had been stimulated with EGF (Figure A.2 [lane 1]). This observation suggested that Par6 overexpression may induce activation of the receptor, although the phosphorylation levels are not detectable. Therefore, I further investigated if EGFR was activated in Par6 overexpressing cells without exogenous EGF stimulation.

Par6 overexpression reduces EGFR protein levels

To confirm that Par6 overexpressing cells had less detectable EGFR protein when compared to 10A and vector control cells, I examined EGFR activation in growing (Day 3), confluent (Day 4), and contact-inhibited (Day 5) cells. Low levels of total EGFR protein and phosphorylated receptor were detected in growing cells (Figure A.3.A [lanes 2-4]), suggesting that the receptor is being activated and subsequently degraded. The low levels of both EGFR and Phosphotyrosine also suggest that EGFR is too labile to detect in growing cells. As the control cells become confluent and contact-inhibited, total EGFR levels were increased (Figure A.3.A, [Lanes 6,7 and 12,13]) when compared to growing cells (Figure A.3.A, [lanes 2,3]), indicating that EGFR is no longer being

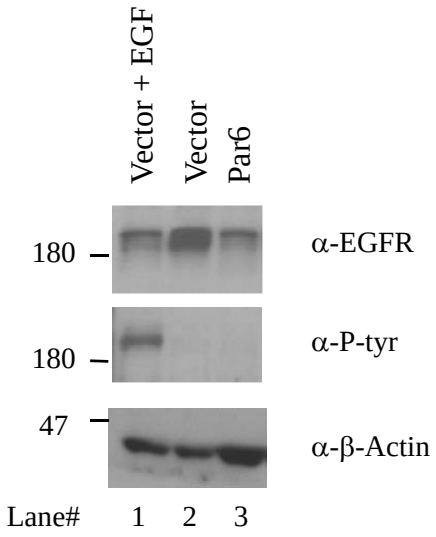

Figure A.2. Par6 overexpression does not promote phosphorylation of EGFR.

MCF-10A cells expressing vector control or Flag-Par6α were grown to confluence and stimulated with 2 ng/ml EGF or left untreated for 15 minutes. Cell extracts were analyzed for activation of EGFR by immunoblotting with a phospho-tyrosine specific antibody..

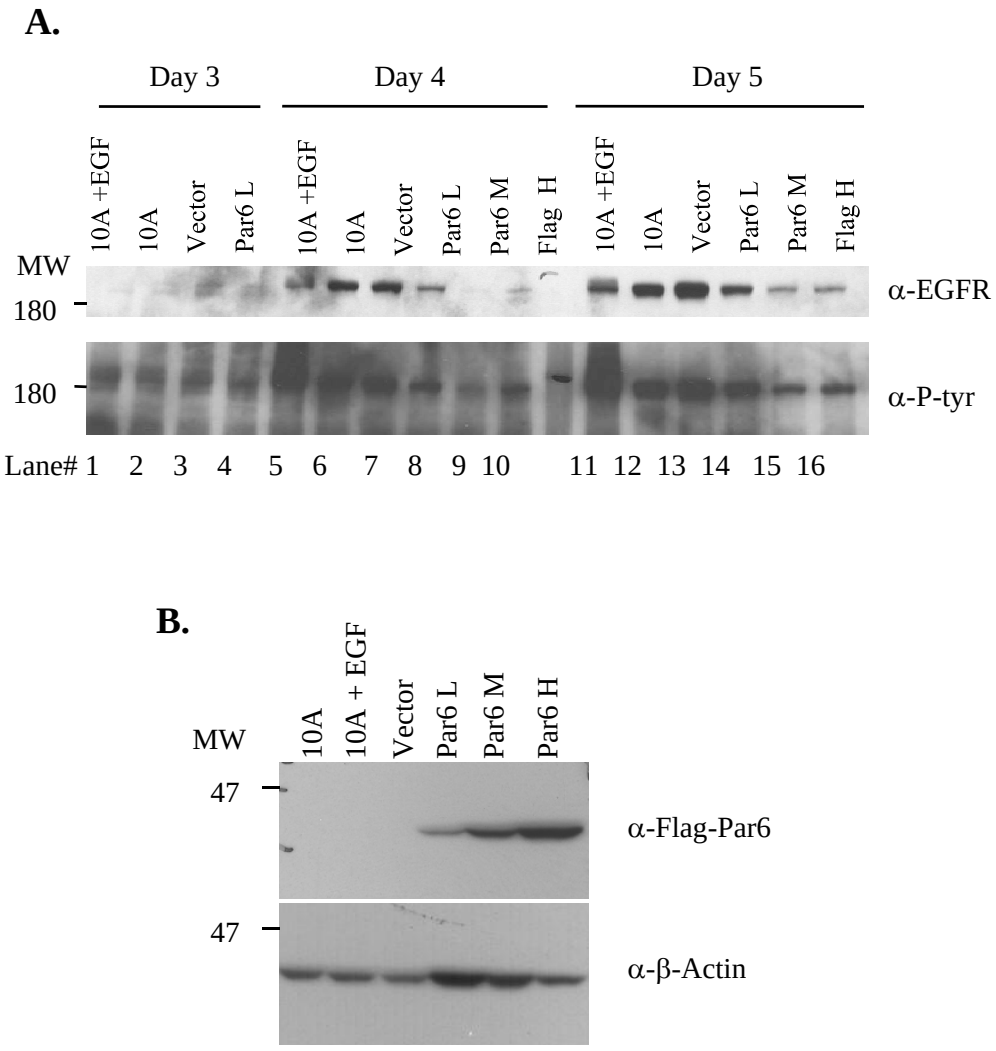

Figure A.3. Par6 overexpression reduces EGFR levels.

(A) MCF-10A cells expressing vector control, Flag-Par6α low (L), medium (M) and high (H) levels of Par6 protein were grown for 3, 4 and 5 days. Each day cells were stimulated with 2ng/ml EGF for 15 minutes or left untreated. Cell extracts were analyzed for activation of EGFR by immunoblotting with phospho-tyrosine specific and EGFR antibodies. **(B)** Extracts from day 5 cells (A) were analyzed for Par6 protein expression by immunoblotting with anti-flag antibody.

activated and degraded in the control cells. However, in Par6 expressing cells total EGFR and phosphotyrosine levels were low even in contact-inhibited cells (Figure A.3.A, [Lanes 15,16]), suggesting that EGFR is being activated and degraded in a similarly to growing cells observed on day 3 (Figure A.3.A [lanes 2,3]). In addition, this experiment was performed in three MCF-10A cell lines that express increasing levels of Par6 protein (Figure A.3.B). Interestingly, I noticed that levels of EGFR were lower in Par6 high expressing cells when compared to the Par6 low expressing cells. This data shows that overexpression of Par6 levels correlated with lower levels of EGFR protein and possibly activation. I also determined that this correlation was specific to EGFR and not ErbB3 another EGFR family member (Figure A.5.A bottom panel). Together, the data in this section shows that there is less detectable EGFR protein in Par6 overexpressing cells. Because there is less detectable protein, I reasoned that EGFR could be activated and subsequently degraded. Therefore, I decided to pursue this line of investigation.

Various protein extraction methods do not alter detection of phosphotyrosine or EGFR in Par6 overexpressing cells

The experiments performed in Figure A.1 and A.2 showed low levels of both EGFR and phosphorlyated receptor. It is possible that the active receptors were located within endosomes and were not solubilized under non-ionic protein extraction conditions. To address this, cells were lysed using two ionic detergent based lysis buffers, RIPA, which contains both a non-ionic (NP-40) and ionic (SDS) detergents and boiling (100º) SDS-Laemmeli buffer to promote solubilization of proteins. Figure A.4 showed that

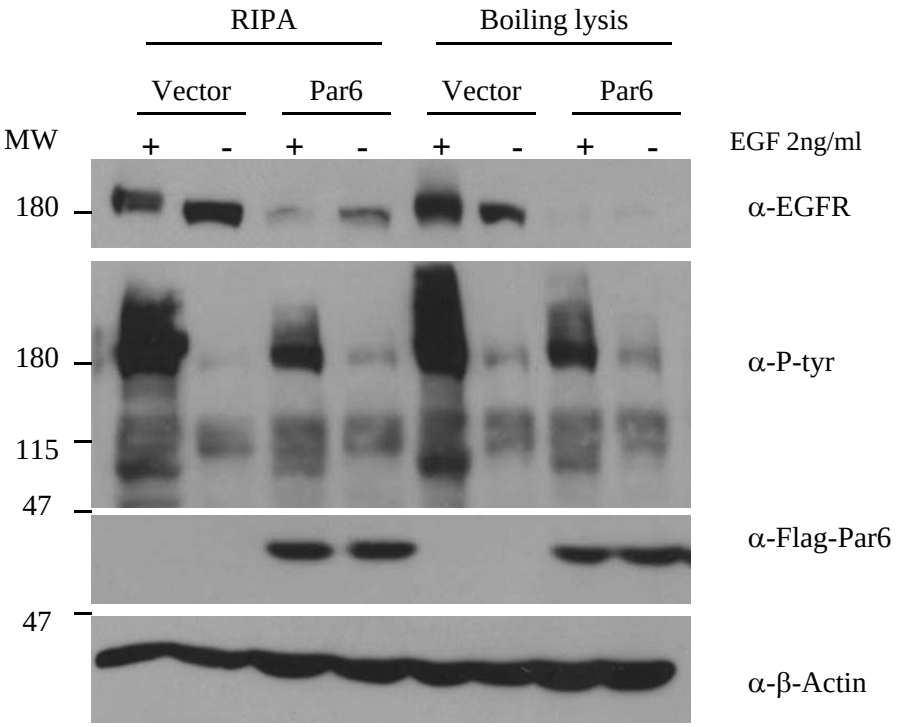

Figure A.4. Various protein extraction methods do not alter detection of phosphotyrosine of EGFR in Par6 overexpressing cells.

MCF-10A cells expressing vector control or Flag-Par6α were grown to confluence and stimulated 2ng/ml EGF for 15 min or left untreated. Cells were then extracted with RIPA buffer or SDS-Laemmeli buffer (100°C) to solubilize proteins located within membrane components. Cell extracts were analyzed for EGFR activation and Par6 protein expression by immunoblotting with phospho-tyrosine specific and EGFR and flag antibodies.

neither cell extraction condition enhanced detection of active EGFR. Therefore there is less detectable EGFR and EGFR phosphorylation in Par6 overexpressing cells.

Inhibition of the proteosome does not increase phosphotyrosine or EGFR levels in Par6 expressing cells

To determine if low EGFR levels in Par6 expressing cells were due to proteasome-mediated degradation of the receptor, I inhibited the proteosome using two inhibitors, MG-132 and Lactacystin (Lee and Goldberg 1998). As expected, addition of the inhibitors blocked degradation of the ligand stimulated EGFR in both control and Par6 overexpressing cells (Figure A.5.A [lanes 3,7] and Figure 6.A [lanes 3,7]). However, there was no increase in EGFR or phosphotyrosine levels in Par6 overexpressing cells in the presence of the proteosome inhibitor (Figure A.5.A [lane 8] and 6.A [lanes 10,12]). Although there was no obvious increase in EGFR phosphotyrosine levels in Par6 overexpressing cells, perhaps the levels were below the threshold of detection by immunoblotting. To further enhance the detectable levels of EGFR phosphorylation I immunoprecipitated EGFR and phosphotyrosine from extracts of cells expressing Par6 and vector control in the presence of a proteosome inhibitor. Under these conditions I did not see an increase in phosphorylation of EGFR in Par6 overexpressing cells (Figure A.5.B [lane 4 compared to lane 7]). While these data suggested that Par6 is not promoting EGFR activation, it is still possible that small amounts of EGFR are becoming activated and endocytosed and degraded through the lysosomal pathway.

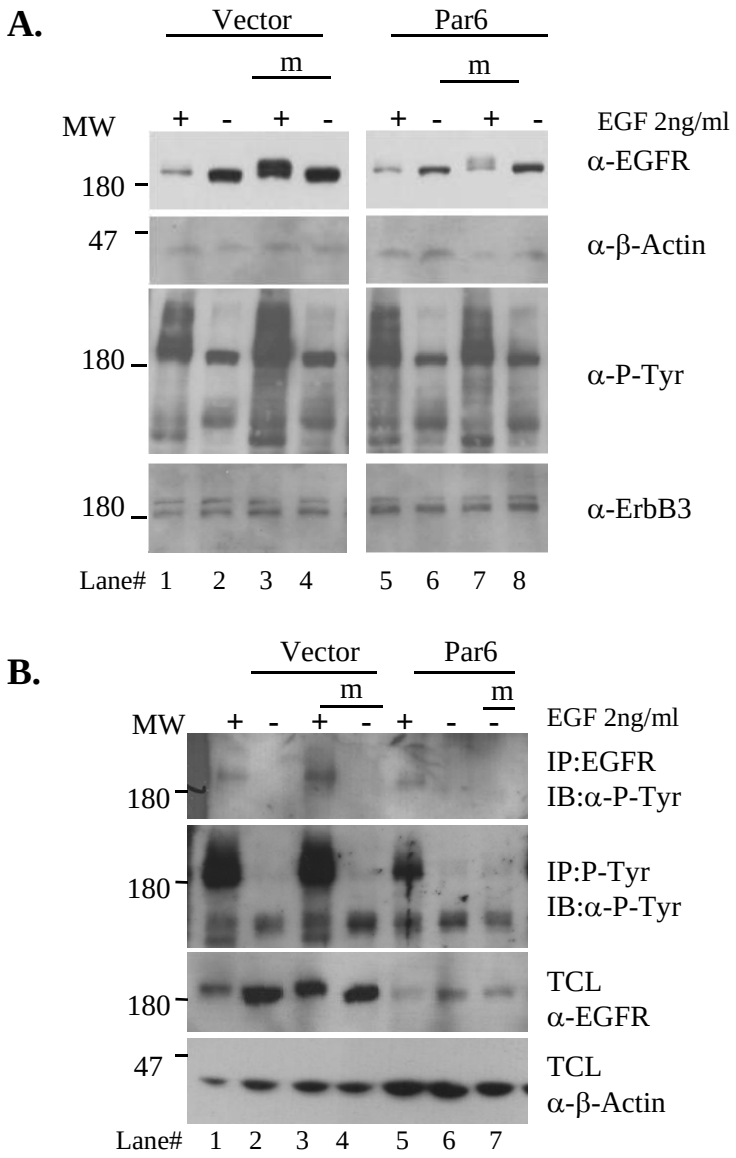

Figure A.5. Inhibition of the proteasome does not increase EGFR levels in Par6 expressing cells

(A) MCF-10A cells expressing vector control or Flag-Par6α were grown for 5 days and left untreated, or pre-treated with 25μm MG-132 (m) for 4 hours and then untreated or stimulated with 2ng/ml EGF 15 min. Extracts were analyzed for EGFR activation by immunoblotting with phospho-tyrosine specific and EGFR antibodies. **(B)** Extracts from MCF-10A cells in (A) were immunoprecipitated with phospho-tyrosine and EGFR specific antibodies. Immunoprecipitates or total cell lysates (TCL) were analyzed for EGFR activation by immunoblotting with phospho-tyrosine specific and EGFR antibodies.

Inhibition of the clathrin and caveolin mediated endocytosis does not increase phospho-tyrosine or EGFR levels in Par6 expressing cells

Active EGFR is primarly endocytosed through clathrin coated pits (Vieira et al. 1996; Wiley 2003), recently there has been evidence that EGFR can be endocytosed through caveolin mediated endocytosis (Sigismund et al. 2005). Therefore, I interfered with both endocytosis mechanisms using two different inhibitors. Interference with endocytosis would prevent EGFR from entering endosomes and thereby prevent EGFR degradation through the lysosomal pathway. I used Bafilomycin A1 an inhibitor of vacuolar-type H^+-ATPase, preventing acidification of endosomal compartments and Filipin III an inhibitor of caveolin mediated endocytosis (Schnitzer et al. 1994). As expected both of these inhibitors stabilized EGFR in ligand stimulated vector control cells (Figure A.6.A. [lane 5] and Figure A.6.B [lane 4]). However, we did not see an increase in EGFR levels or an increase in phosphorylation of EGFR in Par6 overexpressing cells (Figure A.6.A. [lane 11] and Figure A.6.B [lane 8]). These data combined with the proteosome inhibitor data (Figure A.5), show that inhibition of receptor endocytosis and degradation does not enhance detection of activated EGFR in Par6 overexpressing cells.

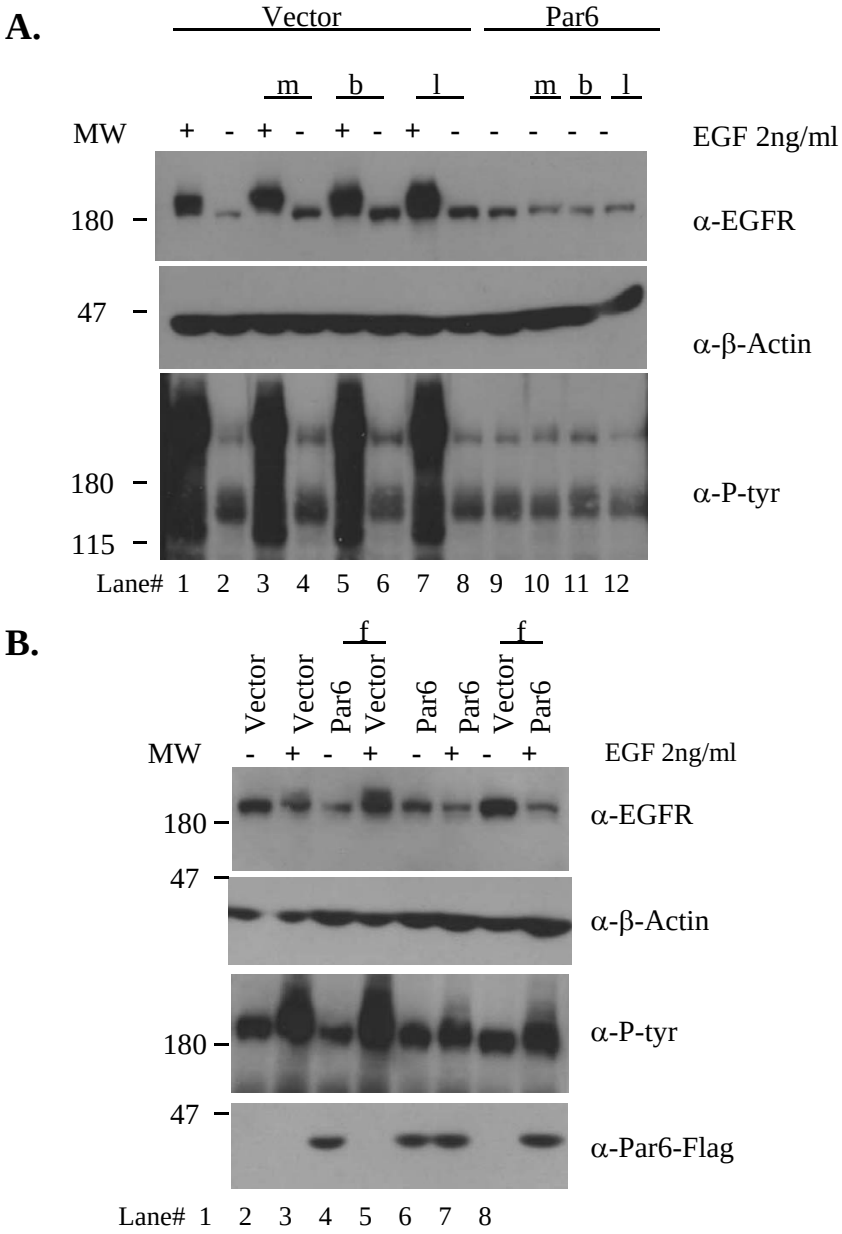

Figure A.6. Inhibition of proteasome, and clathrin or caveolin mediated endocytosis does not increase EGFR protein levels in Par6 expressing cells.

(A) MCF-10A cells expressing vector control or Flag-Par6α were grown for 5 days and left untreated, or pre-treated with 25μm MG-132 (m) for 4 hours or 0.25μm BafilomycinA1 (b) or 10μm Lactacystin (l) and then untreated or stimulated with 2ng/ml EGF 15 min. Extracts were analyzed for EGFR activation by immunoblotting with phospho-tyrosine specific and EGFR antibodies. **(B)** MCF-10A cells grown as in **(A)** were treated with FilipinIII (f) for 1 hour. Extracts were analyzed for EGFR activation by immunoblotting with phospho-tyrosine specific and EGFR antibodies.

Discussion:

The experiments presented in this appendix have determined that Par6 overexpression does not promote activation of EGFR. In addition I have shown that Par6 overexpression correlates with lower levels of EGFR protein expression. The decreased levels of EGFR are not associated with receptor mediated endocytosis and degradation because inhibition of these mechanisms did not restore EGFR levels in Par6 overexpressing cells. Further experiments need to be done to determine if EGFR gene expression is being regulated at the transcriptional or translational level in Par6 overexpressing cells. One experiment that would shed some light on this topic would be to perform quantitative PCR to determine if the levels of EGFR mRNA are equal in control versus Par6 overexpressing cells. The conclusion of this appendix is that Par6 overexpression does not promote activation of EGFR and that there must be an alternative mechanism by which Par6 is promoting activation of MAPK and mammary epithelial cell proliferation.